Transformation of non-malignant breast epithelial cells: Role of alkylating agents and platelet activating factor

A thesis Submitted in partial fulfillment of the requirements

Of the degree of

Doctor of Philosophy

By

Libi Anandi Viswanathan

Reg. No. 20123152

INDIAN INSTITUTE OF SCIENCE EDUCATION AND

RESEARCH PUNE

2017

CERTIFICATE

Certified that the work incorporated in the thesis entitled "**Transformation of non-malignant breast epithelial cells: Role of alkylating agents and platelet activating factor**" submitted by Libi Anandi Viswanathan was carried out by the candidate, under my supervision. The work presented here or any part of it has not been included in any other thesis submitted previously for the award of any degree or diploma from any other University or Institution.

Date: 7th February 2017

Dr. Mayurika Lahiri

Associate Professor

Biology Division, IISER Pune

DECLARATION

I declare that this written submission represents my idea in my own words and where others' ideas have been included; I have adequately cited and referenced the original sources. I also declare that I have adhered to all principles of academic honesty and integrity and have not misrepresented or fabricated or falsified any idea/data/fact/source in my submission. I understand that violation of the above will be cause for disciplinary action by the Institute and can also evoke penal action from the sources which have thus not been properly cited or from whom proper permission has not been taken when needed.

Date: 7th February 2017

Libi Anandi Viswanathan

20123152

Dedicated to my Mom and Dad

For their endless love, support and encouragement.

ACKNOWLEDGEMENTS

The journey of my PhD would not have been possible without the contributions of many people. At this juncture, I would like to express my sincere thanks to all who have contributed in many ways to the success of this work and made it a memorable experience for me. My heartfelt thanks goes out to all of you who provided support, inspiration, mentoring, peer pressure, and motivation along the way.

First and foremost I am grateful to ***Dr Mayurika Lahiri*** *for having given me the opportunity to work under her esteemed guidance. I would like to thank her for her intellectual support and motivation that has guided me throughout the work and helped the accomplishment of the thesis work. I consider myself fortunate to be associated with her, who gave me a decisive turn, a significant boost to my career. I am also thankful to her for all the opportunities she provided to develop my skills; the freedom to think and design experiments independently. Her excitement in each of our achievements is very motivating. Her constant encouragement kept me going. I also appreciate her genuine care and help beyond professional mentoring.*

I would also like to express my sincere regards and gratitude to ***Dr LS Shashidhara****, HOD, Biology, IISER Pune for the all the support he has provided during the past five years, especially for the funding he provided to attending the GRC Conference on Mammary Gland Biology, 2016, Barga, Italy. I would also like to express my sincere thanks to* ***Dr VS Rao****, for all the help and support he provided with regards to funding.*

I am especially indebted to my thesis committee members ***Dr Annapoorni Rangarajan****, Indian Institute of Science (IISc) Bangalore,* ***Dr Sanjeev Galande****, IISER Pune and* ***Dr Richa Rikhy****, IISER Pune, who have been simply unreal. Their timely suggestions and constructive criticism immensely helped in molding the project into what it is today. I would like to express my special thanks to Dr Richa Rikhy for her critical reading of the*

manuscript and for the discussions with her ,which helped me design a few critical experiments during revision of manuscript. I am also grateful to ***Dr. Aurnab Ghose*** *for his valuable guidance and support throughtout the work. The help rendered by Dr Richa Rikhy and Dr Aurnab Ghose with microscopy of 3-dimensional cultures, at a time when I had almost given-up is invaluable.*

My sincere thanks to ***Dr Sourav Banerjee****, National Brain Research Center (NBRC), Manesar, Gurgaon, and his students for providing me training in lentiviral work. I would also like to express my sincere thanks to* ***Dr Manas Kumar Santra****, National Center for Cell Sciences (NCCS), Pune, and his student* ***Debasish*** *for their help with the lentiviral work.*

I would like to take this opportunity to thank ***INSPIRE-DST*** *for providing me with fellowship for my studies. I am indebted to* ***IISER, Pune*** *for providing the infrastructure and facilities.*

I would also like to express my heartfelt thanks to ***Satish*** *for all the help. The discussions, which often ended up in arguments were instrumental in the designing of the project. His open criticism, although often annoying, also triggered thinking and helped foresee the pitfalls of the experiments and re-design them. His help and support, especially during the initial days of my graduate school days, will always be valued. Thank you for being there during both good and bad times throughout this journey.*

Special thanks to ***Vaishali*** *for all her unconditional love, support and help. She has been a patient teacher, a well wisher, and a counselor during times of difficulty. A person I could turn to anytime, in any situation. Thank you so much for everything. I would also like to extend my heartfelt thanks to* ***"Chechi"*** *(****Rintu****). She has not only helped me out with work but also has been a lovely friend, a caring sister, a person with whom I could share my problems. "Queen of Midiprep", my guru for all the bacterial work, thank you for always being there.*

Words are not sufficient to express my deepest sense of gratitude and warm thanks to ***"Bro" (Ashiq)****: an apt example of the proverb "A friend in need is a friend in deed". He has always stepped in selflessly during the most difficult and critical situations. His help and support indeed needs a special mention. Special thanks to him for the help with formatting, without whom this thesis would have been a mess.*

Special thanks to ***Ishtiyaq Khan****,* ***Mahesh Chand*** *and* ***Sachin Holkar*** *for their unconditional help and guidance with troubleshooting my problems with "Cloning" and simplifying the process. Thanks to* ***Mitali*** *for her guidance and advice during the first year of my PhD. Her constant encouragement during the frustration phase of initial standardizations of 3D cultures kept me going without giving up. I am also thankful to* ***Surojit*** *for having initiated the project in the lab.*

I would also like to thank all my friends other that my lab, especially ***Ketakee*** *and* ***Sayali*** *for the helpful and thought provoking discussions and suggestions they provided. Thanks to my batchmates* ***Indu, Manasi, Sampada*** *and* ***Ishtiyaq*** *for their timely support. Indu has been a close friend from day one at IISER. Talking to her has always been refreshing.*

I would also like to thank Bio-admin staff ***Mrinalini, Kalpesh, Piyush, Shabnam*** *and* ***Rupali*** *for taking care of the infrastructure and help simplify the process of procuring reagents. I would also like to express my special thanks to* ***Vijay*** *and* ***IISER microscopy facility.*** *Vijay's help with the image analysis and troubleshooting problems with the microscopy is greatly appreciated. Thank you Vijay and* ***Tanmoy*** *for the help with TIRF microscope during the revision, I would not have been able to finish my work on time without your help.*

Special thanks to present and past Lahirilab members, especially ***Mitali, Sneha, Arijita, Swaroopa, Payal, Satish, Vaishali, Ashiq, Rintu, Abhijit, Rupa, Aishwarya, Vishaka, Kezia, Faseela, Komal, Virender*** *for making Lab feel like a second home. I am grateful*

to them for their continued moral support and maintaining healthy atmosphere in the lab. The time and the moments we enjoyed together will be cherished throughout my life.

I would like to thank ***Satish, Rupa, Ashiq and Ketakee*** *for proofreading of my thesis and their valuable suggestions. Any attempt to acknowledge by name, the help received by me during the thesis work runs the risk of omitting someone. Therefore following must be preceded by sincere thanks to all who rendered their valuable assistance and concerned guidance to me throughout these five years.*

Last, but certainly not the least, my heartfelt deepest gratitude to my parents, my siblings, my husband and in-laws. Thank you ***Mom*** *and* ***Dad*** *for having given me the freedom to pursue my PhD and for the sacrifices and compromises you have made to help me accomplish whatever I have achieved till date. You have contributed irreversibly to the person I have become. I cannot thank you enough. It's only through your love, patience, support and unwavering belief in me, that I've been able to complete this long dissertation journey. My appreciation to* ***my siblings*** *for all the moral support they have provided throughout and tolerating my mood swings. Special thanks to my maternal uncle* ***Hero****, for his guidance in choosing my career and his advice during times of confusion. I would like to express my deep sense of gratitude to* ***my husband*** *for the love, care and support he provided, for the encouraging words when I felt low, for making me laugh even in the toughest of the situations and for patiently listening to all my cribbing. Special thanks to my* ***in-laws*** *for the interest they expressed in my work and their excitement in my achievements which was a source of motivation.*

*And above all my deep thanks to "****The Almighty****" for His blessings and grace that enlightened my path as I travelled through.*

SYNOPSIS

Title: Transformation of non-malignant breast epithelial cells: Role of alkylating agents and platelet activating factor

Name of the Student: **LIBI ANANDI**

Roll number: 20123152

Name of the thesis advisor: Dr. Mayurika Lahiri

Date of Registration: 2nd January 2012

Indian Institute of Science Education and Research (IISER), Pune, India.

Introduction

Worldwide cancer statistics taken in 2012 reveals that among men lung cancer was the most common cancer (12.9% of all new cases) while breast cancer was found to be the most common cancer diagnosed among women (25.2% of all new cases in women) (GLOBOCAN). Breast cancers are caused by a complex combination of genetic and environmental factors. However, statistical data revealed that only 15% of breast cancers are inherited in nature hence highlighting the increased possibility of various other factors contributing to development and progression of cancer (Cancer, 2001). Hanahan and Weinberg, in their review entitled “Hallmarks of Cancer: The next generation” enlisted “genomic instability” and “tumor promoting inflammation” as the characteristics that enable normal cells to become cancerous (Hanahan and Weinberg, 2011). The mammary gland, throughout a woman’s lifetime undergoes extensive and significant remodelling. The rate of differentiation, proliferation and apoptosis in mammary gland is significantly higher as compared to the other tissues of the body. Thus, the gland is susceptible to the occurrence of DNA damage as compared to the other tissues (McCready et al., 2010). Various exogenous and endogenous agents are known to cause DNA damage leading to genomic instability. Alkylating agents are one such class of agents which are used in cancer chemotherapy as well are ubiquitously present as pollutants in the environment. On the other hand, inflammation results in accumulation of

bioactive molecules in the cellular microenvironment. PAF, Platelet Activating Factor, is one such molecule secreted by cells of the immune system. This thesis involves the study of effect of alkylating agents (which induce genomic instability) and PAF (bioactive molecule present in inflammatory microenvironment) on breast epithelial cells. We have used 3D cultures of non-transformed epithelial cells as the model system. The concept of 3D-cultures has emerged as a powerful tool to study the progression of cancer, by overcoming the shortcomings of 2D-culture (3D cultures to a large extent mimics the *in vivo* microenvironment) as well as rodent models (since the cells grown in 3D are of human origin).The breast epithelial cells grown on the basement membrane (as 3D cultures) tend to form acini, which closely resemble the *in vivo* structures. The morphology of these acini is disrupted in malignancy, where an increase in size and elongation of acini was observed (Dey et al., 2009). The acinar structures formed by the epithelial cells aids in distinguishing the normal and transformed phenotype which is difficult in case of 2D cultures. This model provides the added advantage of studying the process of morphogenesis of both non-transformed and transformed breast epithelial cells in a simplified set-up. Establishing a model to study effects of potential physiologically relevant chemicals in a 3D culture environment will serve as a relevant model to delineate the process of cancer initiation and also help in the process for screening cancer therapeutics.

MCF10A, a near diploid, immortalized, and non-tumorigenic breast epithelial cell line, derived from human fibrocystic mammary tissue, was used in the study. Growth factor reduced Matrigel ™ was used as the basement membrane.

The aim of the study was studied the effect of alkylating agents NEU *(N-ethyl-N nitrosourea)*(Bodakuntla et al., 2014) *and* NMU *(N-methyl-N nitrosourea)* as well as PAF (Anandi *et al*., 2016; Libi Anandi, 2016) on non-transformed breast epithelial cells (MCF10A) using 3-dimensional cultures as a model system. The specific objectives were as follows:

OBJECTIVES:

1. Develop a model to study the process of transformation.
2. To delineate the process of transformation following exposure to alkylation damage
    a. *Investigate the phenotypic changes that may occur during transformation.*
    b. *Elucidate the mechanism(s) involved in transformation*
    c. *Identify candidate genes and study their role in transformation.*
3. To investigate the effect of PAF on breast epithelial cells.
    a. Investigate the phenotypic changes that may occur following exposure to PAF.

Effect of alkylation damage on MCF10A cells grown as 3D 'on top' cultures.

Alkylating agents are well known DNA damaging agents known to induce mutations due to the ability to alkylate "N" and "O" positions of DNA leading to A:T to T:A transversions or G:C to A:T transition mutations (Barbaric I, 2007; Engelbergs et al., 2000). Among the various Alkylating agents we used two of the agents namely *N*-nitroso-*N*-ethylurea (NEU) and *N*-nitroso-*N*-methylurea (MNU). NEU and MNU are simple monofunctional S_N1 type-DNA ethylating agent and methyating agent respectively. These agents have been demonstrated to cause mammary tumors in rodent models (Givelber and DiPaolo, 1969; Stoica et al., 1983b). In spite of this, these agents are the prototypical of alkylating agents used in cancer chemotherapy for almost 30 years (Kaina et al., 2010). NEU has been found to be a severely potent transplacental teratogen and an active rat mammary gland genotoxic carcinogen in rodents (Stoica et al., 1983a, 1984). In vitro, NEU has been reported to induce neoplastic transformation of rat mammary epithelial cells (Stoica et al., 1991). NEU is known to induce random mutagenesis. On the other hand, MNU has been found to induce mammary tumors in rat (Gandilhon et al., 1983). It has been reported to be mutagenic in mammalian cells as well as these mutations have been found to be site specific using the HPRT gene Mutation assay (Thomas et al., 2013; Zhang and Jenssen,

1991). MNU-induced mammary cancer in rats has been found to have many similarities to that of human breast cancer (Tsubura et al., 2011). MNU, thus, is a candidate chemical agent which can be used to study the early stages of cancer initiation.

We observed that exposure of non-transformed mammary epithelial cells to alkylating agents resulted in transformation. Exposure to these agents resulted in disruption of the apical and baso-lateral polarity as well as induction of epithelial to mesenchymal transition (EMT) - like phenotype. Acquisition of mesenchymal phenotype was coupled with increased motility as single cells. In addition to motility, we also observed that these cells showed invasive capabilities as well as ability to grow in anchorage independent conditions. Though the histopathological data of mammary tumors in rats induced by these agents suggests resemblance to human tumor specimens, there are no reports pertaining to the mechanism of tumor induction. An attempt to decipher the mechanism of methylation damage induced transformation revealed the central role played by DNA-PK in facilitating the process. In conclusion, this study provides evidences for the carcinogenic potential of alkylating agents and identifies the novel role of DNA-PK in transformation of breast epithelial cells.

An interesting novel observation of this study was the cytoplasmic effects caused by the DNA damaging agents. Apart from Golgi dispersal, similar to that reported by Farber-Katz *et al*, (Farber-Katz et al., 2014) we observed reorganization of the cytoskeleton. Investigation of the mechanism revealed that these cytoplasmic effects were mediated via activated DNA-PK. Further experiments suggest the possible role of JNK and Akt downstream of DNA-PK in re-organizing Actin and eventually the microtubules.

Thus this study not only identifies the novel role of DNA-PK in DNA damage induced transformation but also sheds light on the cytoplasmic effects caused by DNA damage, an area which remains the least explored.

API5, a candidate gene identified to be up-regulated in alkylation damage induced transformation, is a potential oncogene.

Role of API5, Apoptosis inhibitor 5, has been implicated in various cancers. Our study on studying alkylation damage induced transformation identified Api5 as one of the candidate genes which was up-regulated in the transformed cells. Studies concerned with expression of Api5 protein across different types of cancers including colon, liver, lung, pancreas, stomach, kidneys and esophagus showed a significant up regulation of Api5 (Koci et al., 2012). Api5 has also been shown to be up-regulated in B-cell chronic lymphoid leukemia. Kim and colleagues further investigated the role of Api5 in cervical cancer cell metastasis using adhesion and invasion assays and have proposed that Api5 may be involved in invasion of cervical cancer cells, possibly through its role in cell interactions with extracellular matrix (Kim et al., 2000). There are no reports on the role of Api5 in breast cancer, however, up-regulation of Api5 was observed in tamoxifen resistant breast cancer cells and MCF7 cells indicating its possible tumorigenic role (Jansen et al., 2005; Ramdas et al., 2011). Unavailability of information regarding role of Api5 in breast cancer coupled with the up-regulation observed in cells transformed upon DNA damage, instigated the study of its role in breast tumor initiation. To investigate the role of Api5 in breast tumorigenesis, Api5 was stably over-expressed in MCF10A cells using lentiviral mediated gene transfer. MCF10A cells and Api5 over-expressed MCF10A cells were seeded as 3D ‘on top’ cultures on Matrigel^{TM} and maintained for 16 days. We observed that Api5 over expression disrupts the mammary epithelial morphogenesis, enhances cellular proliferation and may result in evasion of apoptosis. Loss of polarity and up-regulation of mesenchymal markers implied the induction of EMT-like phenotype. Furthermore MCF10A cells over-expressing Api5 resulted in the formation of acinar structures with protrusion-like structures implying possible induction of invasion.

Thus, our data implies that Api5 up-regulation in MCF10A cells *per se* is sufficient to transform the cells and suggests possible oncogenic role of Api5 in breast cancer.

Effect of prolonged exposure of Platelet Activating Factor on MCF10A cells grown as 3D 'on top' cultures.

Chronic inflammatory conditions are characterized by the secretion of a number of bioactive molecules in the microenvironment by the cells of the immune system. In order to study role of tumor promoting inflammation in cancer initiation, the potential role of PAF in transformation was explored. Role of various bioactive molecules such as Lysophosphatidic acid, reactive oxygen species and various cytokines, present in the tumor milieu have been well explored. However, role of PAF in breast cancer has not been studied extensively, especially pertaining to its role in breast cancer initiation. This lack of sufficient information coupled with the physiological relevance of this bioactive molecule, prompted us to study the role of this molecule in breast tumorigenesis. We observed that prolonged exposure of non-transformed mammary epithelial cells to PAF disturbed the balance between proliferation and apoptosis thus resulting in formation of abnormal spheroids. Further investigation revealed that PAf induction induced enhanced cellular proliferation and possibly induced invasive phenotypes which were characterized by the formation of protrusion or bulb-like structures. Up-regulation of vimentin, a mesenchymal marker, disruption of apico-basal polarity along with loss of integrity of cell-cell junction was observed suggesting the induction of EMT-like phenotype. Thus, this study for the first time demonstrates the tumorigenic potential of Platelet activating factor in breast epithelial cells and appeals for the detailed study of the process and mechanism thereof; validation of findings in patient samples so as to aid in the development of new effective therapeutic strategies based on tumor profile.

Conclusion:

Taken together our study provides evidences for the carcinogenic potential of alkylating agents as well as reports the ability of PAF to induce phenotypic transformation in breast epithelial cells (Figure 1).

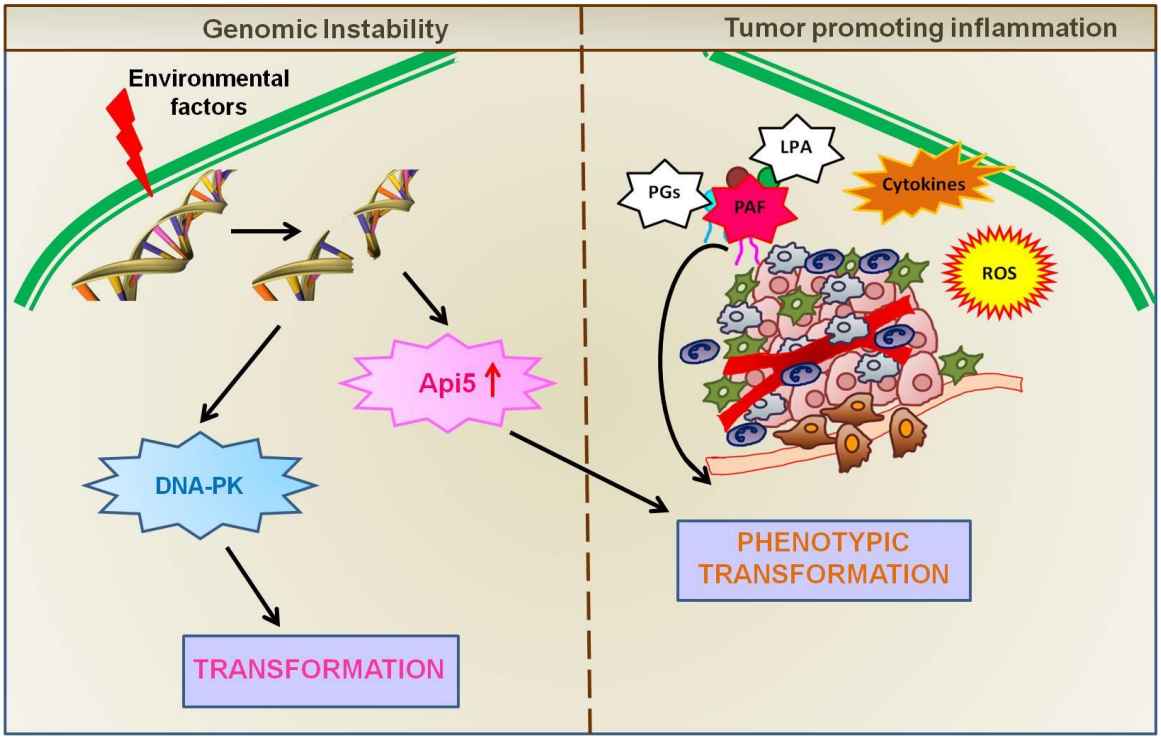

Figure 1: Schematic summarizing the study described in the thesis; Study of "enabling characteristics": Genomic instability and Tumor promoting inflammation. Exposure to alkylating agents through various sources induces DNA damage (and hence genomic instability) and eventually results in transformation which has been found to be mediated via DNA-PK. Up-regulation of Api5, a candidate gene identified in the study, also induces phenotypic transformation. Presence of PAF (component secreted by inflammatory environment) in the microenvironment of non-transformed breast epithelial cells results in Phenotypic transformation.

References:

Anandi, V.L., Ashiq, K.A., Nitheesh, K., and Lahiri, M. (2016). Platelet-activating factor promotes motility in breast cancer cells and disrupts non-transformed breast acinar structures. Oncology reports *35*, 179-188.

Barbaric I, W.S., Russ A, Dear TN (2007). Spectrum of ENU-induced mutations in phenotype-driven and gene-driven screens in the mouse. Environ Mol Mutagen *48*, 124-142.

Bodakuntla, S., Libi, A.V., Sural, S., Trivedi, P., and Lahiri, M. (2014). N-nitroso-N-ethylurea activates DNA damage surveillance pathways and induces transformation in mammalian cells. BMC Cancer *14*, 287.

Cancer, C.G.o.H.F.i.B. (2001). Familial breast cancer: collaborative reanalysis of individual data from 52 epidemiological studies including 58,209 women with breast cancer and 101,986 women without the disease. Lancet *358*, 1389-1399.

Dey, D., Saxena, M., Paranjape, A.N., Krishnan, V., Giraddi, R., Kumar, M.V., Mukherjee, G., and Rangarajan, A. (2009). Phenotypic and functional characterization of human mammary stem/progenitor cells in long term culture. PloS one *4*, e5329.

Engelbergs, J., Thomale, J., and Rajewsky, M.F. (2000). Role of DNA repair in carcinogen-induced ras mutation. Mutation Research *450*, 139-153.

Farber-Katz, S.E., Dippold, H.C., Buschman, M.D., Peterman, M.C., Xing, M., Noakes, C.J., Tat, J., Ng, M.M., Rahajeng, J., Cowan, D.M*., et al.* (2014). DNA damage triggers Golgi dispersal via DNA-PK and GOLPH3. Cell *156*, 413-427.

Gandilhon, P., Melancon, R., Djiane, J., and Kelly, P.A. (1983). N-nitroso-N-methylurea-induced mammary tumors in the rat: role of prolactin and a prolactin-lowering drug. J Natl Cancer Inst *70*, 105-109.

Givelber, H.M., and DiPaolo, J.A. (1969). Teratogenic effects of N-ethyl-N-nitrosourea in the Syrian hamster. Cancer Research *29*, 1151-1155.

Hanahan, D., and Weinberg, R.A. (2011). Hallmarks of cancer: the next generation. Cell *144*, 646-674.

Jansen, M.P., Foekens, J.A., van Staveren, I.L., Dirkzwager-Kiel, M.M., Ritstier, K., Look, M.P., Meijer-van Gelder, M.E., Sieuwerts, A.M., Portengen, H., Dorssers, L.C.*, et al.* (2005). Molecular classification of tamoxifen-resistant breast carcinomas by gene expression profiling. Journal of clinical oncology : official journal of the American Society of Clinical Oncology *23*, 732-740.

Kaina, B., Margison, G.P., and Christmann, M. (2010). Targeting O^6-methylguanine-DNA methyltransferase with specific inhibitors as a strategy in cancer therapy. Cellular and Molecular Life Sciences *67*, 3663-3681.

Kim, J.W., Cho, H.S., Kim, J.H., Hur, S.Y., Kim, T.E., Lee, J.M., Kim, I.K., and Namkoong, S.E. (2000). AAC-11 overexpression induces invasion and protects cervical cancer cells from apoptosis. Lab Invest *80*, 587-594.

Koci, L., Chlebova, K., Hyzdalova, M., Hofmanova, J., Jira, M., Kysela, P., Kozubik, A., Kala, Z., and Krejci, P. (2012). Apoptosis inhibitor 5 (API-5; AAC-11; FIF) is upregulated in human carcinomas in vivo. Oncology letters *3*, 913-916.

Libi Anandi, M.L. (2016). Platelet activating factor leads to initiation and promotion of breast cancer. Cancer Cell and Microenvironment *3*, e1370.

McCready, J., Arendt, L.M., Rudnick, J.A., and Kuperwasser, C. (2010). The contribution of dynamic stromal remodeling during mammary development to breast carcinogenesis. Breast cancer research : BCR *12*, 205.

Ramdas, P., Rajihuzzaman, M., Veerasenan, S.D., Selvaduray, K.R., Nesaretnam, K., and Radhakrishnan, A.K. (2011). Tocotrienol-treated MCF-7 human breast cancer cells show down-regulation of API5 and up-regulation of MIG6 genes. Cancer genomics & proteomics *8*, 19-31.

Stoica, G., Jacobs, R., Koestner, A., O'Leary, M., and Welsch, C. (1991). ENU-induced in vitro neoplastic transformation of rat mammary epithelial cells. Anticancer research *11*, 1783-1792.

Stoica, G., Koestner, A., and Capen, C.C. (1983a). Characterization of N-ethyl-N-nitrosourea--induced mammary tumors in the rat. The American journal of pathology *110*, 161-169.

Stoica, G., Koestner, A., and Capen, C.C. (1983b). Characterization of N-ethyl-N-nitrosourea-induced mammary tumors in the rat. Am J Pathol *110*, 161-169.

Stoica, G., Koestner, A., and Capen, C.C. (1984). Neoplasms induced with high single doses of N-ethyl-N-nitrosourea in 30-day-old Sprague-Dawley rats, with special emphasis on mammary neoplasia. Anticancer research *4*, 5-12.

Thomas, A.D., Jenkins, G.J., Kaina, B., Bodger, O.G., Tomaszowski, K.H., Lewis, P.D., Doak, S.H., and Johnson, G.E. (2013). Influence of DNA repair on nonlinear dose-responses for mutation. Toxicological sciences : an official journal of the Society of Toxicology *132*, 87-95.

Tsubura, A., Lai, Y.C., Miki, H., Sasaki, T., Uehara, N., Yuri, T., and Yoshizawa, K. (2011). Review: Animal models of N-Methyl-N-nitrosourea-induced mammary cancer and retinal degeneration with special emphasis on therapeutic trials. In Vivo *25*, 11-22.

Zhang, L.H., and Jenssen, D. (1991). Site specificity of N-methyl-N-nitrosourea-induced transition mutations in the hprt gene. Carcinogenesis *12*, 1903-1909.

List of Publications:

Research articles

1. **Libi Anandi, V.,** Chakravarty, V., Ashiq, K.A., Bodakuntla, S., and Lahiri, M. A central role for DNA-PK activation in transformation of breast epithelial cells following MNU-induced DNA damage. ***(Manuscript submitted)***
2. **Anandi V Libi**, Ashiq, Nitheesh, Lahiri. Platelet-activating factor promotes motility in breast cancer cells and disrupts non-transformed breast acinar structures. ***Oncology Reports.*** 2016;35(1):179-88.
3. Bodakuntla, S., **Anandi V, Libi**., Sural, S., Trivedi, P and Lahiri, M. (2014) N-nitroso-N-ethylurea activates DNA damage surveillance pathways and induces transformation in mammalian cells. **BMC Cancer** 14 (1): 287. doi:10.1186/1471-2407-14-287.

Review articles

1. **Anandi, L.,** Chakravarty, V. and Lahiri, M. (2016) Investigating two Hallmarks of Cancer - Genome Instability and Tumor Promoting Inflammation. **Indian Society of Cell Biology Newsletter** 35 (2):ISSN: 2349:8307
2. **Libi Anandi, V** and Lahiri,M. Platelet activating factor leads to initiation and promotion of breast cancer. ***Cancer cell and microenvironment.*** 3 (3): e1370 *(Invited Research highlights)*.

TABLE OF CONTENTS

DECLARATION……...iii

ACKNOWLEDGEMENT……v

SYNOPSIS……..……..viii

TABLE OF CONTENTS 1

ABBREVIATIONS 10

ABSTRACT 12

Chapter 1: INTRODUCTION 13

1.1 Breast Cancer 14

1.2 Breast Cancer risk factors 16

1.3 Breast cancer progression 18

1.4 Models of breast cancer 20

1.5 Hallmarks of cancer: The “enabling characteristics” 25

Chapter 2: MATERIALS AND METHODS 33

2.1 Cell lines and culture conditions 34

2.2 Chemicals and antibodies 34

2.3 3D “on top” cultures 35

2.4 Drug treatments 36

2.5 Dissociating cells from 3D cultures 39

2.6 Immunofluorescence of 3D “on top” cultures 39

2.7 Single gel electrophoresis (Comet Assay). 40

2.8 Immunoblot analysis 41

2.9 MTT based cytotoxicity assay 42

2.10 RNA Extraction and cDNA preparation 42

2.11 ts045-VSVG-GFP intracellular trafficking assay 43

2.12 RUSH (Retention using Selective Hook) Assay. 44

2.13 Wound healing Assay..... 45

2.14 Single cell migration assay..... 45

2.15 Collagen Matrigel assay 46

2.16 DQ collagen Invasion Assay..... 46

2.17 Gelatin Zymography..... 46

2.18 Soft agar assay 47

2.19 Microtubule dynamics using EGFP-EB3 48

2.20 Cloning of Api5 into mCherry-CSII-EF-MCS vector..... 48

2.21 Lentiviral production and stable cell line preparation:..... 49

2.22 Statistical Analysis..... 50

Chapter 3: Alkylation damage induces transformation 51

3.1 Background 52

3.2 Results 53

3.2.1 MCF10A cells, when grown on Matrigel™, formed polarized growth arrested spheroids with a monolayer of cells enclosing a hollow lumen. 53

3.2.2 MNU induced DNA damage and affected acinar morphology. 56

3.2.3 Exposure to MNU disrupted baso-lateral polarity. 61

3.2.4 MNU treatment disrupts apical polarity. ,..... 68

3.2.5 MNU treatment impaired intracellular trafficking. 71

3.2.6 MCF10A cells upon exposure to MNU induced Epithelial to Mesenchymal transition. 75

3.2.7 MNU exposure induces migration at the single cell level. 78

3.2.8 MNU treatment induces invasion. 81

3.2.9 Exposure of MCF10A cells, grown as 3D cultures, to MNU during initial days of morphogenesis results in transformation. 84

3.2.10 DNA-PK mediates methylation damage induced Golgi dispersal. 86

3.2.11 DNA-PK activation plays a central role in MNU damage induced transformation. 94

3.2.12 Exposure to NEU *(N*-ethyl-*N* nitrosourea*),* an ethylating agent disrupts basolateral polarity and induces EMT-like phenotype similar to methylating agent. 100

3.3 Discussion 103

Chapter 4: Methylation damage re-organizes the cytoskeleton 108

4.1 Background 109

4.2 Results 109

4.2.1 MNU treatment results in reorganization of microtubules. 109

4.2.2 MNU treatment stabilized microtubules. 113

4.2.3 MNU treatment induced reorganization of microtubules was mediated via actin. 116

4.2.4 MNU treatment induced re-organization of microtubules was mediated by DNA-PK. 119

4.3 Discussion 127

Chapter 5: Api5 over-expression results in phenotypic transformation ... 131
5.1 Background 132
5.2 Results 134
5.2.1 Generation of stable cell line of MCF10A over-expressing Api5..... 134
5.2.2 Api5 over-expression in MCF10A cells induces enhanced cellular proliferation. 137
5.2.3 Api5 over-expression disrupts apico-basal polarity and adherens junctions. 140
5.2.4 Api5 over-expression results in the formation of abnormal structures indicative of EMT-like phenotype. 143
5.3 Discussion 146
Chapter 6: Prolonged exposure to PAF induces phenotypic transformation. 149
6.1 Background 150
6.2 Results 151
6.2.1 MCF10A cells express low levels of PAF-R as compared to malignant cells. 151
6.2.2 PAF induces enhanced cellular proliferation in 3D spheroid cultures. ... 153
6.2.3 PAF exposure induced EMT-like phenotype. 156
6.2.4 PAF exposure disupts basolateral and apical polarity. 158
6.3 Discussion 161
Chapter 7: Conclusion and Future perspectives 166
BIBLIOGRAPHY 176

APPENDIX 199
Appendix I: Media composition 199
Appendix II: Buffers for Immunofluorescence: 200
Appendix III: Buffers for Immunoblotting 202
Appendix IV: Buffers and staining solution for Gelatin Zymograph 203
Appendix V: Cloning of Api5 into CSII-EF-MCS 204
PUBLICATIONS 207
List of Publications: 208
Research articles 208
Review articles 208
Collaborative research articles 208

TABLE OF FIGURES

Figure 1.1: Cancer fact sheet worldwide. 14

Figure 1.2: Age shift in Indian women. 16

Figure 1.3: Morphology of breast cancer progression. 19

Figure 1.4: Schematic showing the process of morphogenesis of breast epithelial cells. 22

Figure 1.5: Different acinar phenotypes observed upon transformation. 24

Figure 1.6: Hallmarks of cancer. 26

Figure 1.7: Cell fate following DNA damage. 28

Figure 1.8: Tumor microenvironment and its components. 30

Figure 2.1: Diagramatic representation of different drug treatments. 37

Figure 2.2: Schematic representing the dosing schedule of different chemicals to study effect of DNA damage on cytoskeleton. 38

Figure 3.1: Representative confocal images of MCF10A acinus. 54

Figure 3.2: MCF10A cells grown on Matrigel^{TM} were polarized. 55

Figure 3.3:Sub-lethal dose of MNU induces DNA damage in MCF10A cells. 58

Figure 3.4: MNU treatment resulted in increase in nuclear volume. 60

Figure 3.5: MCF10A cells lose basal polarity upon exposure to methylating agent. 62

Figure 3.6: Loss of α6-integrin from the basal region of MCF10A acinar cultures upon exposure to methylating agent is not transient. 64

Figure 3.7: Methylation damage results in loss in integrity of adherens junctions. 65

Figure 3.8: Methylation damage results in loss in integrity of adherens junctions 67

Figure 3.9: Apical polarity was lost and Golgi morphology disrupted in cells exposed to methylation damage..... 69

Figure 3.10: MNU damage impaired Golgi to plasma membrane trafficking. 72

Figure 3.11: MNU damage impaired ER to Golgi membrane trafficking. 74

Figure 3.12: Methylation damage induced EMT in MCF10A cells grown as 3D “on top” cultures..... 76

Figure 3.13: Methylation damage induces migration at the single cell level. 79

Figure 3.14: Methylation damage induces invasiveness in MCF10A cells. 82

Figure 3.15: MNU treated cells show enhanced survival in anchorage independent conditions. 85

Figure 3.16: MNU induced DNA damage activates DNA-PKcs which in turn results in Golgi dispersal. 87

Figure 3.17: MNU induced activation of DNA-PK. 89

Figure 3.18: MNU induced Golgi dispersal is via activation of DNA-PK. 90

Figure 3.19: Golgi dispersal observed in MCF10A series is partially reversed following DNA-PK inhibition..... 92

Figure 3.20: DNA-PK plays a role in methylation damage induced EMT..... 95

Figure 3.21: MNU induced migration is inhibited by DNA-PK inhibition..... 96

Figure 3.22: DNA-PK inhibition inhibited invasiveness of MNU treated cells..... 98

Figure 3.23: DNA-PK inhibition results in reduced ability of cells to survive in anchorage independent conditions..... 99

Figure 3.24: NEU exposure disrupts basolateral polarity and induces EMT-like phenotype..... 101

Figure 3.25: Schematic showing the mechanism of MNU-induced transformation. 107

Figure. 4.1: Methylation damage results in up-regulation of α-tubulin in spheroid cultures. 111

Figure 4.2: Exposure of MCF10A cells to MNU re-organizes microtubules 112

Figure 4.3: MNU treatment stabilizes microtubules. 114

Figure 4.4: Methylation damage slows down microtubule dynamics. 115

Figure 4.5: MNU induced microtubule reorganization was actin dependent. 117

Figure 4.6: Methylation damage induced microtubule re-organization is reversed upon DNA-PK inhibition. 121

Figure 4.7: Methylation damage induced persistent microtubule re-organization is reversed upon DNA-PK inhibition. 122

Figure 4.8:Methylation damage induced actin re-organisation is dependent on DNA-PK, JNK and Akt. 123

Figure 4.9: Methylation damage induced microtubule re-organisation is through JNK and Akt. 125

Figure 4.10: Schematic depicting the effect of DNA damge on the cytoskeleton. 130

Figure 5.1: Api5 and TopBP1 are over-expressed following methylation damage. 133

Figure 5.2: Generation of MCF10A cell line over-expressing Api5. 135

Figure 5.3: Api5 over-expression induces enhanced cellular proliferation. 138

Figure 5.4: Api5 over expression disrupts basolateral and apical polarity. 142

Figure 5.5: Api5 over-expression induced EMT-like phenotype..... 144

Figure 6.1: PAF-R expression levels. 152

Figure 6.2: PAF induces enhanced cellular proliferation in MCF10A spheroids. 154

Figure 6.3: PAF exposure results in EMT in MCF10A cells grown as 3D 'on top' cultures. 157

Figure 6.4: Prolonged exposure to PAF resulted in disruption of apico-basal polarity. 159

Figure 6.5: Prolonged exposure of MCF10A cells to PAF disrupts adherens junctions. 160

Figure 6.6: Schematic summarizing the phenotypic transformation phenotypes induced by continuous exposure to PAF. 164

Figure 7.1: Plausible pathways for DNA damage induced transformation. 169

Figure 7.2: Schematic depicting the various phenotypes observed in 3-D “on top” cultures following API5 over-expression. 171

Figure 7.3: Schematic depicting the plausible pathway involved in re-organization of cytoskeleton following DNA damage. 173

Figure 7.4: Plausible pathway of PAF induced transformation predicted based on literature. 175

ABBREVIATIONS

2D	2-dimensional
3D-cultures	3-dimentional cultures
ADH	Atypical Ductal Hyperplasia
CFSE	Carboxyfluorescein succinimidyl ester
CIP	Calf Intestinal Phosphatase
CTCF	Corrected Total Cell Fluorescence
DCIS	Ductal Carcinoma in situ
DDR	DNA Damage Response
DMBA	7,12-Dimethylbenzanthracene
DMNB	4,5-Dimethoxy-2-nitrobenzaldehyde
DMSO	Dimethyl sulfoxide
DSB	Double Strand Breaks
EGF	Epidermal Growth Factor
EMT	Epithelial to Mesenchymal Transition
ERM	Ezrin/Radixin/Moesin
FAK	Focal adhesion kinase
hDlg	human homologue of Drosophila discs large
IDC	Invasive Ductal Carcinoma
IMC	Invasive Mammary Carcinoma
LPA	Lysophosphatidic acid
MAP	Microtubule Associated Proteins
MAPK	Mitogen Activated Protein Kinases
MMP	Matrix metaloproteases
MNU	N-nitroso-N-methylurea
MTT	thiazolyl blue tetrazolium bromide
NEU	N-ethyl N-nitrosourea
NHEJ	Non-homologous end joining
NNK	Nicotine-derived nitrosamine ketone
NNN	N- Nitrosonornicotine
PAF	Platelet activating factor
PAF-AH	Platelet Activating Factor Acetyl hydrolase
PBS	Phosphate buffer saline
PCR	Polymerase Chain Reaction
PFA	Paraformaldehyde
PI3K	Phospho inositol-3- kinase
PVDF	P-polyvinylidene difluoride
RT	Room Temperature
RUSH	Retention using Selective Hook
SDS-PAGE	Sodium Dodecyl Sulphate-Polyacrylamide Gel Electrophoresis

SSB	Single Strand Breaks
SKY	Spectral Karyotyping
SBP	Streptavidin Binding Protein
TBS-T	Tris buffered saline-Tween
TDLUs	Terminal duct lobular units
vsvg	Vesicular Stomatitis Virus G

ABSTRACT

Breast cancer, on a global scale, is the leading cause of death in women. Interestingly approximately only 15% cases are due to inherited mutations. Thus, implying that there are various other factors that contribute to the development as well as progression of cancer. Hanahan and Weinberg, report genomic instability and tumor promoting inflammation as the characteristics that enable cells to acquire the hallmarks of cancer. DNA damage by various agents (exogenous as well as endogenous) is known to result in genomic instability. One such class of compounds is the alkylating agents, which is widely used in cancer chemotherapy as well as present in environmental pollutants. On the other hand, inflammation results in accumulation of bioactive molecules in the cellular microenvironment. PAF, Platelet Activating Factor, is one such molecule secreted by the cells of the immune system. We have studied the effects of alkylating agents (MNU, *N*-methyl-*N*- nitrosourea and NEU, *N*-ethyl-*N*-nitrosourea) as well as PAF on breast epithelial cells using 3D cultures as a model system. We observe that exposure of mammary epithelial cells to alkylating agents or PAF induces epithelial-mesenchymal transition (EMT)-like phenotype along with disruption of the basolateral polarity. Attempt to decipher the mechanism of methylation damage induced transformation revealed the central role played by DNA-PK. Interestingly, we observed that methylation damage resulted in stabilization of microtubules and this effect was also found to be mediated by DNA-PK.

In conclusion, this study provides evidences for the carcinogenic potential of alkylating agents as well as reports the ability of PAF to induce phenotypic transformation in breast epithelial cells.

Chapter 1: INTRODUCTION

1.1 Breast Cancer

With an estimated 1.67 million cases newly reported, breast cancer is the second most common cancer in the world. Worldwide cancer statistics taken in 2012 reveals that breast cancer accounting for 25.2% of all new cases in women is the most common cancer diagnosed among women and contributes to about 13.7% of all cancer deaths (Figure 1.1).

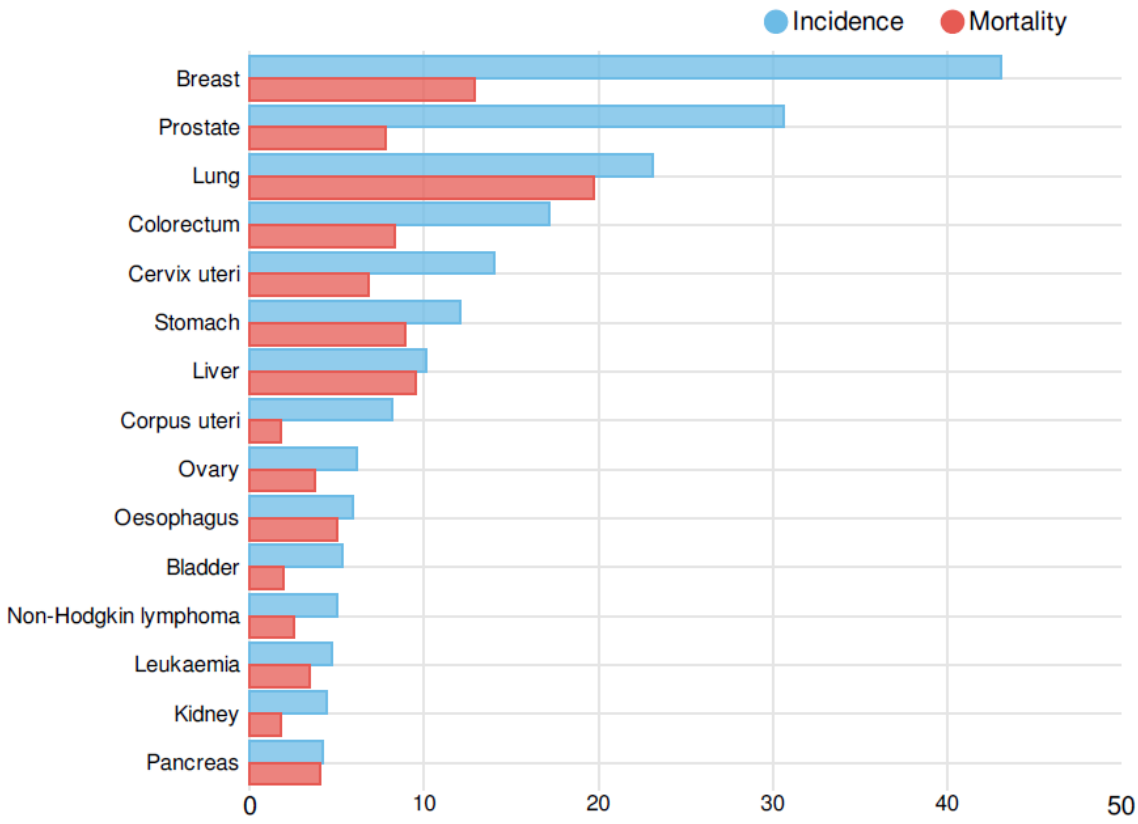

Figure 1.1: Cancer fact sheet worldwide.

The histogram indicates the incidence (blue) and mortality (pink) rates of various cancers wherein breast cancer holds the maximum percentage of incidence and second highest mortality rate worldwide. *(Reproduced from GLOBOCAN 2012)*

In underdeveloped and developing countries, breast cancer has been reported to be the most frequent cause of death, while in developed countries it is the second frequent cause of death. In India, breast cancer is the second most frequently occurring cancer as well as cause for cancer related deaths. In major cities in India, according to the National Cancer Registry program, breast cancer accounts to 25% to 32% of all female cancer cases reported (Agarwal and Ramakant, 2008). The Globocan report released in 2012 estimates 144,937 new cases of breast cancer among Indian women and 70,218 deaths implying that 1 in every 2 women suffering from breast cancer dies of the disease. Recently, a change in the trend of breast cancer occurrence has been observed in India. Apart from the rampant increase in incidence and mortality, there appears to be a shift in the age of occurrence of the disease. The average age of occurrence of breast cancer has been 50-60 years in most of the western countries. In India, over the past few decades there appears to be a shift in the age of disease onset (40-50 years) with more of the younger women getting affected (Chopra et al., 2014) (Figure 1.2). In addition to this, these cancers appear to be more aggressive than the postmenopausal cases. In India, 45.7% of newly diagnosed cases are reported in advanced stages in contrast to that in western countries where the cases reported are in Stage I and stage II. The changing trends in breast cancer incidence and mortality have been attributed to the modernization of women in the urban areas as well as the lack of awareness and screening at early stages. To this end, awareness programs are being conducted to aid in early detection and reduce mortality.

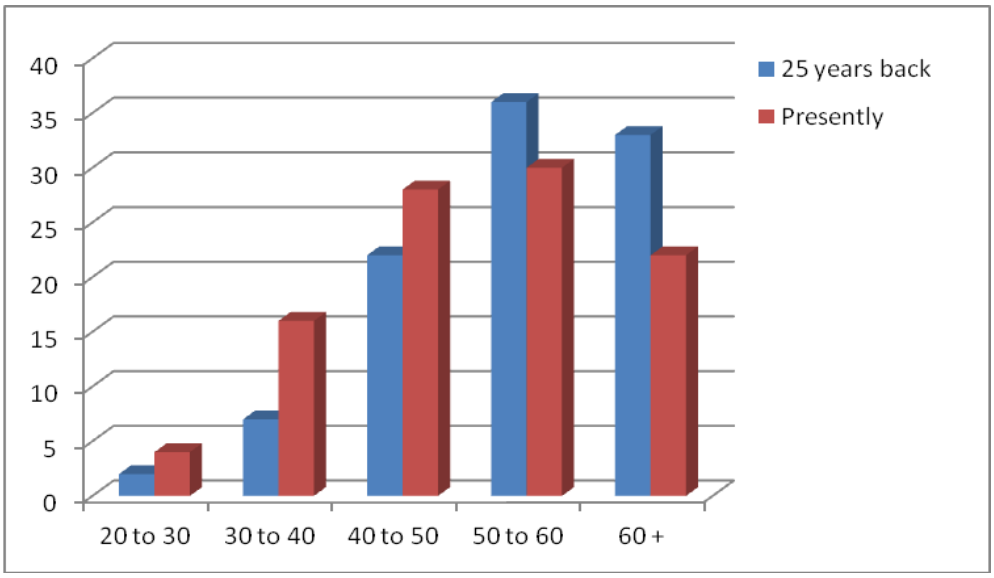

Figure 1.2: Age shift in Indian women.

The bar graph indicates the early onset of breast cancer in Indian women thus implying an age shift of the incidence of disease. *(Reproduced from National Cancer Registry 2011).*

1.2 Breast Cancer risk factors

Women generally are at high risk of developing breast cancer. The various risk factors include but are not limited to, gender, hereditary mutations, early menarche and/or late menopause, nulliparity, late first pregnancy, hormonal therapy, lack of breastfeeding, radiation exposure, dietary factors, sedentary lifestyle, obesity and alcohol intake (Aich et al., 2016; Mustafa et al., 2013). Hereditary mutations refer to mutations in genes which are inherited in an autosomal dominant manner. BRCA1 and BRCA2 germline mutations contribute to a major proportion (20-25%) of hereditary cancers (Ford and Easton, 1995). However, hereditary breast cancers account for only 5% of the total case (Martin and Weber, 2000). Approximately 80% breast cancer patients have no history of breast cancer in their family (Cancer, 2001). Early menarche (less than 12 years) and late menopause (more than 55years) contribute to the risk of developing breast cancer, mainly due to the increased duration of exposure to estrogen during one's life time (Helmrich et al., 1983; Henderson et al., 1988). Nulliparity

has also been associated with increased risk of breast cancer. In addition to this, age of the mother at first pregnancy has also been found to be associated with breast cancer risk. First full time pregnancy before 30-35 years of age poses a lower risk as compared to after 30-35 years. However, the basis for such association is not very clear. Apart from this, women who have had multiple pregnancies are at lower risk as compared to single pregnancy (Helmrich et al., 1983). Hormone replacement therapy (estrogen) taken for a longer duration in postmenopausal women has been associated with increased risk of breast cancer (Porch et al., 2002). On the contrary, oral contraceptives have not been clearly associated with increased risk (Marchbanks et al., 2002). Dietary factors have been shown to have a controversial role in altering the risk of breast cancer. Most of the cases which relate high fat diet to increased risk of cancer reveal that the increased risk is mainly due to obesity and not due to fat in the body. Obesity has been related to breast cancer risk in postmenopausal women (Brown and Allen, 2002; Hirose et al., 2001). Fat cells are known to secrete some estrogen and hence obesity posed risk probably is related to estrogen production. Apart from this physical activity has been consistently linked with breast cancer risk, with women having a sedentary lifestyle being at higher risk of developing cancer as compared to physically active women (Bernstein et al., 1994; Friedenreich et al., 2001). Exposure to high dose radiations during adolescence has been shown to have increased chances of developing breast cancer (Preston et al., 2002). Association between smoking, as well as, alcohol consumption and breast cancer risk are still debatable. There are contradictory reports for the same. However, smoking is known to promote progression of breast cancer (Atkinson, 2003; Chen et al., 2002; Palmer and Rosenberg, 1993). In addition to cigarette smoke exposure to various environmental chemicals such as phthalates (Lopez-Carrillo et al., 2010), Polycyclic aromatic hydrocarbons (Bonner et al., 2005), parabens (Darbre et al., 2004), zeranol (Zhong et al., 2011) have also been demonstrated to increase the risk of developing breast cancer.

1.3 Breast cancer progression

Breast cancer originates in the epithelial cells lining the terminal duct lobular units. It has been known to progress through three different stages namely, ADH (atypical ductal hyperplasia), DCIS (Ductal carcinoma in situ) and finally the IMC (invasive mammary carcinoma) or IDC (Invasive ductal carcinoma), however, the progression not always being in the linear fashion. Nevertheless classifying the stages based on their histological pattern serves as a vital indicator of the possible molecular events which are driving the progression (Polyak, 2008). ADH has been found to develop from the stem cells of the terminal duct lobular units (TDLUs). It is characterized by the partially filled breast duct comprising two epithelial cell types, one of them appearing to be more of the normal kind and the other which may be neoplastic (Allred et al., 2008; Arpino et al., 2005; Page and Dupont, 1993; Page et al., 1985; Wellings and Jensen, 1973). ADH may develop into DCIS which is characterized by neoplastic cells filled in the breast duct. Further this stage becomes invasive (IMC) and results in metastasis at different sites in the body (Allred et al., 2001; Allred et al., 2008; Arpino et al., 2005; Bodian et al., 1993; Carter et al., 1988; Dupont et al., 1993) (Figure 1.3). IDC accounts for almost 20 to 30% of all newly diagnosed cases of breast cancer(Tang et al., 2007).

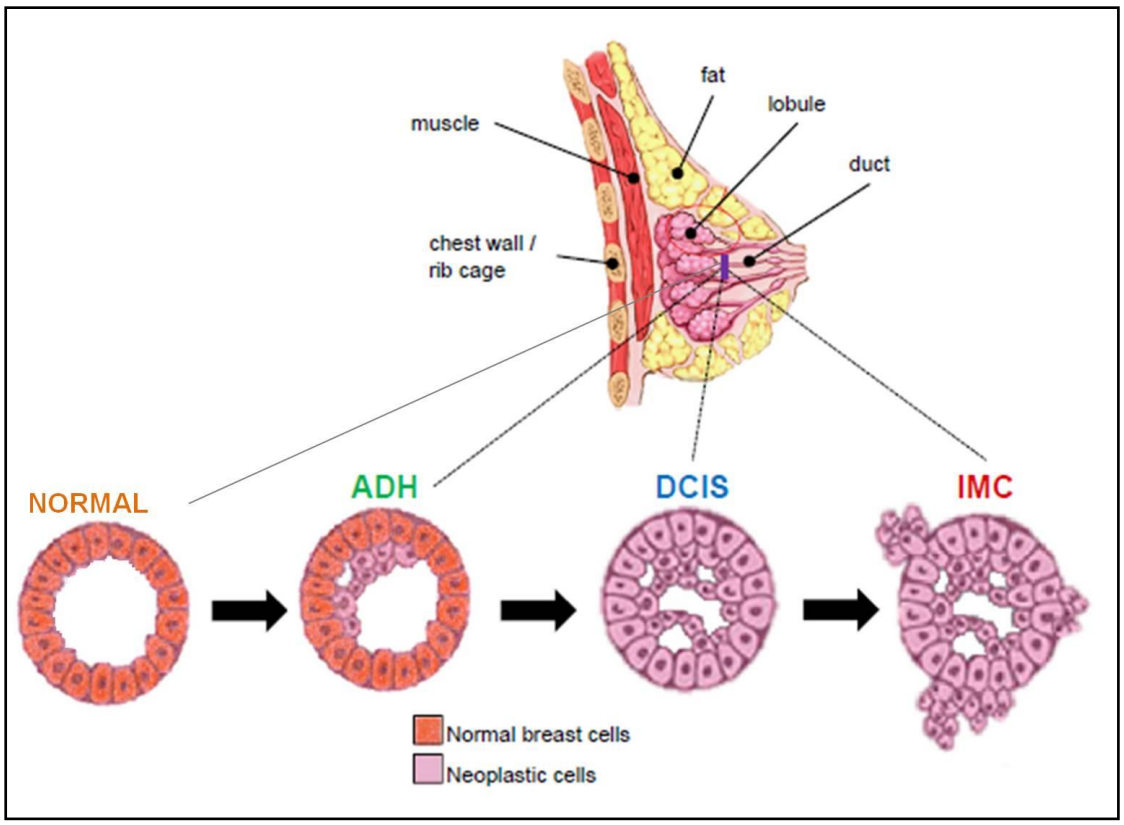

Figure 1.3: Morphology of breast cancer progression.

Pictorial representation of the various morphologies acquired during the progression of breast cancer. The anatomy of breast lobule is enlarged showing the normal acinar morphology and the altered morphologies in case of different breast cancer types (ADH, DCIS, and IMC). *(Adapted from www. breastcancer.org)*

1.4 Models of breast cancer

To study the progression of breast cancer, several models have been developed to date. Breast cancer being extremely heterogeneous, it is very difficult to have a single model to completely recapitulate the disease condition. The establishment of a perfect model to recapitulate such a complex disease is the major challenge at present as none of the available models are able to achieve this (Vargo-Gogola and Rosen, 2007) The selection of a model depends on the hypothesis under investigation and the experimental design.
The commonly used models are herewith listed:

1. *In vivo* models
    a. Chemically induced models;
    b. Genetically Engineered Mice such as transgenics and knockouts;
    c. Xenograft models.
2. *In vitro* models
    a. 2 Dimensional cell cultures or Monolayer culture
    b. 3 Dimensional cell cultures

Each model in its own way has provided valuable insights with regards to cancer biology and paved a way for improvement of the models to mimic the actual disease condition. Rodent models since long have been serving as a valuable tool to study the cellular and molecular aspects of breast tumorigenesis *in vivo*. The established cell lines have till date provided unparalleled insights into the deregulation of cellular machinery during cancer progression. The establishment of 3D-cultures of non-transformed breast epithelial cells and cancerous cells have greatly helped to mimic the *in vivo* conditions *in vitro* and thus has developed into an invaluable tool to delineate the complex interactions occurring within the cells either cancerous or normal and study the effects of genes on the morphology and hence their role in neoplastic transformation. Integrating the existing model systems and using a multi-model system to the betterment would probably serve as a powerful tool to clearly understand the many unanswered

and intriguing questions and thus guide us towards developing novel therapeutics against breast cancer to benefit mankind.

3-dimensional cultures as a model system

Epithelial tissues are widely distributed in the body and perform various specialized functions (Royer and Lu, 2011). These functions have been attributed to the distinct structural organization of these cells within the tissues; this implies that a higher order regulation is imposed by the three dimensional organization of epithelial cells (Dow and Humbert, 2007). This architecture is crucial and the maintenance of its integrity is known to inhibit transformation (Bissell and Radisky, 2001). Most of the human cancers are of epithelial origin (Royer and Lu, 2011) and frequently exhibit disrupted structural organization, thus, demonstrating the importance of tissue architecture and its maintenance in tissue homeostasis (Bissell et al., 1999; Debnath et al., 2003) . Consequently, understanding cancer initiation and progression calls for studying different genes in a functional context rather than studying them individually (Knox, 2010). However, studying genes by manipulating those *in vivo* (animal models) though maintains the functional context but is also cumbersome and poses challenges in tractability. Although enormous information has been gained over the years from 2D cultures, the system lacks the three-dimensional organization as well as many of the crucial micro-environmental cues that are present raising questions over its relevance to *in vivo* scenario (Vargo-Gogola and Rosen, 2007). Recently the concept of three dimensional (3D) cultures has emerged as a powerful tool to study the progression of cancer, wherein the non-malignant breast epithelial cells are grown on a reconstituted basement membrane (Debnath et al., 2003). These cells, from an unpolarized proliferating state undergo differentiation to form polarized growth arrested spheroids (in G_0-G_1phase) at the end of 16 days (Fournier et al., 2006). This process is termed as “morphogenesis” and consists of an orchestra of tightly regulated events represented in the schematic (Figure 1.4): The cells seeded on the extracellular matrix proliferate to form a sphere; cells in the centre undergo apoptosis to form

a lumen while remaining cells in the sphere exhibit polarity characterized by basal surface in contact with the ECM; an apical surface which faces the lumen and intact cell-cell junctions comprising lateral surface (Debnath et al., 2003).

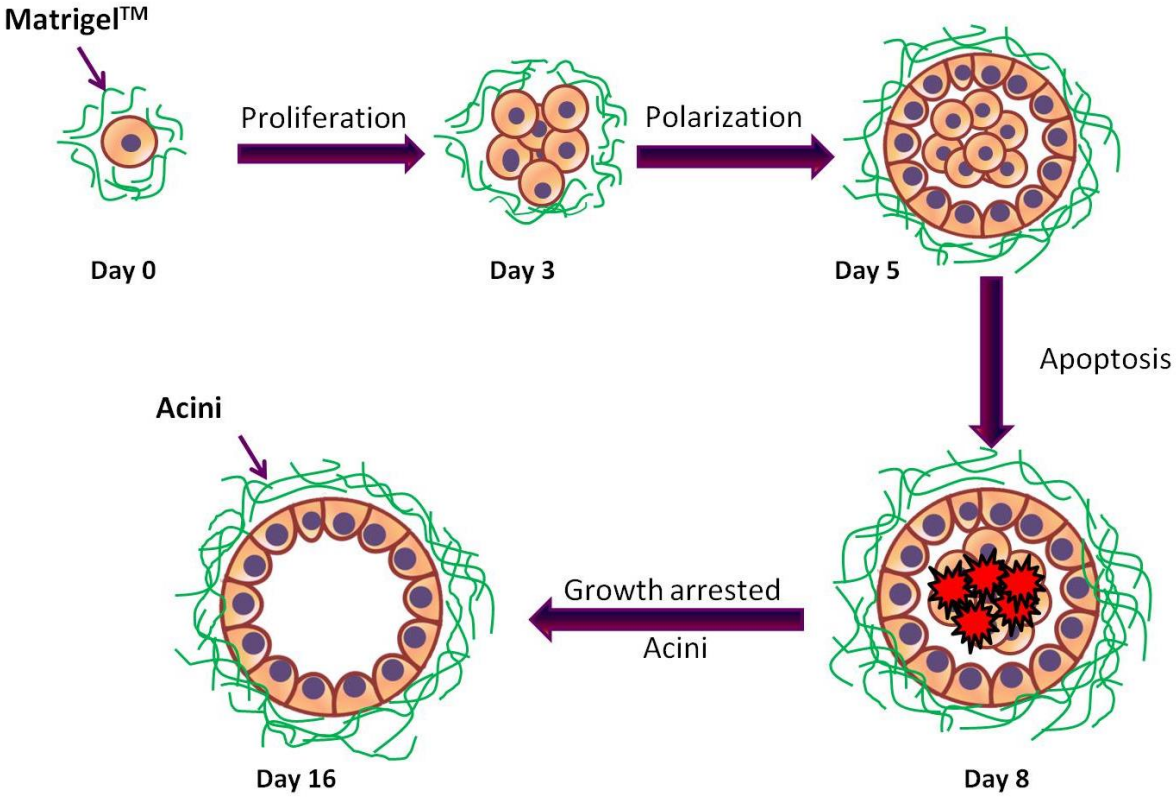

Figure 1.4: Schematic showing the process of morphogenesis of breast epithelial cells.

A single breast epithelial cell when seeded on a bed of laminin rich extracellular matrix, for example Matrigel™ undergoes proliferation and by day 5 leads to the formation of two groups of cells, an outer layer of polarized cells that encloses a cluster of un-polarized cells in the centre. This inner mass of cells eventually undergoes apoptosis by day 8 eventually resulting in the formation of a growth arrested spheroid, called “acini” by day 16, which is characterized by a monolayer of polarized epithelial cells enclosing a hollow lumen.

These spheroids, termed as ‘acini’, closely resemble the acini structures, the smallest functional unit in mammary glands in vivo (Vidi et al., 2013). The disruption of the well-formed polarized architecture is seen in the early stages of breast cancer (Dey et al., 2009). The transformed cells form acini with varied phenotypes (Debnath and Brugge, 2005; Debnath et al., 2003) as depicted in Figure 1.5. The role of genes that influence various features such as the apico-basal polarization, proliferation, invasion, metastasis, apoptosis can be discerned through the differences in the morphology induced by their presence or absence (Debnath et al., 2003). The acinar structures formed by the epithelial cells, can thus, aid in distinguishing the normal and transformed phenotype which is difficult to distinguish in two dimensional (2D) cultures. This feature has thus, laid the foundation to build a platform to study the process of early transformation of breast epithelial cells. This technique can be well exploited to study the role of genes in morphogenesis as well as in breast epithelial cell transformation.

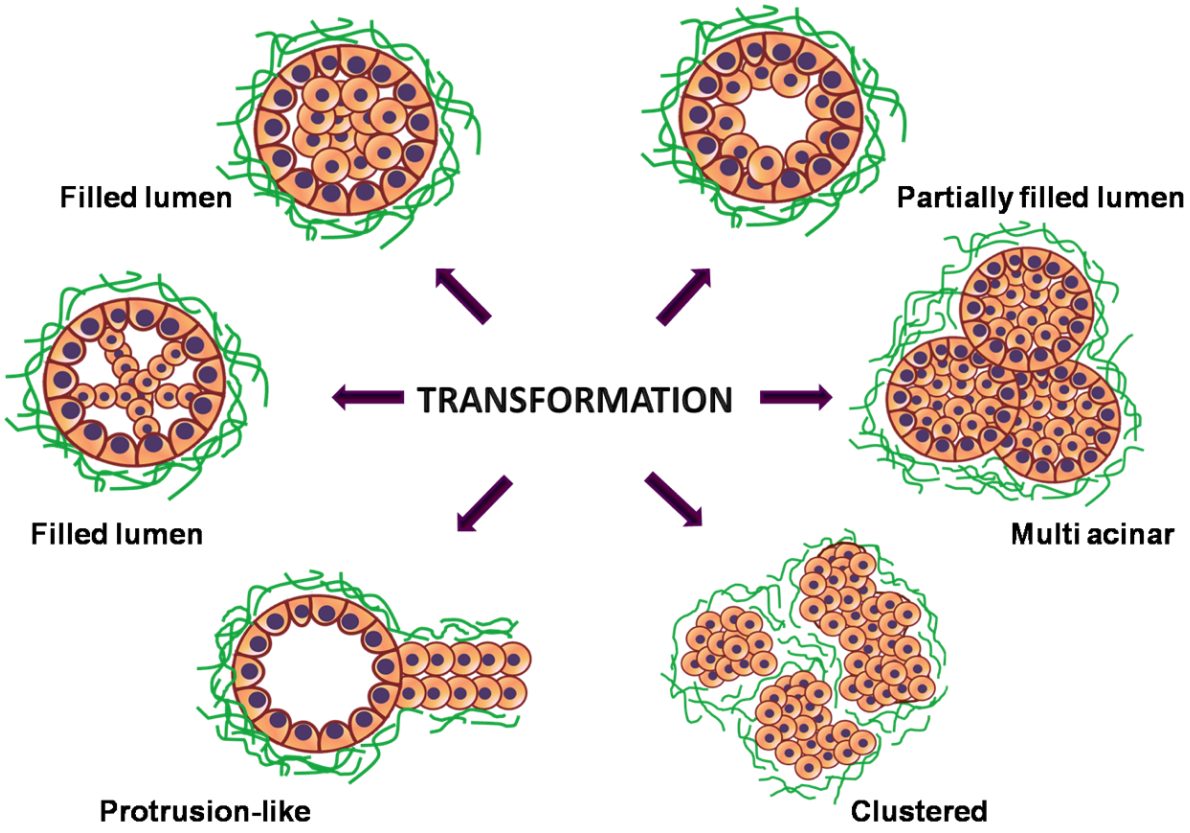

Figure 1.5: Different acinar phenotypes observed upon transformation. Schematic depicting different acinar morphologies observed in transformation. Each of these phenotypes are known to be relevant clinically and have been related to certain genetic signatures. *(Adapted from Debnath et al., 2005)*

The 3D cultures of MCF10A cells have been largely used to study the morphogenesis of breast epithelial cells, which has paved the way to develop models of breast cancer progression. On the same lines, using the MCF10A series of cell lines, a model has been developed in 3-dimensional culture systems which are expected to mimic the progression of breast cancer (Imbalzano et al., 2009). Weaver *et al.*, have modelled the effects of stromal rigidity on morphogenesis of breast epithelial cells, thus delineating the related signalling pathway involved in the process (Paszek et al., 2005). Also, breast cancer cells, grown in 3D culture were used to recognize an 'autocrine loop' which has been found to promote the proliferation of breast cancer cells as well as disrupt the architecture (Kenny and Bissell, 2007). Effects of cyclin D1 over-expression and ErbB2 activation on morphogenesis have been successfully studied using 3D cultures, which was not possible using monolayer cultures (Debnath et al., 2002; Muthuswamy et al., 2001). Effects of integrins, MAPK and PI3K pathways on reversing the cancerous phenotype have been established using 3D cultures (Wang et al., 2002). A novel conditional gene expression system has been developed by Herr *et al.* which permits for the study of sudden withdrawal or introduction of genes (either oncogene or tumor suppressor gene) on the morphology of the 3D structure. This model has been predicted to be a useful tool to study various phenomena such as epithelial to mesenchymal transition, the role of particular oncogenes and its effect on vital processes and drug resistance(Herr et al., 2011). Gilmore's group, using this model system, demonstrated the role activated FAK in tumorignesis which they illustrated was due to acquiring resistance to apoptosis (Walker et al., 2016). Role of various oncogenes and tumor suppressors have been well established using this model system.

1.5 Hallmarks of cancer: The "enabling characteristics"

Hanahan and Weinberg have listed certain capabilities which are acquired by cells during the process of tumor development (Figure 1.6). These characteristics provide the organizing principle to study the multistep, complex process of tumor

development. Apart from these characteristics, they also enlisted two characteristics such as “genomic instability and mutations” and “tumor promoting inflammation” as enabling characteristics, which can foster tumor development. The cells are endowed with genetic alterations mainly due to genomic instability induced either by exogenous or endogenous agents and thus, are driven towards tumor progression. On the other hand, immune system induced inflammation can result in tumor progression by promoting the acquisition of hallmark capabilities.

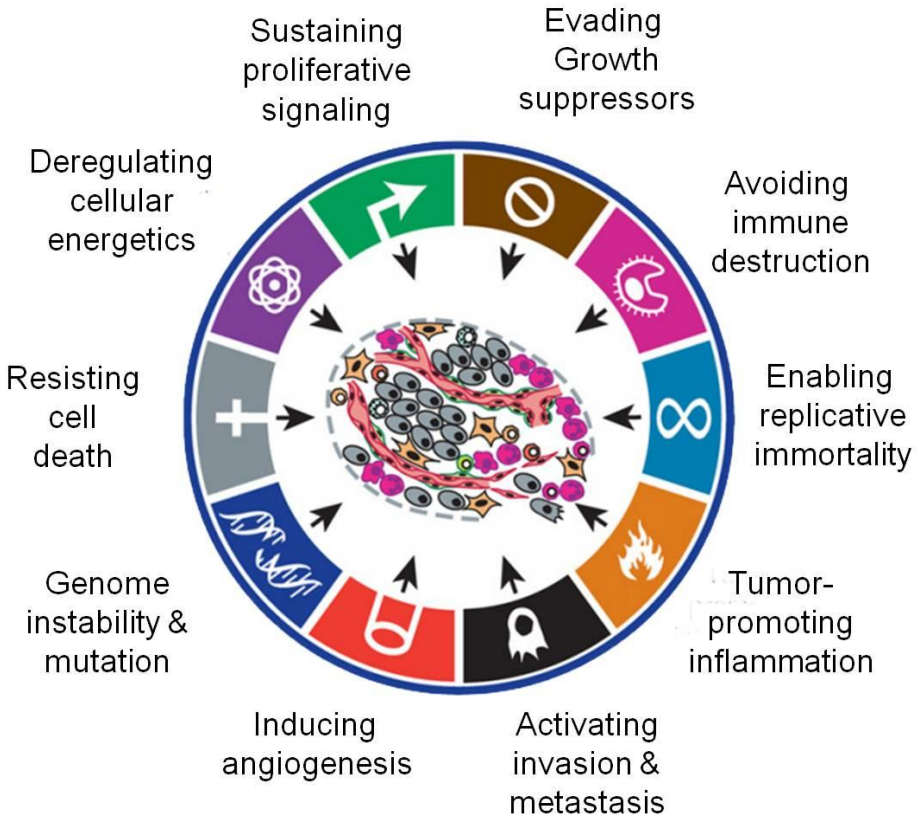

Figure 1.6: Hallmarks of cancer.

Diagramatic representation of the Hallmarks of cancer enlisted by Hanahan and Weinberg *reproduced from* (Hanahan and Weinberg, 2011).

Genomic instability and mutations

We are exposed to a large number of chemicals throughout our lifetime. About two third of the cancers in the United States has been attributed to such exposures. These include chemicals in environmental pollutants, cigarette

smoke, excessive consumption of alcohol, and excessive sunlight exposure as well as exposure to ionizing radiations such as X-rays, γ-rays, alpha particles. All these are potential DNA damaging agents. The cells in the human body (approximately 10^{13}) are predicted to receive DNA lesions occurring at the rate of tens of thousands of lesions per day. There are certain surveillance mechanisms evolved by the cells, commonly known as DNA damage response (DDR), which protect genomic integrity after DNA damage. The aberrant regulation of the DDR leads to genomic instability and results in various cell fates as depicted in Figure 1.7. DNA repair deficiency, mutation prone repair and hyperactive repair systems, lead to accumulation of DNA damage and is intimately related to cancer. The mammary tissue undergoes significant and extensive remodeling throughout a women's lifetime and the rate of proliferation, apoptosis and differentiation are also higher as compared to the other tissues in the body (McCready et al., 2010). Thus, it's susceptibility to the occurrence of DNA damage is higher than the other tissues. Cigarette smoke consists of nitrosoamines NNK (Nicotine-derived nitrosamine ketone) and NNN (*N*- Nitrosonornicotine) which are capable of methylating DNA and causing DNA damage. Chemicals like acridine dye, acriflavin, proflavin and many of the anti-cancer drugs are also capable of causing DNA damage (Crick et al., 1961; Sugino, 1966). Contaminated food or compounds with intrinsic endocrine disrupting capabilities like nonylphenol or factors related to aging (related to telomerase) are some other factors that may give rise to damage. In addition to this, the cancer chemotherapy and radiation therapy are a major source of DNA damage and hence a possible cause of cancer.

In addition to DNA insults induced by exogenous agents, DNA replication is error prone and may also be a reason to DNA mutations and hence a factor to induce cancer. Further, oncogene induced replication stress is considered as the hallmark of cancer (Bartek et al., 2012). Recent studies reveal that the activation of growth-signaling pathways which have been implicated in aging and also in the oxidative stress responses regulation causes DNA replication stress

(Bartkova et al., 2006; Di Micco et al., 2006; Gorgoulis et al., 2005). Replication stress accounts to gross DNA lesions and chromosomal abnormalities. It is hypothesized that replication stress causes chromosomal fragility by causing the destabilization or collapse of the replication forks at vulnerable sites (Feng et al., 2011), thus can endow genetic alterations resulting in cancer initiation and progression.

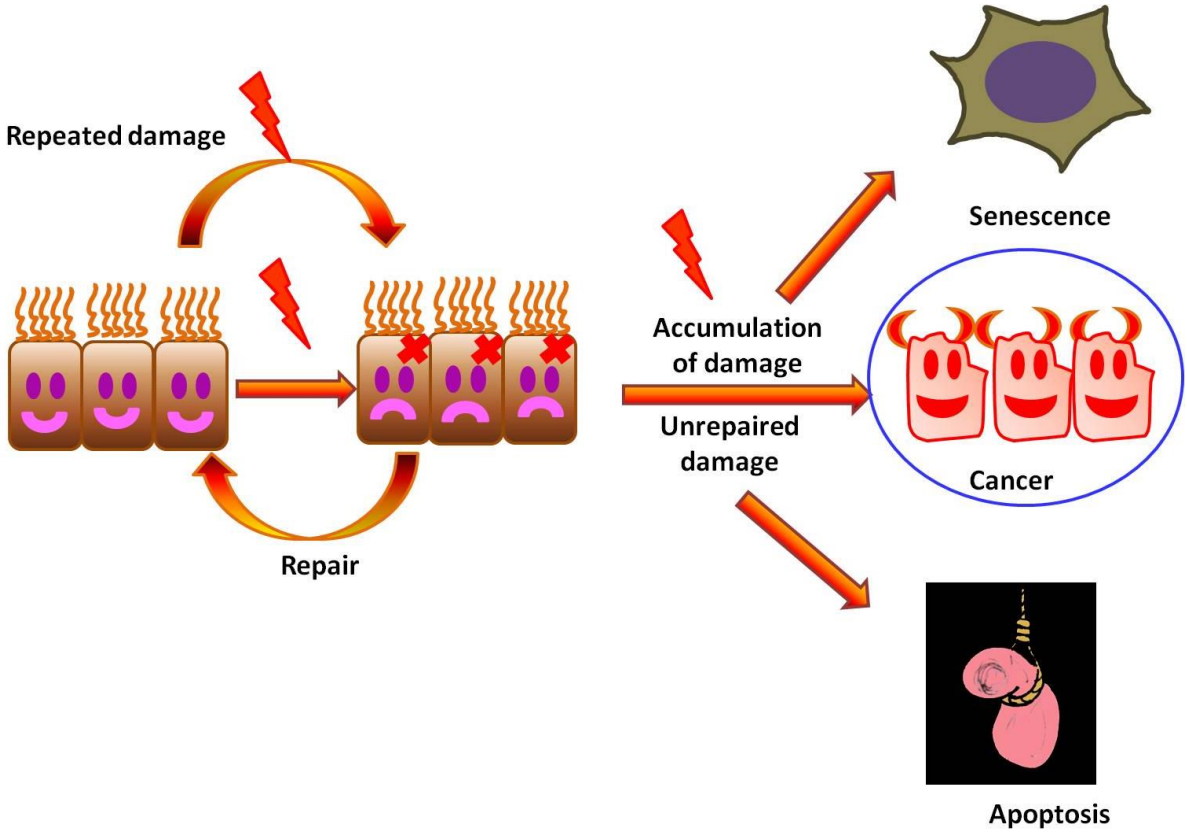

Figure 1.7: Cell fate following DNA damage.

Schematic showing the fate of cell when exposed to DNA damage. Accumulation of DNA damage may lead to three fates, either the cell becomes senescent or it becomes cancerous. If the damage remains unrepaired, it may undergo apoptosis.

Tumor promoting inflammation

Cellular microenvironment has now been reported to be one of the major factors contributing to tumor initiation and progression. Chronic inflammation has been shown to play a pivotal role in cancer initiation and progression. Macrophages and stromal cells secrete bioactive molecules such as cytokines, reactive oxygen species, nitrogen species as well as phospholipid mediators into the surrounding (Figure 1.8). Such a microenvironment is considered to be in an active state. Reactive oxygen and nitrogen compounds can attack DNA leading to chromosomal abnormalities (Cerutti, 1994) that affect various signal transduction pathway(s) (Schreck et al., 1992) or modulate the activity of the stress responsive proteins, genes that regulate cell proliferation, differentiation and apoptosis (Sarafian and Bredesen, 1994). Furthermore, phospholipid mediators such as prostaglandins, lysophosphatidic acid (LPA), Platelet activating factor (PAF) as well as Platelet activating factor-like lipids have been shown to play vital roles in many physiological and pathological conditions including cardiovascular homeostasis, inflammation and various cancer (Chao and Olson, 1993; Du et al., 2010; Prescott et al., 2000; Robert and Hunt, 2001; Ryan et al., 2007; Stafforini et al., 2003; Zhu et al., 2006). All these factors present in the tissue microenvironment can induce as well as promote tumorigenesis.

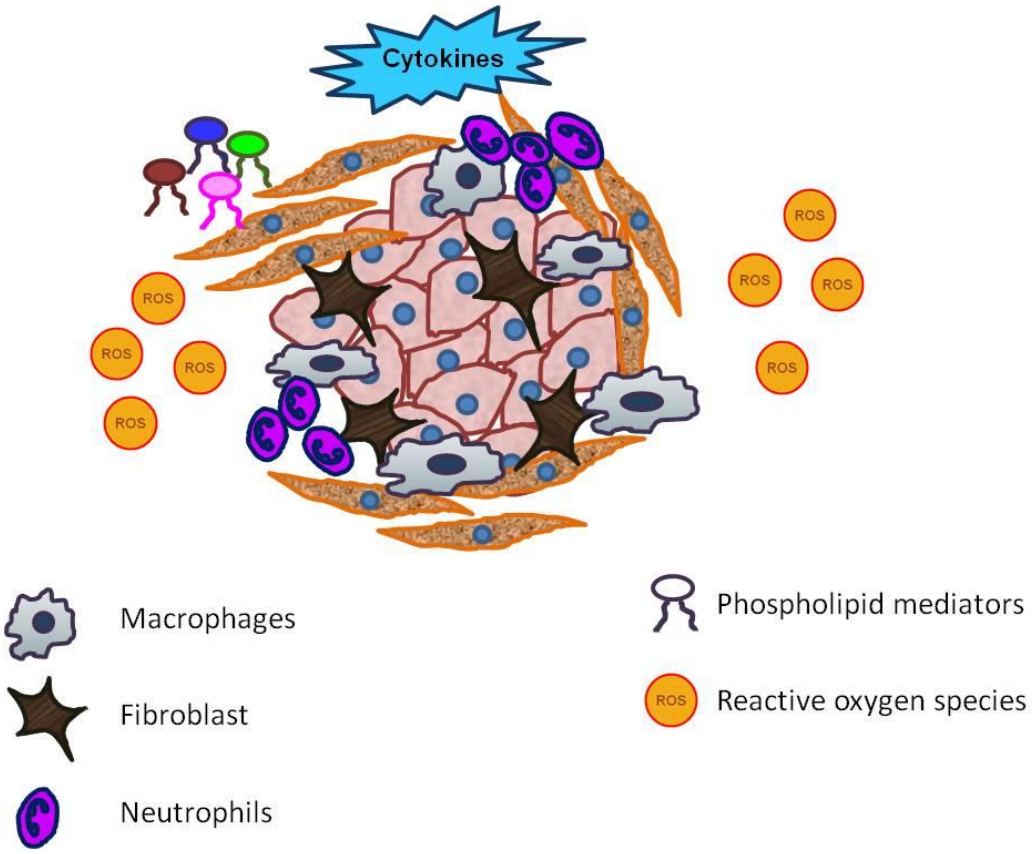

Figure 1.8: Tumor microenvironment and its components.

The tumor microenvironment is composed of several factors such as macrophages, cytokines, fibroblast, neutrophils, phospholipid mediators and reactive oxygen species (ROS) which promote inflammation and play an important role in the initiation and progression of cancer.

Scope of the study-

We have attempted to study the role of the two “enabling characteristics”- Genomic instability and tumor promoting inflammation The work presented in this thesis uses 3D culture of MCF10A cell line as the model system. MCF10A cell line, derived from a subcutaneous mastectomy tissue is a non-tumorigenic cell line, widely being used for 3D cultures.(Tait et al., 1990) These cells are near diploid and considered to be “near normal” breast epithelial cells. The 3D cultures of MCF10A cells, a model of mammary glandular epithelium, have been exploited to study a number of oncogenes and tumor suppressors.

To assess the role of DNA damage in tumorigenesis (Chapter 3), we have used alkylating agents as a source of DNA damage, mainly due to presence of potential alkylating agents in the environment as well as wide use of these agents in chemotherapy. To gauge transformation various phenotypic parameters, including morphology, apico-basal polarity, acquisition of EMT (epithelial to mesenchymal transition), motility, invasiveness as well as anchorage independent growth were studied. We observed that alkylation damage not only disrupted baso-lateral and apcal polarity but also drastically impaired intracellular trafficking. Furthermore, the cells also acquired enhanced motility as single cells and failed to show collective cell migratory capabilities, which was in concordance with the acquisition of mesenchymal phenotype. In addition to motility, we also observed that these cells showed invasive capabilities as well as ability to grow in anchorage independent conditions. Thus, we have demonstrated the potential of alkylating agents to induce transformation. We also identified DNA-PK to be the central player involved in the process of transformation following DNA damage.During the course of the work, we also investigated the dramatic effect of DNA damage on the cytoskeleton (Chapter 4). Rearrangement of the cytoskeleton components mainly the microtubules and actin was observed. DNA-PK was found to mediate this rearrangement too, as a small molecule inhibitor of the kinase activity of DNA-PK could reverse the

rearrangement. Furthermore, we have successfully identified two candidates, Api5 and TopBP1, which may play a role in DNA damage, induced transformation. We also established the possible role of Api5 in inducing phenotypic transformation (Chapter 5).

In a quest to study role of tumor promoting inflammation in cancer initiation, we explored the potential role of Platelet activating factor (PAF) in transformation (Chapter 6). PAF, which is mainly secreted by the cells of the immune system mainly in chronic inflammatory conditions, was used in the study, in an attempt to study the role of certain potential bioactive molecules present in the microenvironment. Role of PAF in breast cancer has not been studied extensively and there are no reports pertaining to its role in breast cancer initiation. The lack of sufficient information coupled with the physiological relevance of this bioactive molecule, motivated us to study the role of this molecule in breast tumorigenesis. We found that prolonged exposure of PAF induced hyperproliferation, disrupted polarity and induced EMT-like characteristics. Thus, we have demonstrated the role of PAF in inducing phenotypic transformation.

Chapter 2: MATERIALS AND METHODS

2.1 Cell lines and culture conditions

MCF10A cell line was a generous gift from Prof. Raymond C. Stevens (The Scripps Research Institute, California, USA). These cells were grown in High Glucose DMEM without sodium pyruvate (Lonza) containing 5% horse serum (Invitrogen), 20 ng/mL EGF (Sigma-Aldrich), 0.5 μg/mL hydrocortisone (Sigma-Aldrich), 100 ng/mL cholera toxin (Sigma-Aldrich), 10 μg/mL insulin (Sigma-Aldrich) and 100 units/mL penicillin-streptomycin (Invitrogen) and were resuspended during sub-culturing in High Glucose DMEM without sodium pyruvate containing 20% horse serum and 100 units/mL penicillin-streptomycin (Invitrogen). The overlay medium in which the cell suspension was made for seeding (assay medium) constitutes of DMEM without sodium pyruvate, 2% Horse serum, hydrocortisone, cholera toxin, insulin, EGF and penicillin-streptomysin. Opti-MEM® used for transfection was obtained from Invitrogen. Cells were maintained in 100 mm tissue-culture treated dishes (Corning, Sigma-Aldrich) at 37°C in humidified 5% CO_2 incubator (Thermo Scientific). The 3D on top cultures were seeded in 8-well chambered cover glass obtained from Nunc Lab-tek, (Thermo Scientific) or 6-well and 12-well dishes (Corning, Sigma-Aldrich) and grown on Matrigel® Basement Membrane Matrix obtained from Corning, Sigma-Aldrich.

2.2 Chemicals and antibodies

N-nitroso-*N*-methylurea (MNU), *N*-nitroso-*N*-ethylurea (NEU), dimethyl sulfoxide (DMSO), thiazolyl blue tetrazolium bromide (MTT), gelatin, biotin and cyclohexamide were purchased from Sigma-Aldrich while 4,5-Dimethoxy-2-nitrobenzaldehyde (DMNB), DNA PK inhibitor was purchased from Tocris Bioscience. Paraformaldehyde (16% w/v aqueous solution) used for immunostaining was bought from Alfa Aeser. DQ™ Collagen type1 was purchased from Thermo Fisher Scientific while rat tail Collagen type 1 from BD Biosciences. Carbamyl PAF (Platelet Activating Factor) was procured from Cayman chemicals. Monoclonal antibodies used for immunofluorescence for

laminin-5 (MAB19562) and α6-integrin (MAB1378) were bought from Millipore, α-tubulin (T6199) and GAPDH (G9545) antibodies were bought from Sigma-Aldrich.

Monoclonal antibodies for immunofluorescence for vimentin (ab92547), β-catenin (ab32572), E-cadherin (ab1416) and DNA-PKcs (phospho T2609, ab18356) were obtained from Abcam while that for hDlg (sc-9961) were obtained from Santa Cruz Biotechnology, Inc. For western blotting, monoclonal antibodies for vimentin (ab8069), N-cadherin (ab12221), Cytokeratin 14 (ab7800), Cytokeratin 19 (ab52625) and polyclonal antibody for Snail (ab180714) were purchased from Abcam. For immunoflurorescence studies, GM130 monoclonal antibody (610822) and for western studies, fibronectin monoclonal antibody (610077), were obtained from BD Biosciences. Polyclonal antibody for pAKT (S437) (9271S) was purchased from Cell Signalling while that for c-Myc (SC 40) was purchased from Santa Cruz Biotechnology Inc. for western blotting. Peroxidase-conjugated AffiniPure goat anti-mouse and anti-rabbit as well as AffiniPure F(ab')$_2$ fragment goat anti-mouse IgG, F(ab')$_2$ fragment specific were obtained from Jackson Immuno Research. 4′, 6-Diamidino-2-phenylindole dihydrochloride (DAPI), Alexa Fluor 568 Phalloidin, Alexa Fluor 488 and 568 were bought from Invitrogen. Anti-VSVG (8G5F11) Antibody (EB0010) purchased from Kerafast was used to selectively mark extracellular domain of VSVG glycoprotein, in trafficking assay.

2.3 3D "on top" cultures

Wells in 8-well chamber coverglass were coated with 50 µl growth factor reduced basement membrane matrix (or Matrigel; BD Biosciences) and allowed to gel at 37°C for 15 minutes. MCF10A cell suspension was prepared in assay medium supplemented with 2% Matrigel and 5 ng/mL EGF. This suspension was added on top of 50 µl Matrigel coat to attain a cell density of 6 X 10^3 cells per well. Cultures were maintained for 16 days at 37 °C and assay medium containing 2% Matrigel and 5 ng/mL EGF was supplemented every 4 days (Debnath et al., 2003). MNU and NEU were added at day 0 and day 2 of culture and maintained

for 16days, while PAF was added on day 4, day 8, day 12, and day 16 of culture and maintained for 20 days.

2.4 Drug treatments

The different drugs used in the study and duration of treatment have been summarized in Table2.1. Alkylating agents were added in the initial days of morphogenesis (Figure 2.1a) to ensure that only cells that incurred damage and survived will form acinar structures which can be further characterized and used for the study. DNA-PK inhibition using 25 μM DMNB was done on Day 15 and Day16 of culture (Figure 2.1a). To mimic the possible *in vivo* scenario cells were subjected to prolonged exposure to 200nM of PAF. PAF was added on Day 0, 4, 8, 12, 16 of culture (Figure 2.1b). To study the re-organization of the cytoskeleton following DNA damage, MNU was added 16 hours post seeding. Following 24 hours of 1 mM MNU exposure, cells were replenished with fresh media and fixed or lysed 24 hours later. Wherever required 25 μM DNA-PK inhibitor (DMNB) for 12 hours, 50 μM ,JNK inhibitor (JNKi; SP60025) for 24 hours , 7.5 μM Akt inhibitor (Akti) for 12 hours, 2.5 μg/ml of Nocodazole was added for 20 minutes while 250 nM of Latrunculin A was added for 10 minutes (Figure 2.2).

Drug	Concentration	Duration
MNU	1 mM	24 hours
DMNB	25 μM	12-24 hours
Nocodazole	2.5 μg/mL	20 minutes
Latrunculin A	250 nM	10 minutes
Taxol	100 nM	24 hours
SP600125	50 μM	24 hours
AKTi	7.5 μM	12 hours
PAF	200 nM	4 days

Table 2.1: Concentrations and duration of treatment

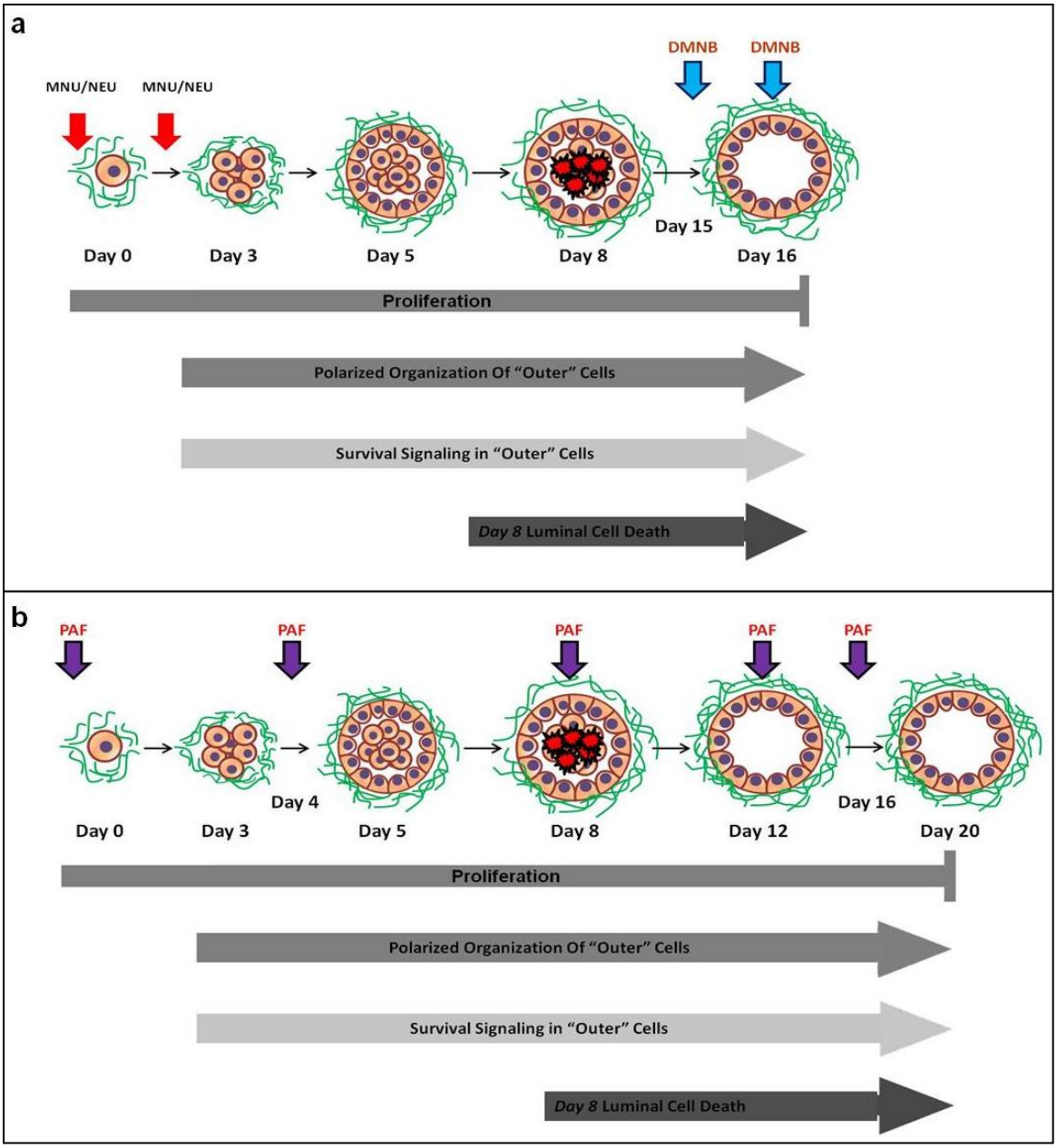

Figure 2.1: Diagramatic representation of different drug treatments.
(a) Schematic depicting the dosing of alkylating agents. NEU and MNU as well as DNA-PK inhibitor, DMNB. (b) Schematic depicting dosing regimen of 200 nM PAF to study effect of prolonged exposure of PAF on non-transformed breast epithelial cells grown as 3D "on top" cultures.

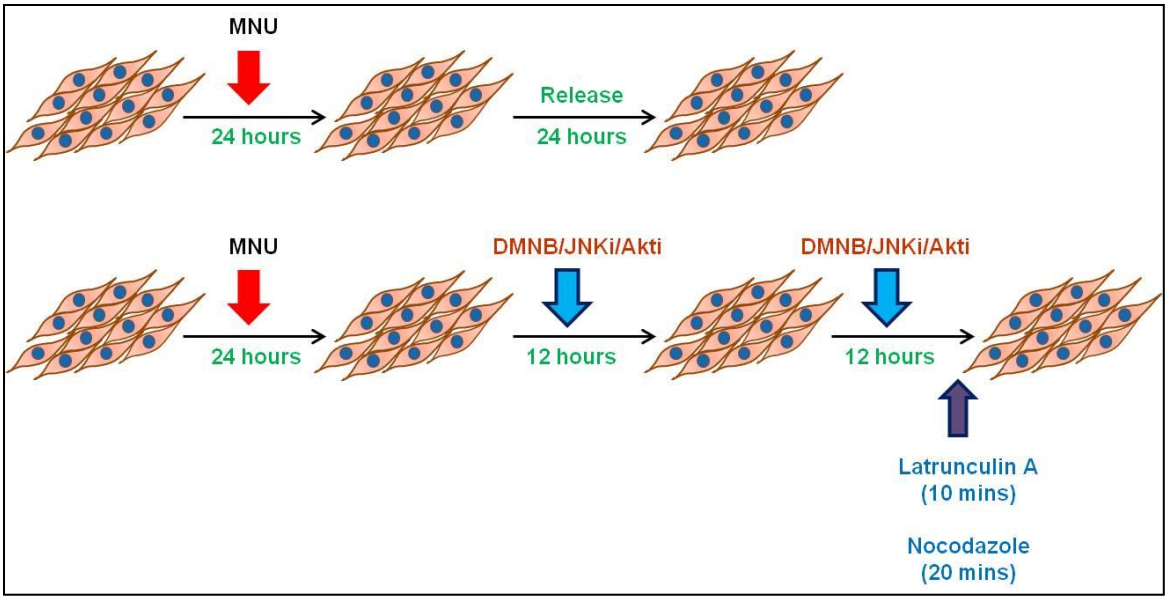

Figure 2.2: Schematic representing the dosing schedule of different chemicals to study effect of DNA damage on cytoskeleton.

2.5 Dissociating cells from 3D cultures

1.5 X 10^6 cells were seeded in 6 well dish coated with 500 µl of Matrigel™. 375 µl of Dispase™ was added per dish. The plate was incubated at 37 °C for 20 minutes. The solution was collected into 1.5 ml micro-centrifuge tubes and further incubated for 10 minutes. The tubes were centrifuged at 900 rpm for 10 mins, supernatant discarded and further resuspended in growth medium. Centrifugation was repeated and the pellet thus formed was again re-suspended in growth medium and plated in a 12 well dish. The cells were monitored for 48 hours (replenished with fresh media after 24 hours). After 48 hours, depending on confluency (approximately 70%) cells were trypsinized and replated in 6 well dish (size of dish depends on confluency). Culture was expanded and cells were frozen down at every passage and later used for the experiments.

2.6 Immunofluorescence of 3D "on top" cultures

On 16th day, the acini were fixed using 4% PFA (freshly prepared in PBS, pH 7.4) for 10 minutes at RT and washed four times with 1X PBS-Glycine for 10 minutes at RT. Cultures were permeabilized using PBS containing 0.5% Triton-X-100 for 10 minutes at 4 °C and were washed three times with PBS for 10 minutes at RT. This step was altered based on the localization of the protein of interest; though the above conditions work well in most cases, for Golgi an additional step of dissolving Matrigel™ with pre-cooled PBS-EDTA (4 °C for 15 minutes) was done. In case of Api5 over-expression studies and PAF treatment wherein the acinar structures were large; permeabilization using PBS containing 0.5% Triton-X-100 for 10 minutes at room temperature was done. For Phospho ERM staining, phosphatase inhibitors 1 mM sodium orthovanadate and 1.5 mM sodium fluoride were added in all above steps. Slides were first blocked with primary blocking solution i.e. 10% [v/v] goat serum in immunofluorescence (IF) buffer for 90 minutes at RT and then with secondary blocking solution (IF buffer containing 10% goat serum and 1% F(ab')2 fragment goat anti-mouse IgG) for 45 minutes at RT. Cultures were stained with primary antibody prepared in secondary blocking

solution, α6-integrin (1:100), β-catenin (1:100), vimentin (1:100); overnight at 4 °C. Coverglasses were washed three times with IF buffer for 20 minutes at RT. Cultures were incubated with secondary antibody prepared in secondary blocking solution, Alexa 488 conjugated donkey anti-rat (1:200), Alexa 488 and 568 conjugated goat anti-mouse IgG (1:200) and Phalloidin 633; for 60 minutes at RT. Slides were washed once with IF buffer for 20 minutes and twice with PBS for 10 minutes at RT. Cultures were counterstained with PBS containing 0.5 µg/ml Hoechst33342 for 10 minutes and washed with PBS for 10 minutes at RT. Prolong anti-fade was added to each well and was allowed to set overnight at 4 °C. 3D structures were visualized under a Zeiss LSM 710 laser scanning confocal microscope. All immunofluorescence images, unless otherwise specified, were captured using 63X oil-immersion objective.

2.7 Single gel electrophoresis (Comet Assay) (Olive and Banath, 2006).

Preparation of slides: Glass slides frosted at one end were dipped in methanol and burnt over flame to remove oil from its surface. The slides were then dipped in to 1% normal melting agarose prepared in Ca^{++} and Mg^{++} free PBS and air dried.

Preparation of cell suspension: MCF10A cells were seeded on 12 well dishes precoated with 250 µl of Matrigel™ at a density of 1.5 X 10^5 cells per well. 1 mM MNU was added to the cells 2 hours following seeding and samples were collected 2 hours and 24 hours following drug addition. For dissociating the acini to obtain single cells, the 12 well dishes were washed with 500 µl of PBS followed by addition of 500 µl of ice-cold PBS-EDTA. The cells were incubated at 4 °C for 30 minutes. The samples were collected into microcentrifuge tubes and centrifuged at 900 rpm for 10 minutes at 4 °C. The supernatant was discarded and the pellet was resuspended in PBS so as to make a cell suspension at a density of 1000 cells/ µl. 10 µl of cell suspension was added to 75 µl of 0.5% LMA (low melting agarose prepared in Ca^{++} and Mg^{++} free PBS) and the mixture was added to the slides with base agarose coating. Cover slip was placed on the

mixture and the slides were placed on ice until the agarose layer hardens. The coverslips were slided off and 80 μl of 1% LMA prepared in Ca^{++} and Mg^{++} free PBS was added to the previously added layer and coverslips were placed. The slides were then placed on ice until it hardens.

Lysing and Electrophoresis: The slides were placed into lysing solutions (recipe in Appendix) and incubated at 37 °C for neutral comet assay and 4 °C for alkaline comet assay for 2 hours. This was followed by placing the slides in electrophoresis tank containing electrophoresis buffer for 20 minutes to equilibrate the slides. Electrophoresis was done at 20 volts and 7 mA current for neutral comet assay and 24 volts and 300 mA for alkaline comet assay. Electrophoresis was done for 25 minutes. Slides were then washed with water and neutralizing buffer for neutral and alkaline comet assay respectively. Further, the slides were stained with 80 μl of 2 μg/ml of EtBr solution for 5 minutes. Excess stain was removed by washing in cold water and slides were mounted using water.

Imaging and data analysis: The slides were visualised immediately under 20X objective of epifluorescence microscope. 50 cells were imaged randomly per slide and the images were analysed using the comet assay plugin in Image J software. Extent of DNA damage was measured by calculating % tail DNA and tail length.

2.8 Immunoblot analysis

MCF10A cells were grown on Matrigel® for 16 days and the spheroids were extracted using ice cold PBS-EDTA or Dispase™ by incubating on ice for 30 minutes. Cell suspension was collected in microcentrifuge tube and centrifuged at 1200 rpm for 10 min at 4 °C. Supernatant was discarded carefully and pellet was mixed with sample buffer. This 3D culture lysate was resolved on SDS-PAGE (sodium dodecyl sulphate polyacrylamide gel electrophoresis) and transferred to PVDF (P-polyvinylidene difluoride) membrane (Millipore). Blocking for non-phospho antibodies was performed in 5% (w/v) skimmed milk (SACO Foods, USA) and for phospho-specific antibodies 4% (w/v) Block Ace (AbD

Serotec) prepared in 1X Tris buffered saline containing 0.1% Tween 20 (1X TBS-T) for 1 hour at RT. Blots were incubated in primary antibody for 3 hours at RT (or for 16 hours at 4 °C) followed by washes with TBS-T, blots were then incubated with peroxidase-conjugated secondary antibody solution in the ratio 1:10,000 prepared in 5% (w/v) skimmed milk in 1X TBS-T for 1 hour at RT following which blots were developed using Immobilon Western Detection Reagent kit (Millipore) and visualised using ImageQuant LAS 4000 (GE Healthcare). Densitometry analysis of images was done using ImageJ software.

2.9 MTT based cytotoxicity assay

MCF10A cells were seeded at a density of 0.5 X 10^4 cells per well in a 96 well flat bottomed tissue culture treated plate (Corning) in growth medium. The cells were maintained for 16 hours at 37 °C. Varying doses of MNU was added to the cells and incubated for 24 hours. Media was aspirated and freshly prepared 0.5mg/ml of MTT solution diluted in growth medium was added to cells. Following 4 hours of incubation at 37 °C, the medium was aspirated and the formazan crystals formed were dissolved by adding 100 μl of DMSO. Absorbance was measured on a Varioskan Flash Multimode Plate Reader (Thermo Scientific) at 570 nm.

2.10 RNA Extraction and cDNA preparation

For extraction of RNA, MCF10A cells seeded on Matrigel® bed made in 6 well plates at a density of 2.5 X 10^5 per well were harvested on day16 by scrapping cells following addition of TRIzol (Ambion). RNA extraction was done using standard protocol. 1ug of RNA was used for preparation of cDNA using 1 µl oligo dT (50 mM; Invitrogen) in RNAse and DNAse free water, dNTP (2.5 mM) and M-MLV-reverse transcriptase (Invitrogen). Amplification was done using the following PCR cycle: 95 °C for 60 sec, 55 °C for 45 sec, 72 °C for 60 sec and final extension for 5 min; 40 cycles. Densitometric analysis was done gel analysis function of ImageJ software and normalised to GAPDH (housekeeping gene) and later with control. Primer sequences used are as listed in Table 2.2:

Gene of interest	Forward	Reverse
Vimentin	TGTCCAAATCGATGTGGATGTTTC	TTGTACCATTCTTCTGCCTCCTG
Twist	CGGAGACCTAGATGTCATTG	ACGCCCTGTTTGTTTGAAT
Snail	ACCACTATGCCGCGCTCTT	GGTCGTAGGGCTGCTGGAA
PAFR	TACTGCTCTGTGGCCTTCCT	CTGCCCTTCTCGTAATGCTC
GAPDH	ACCACAGTCCATGCCATCAC	TCCACACCCTGTTGCTGTA

Table 2.2: Primer sequences used for RT-PCR analysis.

2.11 ts045-VSVG-GFP intracellular trafficking assay

Temperature sensitive mutant of **V**esicular **S**tomatitis **V**irus **G** (vsvg) protein fused with GFP is widely used to study the intracellular trafficking of cells(Hirschberg et al., 1998). 5 X 10^4 cells were seeded in 8 well chamber coverglass and incubated for 16 hours. This was followed by treatment either with DMSO or 1mM MNU for 24 hours. Further, the cells were transfected with pCDM8.1/VSVG^{ts045}-GFP construct using Lipofectamine 2000 in OptiMEM I Reduced Serum Medium (Invitrogen) and then incubated at 37 ^oC for 4 hours. The cells were then re-fed with growth medium and incubated at 40 ^oC for 16 hours. 100 μg/ml of cyclohexamide was added, to inhibit protein synthesis and incubated at 40 ^oC for 30 minutes and then shifted to permissive temperature of 32 ^oC. Cells were fixed at 0, 40, 80 and 120 minutes after shifting. Immunostaining of the surface VSVG molecules was done using antibody specific for the conformation of the molecules following exit from Golgi. The immunostaining was done under non-permeabilization conditions. The cells were immediately washed with wash buffer consisting of 0.1% Sodium azide and 2 % goat serum (this step should be done as quickly as possible to prevent internalization of the molecules) and fixed with 2% PFA (paraformaldehyde) for exactly 15 mins at 4 ^oC. The cells were then washed with wash buffer followed by incubation with Anti-VSVG (8G5F11) antibody (1:1000 dilution) for 1 hour at 4 ^oC.

The slides were washed extensively with wash buffer and then incubated with Alexa Fluor 568 conjugated goat anti mouse antibody (1:100 dilution) at 4 ^{o}C for 1 hour. Further the cells were washed with wash buffer and mounted using Slow fade Gold Anti-fade reagent (Invitrogen). Images were captured in laser scanning confocal microscope LSM710 (Carl Zeiss, GmbH) using 63X objective.
To measure the intensity of cells expressing VSVG molecules ImageJ software was used. Cell boundaries were marked manually and fluorescence measured. Mean cellular fluorescence of a non-transfected cell, in the same field, was measured to account for background fluorescence. To calculate the corrected total cell fluorescence (CTCF), formula used was:
CTCF=Integrated Density- (Area of selected cell X Mean fluorescence of Background readings).

2.12 RUSH (Retention using Selective Hook) Assay.(Boncompain et al., 2012)

MCF10A cells were seeded at a density of 4 X 10^5 cells per well of an 8 well chambered coverglass. Following 1 mM MNU treatment for 24 hours, the cells were transfected with ManII-SBP-EGFP construct (generous gift from Dr Franck Perez, (Institut Curie, Paris, France) using transfectene reagent (Qiagen). The transfection mix used was as follows:

DNA	:1 μg
Enhancer	:6.4 μl
EC Buffer	:Upto 60 μl (DNA +Enhancer +EC buffer)
Transfectene	:8 μl
DMEM (Growth medium)	:350 μl

After 18 hours of transfection, 40 μM Biotin was added and cells were fixed at 0, 10 and 20 minutes following addition and visualized using 63X objective of a laser scanning confocal microscope LSM710 (Carl Zeiss, GmbH). Percentage of cells showing either reporter diffused in cytoplasm, or Golgi or both were calculated and represented as bar graphs.

2.13 Wound healing Assay

Ibidi Culture Inserts, made up of biocompatible silicon, and having a defined cell free space were placed in a 35mm dish. Cell suspension at a density of 5 X 10^5 cells/ml of Growth Medium was prepared and 70 μl suspension was added to both sides of the insert. The cells were incubated with insert at 37 °C for 16 hours. Cells were treated with 10 μg/ml mitomycin C (Sigma) for 2 hours; cells were replenished with fresh medium; insert was removed and the wounds were visualized at 0,12 and 18 hrs under 10X objective of ECLIPSE TS100 (Nikon) microscope. The wound area was measured using ImageJ software, and percentage wound closure was calculated at different time points using the formula

$$\%\, WoundClosure = \frac{Initial\ wound\ area - Final\ wound\ area}{Initial\ wound\ area}\ X\ 100$$

2.14 Single cell migration assay

Cells were dissociated from 3D cultures as mentioned in section 2.5 . The cells were tagged using CFSE (Carboxyfluorescein succinimidyl ester), a cell permeable dye which stains cytoplasm of live cells. For tagging, 4 X 10^4 cells were centrifuged at 900rpm for 5 minutes, media discarded, and the pellet was rapidly resuspended in 2ml of PBS containing 5 μg/ml of CFSE .and incubated at 37 ^oC for 10 minutes. After 10 minutes the cells were centrifuged at 900rpm for 5 minutes, supernatant discarded, resuspended in 2 ml of PBS. This step was repeated again and cells were finally resuspended in 1 ml of Growth medium and 0.5 ml of the suspension was seeded in 8 well chambered coverglass (final seeding density : 20000 cells/ well). Cells were maintained in growth media at 37 ^oC for 16-18 hours. Using stage incubator of Zeiss LSM 710 laser scanning confocal microscopy time lapse imaging was carried at an interval of 2 minutes for 4 hours at 10x magnification. During live cell imaging cells were maintained in L15 media supplemented with horse serum, insulin, hydrocortisone, cholera toxin and EGF. Manual tracking plugin of ImageJ software was used to manually track randomly selected cells. Displacement, distance travelled and velocity of each cell was calculated using Chemotaxis and migration tool software (ibidi GmbH,

Munich, Germany) and were represented as box plot using Graph Pad Prism software (Graph Pad Software, La Jolla, CA, USA).

2.15 Collagen Matrigel assay

Collagen Matrigel assay was performed using protocol described by Muthuswamy's group (Xiang and Muthuswamy, 2006). Collagen was neutralized using 125 μl of 10X PBS, 125 μl of 0.1M sodium hydroxide and 25 μl of 0.1M HCl and this was mixed with Matrigel in the ratio of 1:1. Each well of 8 well chamber cover glass was coated with 50 μl of this Matrigel:Collagen mixture and was incubated for 30 minutes at 37 ^{o}C in the incubator. Further, 6 X 10^4 cells were seeded on this mixture as mentioned in 3D “on top” culture protocol. Media was changed every 4 days. Structures were analyzed by performing immunoflourescence staining for laminin-5 and Phalloidin as mentioned earlier. Images were captured using 63X objective of laser scanning confocal microscope. (Carl Zeiss, GmbH).

2.16 DQ collagen Invasion Assay

Cells were dissociated from day 16 cultures of MCF10A cells treated with or without MNU and DMNB as mentioned in section **2.4**. 2 X 10^4 cells were seeded in 8 well chamber cover glass coated with 1.6mg/ml rat tail Collagen type 1 (neutralized with NaOH) containing 25 μg/ml of DQ collagen type 1 (Invitrogen). 48 hours following incubation, the cells were imaged at 40X magnification using an Olympus IX81 system equipped with a Hamamatsu ORCA-R2 CCD camera. Fluorescence intensity per cell was measured using Image J and the corrected total cellular fluorescence was calculated as mentioned in the section on VSVG cellular-trafficking assay.

2.17 Gelatin Zymography

Conditioned media from untreated MCF10A and MNU- treated MCF10A were collected from the invasion assay and stored at -80 ^{o}C. The cells were lysed and lysates were prepared to serve as loading control. On the day of performing the

experiment, the media was thawed on ice (avoid thawing by hands). The media should be maintained at 4 ^{o}C continuously to prevent the degradation of MMPs. The conditioned media was mixed with 6X non-reducing sample buffer (87 μl of media + 13 μl of 6X sample buffer) and required amount of the mix was loaded on a pre-cooled SDS-PAGE gel containing 0.1% gelatin. The amount of media to be loaded was calculated based on the ratio calculated based on the loading adjustment done (with lysates). The gel was run at 120V at 4 ^{o}C till the dye front is run out. The gel was further incubated in renaturing buffer (2.5 % v/v of Triton X-100 in water) for 30 minutes and this step was repeated. This was followed by washing with water and then incubation in developing buffer (0.5 M Tris-HCl pH-7.8, 2M NaCl, 0.05M $CaCl_2$ and 0.2% Brij35) for 30 minutes at room temperature with gentle shaking. The gel was replenished with fresh developing buffer and kept at 37 °C for 24 hours. The developing buffer was again changed and the gel was incubated overnight at 37 °C. The gel was stained in Coomassie blue staining solution (0.1% w/v Coomassie blue (Sigma-Aldrich), 50% v/v Methanol (Fisher Scientific), 10% v/v Acetic acid (Fisher Scientific and 40% v/v distilled water). The gels were destained using destaining solution (mixture of 50% v/v Methanol, 10% v/v acetic acid and 40% v/v distilled water) to visualize the cleared regions of gelatin against a dark blue background. Further the Gels were washed with water and the gel images were captured using ImageQuant LAS4000 gel documentation system (GE Healthcare).

2.18 Soft agar assay

1.2% and 0.6 % agar solution was prepared in sterile distilled water. 2X DMEM was prepared by dissolving the powdered media (Invitrogen) in sterile distilled water and later adding filter sterilized sodium bicarbonate (3.7gm/L) solution to it. *Preparation of base agar:* 1.2% agar and 2X DMEM were placed in water bath and maintained at 40 °C. 0.75 ml of agar solution was mixed with 0.75ml 2X DMEM supplemented with (2X) growth constituents and added to each 35 mm dish and allowed to cool at room temperature inside the hood (approx. 30 minutes)

Preparation of top layer of agar: MCF10A cells were trypsinized, collected and later resuspended in 2X DMEM. These required volume of cells (1.25 X 10^5 cells) were mixed with 0.75ml of 0.6% agar (maintained at 40 °C) and 0.75 ml of 2X DMEM. 1.5 ml of total volume of mixture was poured above the base layer and placed at 37 °C, 5% CO_2 incubator. Following incubation for 2-3 hours 0.75ml of Growth medium was added to each of the dishes. The plates were maintained for 18 days and replenished with fresh media every 4 days.
Images were acquired using 4X objective of Nikon microscope. 10 random fields per dish were imaged and total number of colonies found per plate was counted manually.

2.19 Microtubule dynamics using EGFP-EB3

MCF10A cells were seeded at a density of 4 X 10^4 cells per well of a 8-well chamber coverglass. Following 16 hours of incubation at 37 °C with 5% CO_2 , 1 mM MNU was added to the cells and incubated for 24 hours. Cells with and without MNU treatment were transfected with EGFP-EB3 construct using Lipofectamine 2000. Using stage incubator of Zeiss LSM 710 laser scanning confocal microscopy time lapse imaging was carried at an interval of 2 seconds for 5minutes at 10x magnification; 5X zoom. During live cell imaging cells were maintained in L15 media supplemented with horse serum, insulin, hydrocortisone, cholera toxin and EGF. The comets were tracked manually using the Manual tracking plugin in ImageJ. 20 microtubules were analyzed per cell. Velocity and the lifetime of the comets/ was calculated.

2.20 Cloning of Api5 into mCherry-CSII-EF-MCS vector

Api5 gene was PCR amplified from Api5-mVenus C1 plasmid using primers with XbaI and NotI restriction sites as overhangs (Details in Appendix V). mCherry-CSII-EF-MCS vector and PCR product (after PCR purification) were digested using XbaI and NotI (New England Biolabs; NEB) for 4 hours. The plasmid ends were dephosphorylated by incubating the digested plasmid with calf intestinal phosphatase (CIP; NEB) during digestion (after 3 hours of digestion) and

incubation was continued at 37ºC for another 1 hour. Digested plasmids were then resolved on a 0.8% agarose gel and the band corresponding to the size of mCherry-CSII-EF-MCS vector (~9kb) was gel extracted and purified using gel extraction kit (Sigma). The amplified product (Api5; ~1.57 kb) following digestion was purified using PCR purification kit (Qiagen) and Api5 was ligated into mCherry-CSII-EF-MCS vector with an insert to vector ratio of 0.075 picomoles: 0.025 picomoles using T4 DNA ligase (NEB) at 25 °C for 90 minutes. Ligation mixture was transformed into DH5α competent cells. Plasmid DNA was isolated from the obtained colonies and screened the colonies by digesting with XbaI and NotI HF to check for insert release. *(For detailed cloning protocol refer Appendix V)*

2.21 Lentiviral production and stable cell line preparation:

HEK293T cells were seeded at a density of 5 X 10^5 in a 35mm dish and incubated for 16 hours at 37 °C. Lipofectamine 2000 (Invitrogen) and Opti-MEM (Invitrogen) were mixed to give Solution 1(10 µl Lipofectamine + 240 µl Opti-MEM), followed by incubation at room temperature for 5 minutes. Meanwhile DNA and Opti-MEM were mixed in the ratio to give Solution 2(1 µg mCherry-CSII-EF-MCS /or mCherry-CSII-EF-MCS-Api5 + 1 µg pCAG-HIVgp + 0.5 µg pCMV-VSV-G-RSV-Rev + Opti-MEM to make up volume to 250 µl). Solution1 and Solution 2 were mixed and incubated for 20 minutes at RT. In the meantime, the cells were preconditioned with Opti-MEM for 20 minutes. After 20 minutes, 250 µl of OPTIMEM was added to the reaction mixture, and 500 µl of the mixture was added to the wells. 24 hours post transfection, 500 µl DMEM containing 30% FBS was added to the cells. For transduction, MCF10A cells were seeded at a density of 5 X 10^5 on a 35 mm dish. 48 hours post transfection viral supernatant was collected, filtered through a 0.45 µm filter and added to MCF10A cells along with 1 ml fresh media supplemented with 8µg of polybrene to increase the transduction efficiency. 48 hours post transduction the cells were replenished with fresh Growth medium.

2.22 Statistical Analysis

Student's t test was used to analyze the statistical significance of tail length while one tailed Mann-Whitney U test was used for % tail DNA. Mann-Whitney U test was also used to analyze the significance of difference between parameters in morphometric analysis of 3D cultures. Data of VSVG trafficking assay was analyzed using Two-way ANOVA to determine the significance of effect of treatment as well as of time on the trafficking. Mann-Whitney U test was used to analyze statistical significance of relative Golgi area and relative fluorescence intensity in DQ^{TM} Collagen invasion assay. $p<0.05$ was considered statistically significant. ***, ** and * indicates $p<0.0001$, $p<0.01$, and $p<0.05$ respectively. Graph Pad Prism software (Graph Pad Software, La Jolla, CA, USA) was used to analyze data and $p < 0.05$ has been considered as significantly different.

Chapter 3: Alkylation damage induces transformation

3.1 Background

Cancer therapeutics is double-edged in their action. The therapies are largely based on inducing DNA damage in rapidly dividing cells and thus kill cancerous cells. However, these agents have been shown to induce mutations in DNA, which can ultimately contribute to tumor development or progression (Kastan & Bartek 2004). This is supported by the report from Fung and colleagues who demonstrated that reversal of DNA damage induced apoptosis resulted in transformation (Tang et al., 2012). Further, Paules group demonstrated that "cancer-predisposition programs" were induced in lymphocytes following DNA damage (Innes et al., 2013).

Alkylating agents are a class of agents used in cancer chemotherapy and form the first line of therapy (Chaney and Sancar, 1996; Cheung-Ong et al., 2013). These act by inducing DNA damage. Apart from therapeutics, exposure to these agents may be through environment mainly nitrosamines present in cigarette smoke, environmental pollutants, dietary sources of nitrodialkylamines as well as through job occupations (Silber et al., 1996). Apart from the exogenous sources, certain endogenous processes are known to generate potential methylating species, which ultimately can alkylate DNA (Barrows and Magee, 1982; Vaca et al., 1988). These agents act by alkylating DNA at “N” or “O” positions, thereby inducing DNA breaks and directing the cell towards apoptosis. These agents are capable of forming 12 different DNA adducts. Apart from this, these agents namely DMBA (7,12-Dimethylbenzanthracene, NEU (*N*-ethyl *N*-nitrosourea and MNU (*N*-methyl *N*-nitrosourea have been used to develop rodent models of different cancers (Gullino et al., 1975; Guzman et al., 1988; Stoica et al., 1983, 1984). Such models developed in early 1960s have been used successfully to screen therapeutics as well as to answer intriguing questions related to tumor progression. However, the exact mechanism of tumor induction has not been elucidated yet. Given that we are exposed to DNA damaging agents in day-to-day life and with breast tissue undergoing constant re-modelling throughout a women’s lifetime, in turn making it vulnerable to acquire and accumulate DNA

damage (Davis and Lin, 2011), the study of mechanism of DNA damage induced transformation in breast epithelial cells becomes imperative.

In this study, we have used two of such agents, namely MNU and NEU to ascertain whether DNA damage can induce transformation and further provide mechanistic insights into the process. We have used 3-dimensional '*on top*' cultures of MCF10A, cells as our model system.

3.2 Results

3.2.1 MCF10A cells, when grown on Matrigel™, formed polarized growth arrested spheroids with a monolayer of cells enclosing a hollow lumen.

3D on-top culture of MCF10A cells was established to study step-wise, the process of transformation using chemical carcinogens, MNU*,* and NEU*.* Following 16 days of culture of MCF10A cells on growth factor reduced basement membrane (Matrigel™), these cells formed growth arrested multicellular acinar structures resembling the epithelial lining of lobules in the breast tissue *in vivo* (Figure 3.1)*.* 3D structures were visualized using 63X oil-immersion objective, under a Zeiss LSM 710 laser scanning confocal microscope.

To confirm the apicobasal polarization of the cells forming the acini, these acini were immunostained with α6-integrin antibody (Figure 3.2a). α6-integrin is a transmembrane extracellular matrix receptor, which maintains contact with the basement membrane. The cells in the acinus which loose contact with the basement membrane undergo apoptosis between day 6 to day 10, thus resulting in the formation of a hollow lumen. β-catenin (Figure 3.2b) and E-cadherin (Figure 3.2c), adherens junction markers, were found to localize at cell-cell junctions and GM130 (Figure 3.2d), a Golgi marker, showed apical orientation (Debnath et al., 2003), all characteristic of normal epithelial cells.

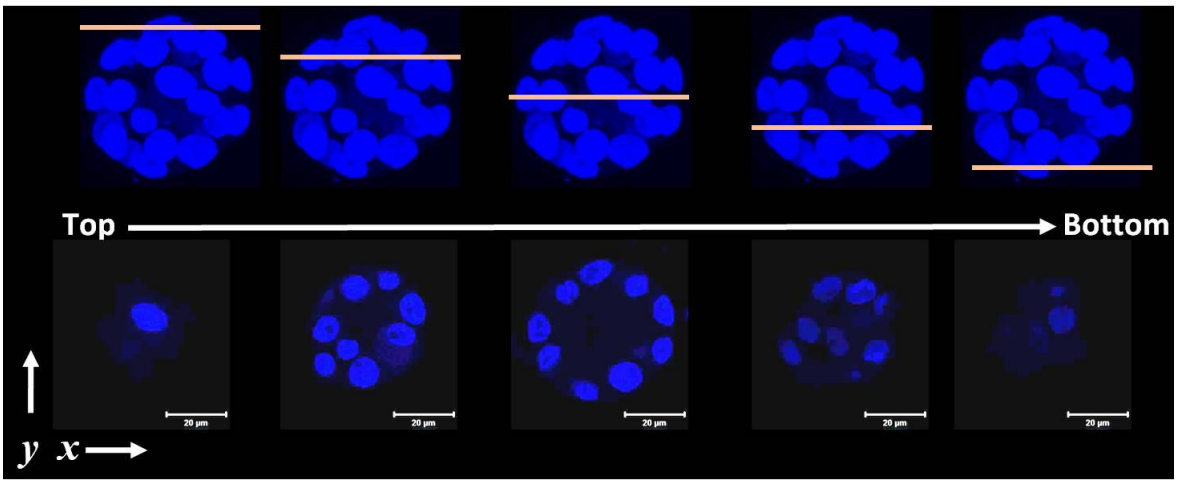

Figure 3.1: Representative confocal images of MCF10A acinus.
DAPI-stained (blue) cross sections (x-y axis) of a Day 16 MCF10A acinus imaged down the z axis. **Upper panel:** 3D construction of confocal 'z' sections each 0.35 μm in thickness. **Lower panel:** Individual optical sections of the spheroid. Scale bar: 20 μm

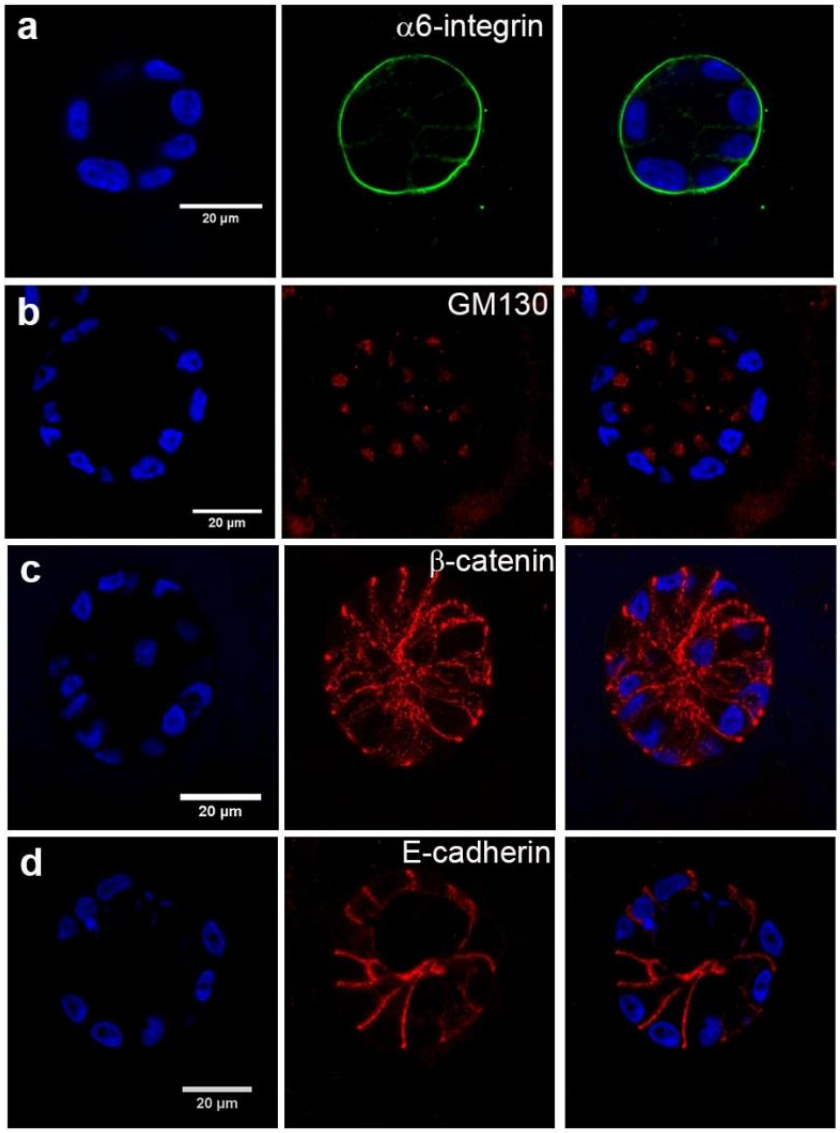

Figure 3.2: MCF10A cells grown on Matrigel™ were polarized.

Day 16 MCF10A acinus immunostained with (a) α6-integrin (b) β-catenin (c) E-cadherin (d) GM130 antibody.: MCF10A cells were grown as 3D-on top cultures for 16 days and were stained with DAPI (blue) to visualize nuclei and with antibody towards α6-integrin (green) to demarcate its attachment with basement membrane; antibody towards β-catenin and E-cadherin to mark the cell-cell junctions and GM130 to mark the apical region. Scale bar: 20 μm.

3.2.2 MNU induced DNA damage and affected acinar morphology.

MTT-based cytotoxicity assay was carried out to select a suitable, sub-lethal dose of MNU. 1 mM was selected as the optimal sub-lethal dose (Figure 3.3a). The cells were exposed to MNU in the initial days of morphogenesis (day 0 and day 2) to ensure that only those cells that acquired damage and finally survived the damage proliferated and differentiated on Matrigel^{TM} could be further analyzed for phenotypes in 3D spheroid cultures. To ascertain whether the sub-lethal dose of MNU selected caused DNA damage under the conditions of the study, Single Cell Gel Electrophoresis (Comet Assay) was performed under both alkaline as well as neutral pH conditions. Comet assay enables visualization of DNA breaks at the single cell level and also helps distinguish between single strand breaks (SSB and double strand breaks (DSB) based on changes in pH conditions wherein alkaline comet assay detects SSBs and alkaline labile breaks while neutral comet assay detects DSBs. MCF10A cells grown as 3D cultures, with or without treatment with 1 mM MNU for 2 hour and 24 hours were subjected to comet assay. We observed that 1 mM MNU induced DNA damage and resulted in the formation of both SSBs (alkaline comet assay) and DSBs (neutral comet assay), characterized by the formation of comets under both alkaline and neutral pH conditions (Figure 3.3b). The extent of DNA damage induced by MNU exposure was measured in terms of tail length (Figure 3.3c and Figure 3.3e) and percentage of tail DNA (Figure 3.3d and Figure 3.3f).

Previous studies convincingly showed that the morphology of acini was disrupted upon transformation (Debnath and Brugge, 2005; Debnath et al., 2003). We tested overall morphology of MCF10A acini after exposure to MNU. Morphometric analysis revealed that MNU treated MCF10A cells lead to formation of smaller acini with fewer cells by day 16 (Figure 3.4a and Figure 3.4b). However, culturing the acini further till day 30 led to a significant increase in volume of acini as well as the number of cells in the treated acini, as compared to control acini where the volume and number of cells in the acini did not change significantly (Figure 3.4c and Figure 3.4d). Change in nuclear architecture is one

of the key features of cancer cells (Zink et al., 2004). To investigate the change in nuclear morphology the 3D reconstructed images of acini were used for nuclear morphometry using Huygens Professional software (SVI, Hilversum, Netherlands). It was observed that the nuclei of cells treated with MNU were larger as compared to that of control. Further, this phenotype was observed in cells in day 30 acini indicating the persistent increase in nuclear volume following DNA damage induced in the early stages of morphogenesis.

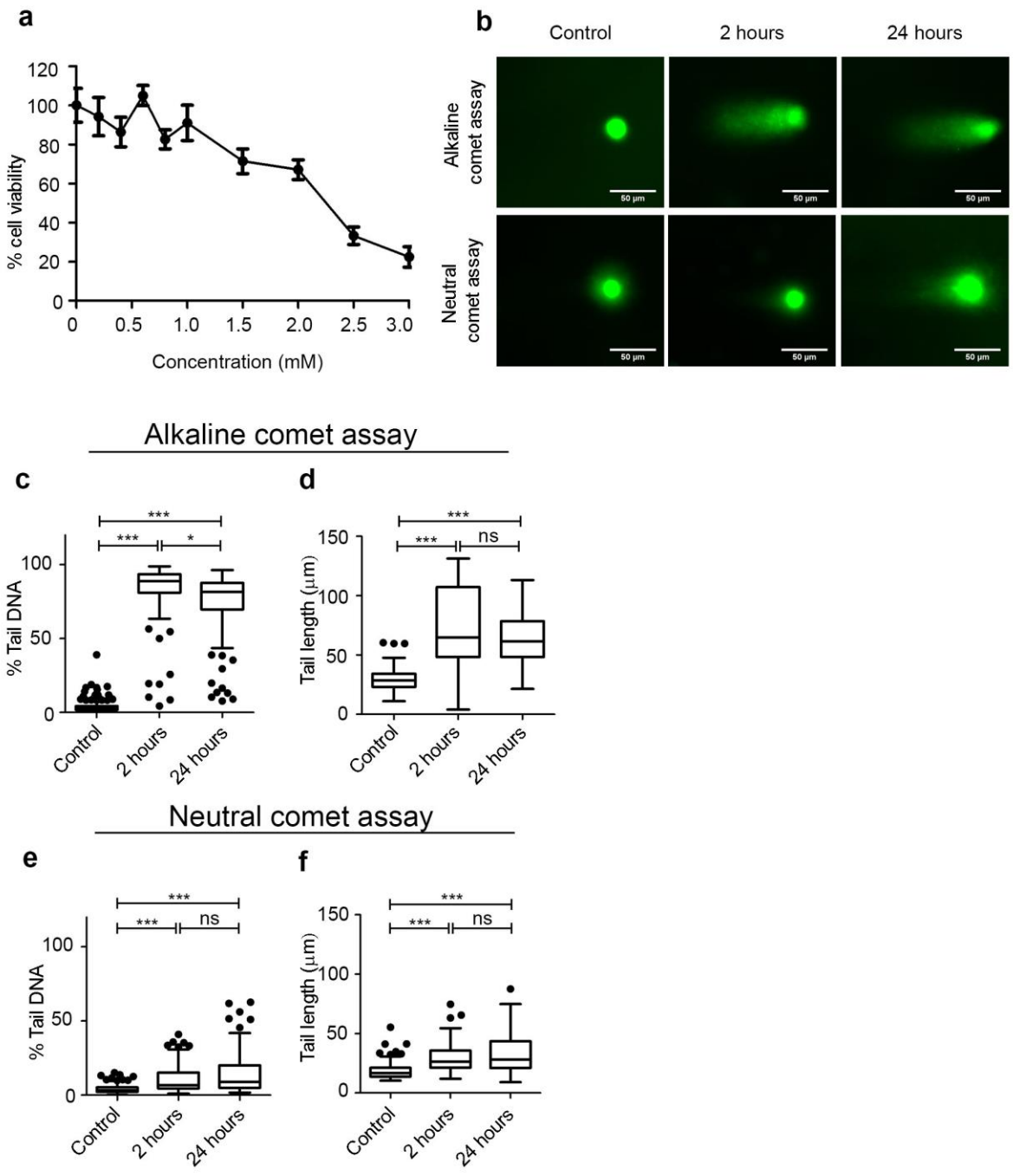

Figure 3.3:Sub-lethal dose of MNU induces DNA damage in MCF10A cells. (a) MTT-cytotoxicity assay was performed over a dose range to identify the sub-lethal dose of MNU to be used for the study. (b) Comet assay was performed in alkaline and neutral conditions. The % tail DNA (c and e) and tail length (d and f) were measured using ImageJ software. Student's t-test was used to analyze the

statistical significance of difference in tail length and % tail DNA. * $p<0.05$ and *** $p<0.0001$ has been considered as significantly different. Data is representative of three independent experiments; 50 nucleoids were scored per experiment. Scale bar: 50 μm

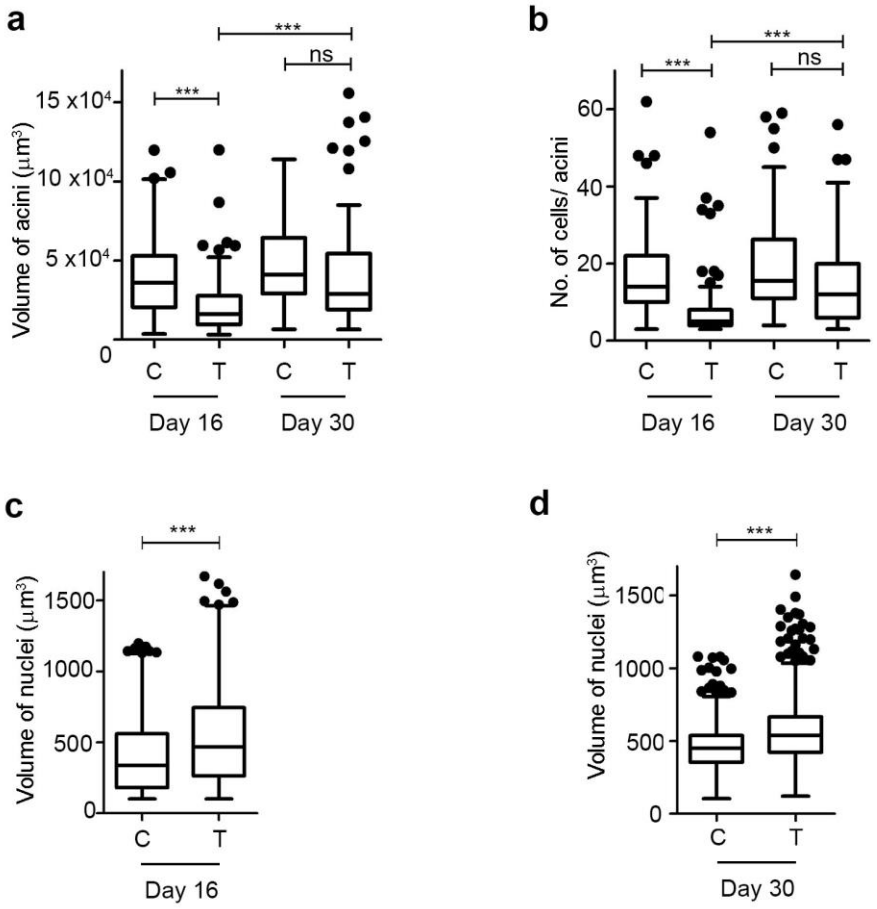

Figure 3.4: MNU treatment resulted in increase in nuclear volume.

MCF10A cells grown as 3D cultures were immunostained with Phalloidin to mark the boundary of the entire acini while DAPI was used to stain the nuclei. Images were captured using Zeiss LSM 710 laser scanning confocal microscope (Zeiss, GmbH) and morphometric analysis was done using Huygens Professional software (SVI, Hilversum, Netherlands). Graph representing (a) volume of day 16 acini and day 30 acini, (b) number of cells per acini on day 16 and day 30; (c) Volume of nuclei of day 16 and (d) day 30 acini. Statistical analysis was performed using One way ANOVA for (a) and (b) while Mann Whitney test for (c) and (d); C denotes control and T denotes treated**.** Data from N>5 independent experiments is pooled and represented. *** $p<0.0001$.

3.2.3 Exposure to MNU disrupted baso-lateral polarity.

Epithelial cells are characterized by their ability to polarize. When these cells get transformed they lose this characteristic (Debnath and Brugge, 2005). To investigate the effect of DNA damage in establishment and maintenance of polarity of the breast epithelial cells, MCF10A cells were grown on Matrigel^{TM} and analyzed using different markers. α6-integrin and laminin-5 are widely used to ascertain the integrity of basal polarity. Upon methylation damage, we observed mislocalization of α6-integrin in 43% acini while a discontinuous staining of both α6-integrin (Figure 3.5a and Figure 3.5b) and laminin-5 (Figure 3.5c and Figure 3.5d) in 33% and 55% of acini respectively. To ascertain whether this effect was transient or persisted beyond day 16, the day 30 acini were subjected to immunofluorescence and localization of α6-integrin was investigated. Loss of α6-integrin from the basal region was observed in majority of the acini (Figure 3.6a and Figure 3.6b).

Further to investigate the integrity of the adherens junctions the day 16 acini were immunostained for E-cadherin and β-catenin. We observed that acini of cells which were exposed to MNU showed reduced E-cadherin at cell-cell junctions (Figure 3.7a and Figure 3.7b). To confirm this phenotype, the cells from acini were dissociated on day 16 and were immunostained for E-cadherin. The phenotype observed (Figure 3.7c) corroborated with that observed in spheroids, thus implying the loss of integrity of cell-cell junctions. β-catenin showed an aberrant staining pattern characterized by cytoplasmic staining (Figure 3.8a and Figure 3.8b). Further hDlg, human homologue of Drosophila discs large tumor suppressor protein, was used to confirm the loss of adherens junctions. Localization of hDlg was found to be reduced at cell-cell junctions (Figure 3.8c and Figure 3.8d). This observation further strengthens our claim of disruption of cell-cell junctions in MCF10A cells treated with MNU in early days of morphogenesis.

Thus, the above results imply the loss of baso-lateral polarity following exposure of breast epithelial cells to DNA damage by MNU.

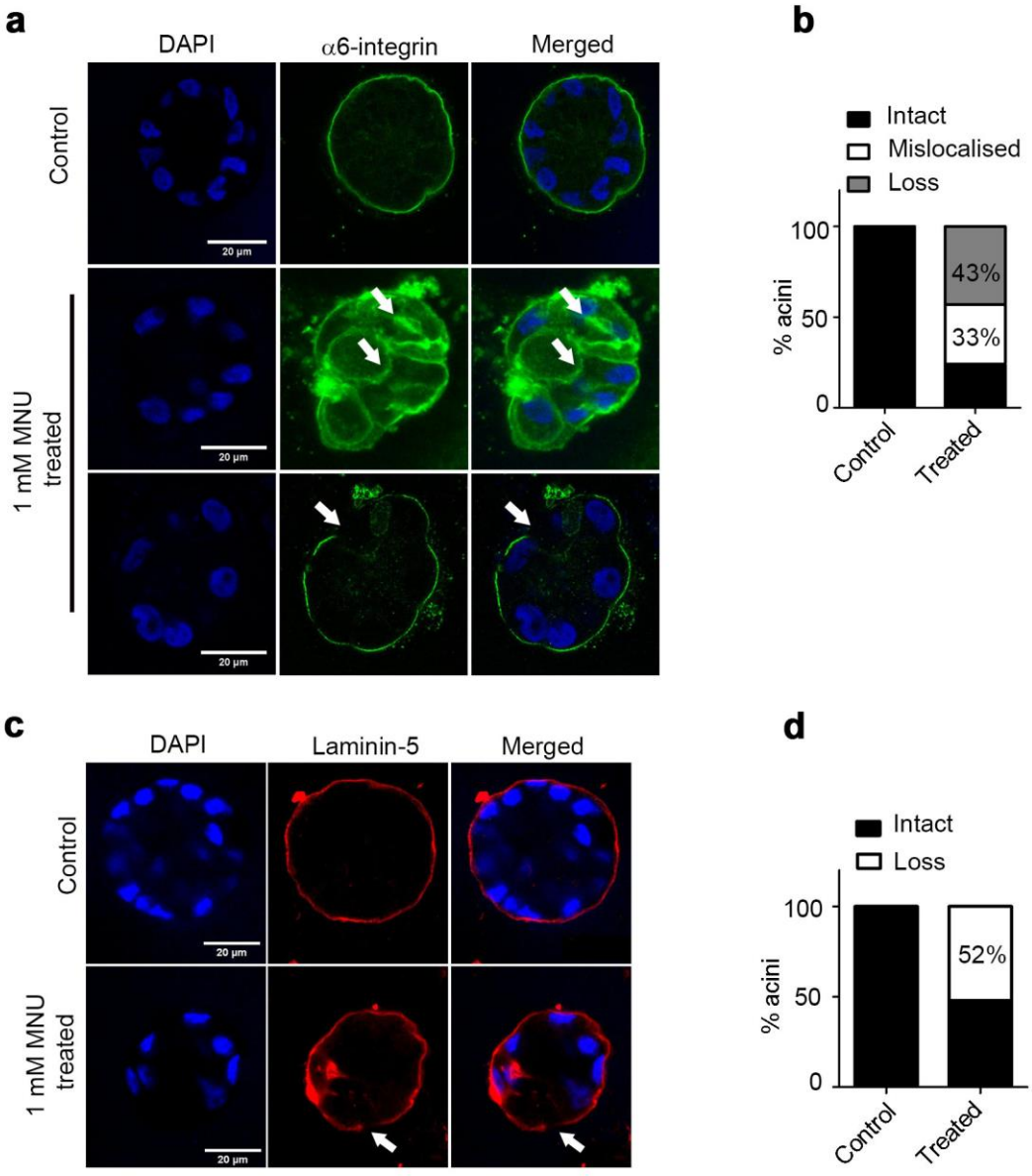

Figure 3.5: MCF10A cells lose basal polarity upon exposure to methylating agent.

Day 16 spheroid cultures were immunostained for basal polarity markers. (a) Representative images of centermost z section of spheroids immunostained with α6-integrin (green). (b) Graph depicting the percentage of acini showing different phenotypes observed with α6-integrin. (c) Representative images of centermost

z section of spheroids immunostained with laminin-5 (red). (d) Graph depicting the percentage of acini showing discontinuous laminin-5. (e) Immunofluorescence images of α6-integrin (green) stained Day 30 spheroids. (f) Graph representing the percentage of acini showing presence of discontinuous α6-integrin. Arrow head (white) indicate the abnormal localisation and loss phenotype. Data is representative of >5 independent experiments. >50 acini were analyzed per treatment group. Scale bar: 20μm.

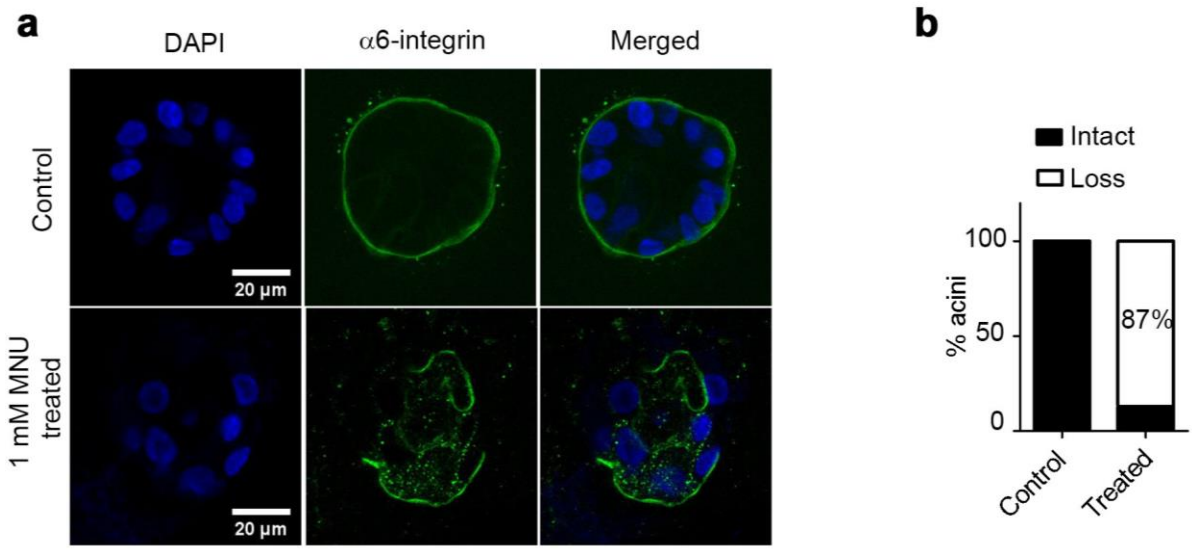

Figure 3.6: Loss of α6-integrin from the basal region of MCF10A acinar cultures upon exposure to methylating agent is not transient.

Day 30 , MCF10A acinar cultures were immunostained for basal polarity markers. (a) Representative images of spheroids immunostained with α6-integrin (green). (f) Graph representing the percentage of acini showing presence of discontinuous α6-integrin. Data is representative of >2 independent experiments. >40 acini were analyzed per treatment group. Scale bar: 20μm.

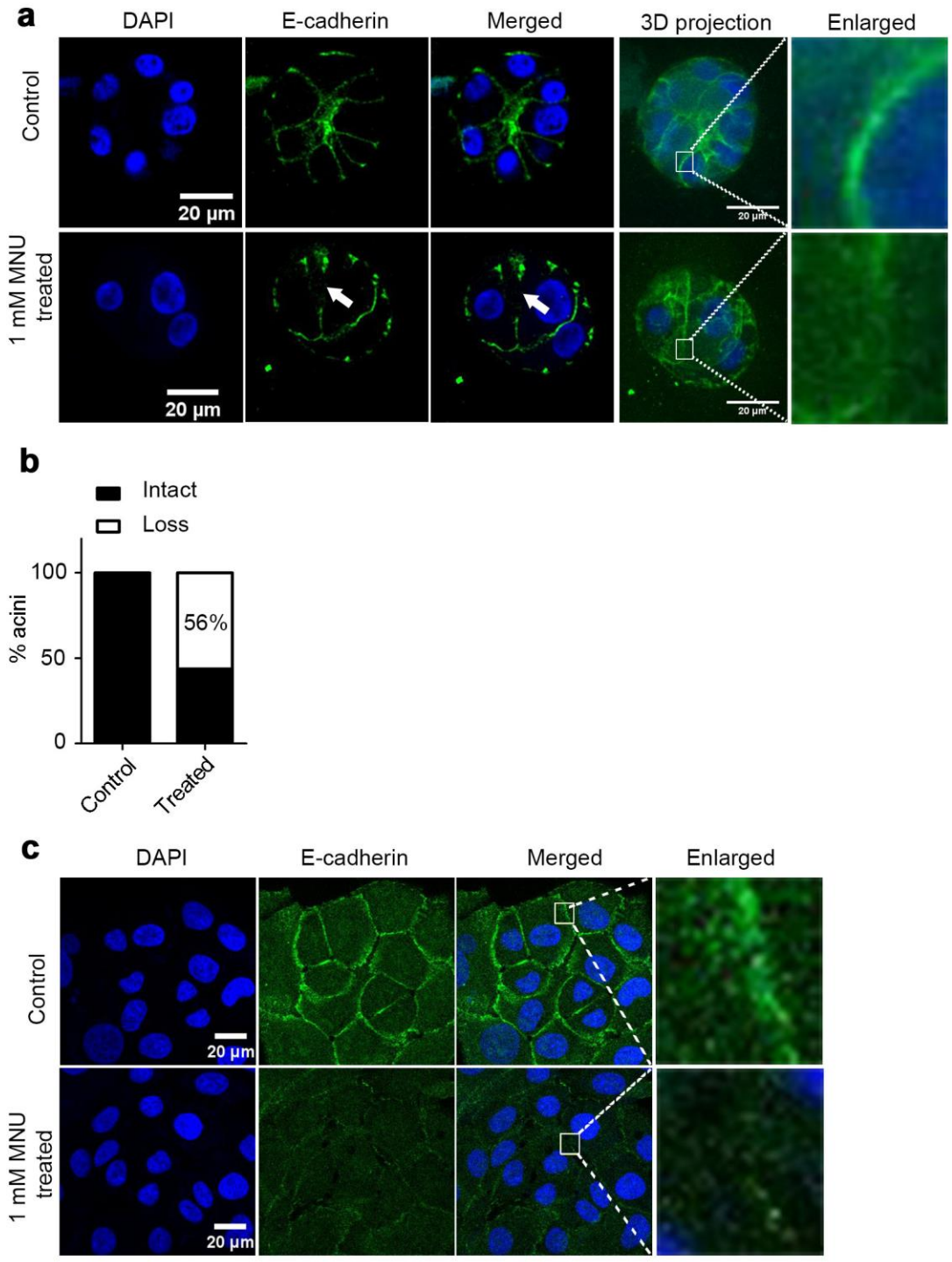

Figure 3.7: Methylation damage results in loss in integrity of adherens junctions.

Day 16 cultures of MCF10A cells were immunostained for markers of adherens junctions and analyzed for their integrity. (a) Representative immunofluorescence images of acini labelled with E-cadherin (green). (b) Graph representing the % of acini showing loss phenotype. (c) Cells from day 16 acini were dissociated using Dispase™ and immunostained for E-cadherin. Data is representative of >5 independent experiments. Scale bar: 20 μm

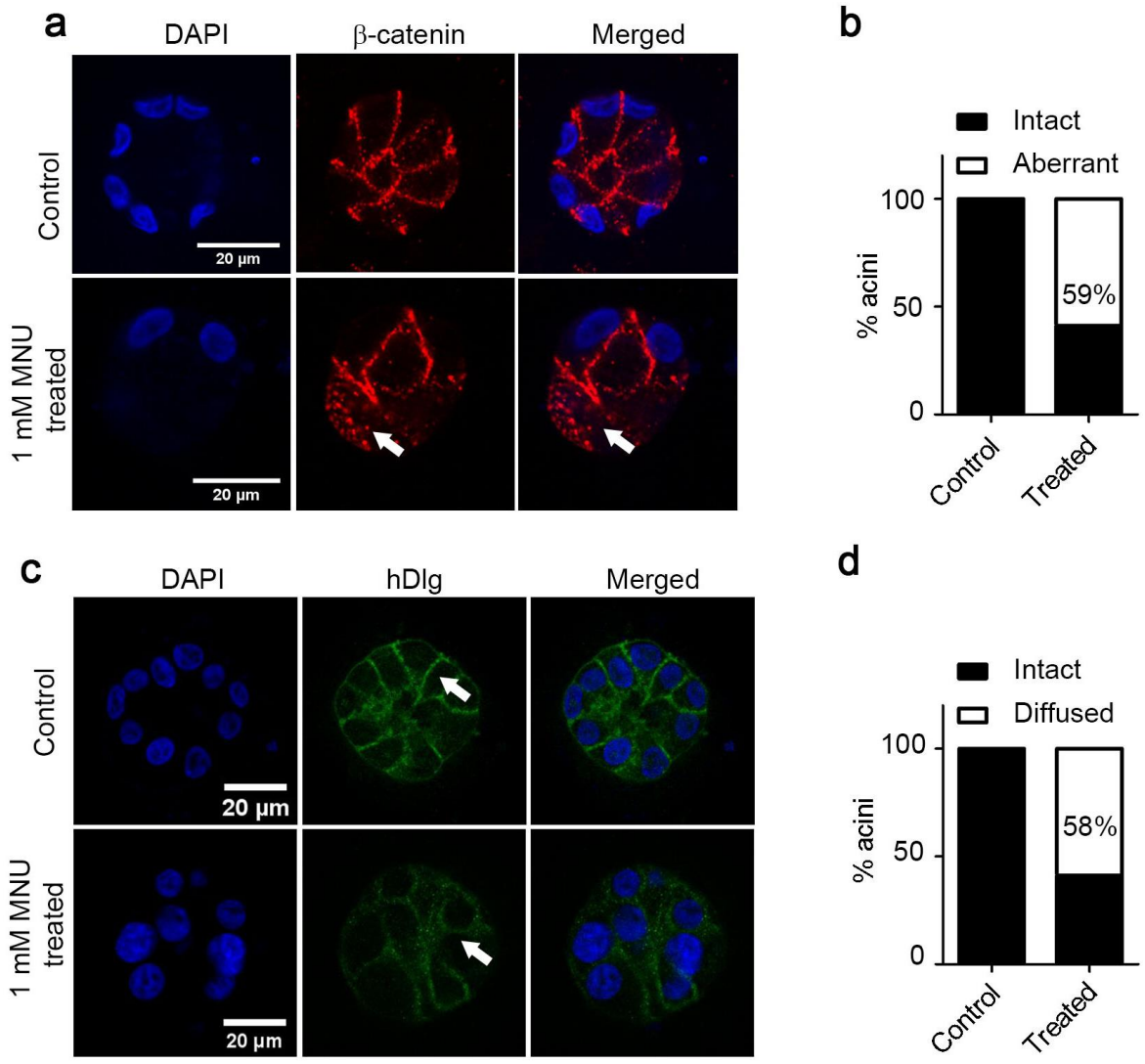

Figure 3.8: Methylation damage results in loss in integrity of adherens junctions

(a) Representative immunofluorescence images of acini labelled with β-catenin (red). (b) Graph representing the % of acini showing aberrant phenotype. (c) Representative immunofluorescence images of acini labelled with hDlg (green). (d) Graph representing the % of acini showing diffused localization on cell-cell junctions. Data is representative of >5 independent experiments. Scale bar: 20 μm

3.2.4 MNU treatment disrupts apical polarity. ,

Loss of apico-basal polarity of epithelial cells is one of the hallmarks of cancer (Debnath and Brugge, 2005). Golgi plays a central role in polarized sorting of proteins to the apical and baso-lateral membranes and thus in establishment and maintenance of polarity. Golgi present in the apical region above the nucleus is widely used to investigate apical polarity in MCF10A spheroids (Aranda et al., 2006). To determine the integrity of apical polarity, GM130, a Golgi marker was used. Interestingly, we observed that the morphology of Golgi in acini formed by cells exposed to DNA damage was disrupted wherein it appeared to be dispersed (Figure 3.9a).

Further quantification of Golgi area revealed that MNU treated cells showed a significant difference and thus confirmed the dispersed phenotype (Figure 3.9b). However, due to dispersed phenotype, GM130 could not be used to investigate apical polarity establishment. Therefore, phospho ERM (ezrin/radixin/moesin known to mark the apical membrane and localize to actin rich structures was used to ascertain integrity of apical polarity. In MCF10A cells phospho ERM is known to mark the plasma membrane and used to mark the apical membrane. The acini formed by MNU treated cells showed a strong basal localization of phospho ERM, thus implying the loss of apical polarity **(**Figure 3.9c and Figure 3.9d). To confirm whether the effect on Golgi was persistent, day 30 acini were analyzed and we observed a similar dispersed phenotype (Figure 3.9e).

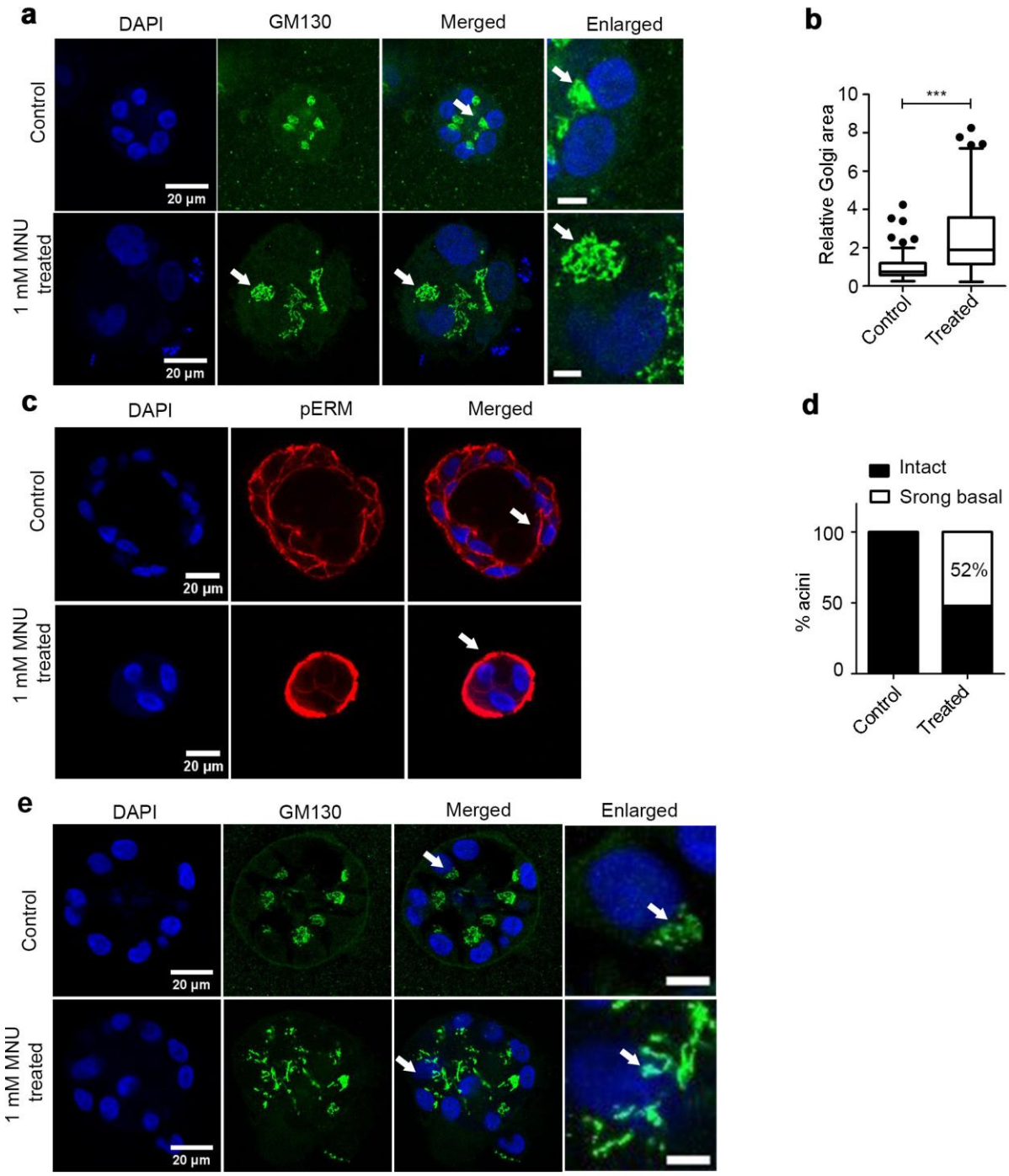

Figure 3.9: Apical polarity was lost and Golgi morphology disrupted in cells exposed to methylation damage.

3D “on top” cultures of MCF10A cells were immunostained for apical polarity markers. (a) Representative immunofluorescence images of day 16 acini labelled

with GM130, a Golgi marker (green). Arrow head (white) indicate the abnormal localisation of Golgi. (b) Graph depicting the relative Golgi area normalized to control was measured using ImageJ software. Mann-Whitney test was used to analyze the statistical significance of differences (c) Representative immunofluorescence images of day 16 acini labelled with phospho ERM (red). Arrow head (white) indicate the abnormal localisation of phospho ERM. (d) Graph representing the % of acini showing strong basal localization of phospho ERM (e) Representative immunofluorescence images of day 30 acini labelled with GM130 (green). Data is representative of >5 independent experiments. *** $p<0.0001$. Scale bar: 20 μm

3.2.5 MNU treatment impaired intracellular trafficking.

To investigate whether the dispersed Golgi was functional, ts045- VSVG intracellular trafficking assay was performed. The assay uses GFP-fused temperature sensitive mutant of VSVG (vesicular stomatitis viral glycoprotein). The VSVG molecules accumulate in the endoplasmic reticulum (ER) at 40 °C (non-permissive temperatures). After shifting the cells to permissive temperature of 32 °C the molecules are synchronously released from ER to Golgi within 40 minutes and to plasma membrane within 120 minutes (Presley et al., 1997). These VSVG molecules are mis-folded and hence can be marked using the conformation specific antibody (clone 8G5F11). The integrity of intracellular trafficking is measured in terms of the ratio of surface VSVG to total VSVG. We found that although by 120 minutes a large proportion of the vsvg molecules reached the surface in untreated cells, in case of treated cells negligible number of molecules reached the surface. Thus, our results revealed that MNU induced disruption of Golgi morphology and also impaired Golgi trafficking (Figure 3.10a and Figure 3.10b). Furthermore, to determine the effect of DNA damage on ER to Golgi trafficking, RUSH assay (**R**etention **U**sing **S**elective **H**ooks assay was performed. Str-KDEL-ManII-SBP-EGFP construct was used where Str-KDEL is the ER hook and ManII-SBP-EGFP is the reporter. Mannosidase II (ManII) localizes in the Golgi, its acceptor compartment. Release of the molecules is coordinated by addition of biotin and is based on the competitive binding affinity of biotin over streptavidin binding protein (SBP). 10 minutes following addition of biotin all the reporter molecules localized at Golgi in majority of the untreated cells, while in MNU damaged cells the molecules failed to completely localise in Golgi in a large proportion of cells even by 20 minutes(Figure 3.11a-c). These results imply that MNU damage impaired the ER to Golgi trafficking. Since the percentage of cells showing localization of reporter to Golgi increased by 20 minutes, it can be inferred that the trafficking is only impaired and not completely abrogated.

Taken together, the above experiments demonstrate the ability of methylation damage to not only disrupt apical polarity but also to disrupt Golgi morphology and impair intracellular trafficking.

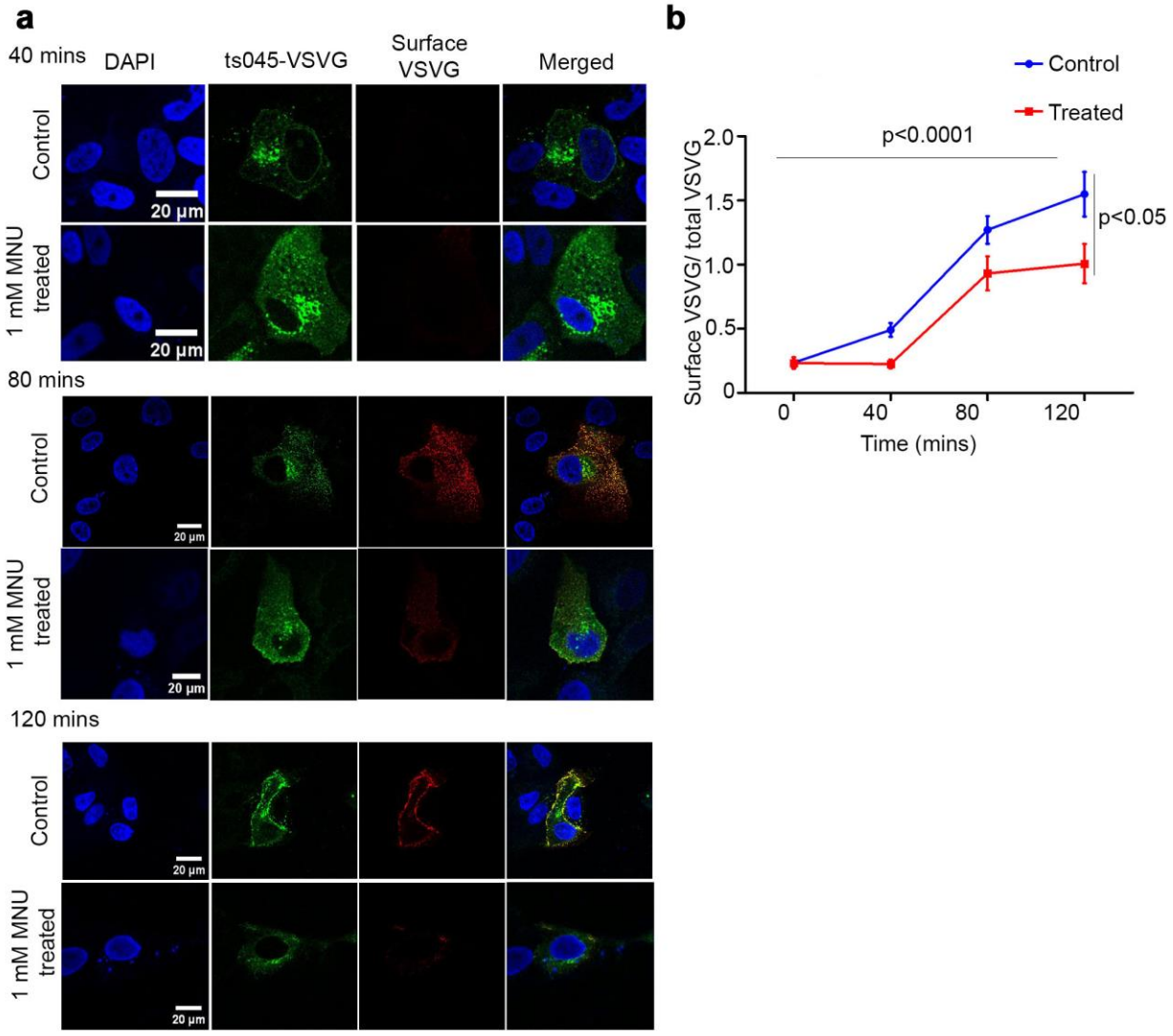

Figure 3.10: MNU damage impaired Golgi to plasma membrane trafficking. MCF10A cells grown as monolayers with and without 1 mM MNU treatment for 24 hours were transfected with ts045 VSVG-GFP construct. The cells were incubated at 40°C (non-permissive temperature). Following shift to 32°C (permissive temperature), samples were collected at pre-determined time-points and surface VGVG molecules were immune-stained under non-permeabilizing conditions with antibody specific to the conformation of surface molecules.

Representative images of cells incubated at 32°C for (a) 40 minutes, 80 minutes and 120 minutes. (b) Graph represents mean +/- SEM of the relative ratio of surface VSVG molecules (red fluorescence) to total VSVG molecules (green fluorescence). Statistical significance of effect of MNU and time on trafficking of VSVG molecules was determined using Two way ANOVA. $p<0.05$ has been considered to be statistically significant. Data represented is pooled from three independent experiments. Scale bar: 20 μm

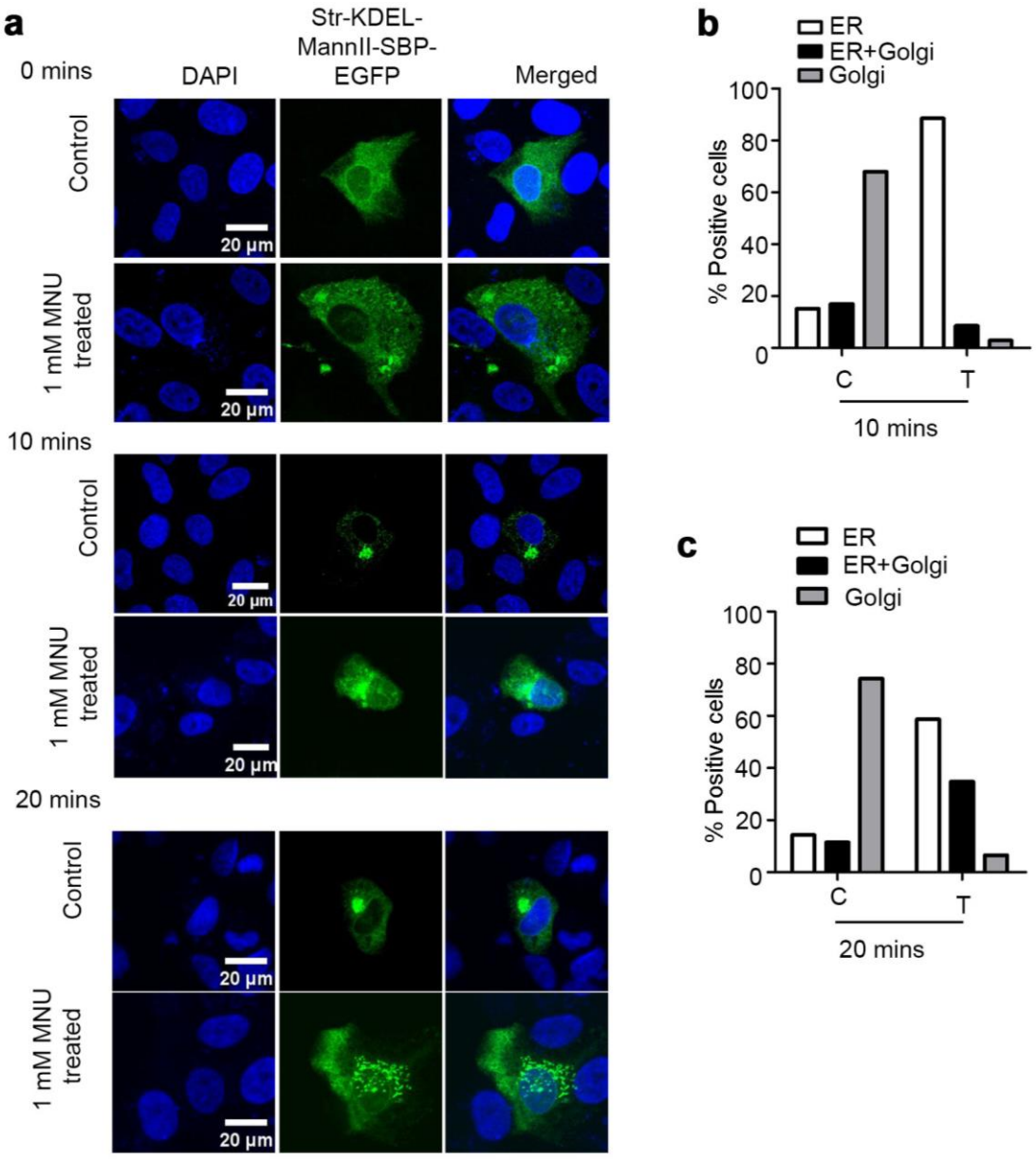

Figure 3.11: MNU damage impaired ER to Golgi membrane trafficking.

(a) Monolayer cultures of MCF10A cells, with and without 1 mM MNU treatment for 24 hours were transfected with Str-KDEL-ManII-SBP-EGFP construct The reporter (green) release was observed at 0, 10 and 20 minutes upon biotin addition. Graph representing the localization of the reporter in (b) 10 minutes and (c) 20 mins following biotin addition. C denotes control and T denotes 1 mM MNU treated cells. Data is representative of three independent experiments. Scale bar: 20 µm.

3.2.6 MCF10A cells upon exposure to MNU induced Epithelial to Mesenchymal transition.

Loss of apico-basal polarity coupled with loss of intact adherens junctions results in epithelial to mesenchymal transition (EMT). To ascertain if MCF10A cells following MNU damage underwent mesenchymal transition, the day 16 acini were immunostained for vimentin, a mesenchymal marker. We observed a significant upregulation of vimentin in 69% of acini formed by the MNU treated cells (Figure 3.12a and Figure 3.12b). In addition to this the lysates obtained from 3D cultures were immunoblotted and probed for various epithelial and mesenchymal markers. We observed upregulation of mesenchymal markers such as vimentin, fibronectin, N-cadherin and snail where as a down regulation of epithelial markers such as, E-cadherin, cytokeratin 14 and cytokeratin 19 (Figure 3.12c). Similar profile was also observed at the transcript level, wherein twist, Snail and vimentin, all mesenchymal markers showed an upregulation (Figure 3.12d).

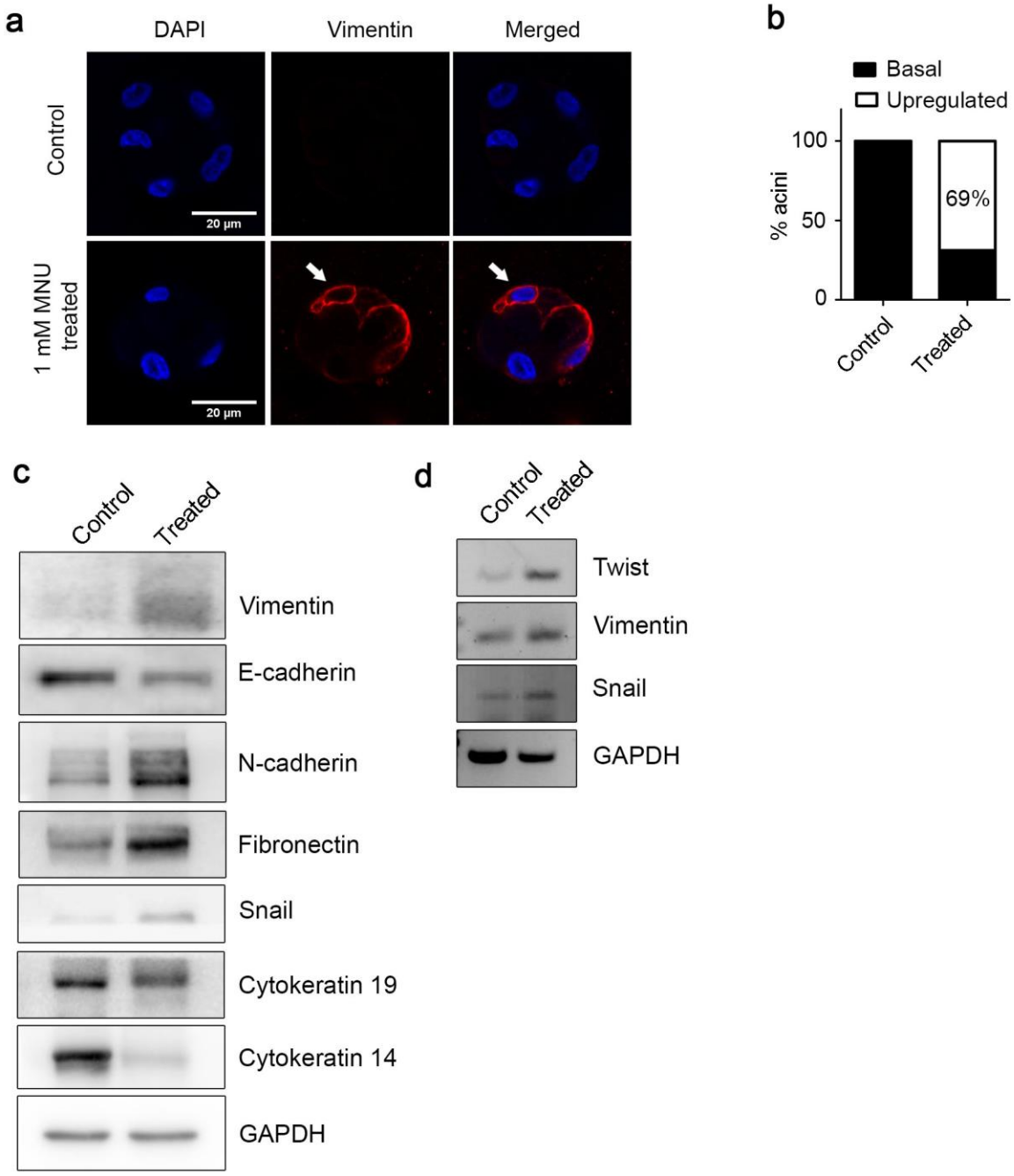

Figure 3.12: Methylation damage induced EMT in MCF10A cells grown as 3D "on top" cultures.

(a) Day 16 cultures of MCF10A cells were immunostained for vimentin, a mesenchymal marker (red). Arrow head (white) indicates the staining of vimentin. (b) Graph representing the % of acini showing upregulation of vimentin. (c) Day

16 acini were lysed and immunoblotted for mesenchymal markers like vimentin, N-cadherin, fibronectin and Snail and epithelial markers such as E-cadherin, cytokeratins 14 and 19. (d) RNA was extracted from day 16 cultures, cDNA prepared and used to investigate the level of mesenchymal markers, twist, vimentin and Snail at the transcript level. Data is representative of >5 independent experiments. Scale bar: 20 μm.

3.2.7 MNU exposure induces migration at the single cell level.

Acquisition of mesenchymal phenotype is usually coupled with increased migratory ability. To determine whether the cells treated with MNU exhibited enhanced migration, both collective cell migration and migration at single cell level was studied. Collective cell migration was studied using wound healing assay. The wound area at different timepoints was measured using ImageJ software and the percentage wound closure calculated. The data revealed that the methylation damage did not affect collective cell migration (Figure 3.13). Since we observed loss of cell-cell contact and induction of EMT in MNU treated cells, we investigated whether the motility at the single cell level is affected. To study this, cells tagged with CFSE (Carboxyfluorescein succinimidyl ester). CFSE is a cell permeable dye which selectively stains the cytoplasm of live cells by covalently binding to the intracellular amine sources. The CFSE stained cells were seeded sparsely and time-lapse imaging was done with images being captured at an interval of 2 minutes. The cells were tracked using Manual tracking plugin of ImageJ and this was followed by analysis of motility parameters using Chemotaxis and migration tool. We found that cells treated with MNU were more motile and traversed longer distance as compared to the untreated cells thus suggesting the acquisition of migratory behaviour.

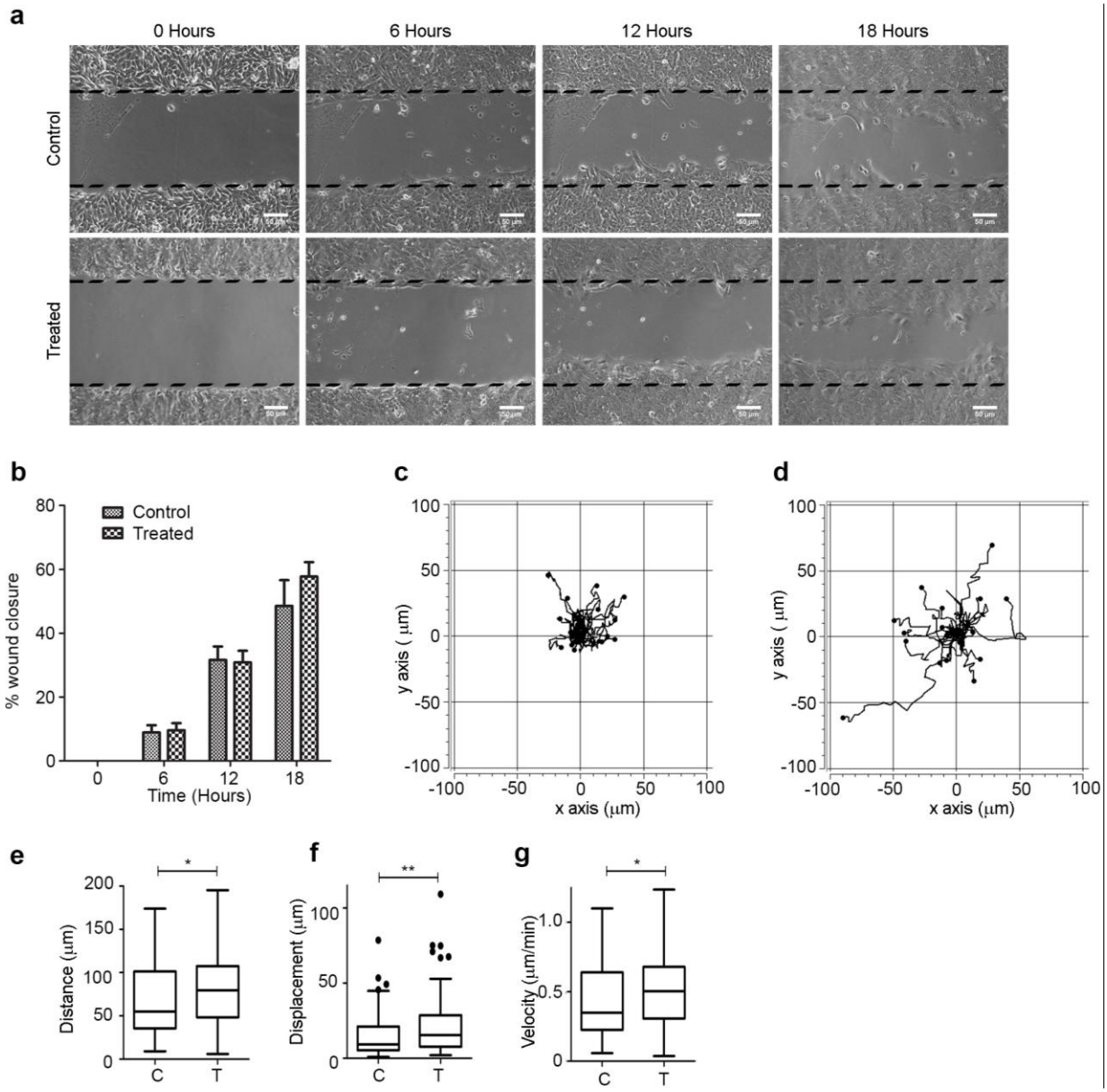

Figure 3.13: Methylation damage induces migration at the single cell level. MCF10A cells dissociated from day 16 acini were subjected to wound healing assay using ibidi inserts and single cell migration assay. (a) Representative images of wound healing assay. Cells were seeded in the ibidi inserts, treated with mitomycin C for 2 hours and images acquired after pre-determined time points. (b) Graph representing the % wound closure. Time lapse images of dissociated cells stained using CFSE dye and seeded at low confluency were acquired at 2 minutes interval for 160 minutes. Cells were tracked manually using

the Manual tracking plugin of ImageJ and analyzed using Chemotaxis and Migration tool (Ibidi GmbH, Munich, Germany) to measure the various parameters. Trajectory plots of a few randomly selected (c) untreated (d) MNU treated cells obtained using Chemotaxis and Migration tool. Box plots representing (e) accumulated distance (f) Euclidean distance (g) velocity. Mann-Whitney test was used to test the statistical significance of data. *P < 0.05, **P < 0.01. Data is representative three independent experiments, > 150 cells per treatment group.

3.2.8 MNU treatment induces invasion.

EMT is considered as a crucial event preceding the attainment of invasive potential during the complex process of cancer progression (Christiansen and Rajasekaran, 2006; Thiery, 2003). Given that MNU treatment induced EMT in MCF10A cells, we investigated whether it also induced invasiveness. To study invasion, we used the Collagen:Matrigel invasion assay. In this assay, Collagen and Matrigel™ are mixed in equal ratios to alter the matrix stiffness so as to allow the formation of inter-acinar bridges which indicate the ability of cells to invade (Xiang and Muthuswamy, 2006). Surprisingly in our study we observed that though the untreated cells differentiated to form acinar structures, the MNU treated cells failed to form such structures and instead grew as sheets. These sheets of cells resembled the duct-like structures as described by Dhimolea *et al* (Dhimolea et al., 2010). Immunostaining of laminin-5 revealed its mis-localization into the cytoplasm in the duct like structures formed by the cells treated with MNU (Figure 3.14a). This phenotype has been reported in the cells at the invasive fronts in epithelial cancers (Giannelli and Antonaci, 2000). Apart from this, the MNU treated cells exhibited elongated morphology characteristic of mesenchymal cells, further supporting our claim of MCF10A cells acquiring mesenchymal characteristics. However, since the assay did not aid in determining the acquisition of invasiveness we performed DQ collagen™ invasion assay. DQ collagen™, Dye quenched collagen, is non-fluorescent in it's native state. Following cleavage by matrix metalloproteinases (MMPs), fluorescence is emitted, thus indicating ability of cells to invade. In our study, we observed enhanced fluorescence in collagen bed invaded by MNU treated cells thus suggesting the invasive potential of these cells (Figure 3.14b and Figure 3.14c). To further confirm the enhanced secretion of active MMPs, the conditioned media of cells dissociated from day 16 3D cultures was subjected to gelatin zymography. Presence of significantly higher amounts of active MMP-9 in media was detected, thus confirming the induction of invasiveness in breast epithelial cells following methylation damage (Figure 3.14d).

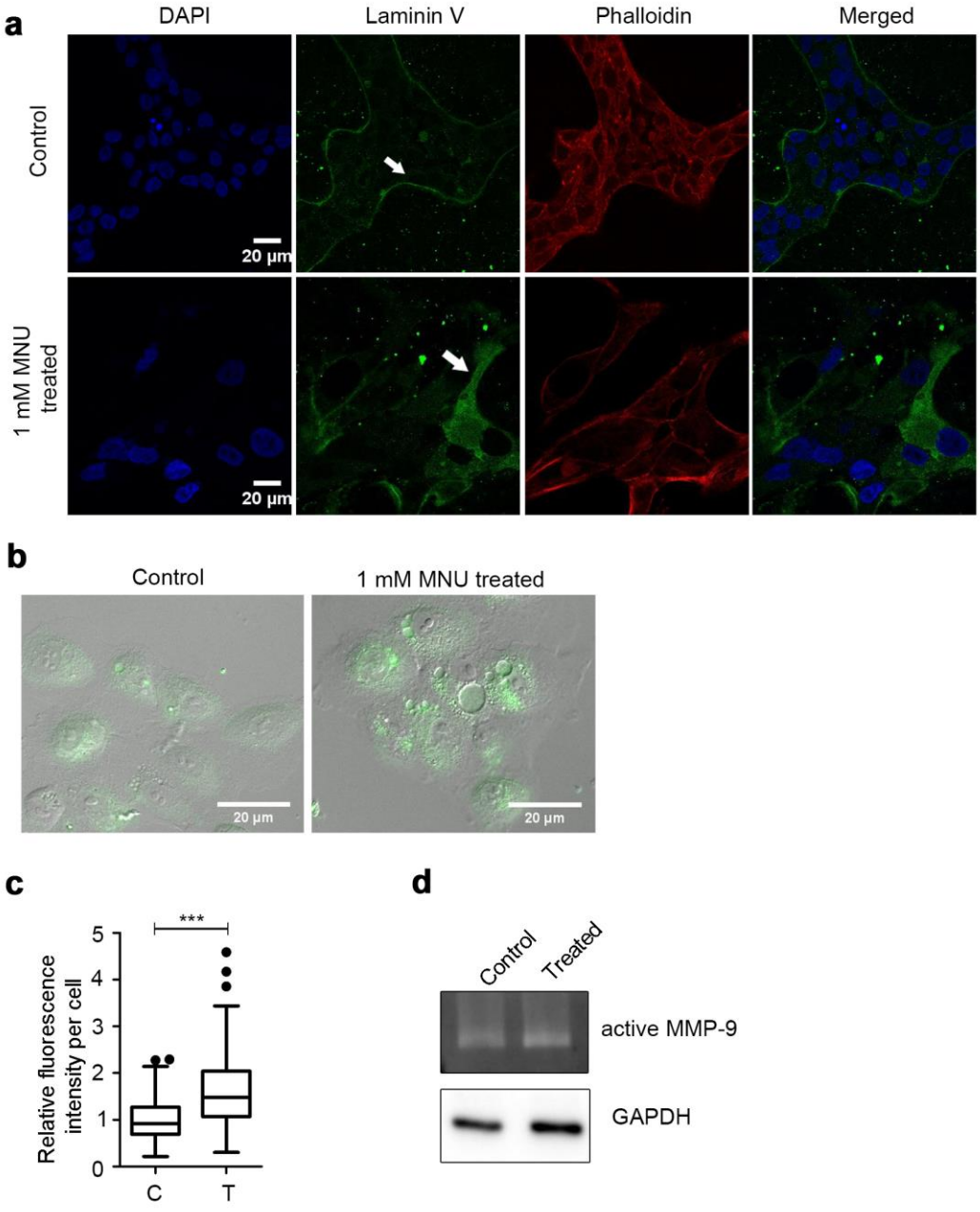

Figure 3.14: Methylation damage induces invasiveness in MCF10A cells.
(a) Representative images of MCF10A cells grown on matrix containing Collagen and Matrigel^{TM} in the ratio 1:1, for a period of 16 days immunostained with laminin-5 (green) and phalloidin, a actin staining dye (red). Nuclei were counter stained with Hoechst 33342 (blue). Arrow head (white) indicate the abnormal localisation of laminin-5. Cells dissociated from day 16 acini were seeded on

Collagen containing DQ^{TM} collagen. (b) Representative images of untreated and treated cells 48 hours following seeding. (c) Graph representing the relative fluorescence intensity of DQ collagen bed measured using ImageJ software. The absolute fluorescence intensities have been normalized to that of control. Mann-Whitney test was used to analyze the statistical significance of difference. (d) Conditioned media from DQ^{TM} collagen invasion assay was collected and subjected to Gelatin zymography to obtain the bands of clearance due to gelatinase activity of active-MMP-9. C denotes control and T denotes treated. Data is representative of >2 independent experiments. *** $p<0.0001$. Scale bar: 20 μm.

3.2.9 Exposure of MCF10A cells, grown as 3D cultures, to MNU during initial days of morphogenesis results in transformation.

To ascertain whether the changes observed and reported above are only due to phenotypic transformation or the cells had undergone malignant transformation, soft agar assay, the most stringent *in vitro* assay of transformation was performed. Cells dissociated from day 16 acini were used for the assay. Single cell suspension of cells was grown in 0.3% agar for 18 days, following which viable colonies were identified using 1 mg/ml MTT. MTT is a tetrazolium salt which is metabolized by the cells to form purple formazan crystals. Colonies were counted from 10 randomly selected fields per dish and mean was calculated. We observed that in contrast to untreated cells which fail to survive in anchorage independent conditions, MNU treated cells formed colonies and were viable (Figure 3.15a and Figure 3.15b). Thus, these results signify that methylation damage induced by MNU in non-transformed breast epithelial cells results in malignant transformation.

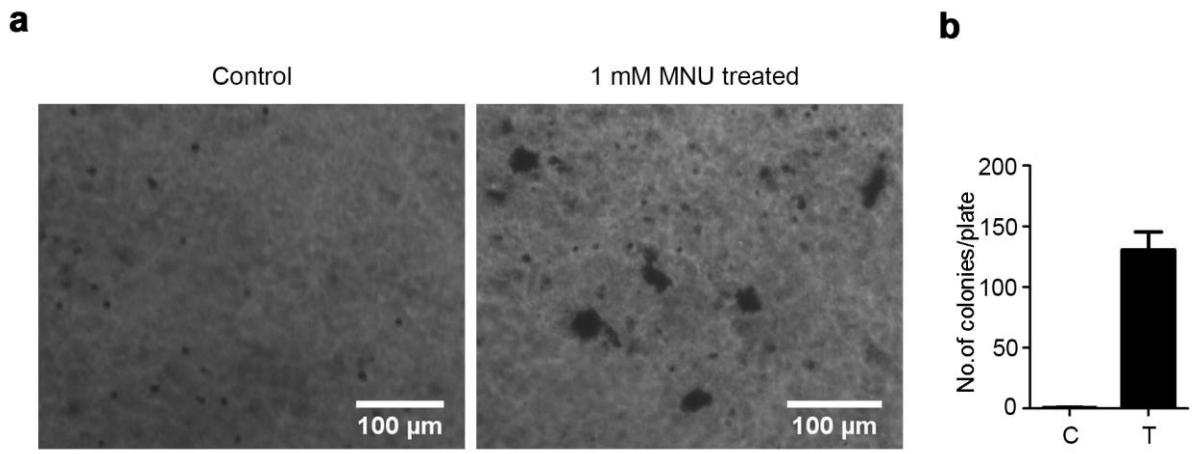

Figure 3.15: MNU treated cells show enhanced survival in anchorage independent conditions.

Untreated and treated cells from day 16 acini were dissociated using Dispase™ and seeded in 0.3% agar over a 0.6% agar layer. Following 18 days of culturing, the cells were treated with 1 mg/ml of MTT solution for 30 minutes and images of viable colonies were captured using 4X objective of Nikon microscope. (a) Representative images of soft agar assay. (b) Graph representing mean +/- standard error of total number of colonies present in 10 randomly selected fields per treatment group. C denotes control and T denotes treated. Data is representative of two independent experiments performed in triplicates. Scale bar: 100 μm.

3.2.10 DNA-PK mediates methylation damage induced Golgi dispersal.

Golgi dispersal observed in MNU treated cells was the most striking phenotype in our study. A similar dispersed Golgi phenotype has also been observed in cancers (Byrne et al., 2015; Petrosyan et al., 2014). A recent report by Farber-Katz *et. al.,* corroborated with our observation and demonstrated that activation of DNA-PK, one of the apical kinase in DDR (DNA Damage Response) pathway, mediated the dispersal of Golgi through the hyperactivation of GOLPH3/MYO18/F-actin axis (Farber-Katz et al., 2014). In addition to this, they also reported that the dispersal was essential for the survival of the cells following damage. We investigated whether MNU induced damage activated DNA-PK under the conditions of our study. We observed that DNA-PKcs, the catalytic sub-unit of DNA-PK, was activated within 10 minutes of DNA damage (Figure 3.16a). Golgi dispersal was observed 4 hours after damage, thus confirming that DNA-PK activation preceded Golgi dispersal (Figure 3.16b and Figure 3.16c). To ascertain whether activation of DNA-PK was linked to Golgi dispersal, we used 25 μm DMNB, a small molecule selective inhibitor of kinase activity of DNA-PK. Inhibition of DNA-PK (Figure 3.17a and Figure 3.17b) resulted in reversal of Golgi dispersal (Figure 3.18a and Figure 3.18b). Interestingly, the cells dissociated from day 16 acini also showed dispersed phenotype which was reversed following inhibition of DNA-PK kinase activity (Figure 3.18c and Figure 3.18d). Taken together these results imply that there is a constitutive activation of DNA-PK following DNA damage which resulted in persistently dispersed Golgi. Interestingly, MCF10A series of cell lines, which are widely used to answer intriguing questions of cancer progression, also showed dispersal of Golgi in premalignant MCF10AT1 and malignant MCF10CA1a cell lines. Surprisingly, the dispersed phenotype was to some extent reversed by treatment with DMNB (Figure 3.19a-c), thus implying the possible role of DNA-PK in dispersed Golgi in the two cell lines.

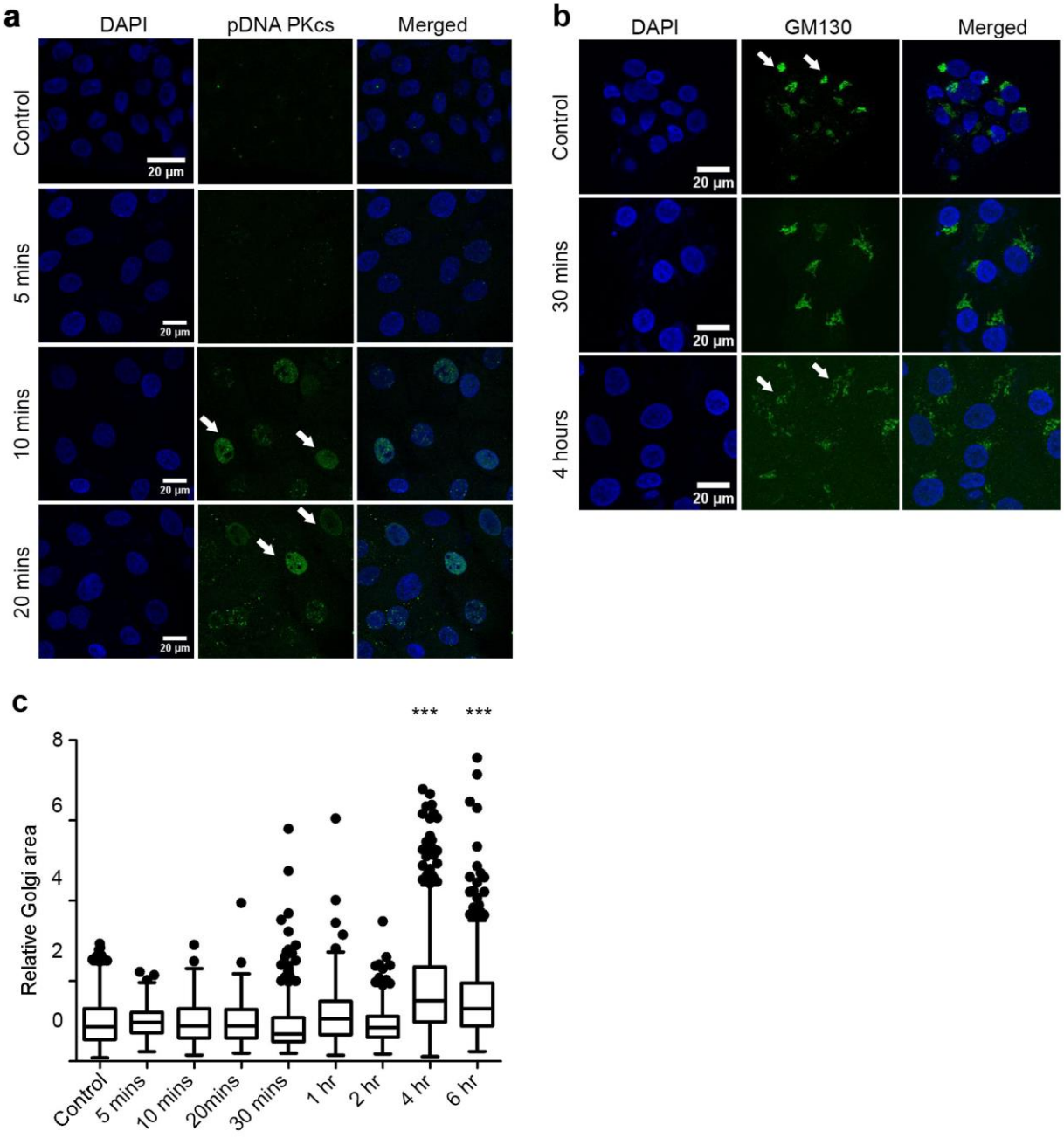

Figure 3.16: MNU induced DNA damage activates DNA-PKcs which in turn results in Golgi dispersal.

Monolayer cultures of MCF10A cells were treated with 1 mM MNU and immunostained after predetermined time-points. (a) Representative images of MCF10A cells immunostained for phospho DNA-Pkcs (S2605) (green). Arrow head (white) mark representative cells with nuclei marked for phospho DNA-

PKcs . (b) Representative images of MCF10A cells immunostained for GM130 (green), a cis Golgi element. Arrow head (white) marks cells with intact as well as dispersed Golgi morphology. (c) Graph depicting the relative Golgi area normalized to control across different time-points. One way ANOVA (Kruskal walis test) was used to test the statistical significance in the relative Golgi area. $p<0.0001$ has been considered statistically significant. *** $p<0.0001$. Data is representative of three independent experiments. Scale bar: 20 μm

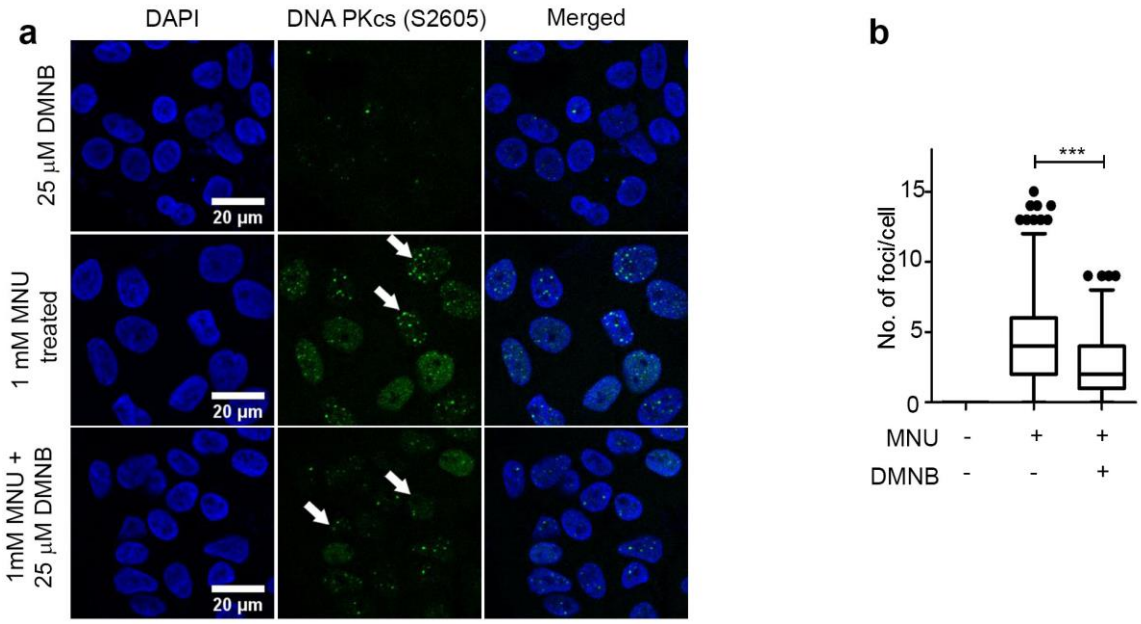

Figure 3.17: MNU induced activation of DNA-PK.

MCF10A cells grown as monolayer cultures were treated with 1 mM MNU with and without DMNB, DNA-PK inhibitor and were immunostained. (a) Representative images of MCF10A cells immunostained for pDNA-Pkcs (S2605) (green). (b) Graph representing the number of pDNA-PKcs foci per cell.

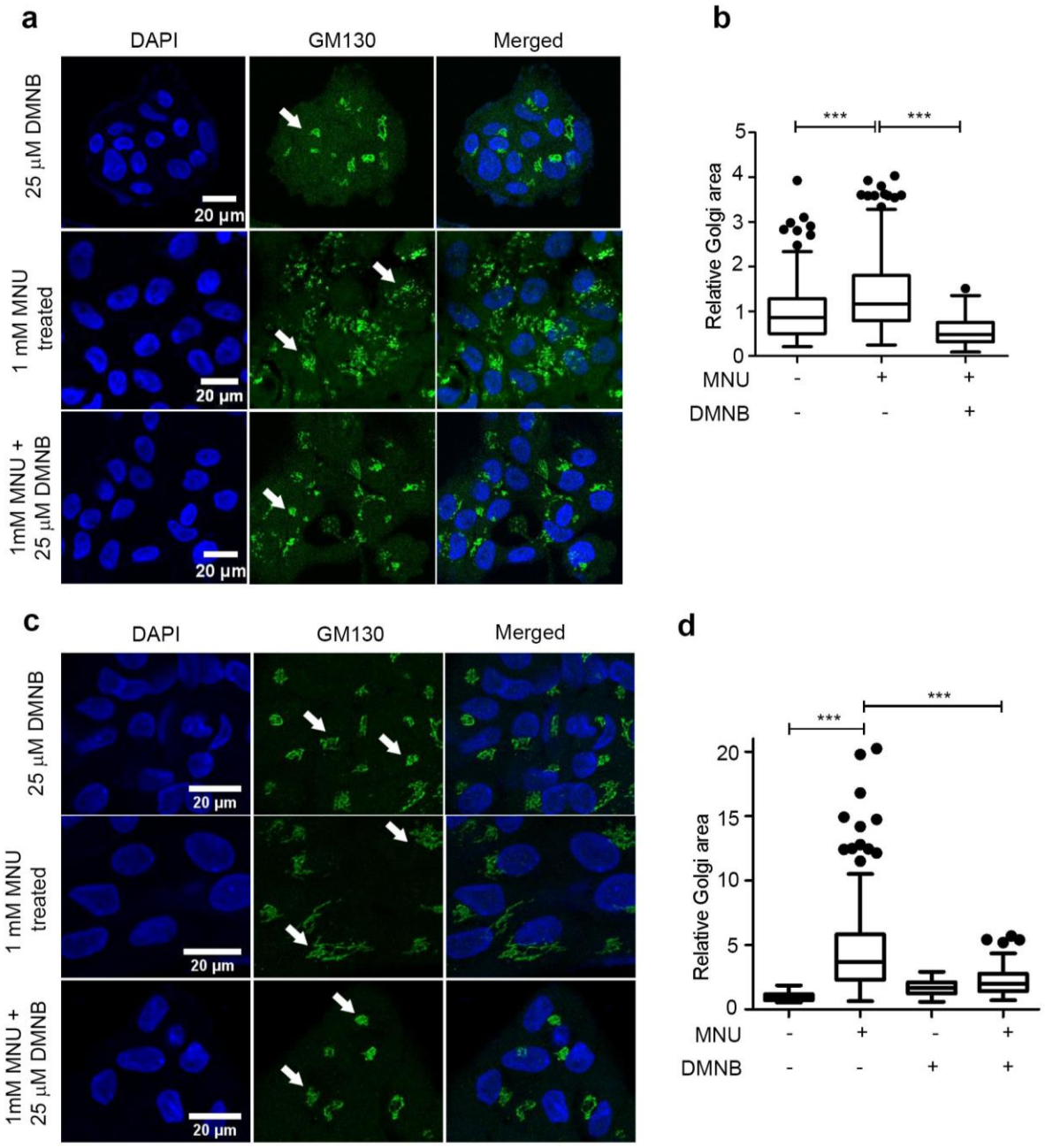

Figure 3.18: MNU induced Golgi dispersal is via activation of DNA-PK. MCF10A cells grown as monolayer cultures were treated with 1 mM MNU with and without DMNB, DNA-PK inhibitor and were immunostained. (a) Representative images of MCF10A cells immunostained for GM130 (green), a cis Golgi element. (b) Graph depicting the relative Golgi area normalized to control across different treatments. (c) Cells dissociated from day 16 acini were

grown as monolayers and immunostained for GM130 (green). (d) Graph depicting the relative Golgi area normalized to control across different treatments. One way ANOVA (Kruskal walis test) was used to test the statistical significance in the relative Golgi area. $p<0.0001$ has been considered statistically significant. *** $p<0.0001$. Data is representative of >3 independent experiments. Scale bar: 20 μm.

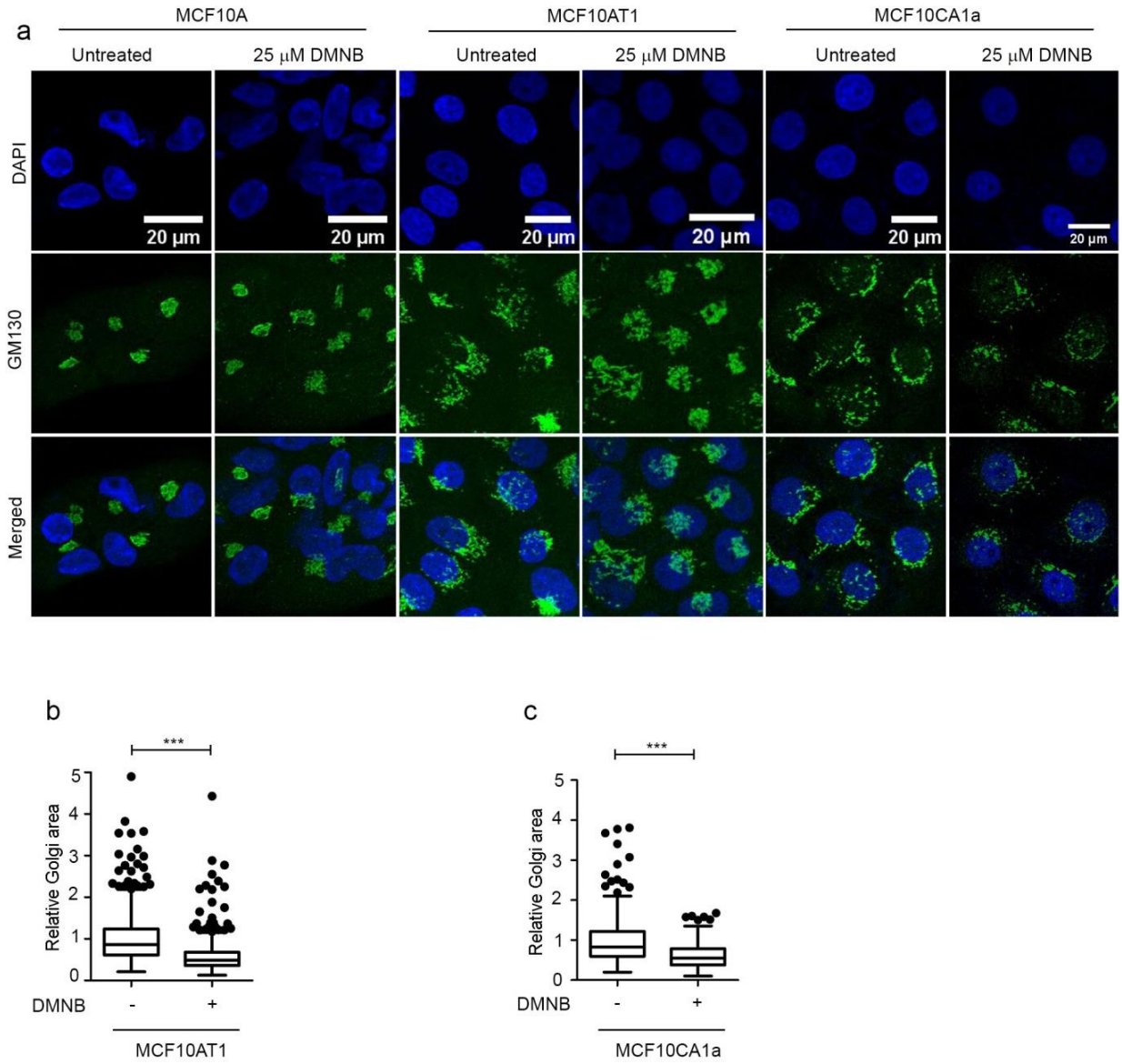

Figure 3.19: Golgi dispersal observed in MCF10A series is partially reversed following DNA-PK inhibition.

MCF10 series of cell lines, namely non tumorigenic MCF10A; pre-malignant MCF10AT1 and malignant MCF10CA1a, were grown as monolayers, treated with 25 μM DMNB, DNA-PK inhibitor, and immunostained for GM130, Golgi marker. The Golgi area was measured using ImageJ software and normalized to control. (a) Representative images of the three cell lines immunostained for GM130 and nuclei counter stained with Hoechst 33342. (b) Graph representing the relative Golgi area of MCF10AT1 cell line with and without 25 μM DMNB treatment. (c)

Graph representing the relative Golgi area of MCF10CA1a cell line with and without 25 μM DMNB treatment. Mann-Whitney test was used to analyze the statistical significance of difference in relative Golgi area. Data is representative of three independent experiments. *** $p<0.0001$. Scale bar: 20 μm

3.2.11 DNA-PK activation plays a central role in MNU damage induced transformation.

DNA-PK has been implicated to play differential role in various cancers. Its role in breast cancer remains elusive. Since we observe a probable constitutive activation of DNA-PKcs (implied by the persistent dispersal of Golgi) in our study, we questioned whether the transformation phenotype induced by MNU was mediated via DNA-PK. To answer this, we exposed MNU treated cells to 25 μm DMNB, inhibitor of DNA-PK kinase activity and investigated the integrity of the adherens junctions. We observed the relocalization of E-cadherin following DMNB treatment (Figure 3.20a). In addition to this, day 16 cultures were treated with 25 μm DMNB twice for 12 hours each, and lysates were collected. Immunoblot analysis showed a reduction in the levels of mesenchymal markers namely vimentin, fibronectin and N-cadherin which were upregulated in cells treated with MNU (Figure 3.20b). To discern the effects of DNA-PK inhibition on the migratory ability of the transformed cells, single cell migration assay was performed on cells dissociated from MNU treated acini after DMNB exposure. We observed a reduction in the migratory ability of the cells following DMNB treatment (Figure 3.21a to Figure 3.21b), thus implying that DNA-PK activation resulted in the increased motility of the transformed cells. Furthermore, DQ^{TM} collagen invasion assay (Figure 3.22a and Figure 3.22b) and gelatin zymography (Figure 3.22c) revealed that inhibition of DNA-PK inhibited invasion. Besides this, cells treated with MNU also showed reduced survival in anchorage independent conditions upon inhibition of DNA-PK (Figure 3.23a and Figure 3.23b).
Taken together, these results signify the central role played by DNA-PK in DNA damage induced transformation.

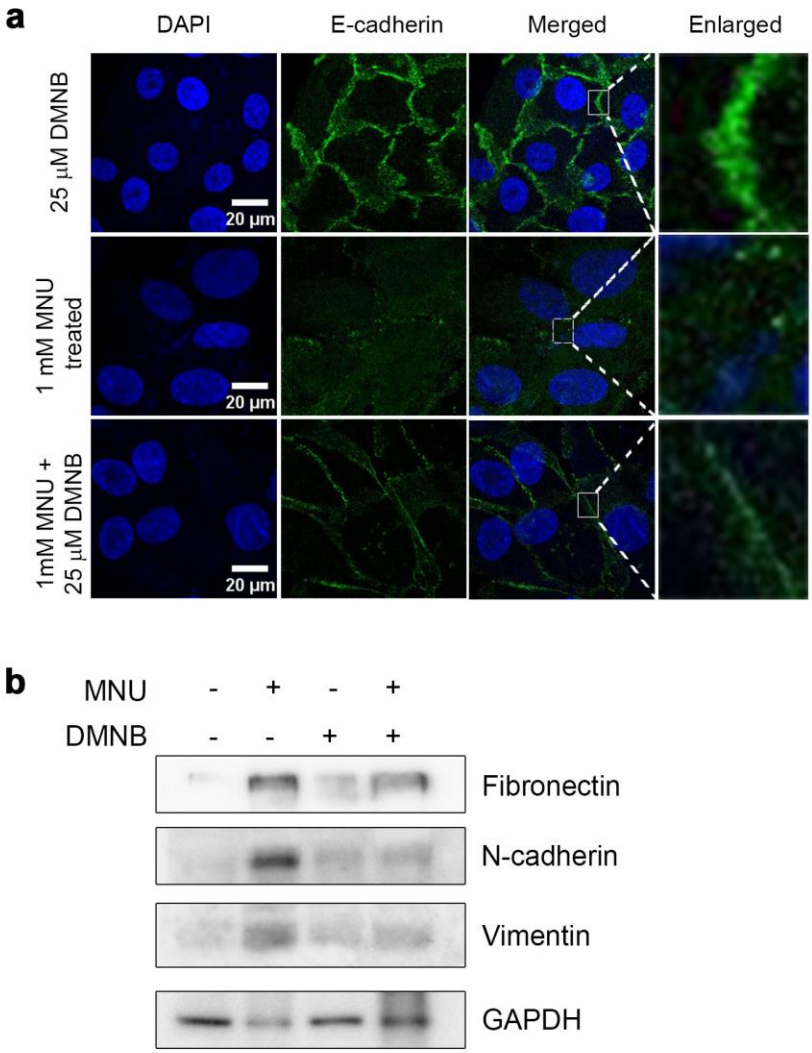

Figure 3.20: DNA-PK plays a role in methylation damage induced EMT.

(a) Monolayer cultures of MCF10A were treated with 1 mM MNU for 24 hours on day0 as well as day2 followed by treatment with 25 μm DMNB twice 12 hours each and immunostained with E-cadherin. Nuclei were counterstained with Hoechst 33342. (b) Day 16 3D spheroids were treated with 25 μM DMNB twice for 12 hours, were lysed, immunoblotted and probed for mesenchymal markers such as vimentin, fibronectin and N-cadherin. Data is representative of three independent experiments. Scale bar: 20 μm

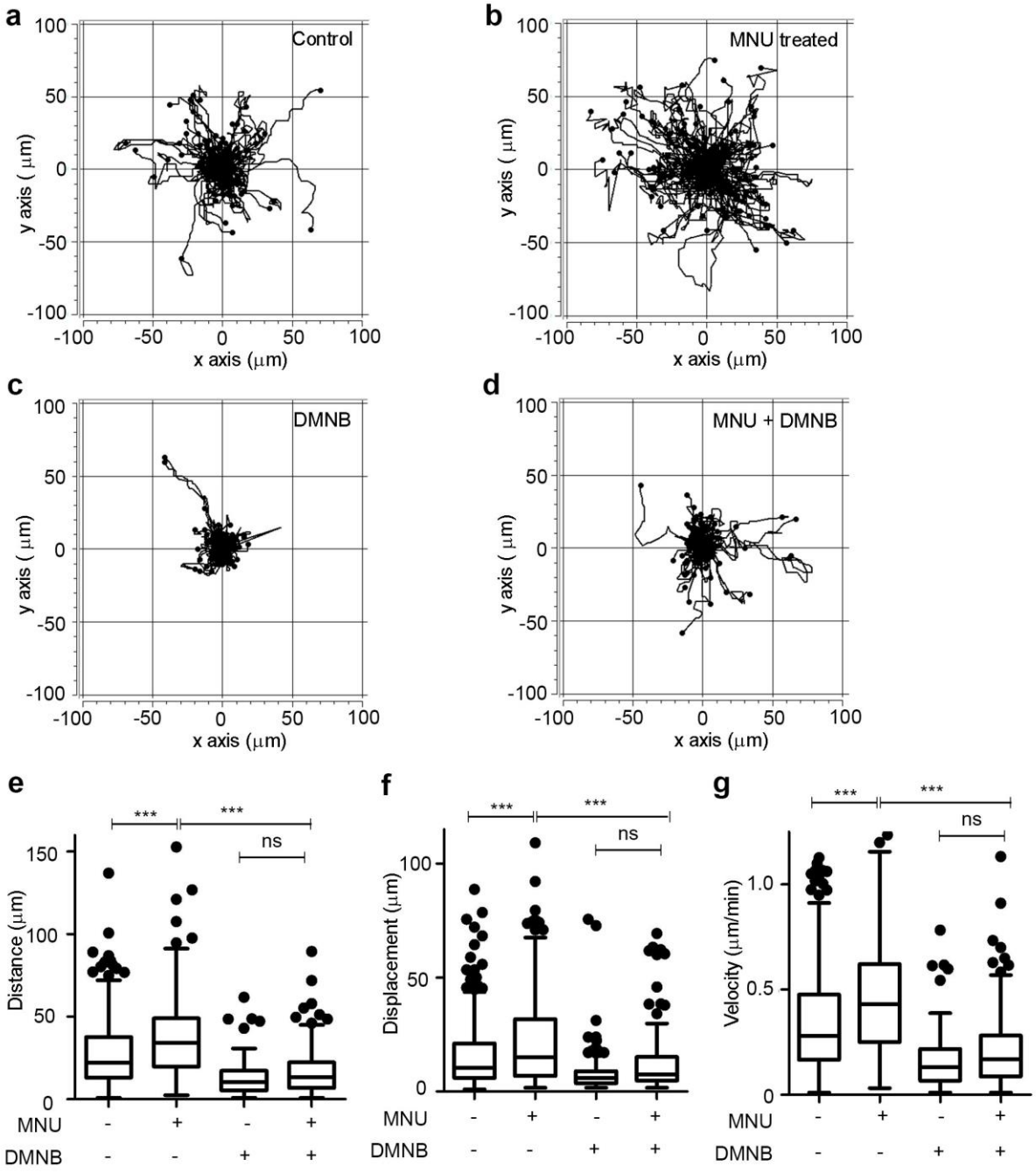

Figure 3.21: MNU induced migration is inhibited by DNA-PK inhibition.
MCF10A cells dissociated from day 16 acini were subjected to single cell migration assay. Time lapse images of dissociated cells stained using CFSE dye and seeded at low confluency were acquired at 2 minutes interval for 160 minutes. Cells were tracked manually using the Manual tracking plugin of ImageJ software and analyzed using Chemotaxis and Migration tool (ibidi GmbH,

Munich, Germany) to measure the various parameters. Trajectory plots of a few randomly selected (a) untreated (b) MNU treated (c) DMNB treated (d) MNU and DMNB treated cells obtained using Chemotaxis and Migration tool. Box plots representing (e) accumulated distance (f) Euclidean distance (g) velocity. One way ANOVA (Kruskal walis test) was used to test the statistical significance of data. ***$p < 0.0001$. Data is representative of three independent experiments.

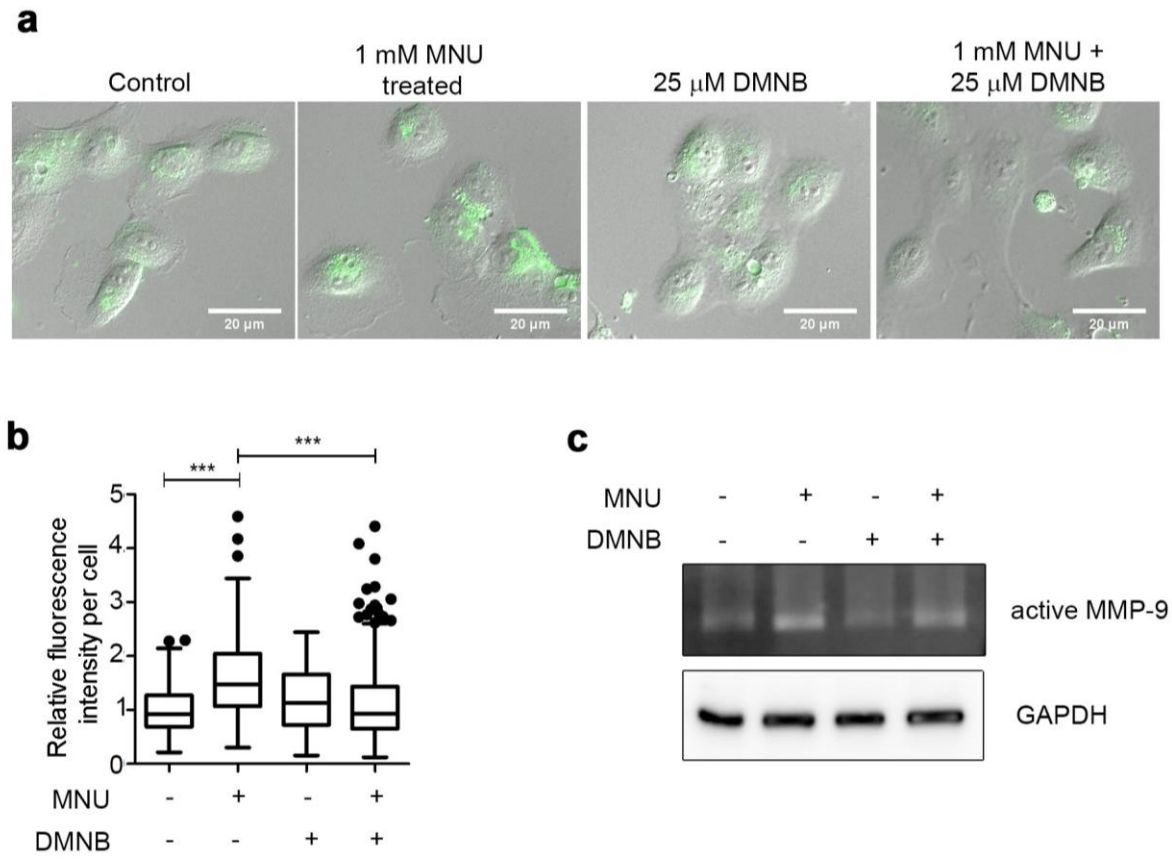

Figure 3.22: DNA-PK inhibition inhibited invasiveness of MNU treated cells. Cells dissociated from day 16 acini were seeded on collagen containing DQ™ collagen and imaged after 48 hours using Olympus IX81 system. Fluorescence intensity was measured using ImageJ. (a) Representative images of cells 48 hours post seeding on collagen. (b) Graph representing the relative fluorescence intensity normalized to control. Data is representative of two independent experiments. One way ANOVA (Kruskal walis test) was used to test the statistical significance of data. (c) Conditioned media from DQ™ collagen assay was subjected to Gelatin zymography. Representative images of Coomassie gel showing gelatinase activity of active MMP-9. ***$p < 0.0001$. Scale bar: 20 μm

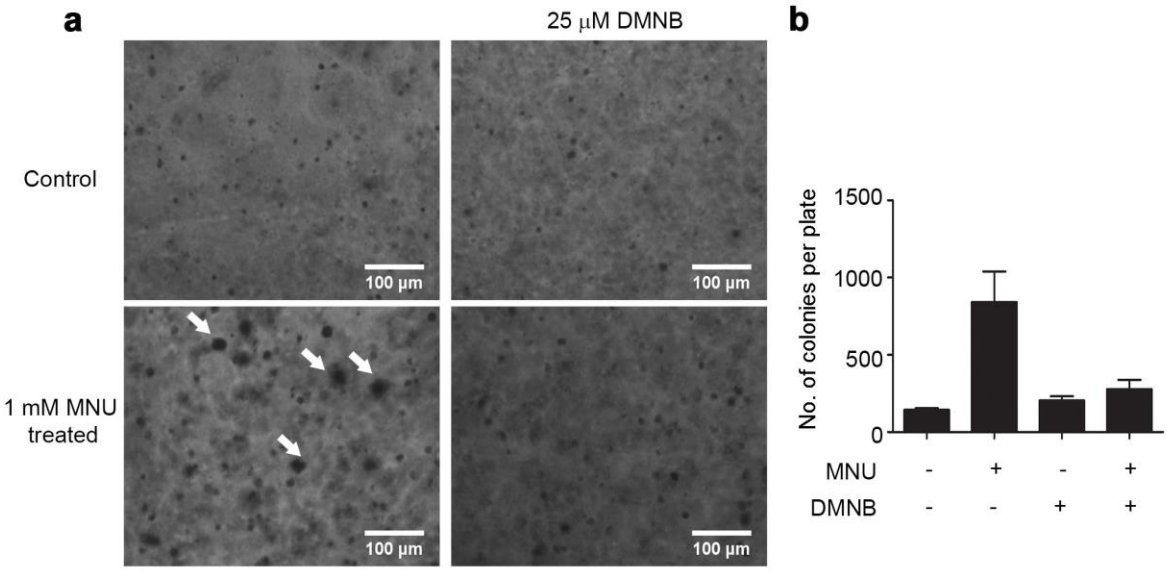

Figure 3.23: DNA-PK inhibition results in reduced ability of cells to survive in anchorage independent conditions.

Cells dissociated from acini of day 16 cultures were mixed with 0.3% agar and grown in a dish pre-coated with 0.6% agar for 18 days. 1 mg/ml of MTT was used to mark the colonies. 20 random fields were selected and colonies were counted to determine the number of colonies per dish. (a) Representative phase contrast images of one of the fields per treatment imaged using 4X objective of Nikon microscope. White arrows indicate the colonies formed by cells on soft agar. (b) Graph representing mean +/- standard error of the number of colonies per dish counted from 20 randomly selected fields. Data is representative of two independent experiments performed in triplicates. Scale bar: 20 μm.

3.2.12 Exposure to NEU *(N*-ethyl-*N* nitrosourea*),* an ethylating agent disrupts basolateral polarity and induces EMT-like phenotype similar to methylating agent.

N-nitroso-*N*-ethylurea (NEU) is a monofunctional S_N1 type-DNA ethylating agent. NEU has been found to be a severely potent transplacental teratogen (Givelber and DiPaolo, 1969) and an active rat mammary gland genotoxic carcinogen in rodents (Stoica et al., 1983). NEU has been reported to induce neoplastic transformation of rat mammary epithelial cells. (Stoica et al., 1991). Previous studies in the lab have demonstrated the ability of NEU to induce DNA strand breaks (Bodakuntla et al., 2014). To study the effect of NEU on MCF10A cells, dosing regimen similar to MNU was followed. Different doses of NEU were added to 3D cultures ranging from 2 mM NEU to 5mM NEU. Lowest dose of NEU, 2 mM, which disrupted polarity, was used in this study. 2 mM NEU was used as the sub-lethal dose. We observed both mis-localization of α6-integrin as well as loss phenotype in a few acini (Figure 3.24a). Further laminin-5 also showed a discontinuous staining in basal region indicating loss of basal polarity (Figure 3.24b). Further, we also observed loss of E-cadherin from the cell-cell junctions (Figure 3.24c) and aberrant β-catenin staining (Figure 3.24d) similar to that observed following MNU treatment. Vimentin, the mesenchymal marker, was also found to be up-regulated (Figure 3.24d). Thus, taken together, NEU was also capable of inducing transformation of non-transformed breast epithelial cells.

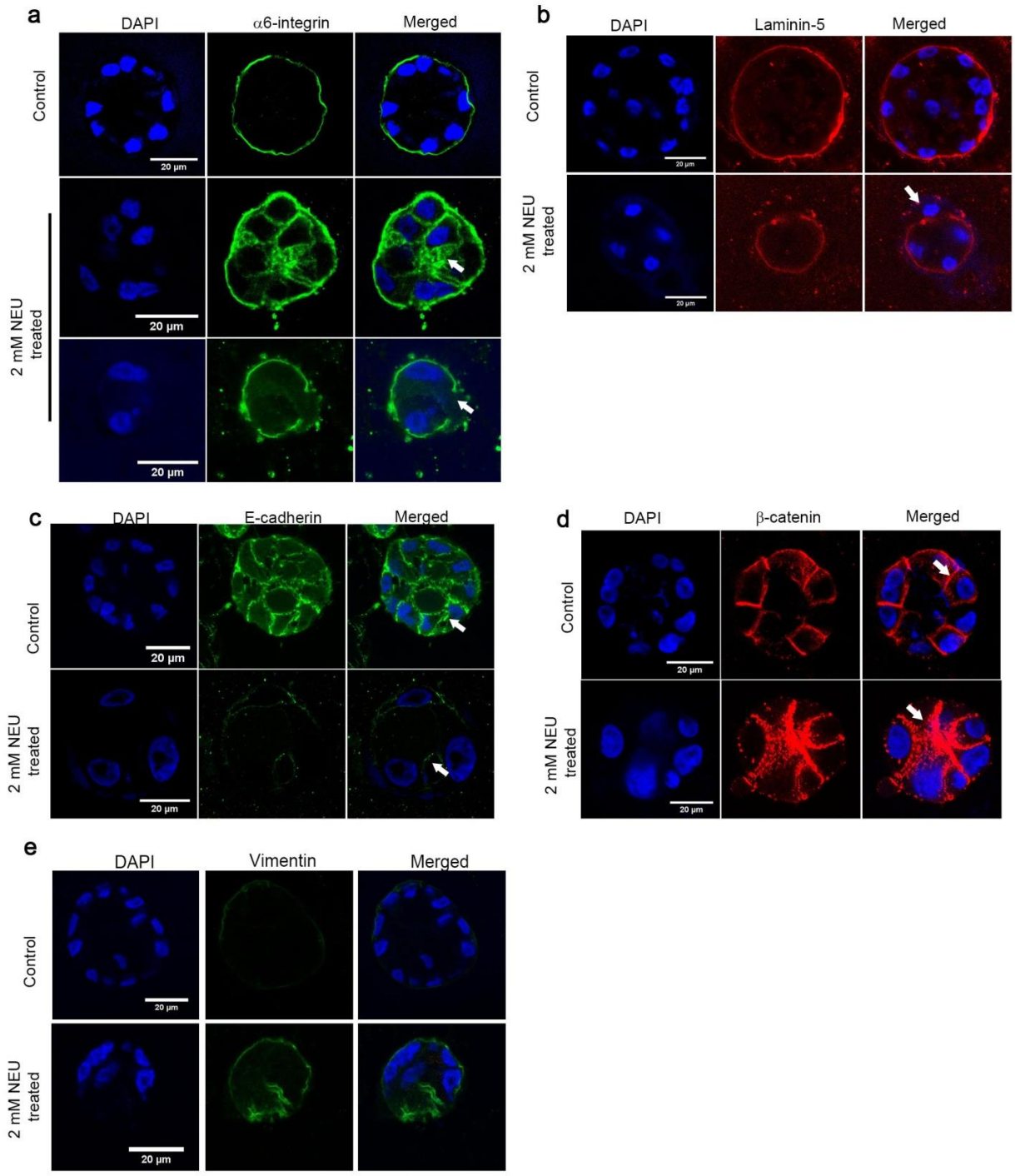

Figure 3.24: NEU exposure disrupts basolateral polarity and induces EMT-like phenotype.

Day 16 cultures of MCF10A cells treated 2 mM NEU, were immunostained for markers of basolateral polarity as well as mesenchymal markers and analyzed

for their integrity. (a) Representative immunofluorescence images of acini labelled with (a) α6-integrin (green) (b) laminin-5 (red) (c) E-cadherin (green) (d) β-catenin (red) (e) Vimentin (green). Arrows (white) indicate the disruption observed in the polarity markers used. Data is representative of >5 independent experiments. Scale bar: 20 μm

3.3 Discussion

Understanding the mechanism of tumor initiation and progression and identification of key players involved contributes in the development of novel therapeutic strategies. In this study we illustrate the potential of DNA damaging agents to induce transformation of breast epithelial cells through the activation of DNA-PK. In general, exposures to DNA damaging agents are mainly through the environment as well as due to cancer chemotherapy. DNA damage surveillance mechanisms repair damaged DNA and safeguard the genome. However, our study demonstrates that mechanism itself can result in tumorigenesis. Our study, illustrates for the first time the role of DNA-PK, a key protein involved in DDR, in breast tumorigenesis.

DNA-PK is a holoenzyme made up of two regulatory subunits Ku70 and Ku80 as well as a catalytic subunit, DNA-PKcs, responsible for the kinase activity (Anderson and Lees-Miller, 1992; Yoo and Dynan, 1999). DNA-PK has been demonstrated in various studies to have diverse functions (Goodwin and Knudsen, 2014). The major role played by this complex is in the NHEJ pathway of DDR following formation of DSBs. Inhibition of DNA-PKcs has been reported to result in increased sensitivity to genotoxic agents (Morozov et al., 1994). Besides its well-established role in DDR, DNA-PK has been illustrated to regulate transcription of various genes by phosphorylating transcription factors such as c-Myc, c-Jun, Sp1, Oct-1, and p53 (Lees-Miller, 1996). It has also been reported to play a vital role in cell cycle. Known as a critical player in safeguarding the genome, DNA-PK has been reported to regulate the entry into mitosis depending on presence or absence of DNA damage, thus contributing to genomic stability (Lee et al., 2011). On the contrary it is also known to promote genomic instability and chemo-resistance mediated by Snail1 (Kajita et al., 2004; Pyun et al., 2013). However its role in cancer is ambiguous. PRKDC, the gene encoding for DNA-PKcs, has been found to have low expression in lung cancers (Hsia et al., 2014), ovarian cancers (Shao et al., 2007) as well as gastric cancer (Lee et al., 2007), while a higher expression has been reported in hepatocellular carcinoma (Cornell

et al., 2015), prostate cancer (Goodwin et al., 2015) and in melanomas (Kotula et al., 2015). Recent reports suggest over-expression of DNA-PKcs regulates metastasis of prostate cancer cells through a transcription regulation (Goodwin et al., 2015). Furthermore, DNA-PK inhibition was found to inhibit formation of primary melanoma, delayed metastasis to lymph nodes as well as inhibited secretion of MMPs (Kotula et al., 2015). However its role in breast cancer remains elusive. Cimmino *et. al*. identified PRKDC as one of the genes being upregulated in breast cancer patients which was also found to be associated with reduced survival (Cimino et al., 2008). This result was in concordance with the data collected by van de Vijver *et al* (van de Vijver et al., 2002) and Sotirou *et al* (Sotiriou et al., 2006). These reports further support our hypothesis of the role of constitutively activated DNA-PKcs in DNA damage induced transformation.
MNU, a prototypic SN1 methylating agent, is capable of methylating DNA at *O6* positions of guanine, a lesion which is considered to be the most mutagenic as well as cytotoxic (Kondo et al., 2010). It has also been shown to induce DNA strand breaks (Menke et al., 2000). We found that the DNA damage induced apart from causing DSBs and SSBs also disrupted Golgi morphology impairing trafficking. This Golgi phenotype was in corroboration with report by Farber-Katz *et al.*(Farber-Katz et al., 2014), wherein the dispersed phenotype was attributed to the activation of DNA-PK. The dispersal of Golgi observed in our study was also found to be reversed upon inhibition of DNA-PK using DMNB, a small molecule inhibitor. Golgi being a central organelle in polarized sorting of proteins, disruption of its function could result in disruption of polarity of epithelial cells. Investigation of effect of methylation damage in establishment of polarity, we observed disruption of apical as well as basolateral polarity. Laminin-5 apart from being lost from the basal region of acinar structures was found to be mis-localized to cytoplasm in altered stiffened extracellular matrix. This phenotype can also be explained by the impaired trafficking resulting in accumulation of the protein in the cytoplasm. This phenotype has also been referred in literature to be indicative of invasive phenotype. Invasive cells are known to breakdown the

basement membrane so as to invade the nearby tissue and disseminate to distant organs (Vidi et al., 2013) . Similar loss phenotype of laminin-5 was observed in our study. We also observed that most of the acini formed by cells exposed to DNA damage showed loss of α6-integrin from the basal region. α6β4-integrin subunits are involved in the formation of hemidesmosomes in epithelial cells (Sonnenberg et al., 1991). Down-regulation of this α6-integrin subunit has been observed in cells metastasizing to the pleural cavity and parenchyma (Natali et al., 1992).Thus these results suggest the possible induction of invasiveness in cells following DNA damage. This was later confirmed by DQ™ collagen invasion assay as well as assessing the presence of active MMP-9 in the conditioned media. EMT which is one of the initial processes in invasion was also found to be induced in the MNU treated cells. These cells also gained ability to survive under anchorage independence conditions, which is considered the most stringent criteria to identify transformed cells. The varied phenotypes namely EMT, invasion and anchorage independence besides Golgi dispersal, induced by DNA damage was reversed following inhibition of DNA-PK, thus confirming the central role played by DNA-PK in methylation damage induced transformation. Interaction between Snail1 and DNA-PK has been reported to result in increased activity of Snail1 (Pyun et al., 2013). Increased Snail activity results EMT, which confers to the results of our study where an upregulation of Snail1 was observed.

Taken together our study showed that activation of DNA-PKcs following methylation damage orchestrated Golgi dispersal and impaired trafficking thus, resulting in loss of basolateral polarity. Use of DNA-PK inhibitor on day 16 cultures, down-regulated mesenchymal markers as well as inhibited invasion. Further, Golgi dispersal was reversed following DNA-PK inhibition even after 30 days of incurring damage. These results suggest the constitutive activation of DNA-PK following DNA damage. This can be explained by the autophosphorylation tendency of DNA-PK. In addition to this, loss of basal polarity has been found to reduce the efficiency of repair of DSBs (Vidi et al.,

2012). This would either result in constitutive activation of DNA-PK or result in accumulation of chromosomal aberration when these cells enter cell-cycle and thus lead to carcinogenesis. Further, another striking feature noted in the study was the increase in nuclear volume. Increase in nuclear volume can be attributed to possible increase in nuclear content resulting due to mis-segregation of chromosomes. MNU is known to induce sister chromatid exchange and thus the increase in nuclear volume. (Bouffler et al., 2000; Neft and Conner, 1989; Neft et al., 1989). However, further investigations are needed to confirm the change in nuclear content of MNU treated cells. Detailed metaphase spread analysis or SKY might help in understanding this intriguing question.

Field,S. J and group in their study have illustrated that DNA damage by various agents including radiations, induced dispersal of Golgi (Farber-Katz et al., 2014). Further NEU and MNU result in different kind of mutations wherein NEU is known to induce random mutations (Acevedo-Arozena et al., 2008) while MNU is known to induce mutations at specific sites defined by a particular consensus sequence (Baumgart et al., 1993). The ability of NEU to induce transformation with phenotypes similar to that induced by MNU indicates that the effect caused by methylation damage is due to the DNA-damage induced in general and not specific to the chemical used. Further, given the vital role of DNA-PK in NHEJ pathway of DDR and NHEJ being the repair pathway active throughout all phases of cell cycle, the Golgi dispersal induced by activation of this holoenzyme maybe responsible for the transformation phenotype.

In sum, we have herewith established a model for DNA damage induced transformation and provided mechanistic insights into the process. We have demonstrated that the transformation following DNA damage occurred via DNA-PK mediated Golgi dispersal and impaired cellular trafficking (Figure 3.25). This study highlights the consequences of DNA damage and illustrates the novel role of DNA-PK in the process of transformation. Thus, use of inhibitor to DNA-PK as an adjuvant to chemotherapy can prove to be beneficial. Nevertheless, there could be multiple pathways which may synergistically contribute to the

transformation apart from the mechanism summarized in the Figure 3.25. This calls for further interrogation into the process and explore the other pathways so as to aid in identifying the various molecular players involved. The information thus gathered can then be used to design novel therapeutic strategies or modify the present strategies. The model established in this study can be further exploited to study alternate pathways as well as can be used for screening of therapeutics. In addition to this, such a model can be also be used to understand how early transformation occurs and identify the initial set of gene(s) that get deregulated in the process of transformation. Understanding this phenomena and recognition of key candidate genes as biomarkers could further help to design novel or modify available therapeutic strategies.

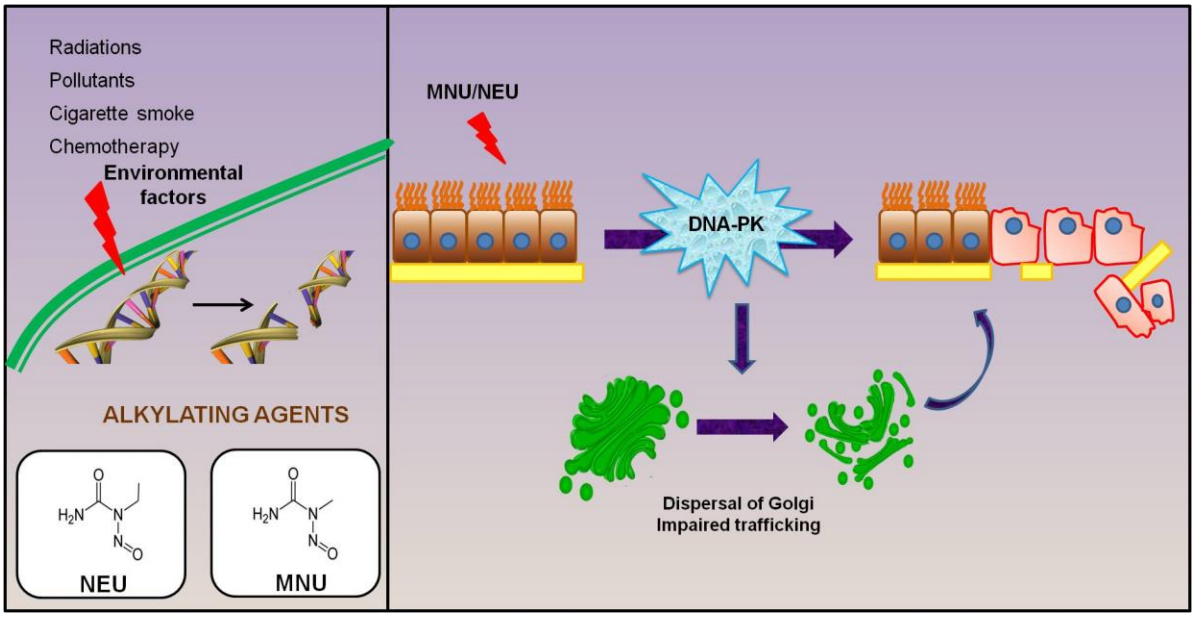

Figure 3.25: Schematic showing the mechanism of MNU-induced transformation.

MNU damage activated DNA-PKcs, which led to Golgi dispersal and impaired trafficking to the plasma membrane. This phenomenon resulted in disruption of polarity, induced EMT-like phenotype and invasion in breast epithelial cells grown as 3-dimensional cultures.

Chapter 4: Methylation damage re-organizes the cytoskeleton

4.1 Background

In the previous chapter we reported MNU to induce dispersal of Golgi and impair intracellular trafficking. Apart from Golgi, the other major component of intracellular trafficking machinery is the cytoskeleton mainly actin and microtubules. Actin, microtubules, MAP (microtubule associated proteins) as well as the motor proteins dynein and kinesin coordinate with Golgi to efficiently sort the proteins to the respective domains (Valderrama et al., 2001; Vaughan, 2005) and are thus known to play a vital role in establishment and maintenance of epithelial polarity (Musch, 2004).In addition to this, the cytoskeleton mainly microtubules and actin, are known to play a crucial role in maintenance of Golgi structure (Burkhardt, 1998; Wehland et al., 1983). On the other hand, Golgi has been found to stimulate nucleation of microtubules (Chabin-Brion et al., 2001). Considering these interrelationships between actin, microtubules, Golgi and epithelial cell polarity along with observing the effects of DNA damage on polarity as well as trafficking, we investigated whether DNA damage affected the cytoskeleton.

4.2 Results

4.2.1 MNU treatment results in reorganization of microtubules.

To investigate the effect of methylation damage on microtubules, day 16 spheroid cultures were immunostained with α-tubulin. We observed an increased intensity as well as abnormal staining pattern as compared to the untreated cells (Figure. 4.1a and Figure. 4.1b). To further confirm, whether increase in intensity was due to up-regulation of α-tubulin, Day 16 acinar cultures were lysed and lysates were immunoblotted (Figure. 4.1c). Interestingly, we found a significant up-regulation of α-tubulin. As reported in the previous chapter, DNA-PK activation was observed within 10 minutes of DNA damage while Golgi was dispersed by 4hours. To determine how early the microtubules were affected, microtubule organization was studied by time course experiments. A visible change in the microtubule organization was observed by 48 hours (Figure 4.2a).

The cells dissociated from the acini were also subjected to immunostaining and a similar phenotype was observed, thus suggesting the re-organization of the microtubule induced was a persistent change and was responsible for the abnormal staining observed in the spheroids (Figure 4.2b)

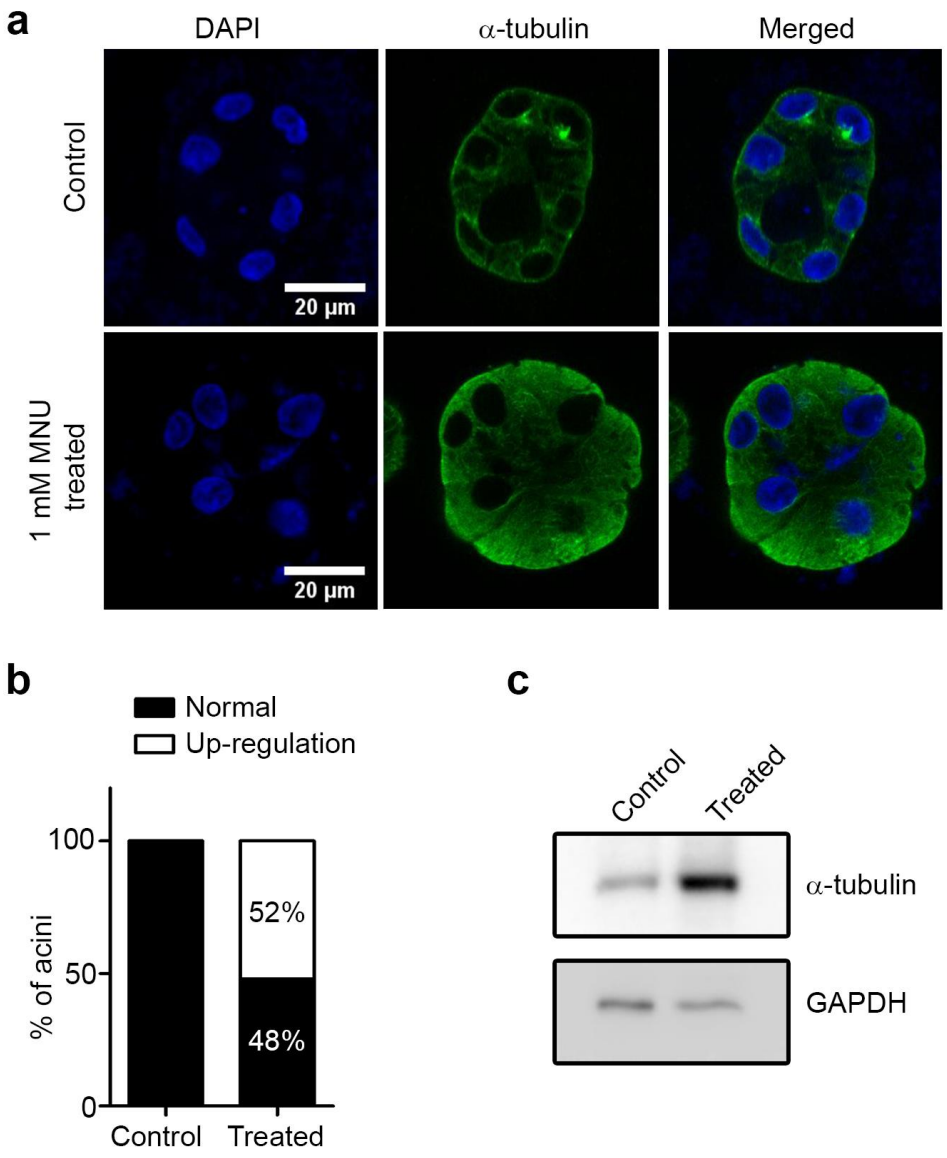

Figure. 4.1: Methylation damage results in up-regulation of α-tubulin in spheroid cultures.

MCF10A cells grown as 3D "on-top" cultures were exposed to 1mM MNU in the initial days of morphogenesis (day0, day 2) (a) Representative images of acinar cultures immunostained for α-tubulin (green), nuclei counterstained with Hoechst 33342 (blue) (b) Graph representing the % of acini showing upregulation. (c) Lysates of acini cultures were immunoblotted and probed for α-tubulin. Data is representative of 3 independent experiments. Scale bar: 20μm.

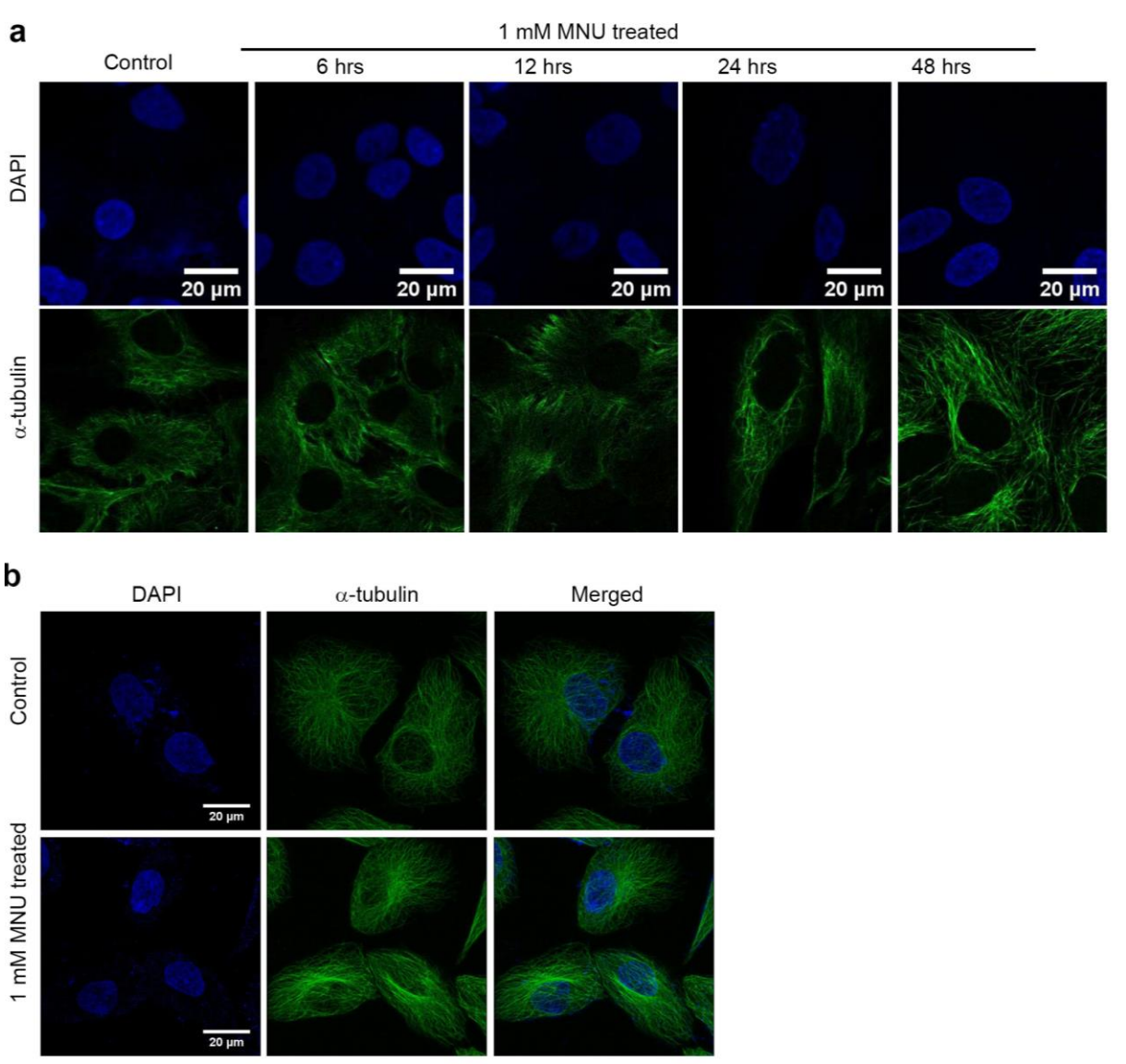

Figure 4.2: Exposure of MCF10A cells to MNU re-organizes microtubules

(a) Monolayer cultures of MCF10A cells were exposed to 1 mM MNU, collected at different timepoints and immunostained for α-tubulin (green), nuclei counterstained with Hoechst 33342 (blue) (b) Cells dissociated from the 3D cultures were immunostained for α-tubulin (green), nuclei counterstained with Hoechst 33342 (blue). Data is representative of 3 independent experiments. Scale bar: 20μm.

4.2.2 MNU treatment stabilized microtubules.

To investigate whether the change in the organization of the microtubules was due to stabilization we compared the phenotypes with that of taxol, a well known microtubule stabilizing agent and nocodazole, a destabilizing agent (Figure 4.3). We observed close resemblance of MNU induced phenotype with that of taxol, implying methylation damage probably stabilized the microtubules. To further confirm this inference, microtubule dynamics were studied using live cell imaging of cells transfected with GFP-EB3 construct. These results corroborated with our phenotypic observation and confirmed that microtubules in cells exposed to DNA damage were stabilized which was characterized by the slow polymerization: slower speed of comets (Figure 4.4a and Figure 4.4b) and longer lifetime of EB3-comets (Figure 4.4c and Figure 4.4d) as compared to the untreated cells.

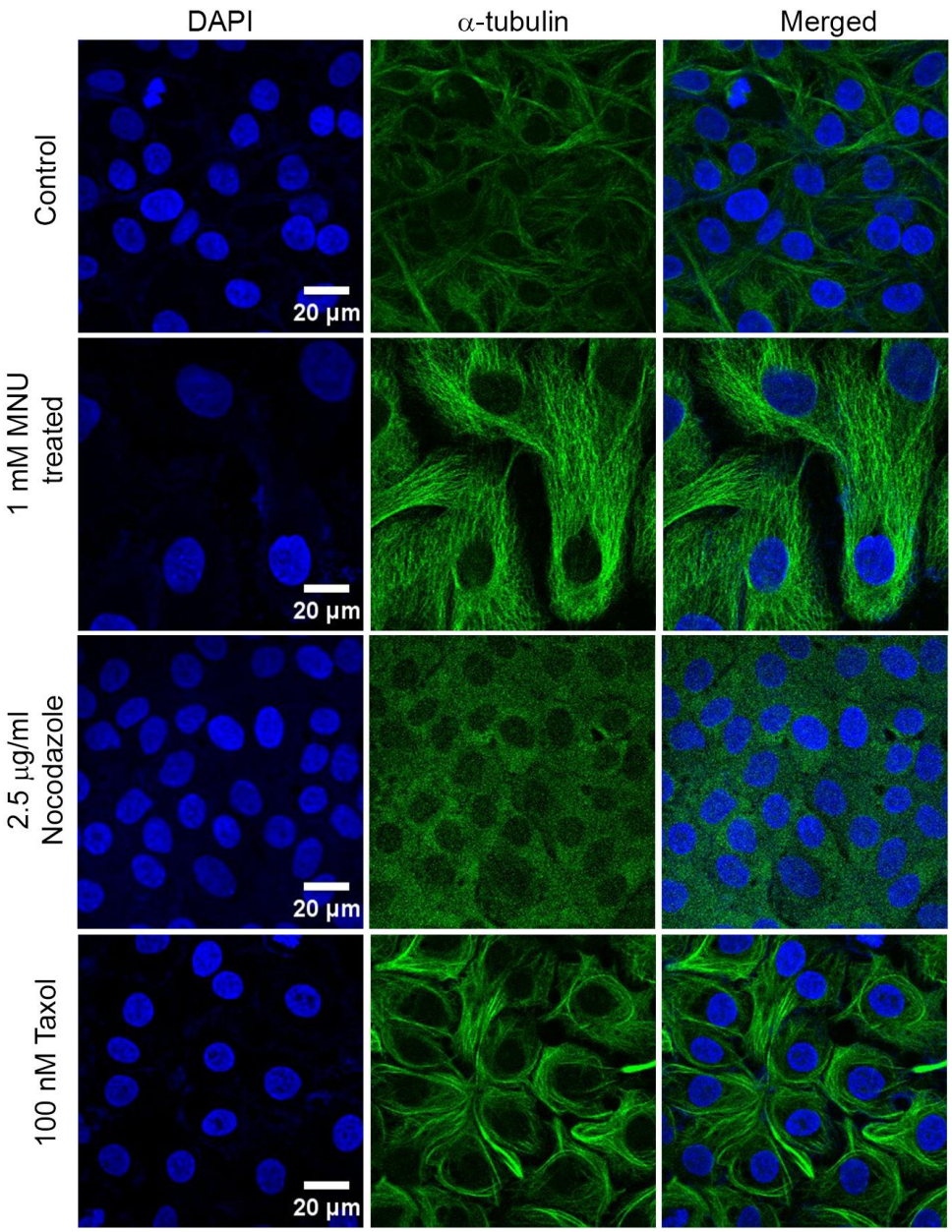

Figure 4.3: MNU treatment stabilizes microtubules.

MCF10A cells grown as monlayer cultures were treated with 1 mM MNU for 24 hours or 2.5 μg/ml of Nocodazole for 20 minutes or 100 nM Paclitaxel (Taxol) for 24 hours. The cells were fixed 48 hours post MNU addition and immunostained for α-tubulin (green), nuclei counterstained with Hoechst 33342 (blue). Data is representative of three independent experiments. 20 micrtoubules per cell were analyzed Scale bar: 20μm.

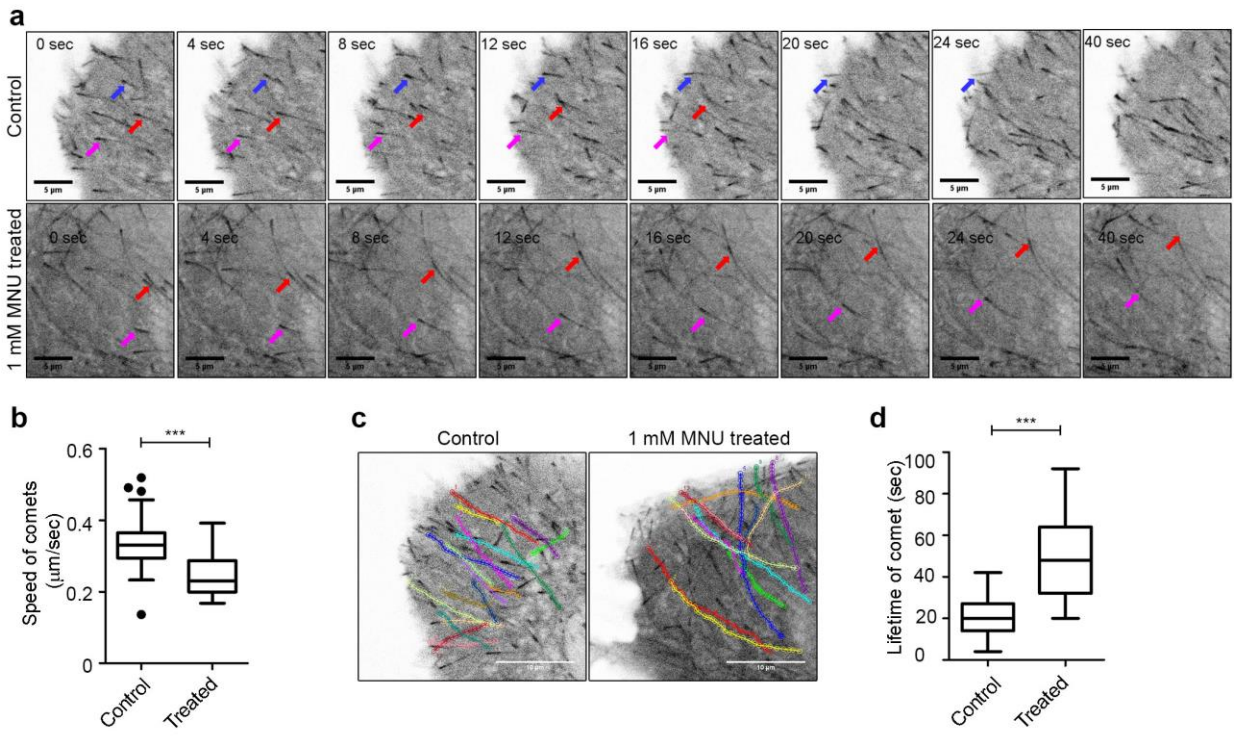

Figure 4.4: Methylation damage slows down microtubule dynamics. Monolayer cultures of MCF10A cells were treated with 1 mM MNU for 24 hours, transfected with EGFP-EB3, microtubule +TIP marker. Time lapse microscopy was done and comets tracked using Manual tracking Plugin, ImageJ. (a) Representative confocal images captured at different timepoints during live-cell imaging. Arrows mark the EB3 comets at each timepoints. (b) Graph representing the quantification of the speed of the EB3 comets reflecting the rate of polymerization. (c) Representative confocal images with overlay of track length travelled by comet reflecting the lifetime of the EB3 comet. Colour coded arrows have been included to mark a few of the EB3 comets being tracked. (d) Graph representing the quantification of lifetime of the EB3 comets. Data is representative of >2 independent experiments. 20 microtubules per cell were analyzed Scale bar: 5µm.

4.2.3 MNU treatment induced reorganization of microtubules was mediated via actin.

MCF10A cells shows the presence of transcytoplasmic actin stress fibres, characteristic of epithelial cells, which was absent in cells exposed to 1mM MNU (Figure 4.5a). Actin appeared to exist as thick bundles, which could not be differentiated into discrete stress fibres, appeared to be diffused at the cell-cell junctions in MNU treated cells (Figure 4.5a). Further, we also observed that at cell-cell junctions circumferential actin belt observed in untreated cells were transformed into fragments which were nearly perpendicular to the cell-cell contact regions (Figure 4.5a). To investigate the interdependence between microtubule and actin phenotypes observed, effect of Latrunculin A (250 nM; inhibitor of actin polymerization) on microtubule organization and effect of nocodazole (2.5 μg/ml microtubule destabilization agent) on actin organization was studied. Interestingly, the microtubule reorganization was reversed upon inhibition of actin polymerization; however there was no effect on actin organization upon microtubule depolymerisation (Figure 4.5b). Taken together, these results imply that the DNA damage induced microtubule organization was mediated via actin re-organization. However, study of actin dynamics would shed light over the phenotype observed.

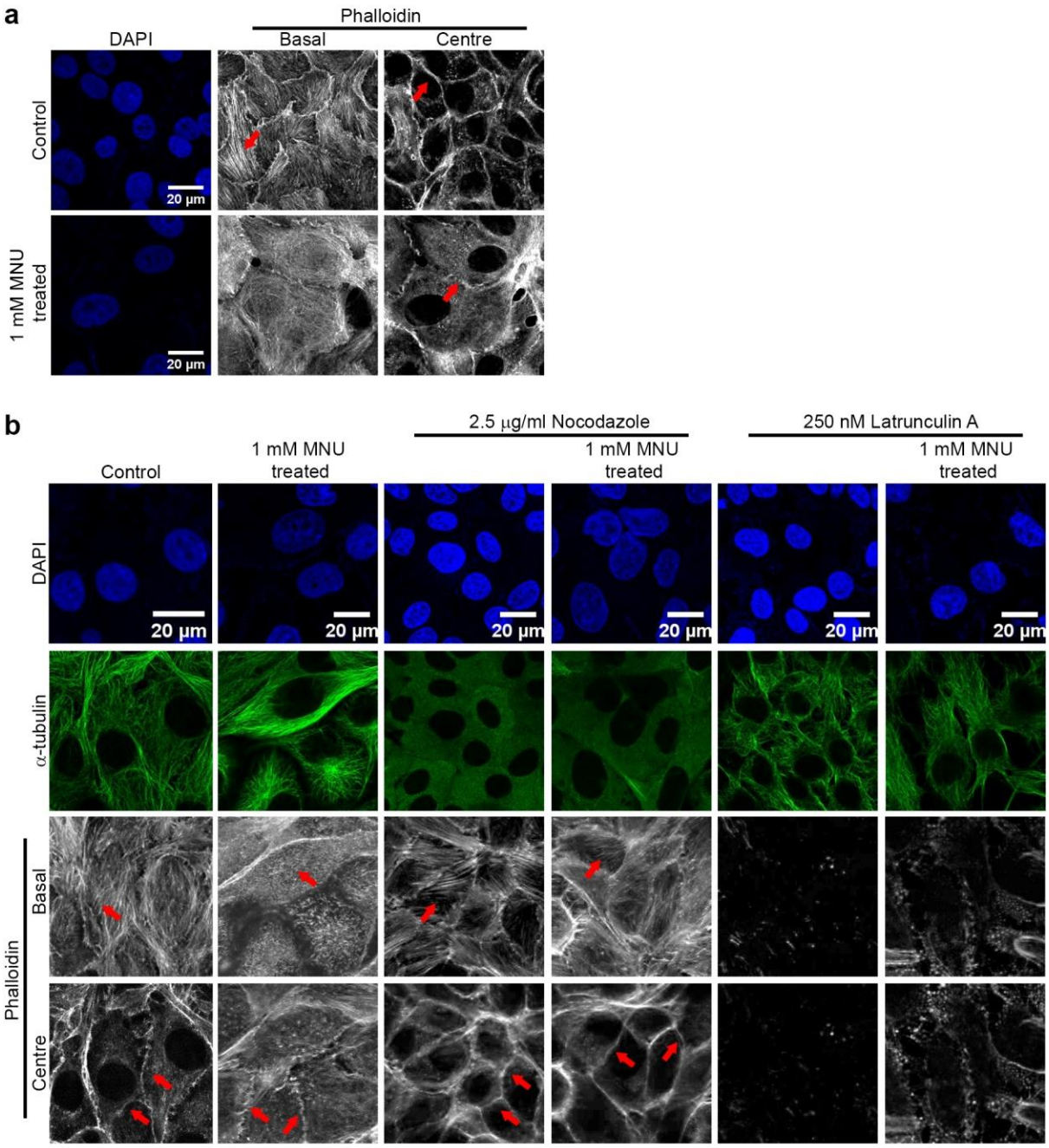

Figure 4.5: MNU induced microtubule re-organization was actin dependent. Monolayer cultures of MCF10A cells were treated with 1 mM MNU for 24 hours. Representative confocal images of basal and centre z-stack of cells stained with Phalloidin to mark actin (grey) (b) Representative confocal images of cells stained with α-tubulin (green), Phalloidin marking actin (grey) and nucleus

counterstained with Hoechst 33342. Untreated and 1 mM MNU treated cells with or without treatment with 2.5 μg/ml of Nocodazole (microtubule destabilizing agent) and with or without treatment with 250 nM Latrunculin A (actin polymerization inhibitor). Arrows (red) mark the regions for comparison of different actin phenotype observed. Data is representative of >2 independent experiments. Scale bar: 20μm.

4.2.4 MNU treatment induced re-organization of microtubules was mediated by DNA-PK.

Since DNA-PK was found to play a central role in MNU induced transformation, we investigated whether the re-organization of actin and microtubules was also via activation of DNA-PK. Microtubule reorganization was found to be reversed characterized by the re-appearance of radially araanged microtubules and disappearance of the parallel arrangement of microtubules(Figure 4.6). Similar reversal was observed in the cells dissociated from day 16 spheroid cultures following DNA-PK inhibition (Figure 4.7). Actin stress fibers began to reappear in cells, with circumferential actin belt being partially reformed (Figure 4.8a). Given that JNK pathway and Akt pathway have been associated closely with DNA damage as well as microtubule organization coupled with the well-established association or interaction of Akt with actin, we investigated the possible role of the two pathways in the re-organization. Investigation of the temporal activity profile for the players revealed that activation of pJNK occurred at 20 minutes and that of Akt at 30 minutes (Figure 4.8b). We observed DNA-PK activation at 10 minutes (Chapter 3) thus, suggesting the possibility of JNK and Akt to act downstream of DNA-PK; and Akt downstream of JNK. To further confirm this, inhibitors of the three key players were used and the activation was investigated. We observed that inhibition of DNA-PK kinase activity using 25 μM DMNB inhibited both JNK as well as Akt activation (Figure 4.8c); while inhibition of JNK activity using 50 μM SP 600125 inhibited Akt activation (Figure 4.8c); thus confirming the signalling cascade to be in the order of DNA-PK, JNK and Akt. Inhibition of Akt using 7.5 μM Akt inhibitor (Millipore) did not affect pJNK (Figure 4.8d). We also investigated the effect of the inhibitors to the three key molecules on the microtubule and actin organization. Actin organization appeared to be partially reversed. Following inhibition of JNK and Akt, transcytoplasmic stress fibres appeared to form again along with circumferential actin bundles reappearing (Figure 4.8e and Figure 4.8f). A reversal of microtubule re-organization was also with the inhibitors, suggesting the involvement of DNA-PK,

JNK and Akt in MNU induced microtubule re-organization (Figure 4.9). Thus, these results imply that the effect on cytoskeleton following DNA damage was mediated by DNA-PK, JNK and Akt However, Akt does not possess the consensus sequence needed for phosphorylation by JNK, thus calling for further investigation of the intermediate players of the predicted pathway.

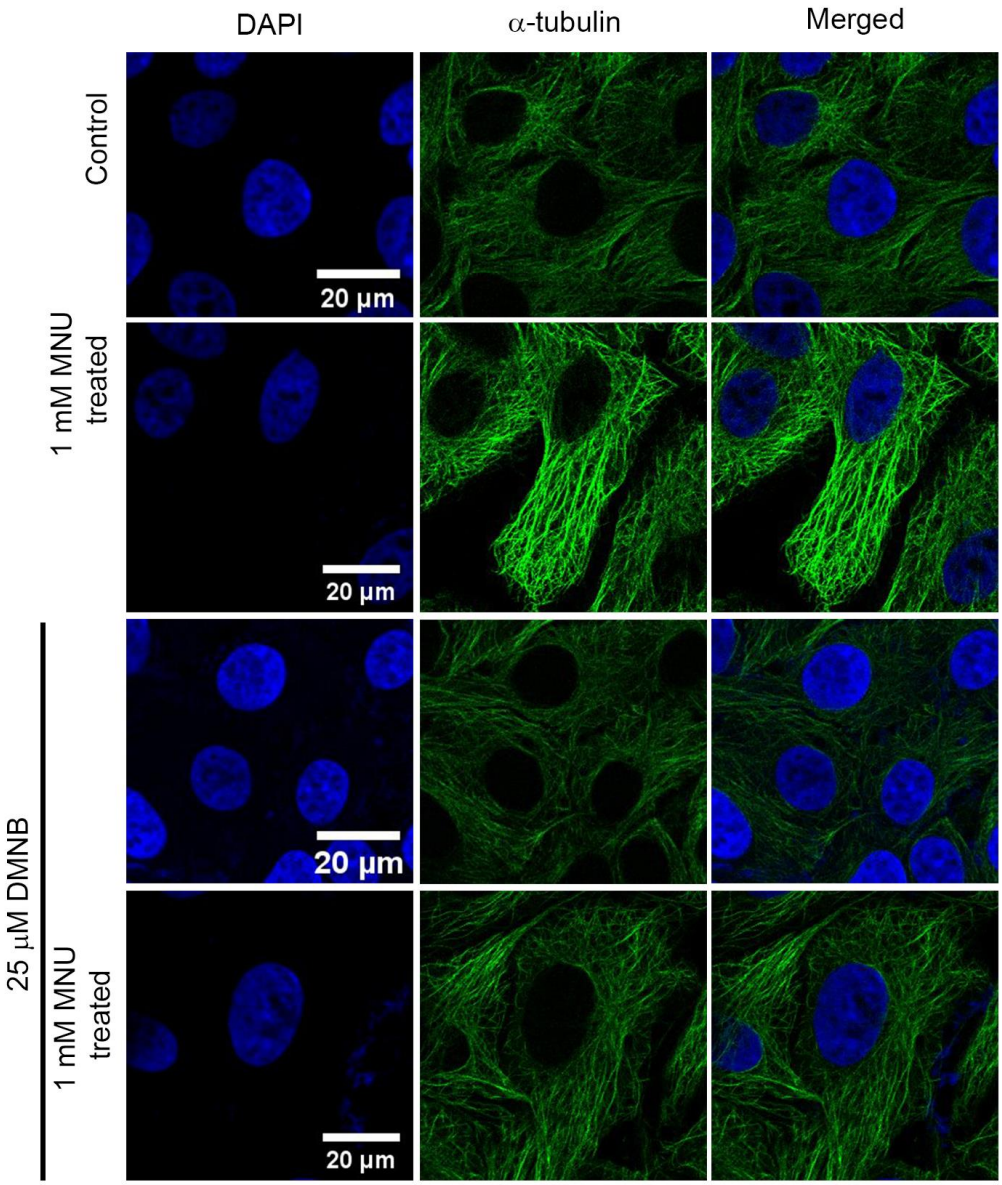

Figure 4.6: Methylation damage induced microtubule re-organization is reversed upon DNA-PK inhibition.

Monolayer cultures of MCF10A cells were treated with 1 mM MNU for 24 hours. Representative confocal images of cells stained with α-tubulin (green) and nucleus counterstained with Hoechst 33342. Untreated and 1 mM MNU treated cells treated with two doses of 25 μM of DMNB for 12 hours each, with and without MNU treatment. Data is representative of three independent experiments. Scale bar: 20μm.

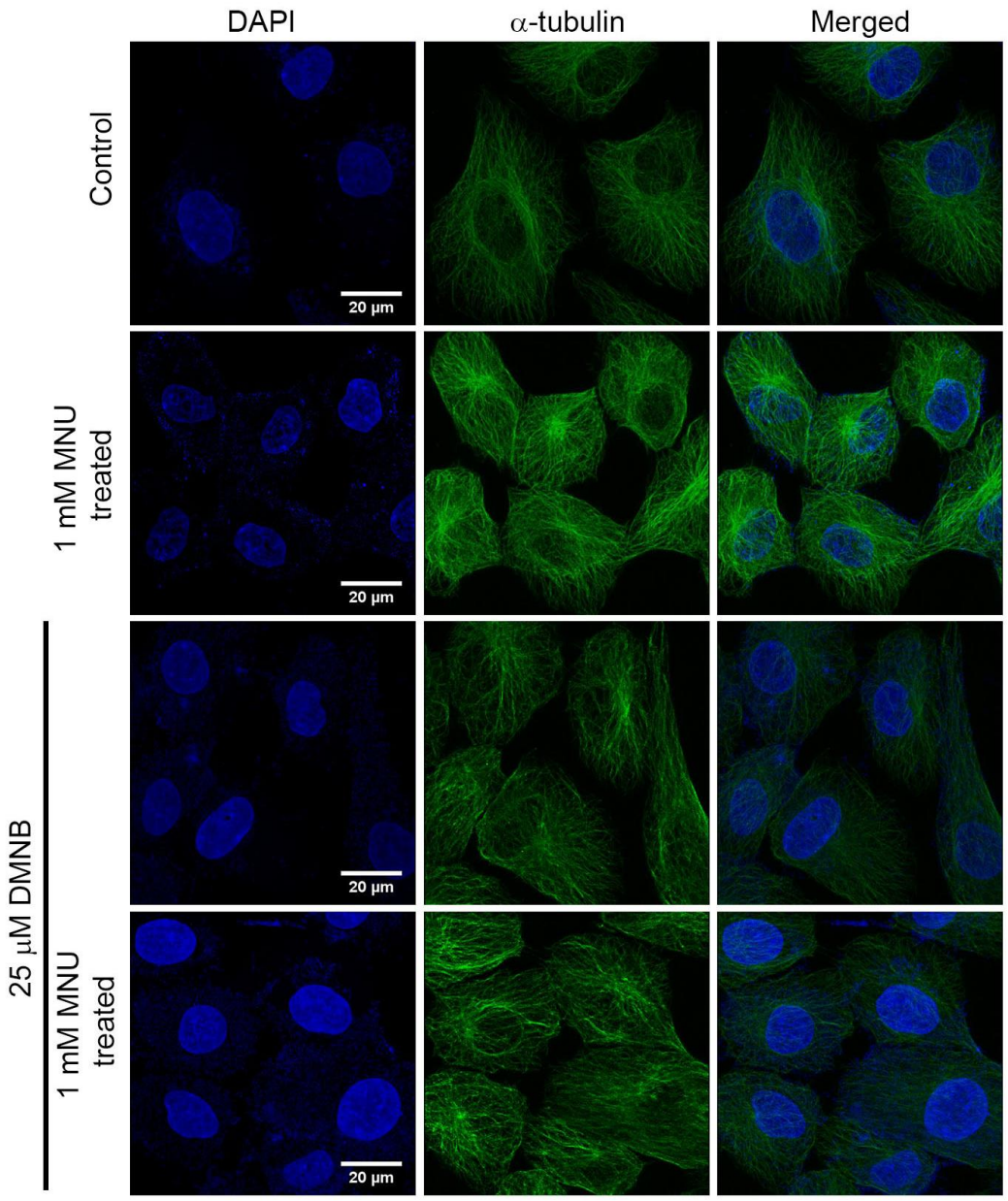

Figure 4.7: Methylation damage induced persistent microtubule re-organization is reversed upon DNA-PK inhibition.

Cells dissociated form day 16 cultures of acini formed by untreated and MNU treated cells, treated with two doses of 25 μM of DMNB for 12 hours each and immunostained for α-tubulin (green) and nucleus counterstained with Hoechst

33342 (blue). Representative 3D projection images are shown. Data is representative of two independent experiments. Scale bar: 20μm.

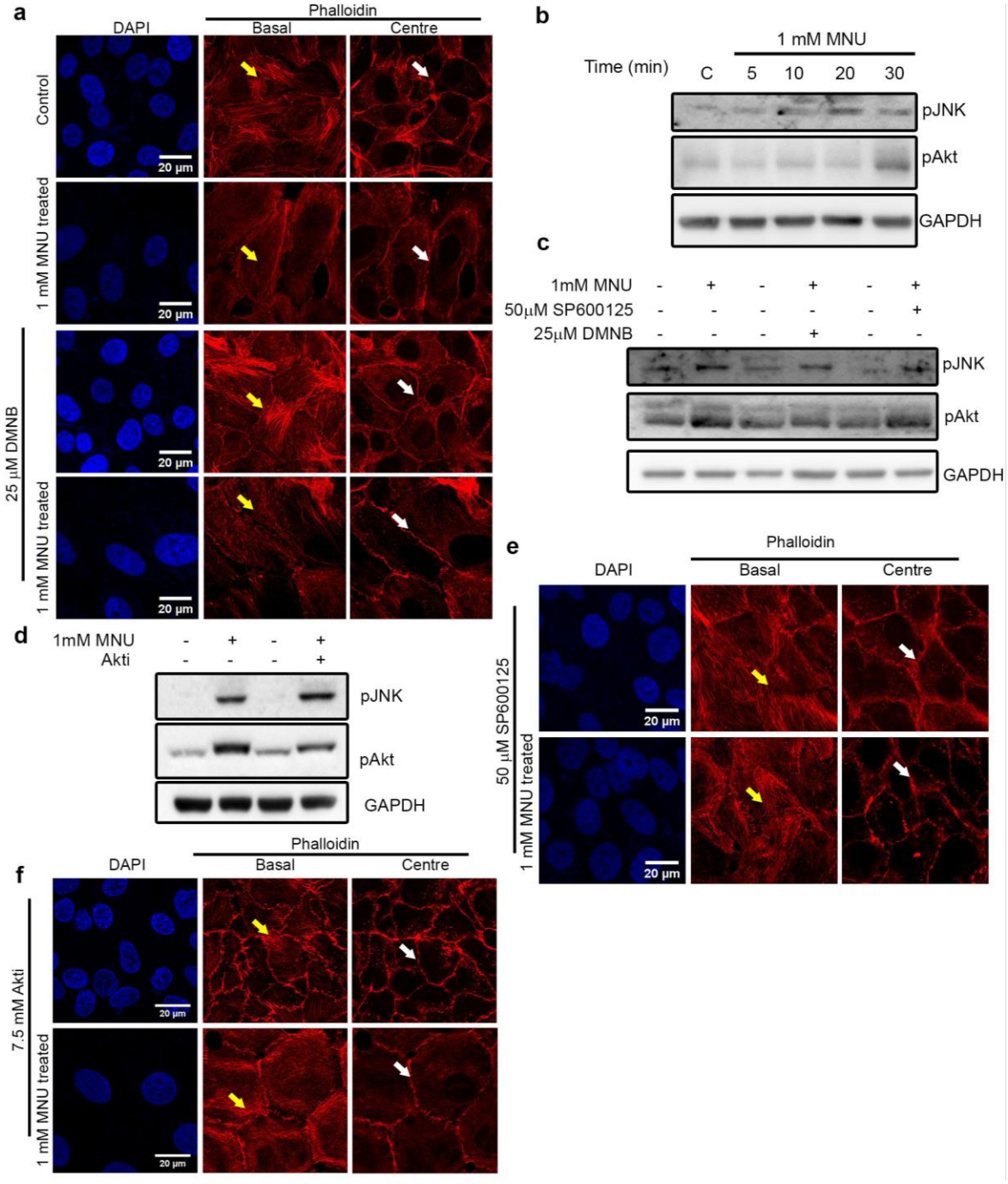

Figure 4.8: Methylation damage induced actin re-organisation is dependent on DNA-PK, JNK and Akt.

Monolayer cultures of MCF10A cells were treated with 1 mM MNU for 24 hours. Representative confocal images of Actin stained with Phalloidin (red) and nucleus counterstained with Hoechst 33342. (a) Untreated and 1 mM MNU treated cells, cells treated with two doses of 25 μM of DMNB for 12 hours each, with and without MNU treatment. Monolayer cultures of MCF10A cells treated with MNU with or without inhibitors of DNA-PK, JNK and Akt were lysed and lysates were immunoblotted. (b) Temporal activation profile of JNK and Akt following DNA damage. (c) Activation profile of JNK and Akt following inhibition of DNA-PK and JNK. (d) Activation profile of JNK and Akt following inhibition of Akt. Representative confocal images of cells with Actin stained using Phalloidin (red) and nucleus counterstained with Hoechst 33342: (e) Cells treated with 50 μM of SP600125, JNK inhibitor for 24 hours, with and without MNU treatment. (f) Cells treated with 7.5 μM of Akt inhibitor for 24 hours, with and without MNU treatment. Arrows (yellow and white) mark regions for comparison of various actin phenotype observed both in the basal as well as the central region. Data is representative of >2 independent experiments. Scale bar: 20μm.

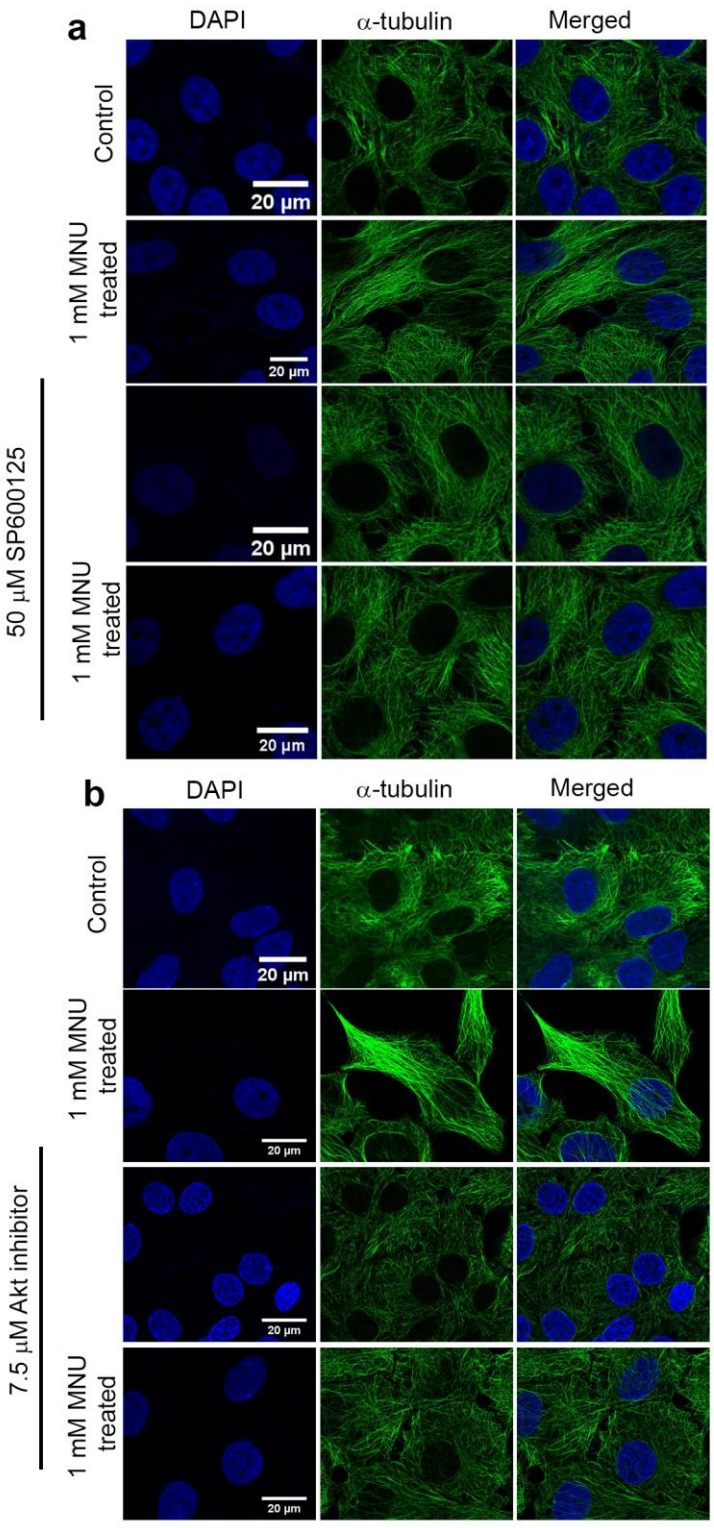

Figure 4.9: Methylation damage induced microtubule re-organisation is through JNK and Akt.

Monolayer cultures of MCF10A cells were treated with 1 mM MNU for 24 hours. Representative confocal images of cells stained with α-tubulin (green) and nucleus counterstained with Hoechst 33342 (a) Cells treated with 50 μM of SP600125, JNK inhibitor for 24 hours, with and without MNU treatment. (b) Cells treated with 7.5 μM of Akt inhibitor for 24 hours, with and without MNU treatment. Data is representative of >2 independent experiments. Scale bar: 20μm.

4.3 Discussion

Golgi is an important organelle involved in establishment of polarity in epithelial cells (Matter and Mellman, 1994). It plays a central role in asymmetric distribution of proteins thus aiding the creation of apical and basal domain in epithelial cells (De Matteis and Luini, 2008; Rodriguez-Boulan et al., 2005). Actin, microtubules, MAP (microtubule associated proteins) as well as the motor proteins dynein and kinesin coordinate with Golgi to efficiently sort the proteins to the respective domains (Valderrama et al., 2001; Vaughan, 2005). In addition to this, microtubules and actin, are known to play a crucial role in maintenance of Golgi structure (Burkhardt, 1998). Actin has been found to act as a molecular scaffold, involved in the deformation of membranes and abscission and/or propelling of vesicles (Anitei and Hoflack, 2011; Insall and Machesky, 2009), while microtubules along with the motors kinesin and dyenin are well known to be actively involved in anterograde transport of cargos (Caviston and Holzbaur, 2006).

Given that DNA damage induced by MNU altered morphology of Golgi, as well as impaired intracellular trafficking we investigated whether it affected microtubules and actin. The organization of microtubules, defined by their abnormal arrangement, was a striking phenotype observed apart from their up-regulation. The radial organization of microtubules in MCF10A cells were found to be disrupted and more of parallel arrangement of relatively thick strands was observed. This data corroborates with the report by Guilford's group, where similar rearrangement was induced upon E-cadherin knock down (Chen et al., 2014). Our study (Chapter 3) also showed a down-regulation of E-cadherin in MNU transformed cells thus, implying the possible link between E-cadherin loss and microtubule re-organization. Loss of E-cadherin and the well- established role of actin in adherens junctions maintenance /establishment promted us to investigate the organisation of actin following DNA damage. Interestingly, actin also showed an abnormal striking feature. The stress fibres were almost lost in the MNU treated cells as well as cells transformed by MNU. The circumferential

actin bundles were also disrupted and more diffused cell-cell junctions were observed which was in concordance with the report by Ayollo *et. Al.,* where the authors linked this phenotype to transformation and an indication of loss of "contact paralysis" (Ayollo et al., 2009). Contact paralysis is the property of non-transformed cells to inhibit formation of protrusions by establishing stable cell-cell contacts (Ayollo et al., 2009; Zoller et al., 1997). It is also known that this phenotype results in enhanced cell motility which was also observed in our study (Chapter 3). Close relationship exists between actin and microtubule organization (Etienne-Manneville, 2004). Investigation of the link between the two components of the cytoskeleton following DNA damage revealed that microtubule re-organization was mediated by actin. DNA-PK plays a role in microtubule dynamics during mitosis (Goodwin and Knudsen, 2014), its activation hyper activates GOLPH3/MYO18/F-actin axis leading to Golgi dispersal (Farber-Katz et al., 2014)these coupled with the central role played by it in MNU induced transformation (Chapter 3) suggests a possible role of DNA-PK in altering the organization of the cytoskeleton. Inhibition of DNA-PK kinase activity not only reversed the microtubule reorganization but also actin phenotype was reversed. This may be attributed to the direct effects of inhibition of DNA-PK on actin or to the restoration of E-cadherin seen following DNA-PK inhibition (Chapter 3). Nuclear actin filament assembly mediated by Formin -2 and Spire-½ following DNA damage has been shown to be essential for efficient DNA repair (Belin et al., 2015). Apart from this, association of DSB repair proteins with polymeric actin has been illustrated to be important for efficient repair which is mainly mediated through stabilization of Ku heterodimer, a component of DNA-PK holoenzyme (Andrin et al., 2012). This calls for further investigation to characterize the effect of DNA damage on actin as well as decipher the exact mechanism.

Following DNA damage, JNK has been known to be phosphorylated by DNA-PK. In addition to this, DNA-PK is also known to phosphorylate Akt at Serine 473. JNK and Akt both are known to closely regulate microtubule organization. PI3K-Akt pathway is known to stabilize microtubules in fibroblasts (Onishi et al., 2007)

and up-regulation of this pathway has been associated with acquisition of resistance to microtubule targeting drugs in prostate cancer (Liu et al., 2015). Furthermore, JNK pathway has been shown to be involved in Wnt-mediated microtubule stability (Ciani and Salinas, 2007). Our study also revealed the possible stabilization of microtubules following DNA damage. In addition to this, actin filament remodelling has been demonstrated to be regulated via activation of Akt (Qian et al., 2004) as well as by JNK activation (Kulshammer and Uhlirova, 2013; Rudrapatna et al., 2014). Investigation of whether JNK and Akt were involved in reorganization of the cytoskeleton revealed the dependence of re-organization on the activity of these two players. Taken together, it appears that DNA-PK mediated actin remodeling and microtubule re-organization was via JNK and Akt pathway. However, further studies are needed to discern the orchestra of events.

In sum, we have demonstrated for the first time the effect of DNA damage on the cytoskeletal organization. The preliminary data presented in this chapter draws our attention to the possible cytoplasmic effects of DNA damaging agents (Summarized in Figure 4.10). However, further investigation into the precise mechanism is essential to decipher the pathway and identify the possible targets. Use of pharmacological inhibitors to these targets may contribute to improve the existing therapies.

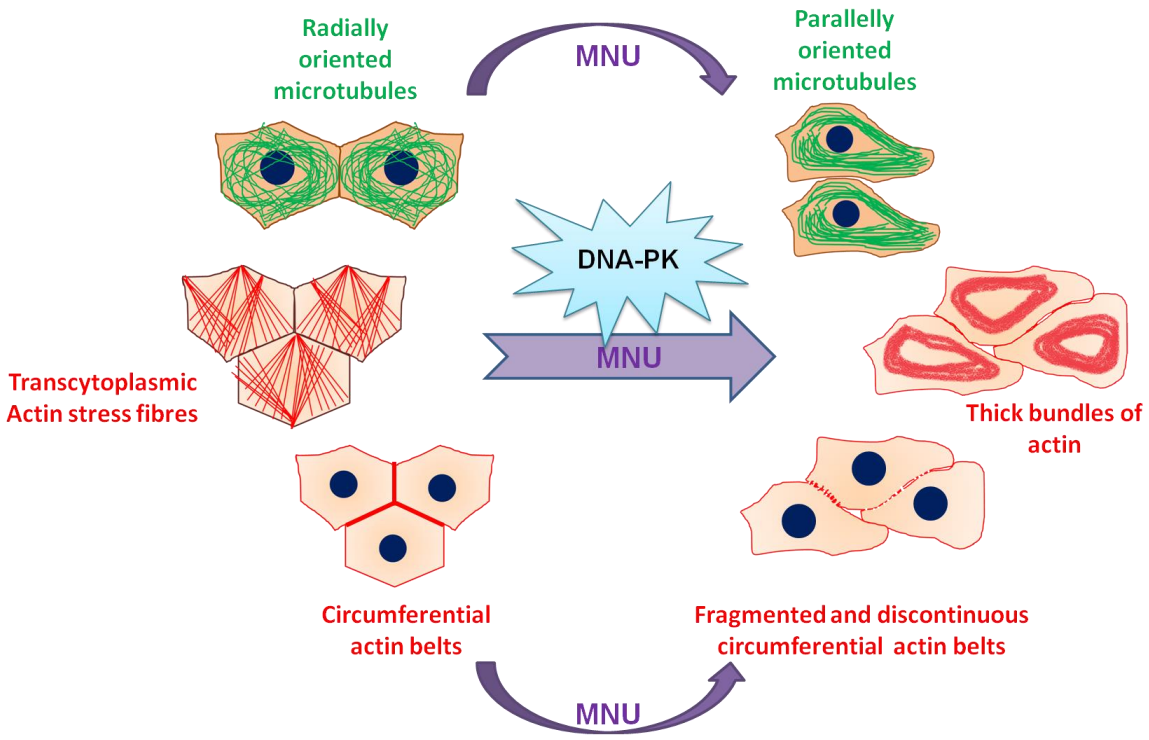

Figure 4.10: Schematic depicting the effect of DNA damge on the cytoskeleton.

Chapter 5: Api5 over-expression results in phenotypic transformation

5.1 Background

Although DNA damage induced transformation was found to be mediated by DNA-PK, involvement of other pathways and molecular players cannot be overruled. In order to identify the other possible molecular players, we investigated the expression of various proteins which play a role in DNA damage surveillance pathway and are implicated in cancers. We observed an up-regulation of two key proteins, Api5 and TopBP1 (Figure 5.1), both of which have been found to be up-regulated in various cancers. Api5, apoptosis inhibitor 5, is an oncogene, up-regulated in bladder cancers, lung cancer (Sasaki et al., 2001; Wang et al., 2010) colon, pancreas, esophagus (Koci et al., 2012), and B-cell chronic lymphoid leukemia (Krejci et al., 2007) as well as has been shown to induce invasion in cervical cancers (Kim et al., 2000). However, role of Api5 in breast cancer is unknown. Nevertheless, up-regulation of Api5 was reported in tamoxifen resistant breast cancer cells by Jansen *et. al.* Further, it was also found to be down-regulated in tocoterinol treated MCF7 and thus the authors report it to be a possible potential target for breast cancer therapy.(Ramdas et al., 2011). Although these reports coupled with upregulation of Api5 observed by us in MNU transformed cells, allude to the possible role of Api5 in breast cancer, the exact role remains elusive. This study aims to establish the possible role of Api5 in breast tumorigenesis using 3-dimesional spheroid cultures.

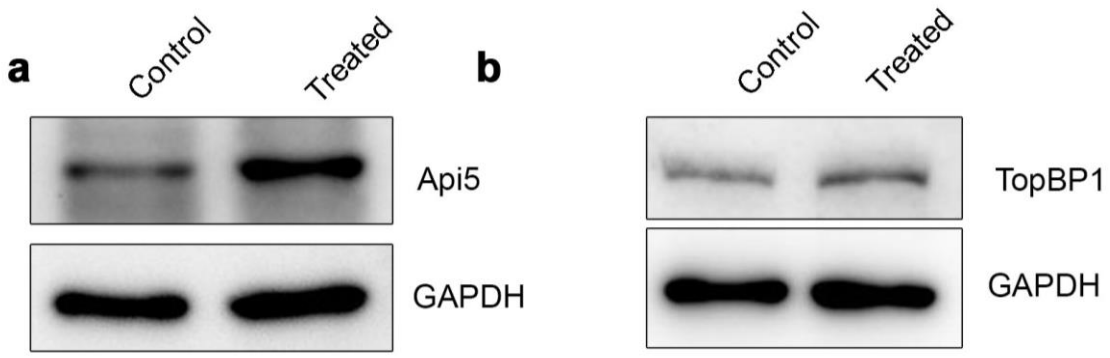

Figure 5.1: Api5 and TopBP1 are over-expressed following methylation damage.

MCF10A cells with or without MNU treatment were grown as 3D ‘on top’ cultures. The acini were lysed on day 16 and immunoblotted for (a) Api5 (b) TopBP1. The data is representative of >3 independent experiments.

5.2 Results

5.2.1 Generation of stable cell line of MCF10A over-expressing Api5.

To elucidate the role of Api5 in breast tumorigenesis, Api5 was over-expressed in MCF10A cells using lentivirus mediated gene delivery system. Full length Api5 was PCR amplified from mVenus-Api5 vector (available in lab) and was cloned into CSII-EF-MCS-mCherry vector (Appendix V) (procured from RIKEN BRC DNA BANK) between Not1 and Xba1 sites. The clones obtained were subjected to double digestion using Not1 and Xba1 to check for release of insert and positive clones were confirmed by sequencing. Further, the positive clones were transfected into HEK 293T cells (Human Embryonic Kidney cell line) and tested for fluorescence (Figure 5.2a) as well as lysates were immunoblotted to detect both endogenous as well as over-expressed Api5 (Figure 5.2b). Further, to generate the stable cell line lentiviral mediated gene delivery was used. Lentiviral particles were prepared by transfecting HEK 293T cells with the either empty vector (CSII-MCS-EF-mCherry) or Api5 construct (CSII-MCS-EF-mCherry-Api5) along with the packaging plasmids. MCF10A cells were transduced with aid of 8 μg/ml polybrene (Figure 5.2c). The cell lines thus generated, MCF10A-mCherry and MCF10A-Api5 were used for the study (Figure 5.2d).

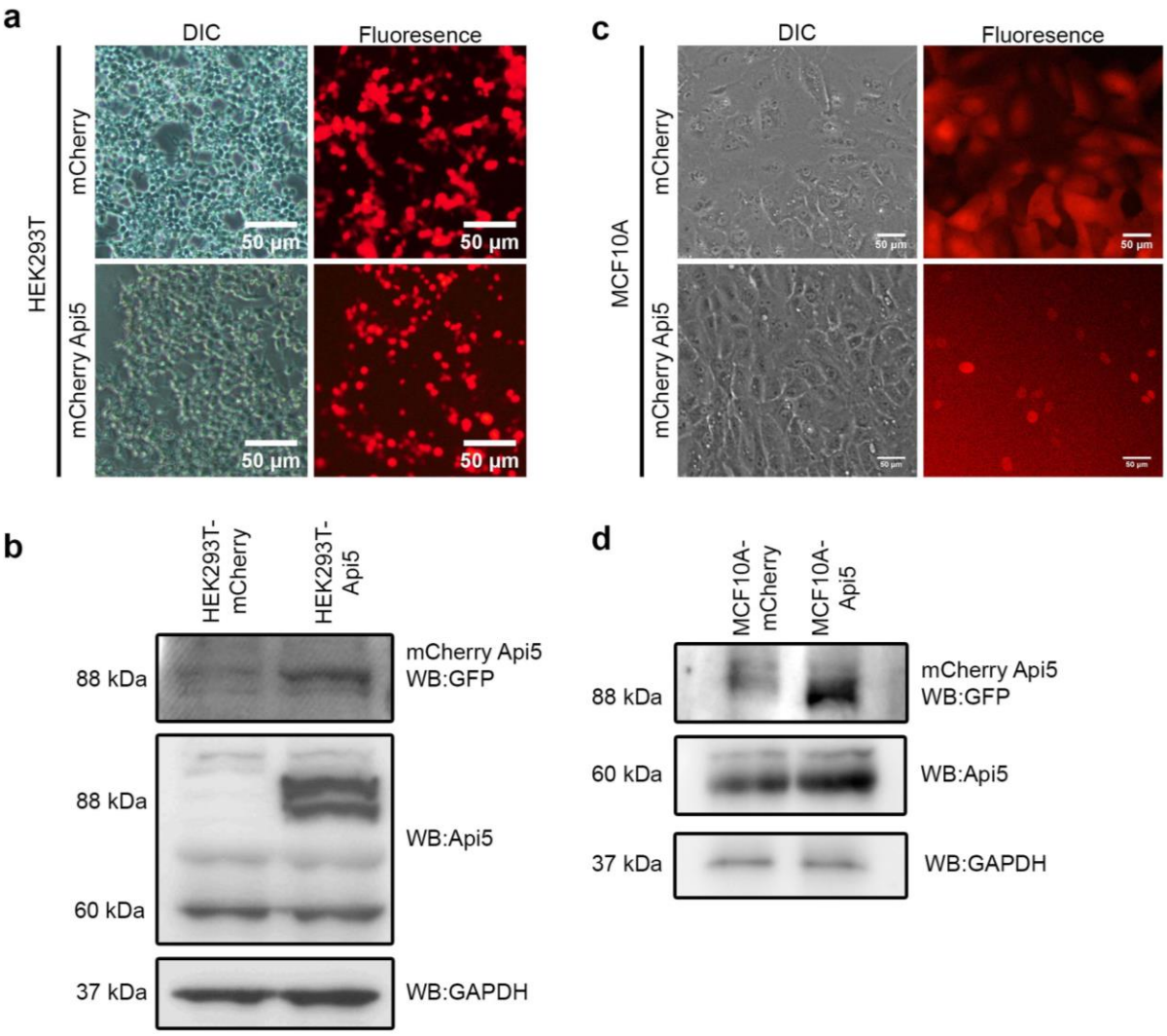

Figure 5.2: Generation of MCF10A cell line over-expressing Api5.

(a) Representative images of HEK 293T cells transfected with CSII-MCS-EF-mCherry and CSII-MCS-EF-mCherry-Api5 to check for the positive clones. (b) Lysates of the transfected HEK 293T cells were immunoblotted against GFP to detect the over-expressed protein; Api5 to detect the endogenous protein; and GAPDH was used as a loading control. (c) Representative images of MCF10A cells transduced with lentiviral particles carrying CSII-MCS-EF-mCherry and CSII-MCS-EF-mCherry-Api5 constructs. (d) Lysates of the transduced MCF10A cells grown as 3D cultures were immunoblotted against GFP to detect the over-expressed protein; Api5 to detect the endogenous protein; and GAPDH was used

as a loading control. Data is representative of >2 independent experiments. Scale bar: 50 μm

5.2.2 Api5 over-expression in MCF10A cells induces enhanced cellular proliferation.

MCF10A cells either expressing empty vector or the over-expression construct was grown on a bed of Matrigel^{TM} for 16 days and the acinar structures formed were scored for the phenotypes. The Api5-overexpressing MCF10A cells appeared to form acini which were larger than the empty vector controls (Figure 5.3a and Figure 5.3b). Morphometric analysis using Huygens Professional software (SVI, Hilversum, Netherlands) revealed a significant increase in acinar volume and surface area. An increase in the number of cells per acini was also observed (Figure 5.3c). To ascertain whether the increase in the number of the cells was due to enhanced cellular proliferation, immunostaining of Ki67 was done. Presence of more than six Ki67 positive cells per acini is indicative of enhanced cellular proliferation (Wu and Gallo, 2013). Api5 over-expression resulted in the formation of acini with more than six Ki67 positive cells thus implying that Api5 over-expression enhanced cellular proliferation (Figure 5.3d and Figure 5.3e). Lumen formation and maintenance in the acinar structures is attributed to a balance between proliferation and apoptosis. Loss of this balance could disrupt the lumen phenotype (Debnath et al., 2002). The luminal phenotype of MCF10A-Api5 acini corroborated with Ki67 staining pattern, wherein we observed a disruption of the cleared luminal phenotype in acini formed by Api5 over-expressing cells (Figure 5.3f and Figure 5.3g).

Thus, these results suggest that Api5 over-expression induces enhanced cellular proliferation.

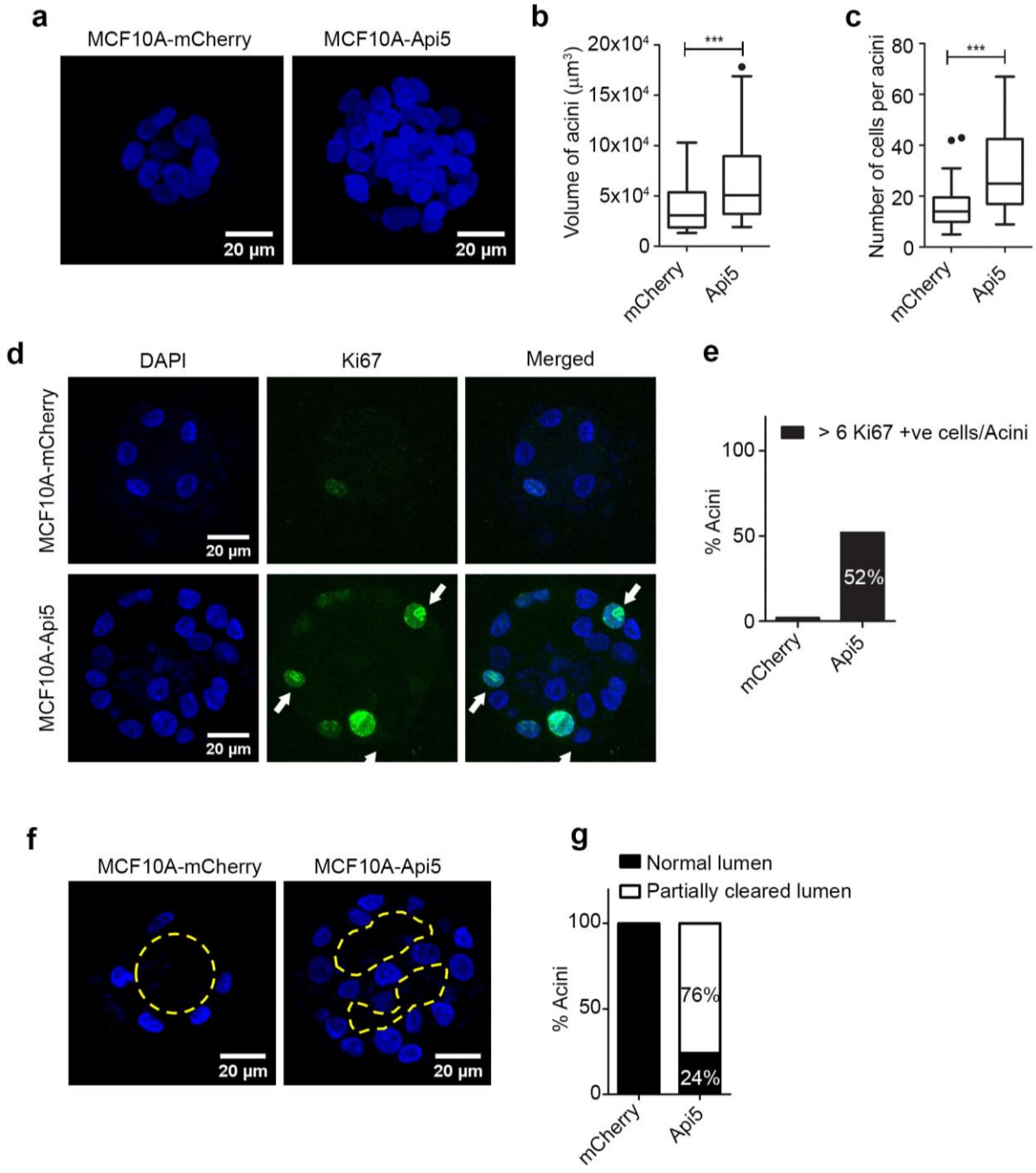

Figure 5.3: Api5 over-expression induces enhanced cellular proliferation. Day 16 3D cultures MCF10A and MCF10A-Api5 cells immunostained with Phalloidin to mark the boundary of the entire acini while DAPI was used to stain the nuclei. Images were captured using Zeiss LSM 710 laser scanning confocal microscope (Zeiss, GmbH) and morphometric analysis was done using Huygens

Professional software (SVI, Hilversum, Netherlands). (a) Representative 3D re-constructed confocal images of acini formed. Graph representing **(**b) volume of acini and (c) number of cells per acini. (d) Representative confocal images of spheroids immunostained for Ki67, proliferation marker. Arrows (white) mark the Ki67 positive nuclei. (e) Graph representing the % of acini showing more than 6 Ki67 positive cells. (f) Representative images of acini formed by MCF10A and MCF10A-Api5 cells showing the presence of disrupted lumen in acini formed by Api5 over-expressed cells. Yellow dotted lines mark the boundary of the lumen. (g) Graph representing the percentage of acini showing disrupted lumen. Data is representative of >4 independent experiments. >60 acini were analyzed per cell line group. Scale bar: 20 μm.

5.2.3 Api5 over-expression disrupts apico-basal polarity and adherens junctions.

In order to study the effect of Api5 on establishment and maintenance of apico-basal polarity, α6-integrin was used as the basal region marker. We observed over-expression of Api5 to result in discontinuous staining at the basal region indicative of loss of basement membrane, observed in case of invasive cells which break the basement membrane to invade the nearby tissue (Vidi et al., 2013) (Figure 5.4a and Figure 5.4b). Apical polarity marked by the localization of Golgi was also found to be disrupted with most of the Api5 over-expressing spheroids exhibiting basal/lateral localization of GM130 (Figure 5.4c and Figure 5.4d). To ascertain the integrity of the cell-cell junctions, localization of E-cadherin was investigated. Unlike the MCF10A-mCherry cells which formed acini with intact cell-cell junctions, MCF10A-Api5 acini showed diffused staining of E-cadherin at cell-cell junctions implying loss of cell-cell adhesion (Figure 5.4e and Figure 5.4f).

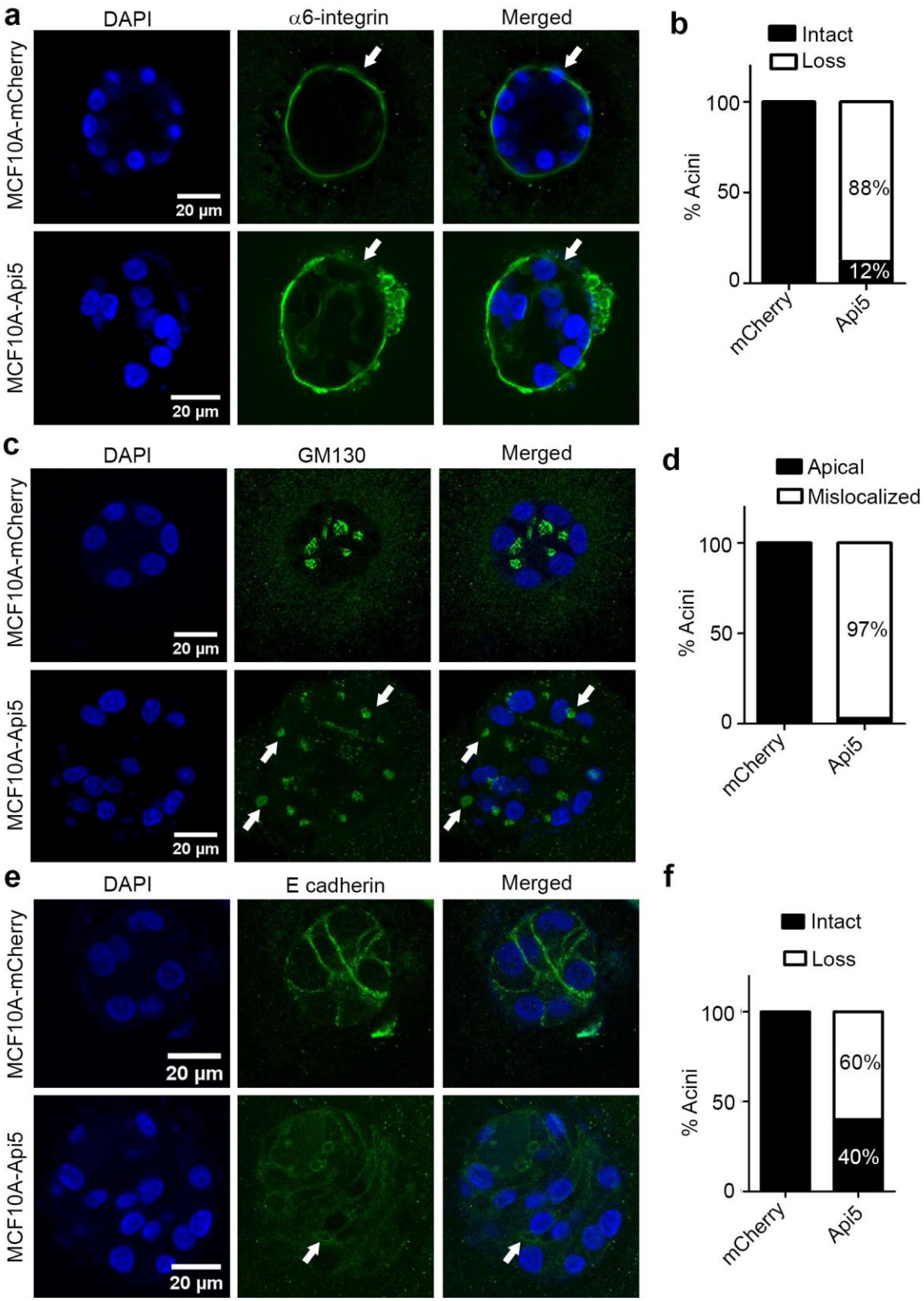
a
DAPI
α6-integrin
Merged
MCF10A-mCherry
MCF10A-Api5
20 μm
b
Intact
Loss
% Acini
100
50
0
88%
12%
mCherry
Api5
c
DAPI
GM130
Merged
MCF10A-mCherry
MCF10A-Api5
20 μm
d
Apical
Mislocalized
% Acini
100
50
0
97%
mCherry
Api5
e
DAPI
E cadherin
Merged
MCF10A-mCherry
MCF10A-Api5
20 μm
f
Intact
Loss
% Acini
100
50
0
60%
40%
mCherry
Api5

Figure 5.4: Api5 over expression disrupts basolateral and apical polarity. MCF10A-mcherry and MCF10A-Api5 cells were grown as 3D “on top” cultures and maintained for 16 days. Representative images of confocal images of centre z section spheroids immunostained with α6-integrin (green). (b) Graph depicting the percentage of acini showing loss phenotype observed with α6-integrin. (c) Representative images of centermost z section of spheroids immunostained with GM130 (green). (d) Graph depicting the percentage of acini showing mislocalization of GM130. (e) Representative immunofluorescence images of E-cadherin (green). (f) Graph representing the percentage of acini showing loss of E-cadherin from adherens junction. Arrows (white) mark the regions for comparison of localization polarity markers. Data is representative of >2 independent experiments. >40 acini were analyzed per cell line. Scale bar: 20 μm.

5.2.4 Api5 over-expression results in the formation of abnormal structures indicative of EMT-like phenotype.

Loss of apico-basal polarity as well as loss of cell-cell contacts are the key features acquired by the cells when they undergo epithelial to mesenchymal transition. The morphology of acini formed by cells which undergo such transitions is found to be altered characterized by the presence of protrusion-like or bulb-like structures (Debnath and Brugge, 2005). The spherical spheroids formed by MCF10A upon Api5 over-expression were found to be distorted and bulb-like structures were seen (Figure 5.5a and Figure 5.5b). To investigate whether the Api5 over-expressed cells had undergone EMT we immunostained day 16 acini with vimentin, a mesenchymal marker and observed a marked up-regulation (Figure 5.5c and Figure 5.5d), which was further confirmed with immunoblotting. Immunoblot analysis of other mesenchymal markers namely, fibronectin and N-cadherin showed up-regulation (Figure 5.5e).
Thus, these results imply that Api5 over-expression in MCF10A induced EMT.

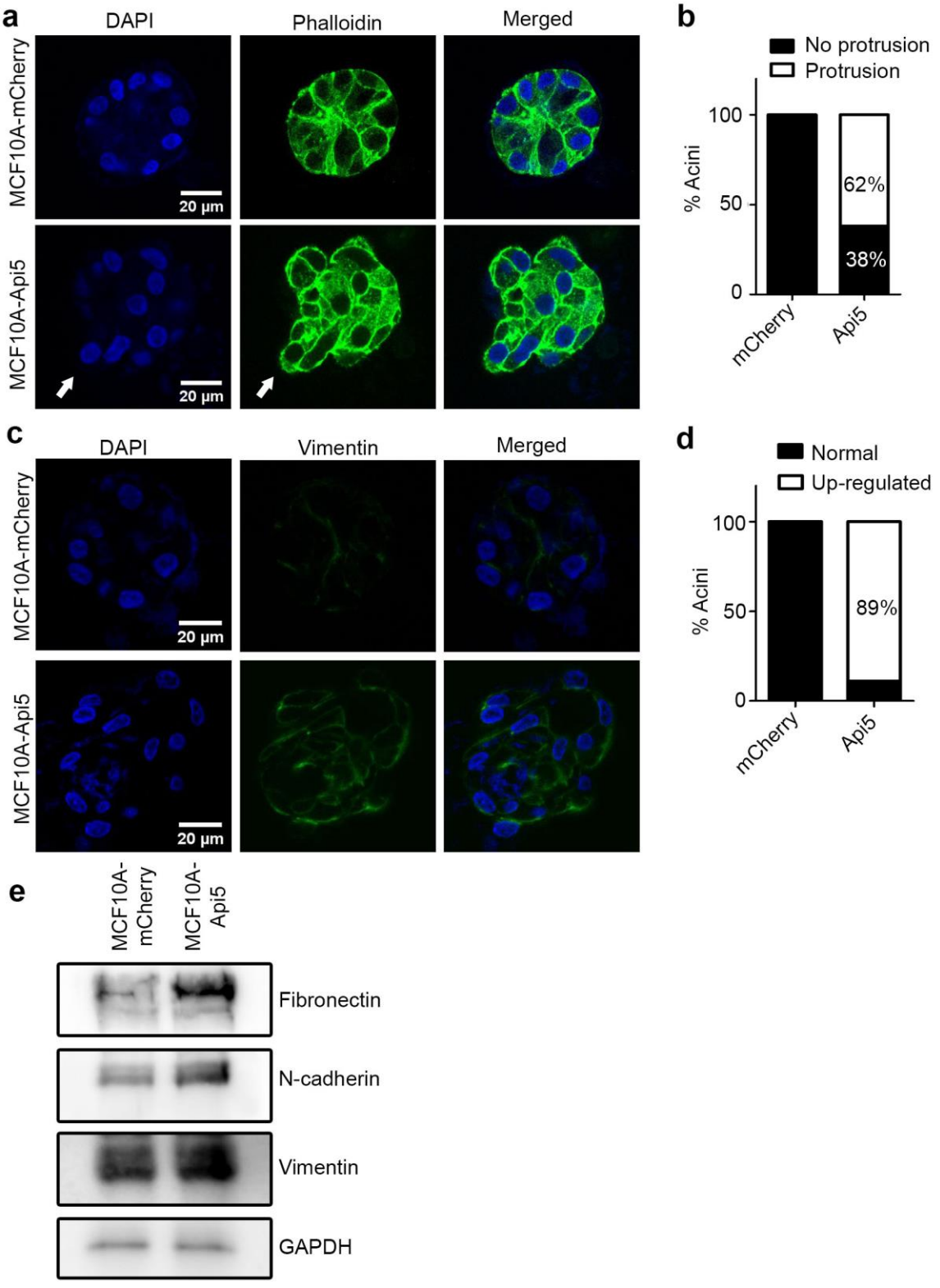

Figure 5.5: Api5 over-expression induced EMT-like phenotype.

Day 16 cultures of MCF10A cells were immunostained with phalloidin and analyzed for presence of ‘protrusion-like’ or ‘bulb-like’ structures. (a) Representative immunofluorescence images of acini labelled Phalloidin (green). Arrow (white) marks the protrusion-like structure.(b) Graph representing the percent of acini showing presence of ‘protrusion-like’ phenotype. (c) Representative immunofluorescence images labelled with vimentin (green). (d) Graph representing the percent of acini showing upregulation of vimentin. (e) Day 16 acini were lysed and immunoblotted for mesenchymal markers like vimentin, N-cadherin, and fibronectin. Data is representative of >2 independent experiments. >40 acini were analyzed per cell line. Scale bar: 20 μm.

5.3 Discussion

Most of the genes which have been implicated as breast cancer susceptible genes are found to be involved in the DNA damage response pathways namely, BRCA1, BRCA2, CDH1, PTEN, STK11, TP53, ATR, ATM, BARD1, BRIP1, CHEK2, ERBB2, NBN, PALB2, RAD50, and RAD51 genes. In the quest of identification of candidate genes that may play a role in DNA damage induced transformation, we screened for a few genes, among which Api5 was found to be up-regulated. Api5, also known as AAC-11 (anti apoptosis clone 11) was primarily identified as an apoptosis inhibitor, which provided survival advantage to cervical cancer cells upon serum starvation (Tewari et al., 1997) and as well as evaded DNA damage induced apoptosis (Rigou et al., 2009). Api5, a nuclear protein, has been found to be up-regulated in multiple cancers. Although its role in various cancers has been studied to some extent, its role in breast cancer is not yet established. In this study we have demonstrated the possible role of Api5 in breast tumorigenesis using 3-dimensional cultures. Modulation of activity of a single gene or a small subset of genes has been shown to be sufficient for disruption of polarized MCF10A (mammary non-tumorigenic epithelial cell line) acinar structures (Chen et al., 2010; Guo et al., 2010; Henry et al., 2011). Exploiting this feature, we investigated whether over-expression of Api5 was sufficient to induce transformation of non-transformed breast epithelial cells. Acini formed by transformed cells exhibit altered morphology. Api5 over-expression resulted in the formation of spheroids which had a larger volume as compared to that of control. The acinar morphology is maintained in non-transformed cells due to equilibrated balance between proliferation and apopotosis. Thus, such a phenotype could be hypothesized as an outcome of “enhanced cellular proliferation” or “evasion of apoptosis” or both, two important “hallmarks of cancer” (Hanahan and Weinberg, 2011). Enhanced number of cells in the MCF10A-Api5 acini being positive for Ki67, at day 16 indicated enhanced cellular proliferation, since by this day of morphogenesis cells in the non-transformed acini undergo growth arrest (Debnath et al., 2003). This result was in

corroboration with the report by Garcia-Jove Navarro *et al.,* where Api5 was demonstrated to regulate cellular proliferation (Garcia-Jove Navarro et al., 2013). Further the lumen in the MCF10A-Api5 acini showed presence of cells in the luminal space. This phenotype could be either due to enhanced proliferation resulting in partially filled lumen or due to the apoptosis inhibitory effect of Api5 resulting in partially cleared lumen. Luminal clearance has been attributed to anoikis and apoptosis mediated through BIM (a pro-apoptotic BH3-only BCL family protein), which is induced by day 8 in case of breast epithelial cells (Reginato et al., 2005). The resistance to apoptosis by Api5 has been demonstrated to be mediated via FGF2 up-regulation which finally results in ERK activation driven degradation of pro-apoptotic factor BIM (Noh et al., 2014). Considering these two independent reports, we can predict the possible role of Api5 in lumen formation. Owing to the delayed clearance of lumen observed upon over-expression of BCL2 (an apoptosis inhibitor, implicated in lumen clearance) in MCF10A, the involvement of other pathways other than apoptosis in clearance of lumen has been implicated (Debnath et al., 2002; Lin et al., 1999). Thus, taking into consideration all these reports, presence of partially cleared lumen in MCF10A-Api5 acini may be attributed to apoptosis inhibition caused by degradation of BIM by Api5. However, detailed investigation of Ki67 positive cells in the MCF10A-Api5 acini revealed that the cells in lumen stained positive for Ki67, thus attributing the luminal phenotype to enhanced cellular proliferation. This warrants further investigation to establish if the effect observed was merely due to enhanced cellular proliferation or also due to apoptosis inhibition. The presence of bulb-like or protrusion-like structures in MCF10A-Api5 acini suggests the possible role of Api5 in EMT, which was further confirmed by the up-regulation of vimentin. This observation is supported by literature wherein its over-expression has been observed in metastatic cells as compared to the normal as well as primary cervical tissues (Kim et al., 2000). Consistent with this report, we observed loss of α6-integrin, the subunit of integrin receptors which forms hemidesmosomes (Sonnenberg et al., 1991), from the basal region. The

loss phenotype is also considered as an indicative of invasive phenotype wherein cells are known to break open their basement membrane so as to invade nearby tissue and disseminate to distant sites of metastasis(Vidi et al., 2013). In addition to this, loss of α6-integrin has been correlated to acquisition of metastatic ability and disseminating to the pleural cavity (Natali et al., 1992). Supporting this, Api5 has also been illustrated to induce invasion in cervical cancer cells through activation of ERK which eventually activated MMP-9 (Song et al., 2014). With the possibility of induction of EMT we also observed loss of adherens junction as illustrated by the loss of E-cadherin from the cell-cell junctions. This phenotype is also a prerequisite for attainment of mesenchymal phenotype. Loss of basolateral polarity characterized by loss of α6-integrin as well as loss of E-cadherin was also coupled with mis-localization of Golgi from the apical domain, suggesting loss of apical polarity.

Taken together, this study illustrates the potential of Api5 to induce phenotypic transformation of non-transformed breast epithelial cells. Thus, it can be concluded that Api5 may possibly play a role in breast tumorigenesis. However further validation of the findings are essential to confirm the same. Further, translation of the findings in clinical samples will provide further insight into the process of tumorigenesis and validate the use of Api5 as a biomarker. Clinical samples of patients with relapse after chemotherapy can be analyzed to establish association. Discerning the pathway(s) will help in designing novel therapeutics strategies to prevent relapse.

Chapter 6: Prolonged exposure to PAF induces phenotypic transformation.

6.1 Background

PAF, platelet activating factor, is a phospholipid mediator secreted by macrophages, neutrophils as well as endothelial cells. Apart from this, Bussolati *et al* reported secretion of PAF by breast cancer cells under growth factor stimulation (Bussolati *et al*., 2000). In addition to this, Camussi's group reported presence of PAF in the microenvironment of breast cancer tissues of patients. Apart from this, cigarette smoke is considered as one of the factors which result in the accumulation of PAF in tissue by inhibiting PAF-AH (PAF acetyl hydrolase) (Kispert *et al*., 2015; Sharma *et al*., 2011). Thus, these reports suggest the presence of this mediator in the microenvironment of the cells. Although role of PAF and PAF-R in various cancers has been well studied, there are very few reports pertaining to its role in breast cancer. The role of PAF in promoting cellular motility and invasion of breast tumor cells has been shown by Bussolati *et al* (Bussolati *et al*., 2000). Accumulated PAF has been shown to enhance adherence of metastatic breast cancer cells to lung endothelium (Kispert *et al*., 2014). However, role of PAF in breast cancer initiation remains elusive. Given the presence of PAF in the microenvironment either due to chronic inflammation, exposure to cigarette smoke or UV radiations as well as by breast cancer cells themselves, it makes it essential to unravel the effect of PAF on breast epithelial cells.

This work aims to study the effect of PAF on breast epithelial cells using the established 3D culture system of MCF10A cells. To investigate whether PAF induced transformation, MCF10A were grown on a bed of growth factor-reduced Matrigel™ with continuous exposure to 200 nM PAF. These cultures were maintained for a period of 20 days. The spheroids thus formed were scored for phenotypic changes.

6.2 Results

6.2.1 MCF10A cells express low levels of PAF-R as compared to malignant cells.

PAF-R expression has been related to the tumorigenic potential of cells as well as knock-down of the receptors has been demonstrated to have inhibitory effect on tumor progression (Cellai et al., 2006; Robert and Hunt, 2001). We investigated the PAF-R status in MCF10A as well as in two other breast cancer cells, MDA-MB 231 and MCF-7s, using RT-PCR. PAF-R expression levels in these cell lines were correlated with their tumorigenic potential. MDA-MB 231 and MCF-7 cells showed increased expression of PAF-receptors while MCF10A showed weak expression (Figure 6.1a and Figure 6.1b). We further investigated the effect of PAF on the expression of PAF-R. The three cell lines were exposed to PAF for 24 hours and expression levels of PAF-R was determined. However we observed no appreciable change in the levels of the receptor with increase in dose of PAF (Figure 6.1c and Figure 6.1d).

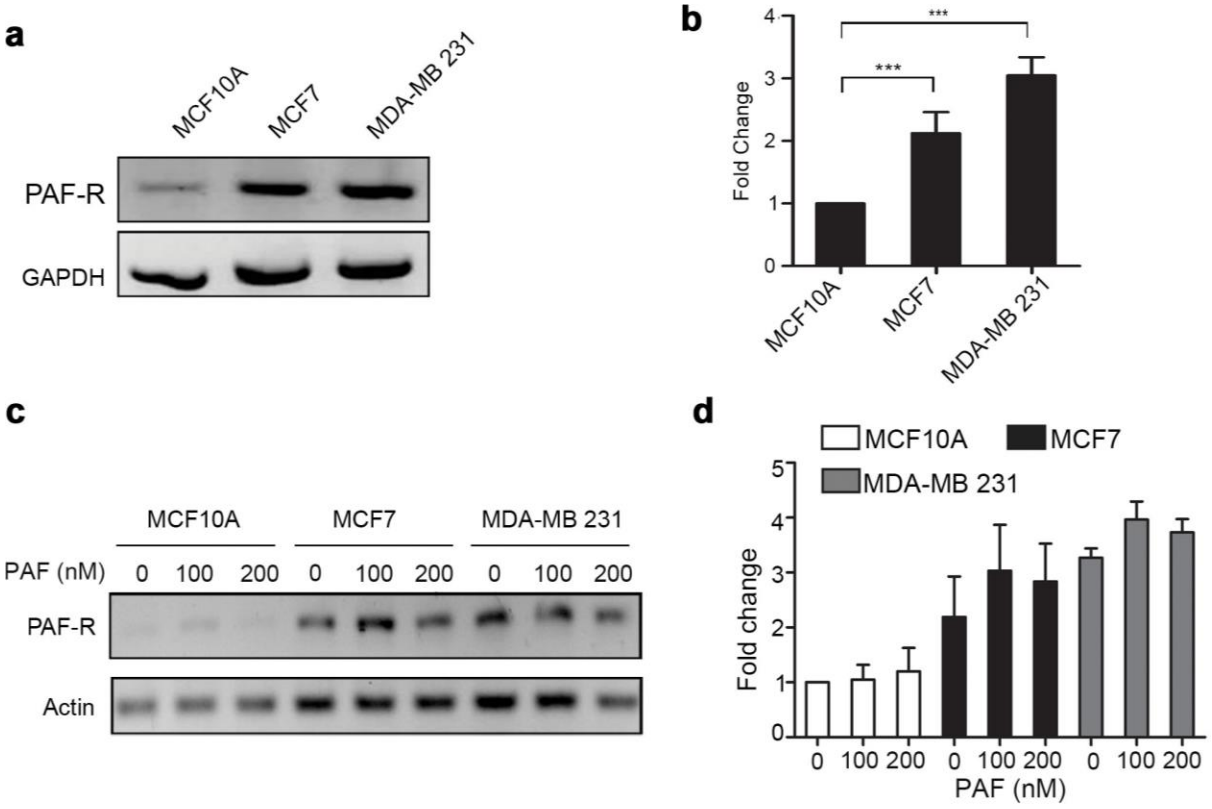

Figure 6.1: PAF-R expression levels.

(a) RT-PCR analysis of PAF-receptor expression in MCF10A (non-transformed breast epithelial cell line), breast cancer cell lines MCF-7 (breast adenocarcinoma) and MDA-MB 231 (invasive ductal carcinoma) (b) Graphs represent mean +/- SEM fold change of expression level normalized to PAF-R expression in MCF10A. (c) RT-PCR analysis of PAF-R expression in MCF10A, MCF-7 and MDA-MB 231 cells treated with 100 and 200 nM PAF for 24 hours. (d) Graphs represent mean +/- SEM fold change of expression level normalized to PAFR expression in untreated MCF10A PAF-R expression levels.

6.2.2 PAF induces enhanced cellular proliferation in 3D spheroid cultures.

Previous work in the lab demonstrated that induction with 200 nM PAF enhances migration of MDA-MB 231 cells. To study effect of PAF on MCF10A cells, considered as 'near normal' breast epithelial, the cells were grown on Matrigel^{TM} in the presence and absence of PAF for 20 days. We observed that when cells were grown in presence of PAF, the cells resulted in the formation of acinar structures which had a larger volume (Figure 6.2a). Consistent with this finding, we also observed significant increase in the number of cells per acini (Figure 6.2b). Luminal phenotype was also disrupted with a significant number of acini having multiple layers of cells enclosing the luminal space (Figure 6.2c and Figure 6.2d). All these phenotypes demonstrate the ability of PAF to induce proliferation of breast epithelial cells, implying possible attainment of hyperproliferative state, referred to as "escape from proliferative state", one of the "hallmarks of cancer" (Hanahan and Weinberg, 2011). To ascertain this, the acini were immunostained for Ki67, a proliferation marker. Presence of more than six Ki67 positive cells per acini is indicative of hyperproliferation (Wu and Gallo, 2013). We observed a significant number of acini exhibiting this phenotype, confirming that PAF induced proliferation of non-transformed breast epithelial cells (Figure 6.2e and Figure 6.2f).

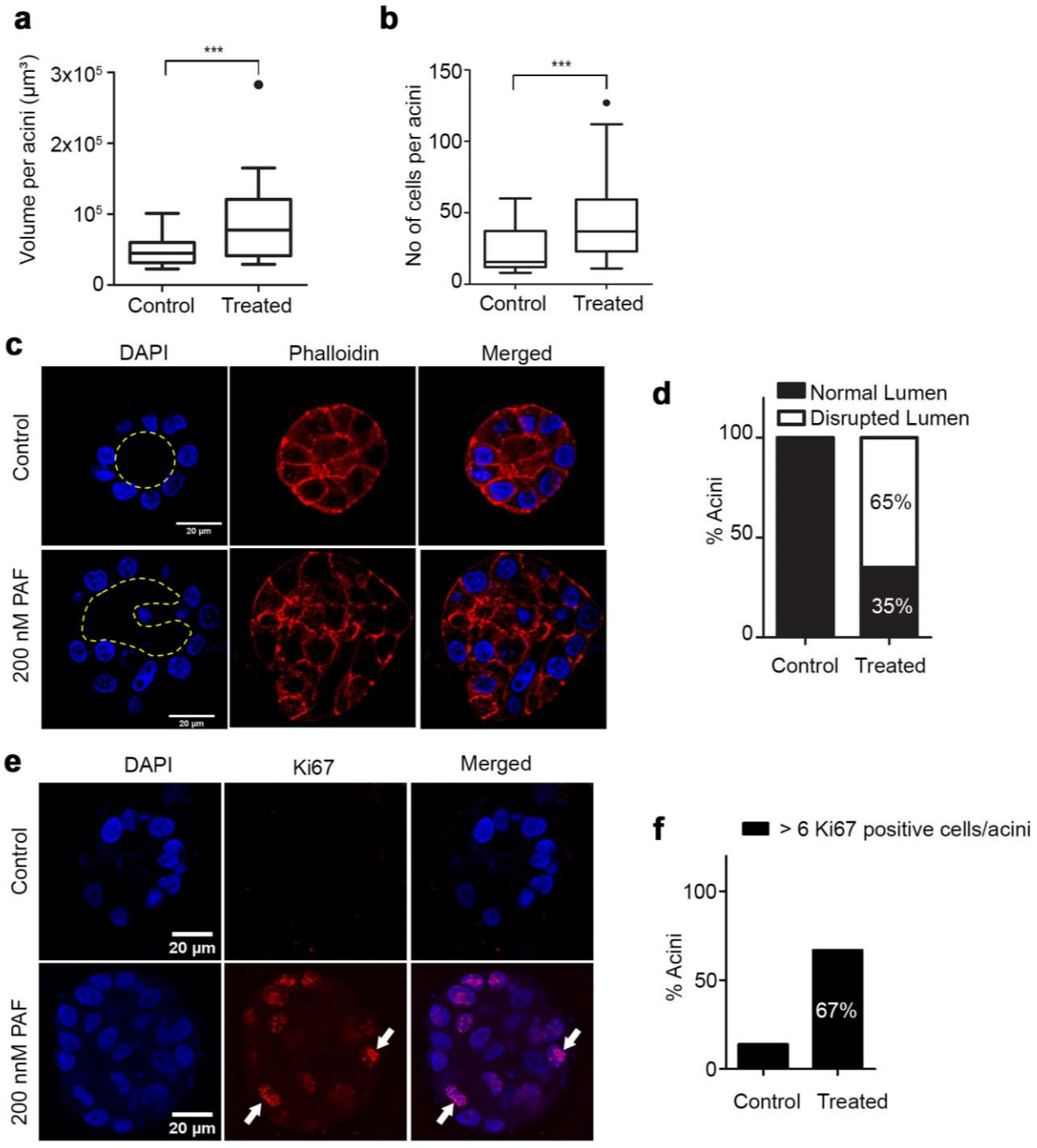

Figure 6.2: PAF induces enhanced cellular proliferation in MCF10A spheroids.

MCF10A cells grown as 3D cultures in presence or absence of 200 nM PAF were immunostained with Phalloidin to mark the boundary of the entire acini and nuclei were counterstained with Hoechst 33342. Images were captured using Zeiss

LSM 710 laser scanning confocal microscope (Zeiss, GmbH) and morphometric analysis was done using Huygens Professional software (SVI, Hilversum, Netherlands). Graph representing (a) volume of acini, (b) number of cells per acini; (c) Representative confocal images depicting the luminal phenotype in acini formed by untreated and 200 nM PAF treated cells. Yellow dotted lines mark the boundary of lumen. (d) Graph representing the percentage of acini showing disrupted luminal phenotype. (e) Representative images of day 20 acini immunostained with Ki67 (red). White arrows indicate the Ki67 positive cells in the acini. (f) Graph representing the percentage of acini showing presence of more than six Ki67 positive cells. Data from N>3 independent experiments is pooled and represented. ~40 acini per treatment condition were analyzed.

6.2.3 PAF exposure induced EMT-like phenotype.

Another striking feature of the acini grown in presence of PAF was the formation of “protrusion-like” or “bulb-like” structures (Figure 6.3a and Figure 6.3b). Such structures are known to be characteristic features of invasiveness or migratory cells. Cells grown on 3D substrata that have undergone epithelial-mesenchymal transition (EMT) give rise to protrusion-like structures. When a few cells migrate into such protrusions, these structures may appear as “bulb-like” structures (Godinho *et al*., 2014; Oyanagi *et al*., 2012) . With the known role of PAF in inducing motility of different kinds of cells including breast cancer cells, these abnormal structures imply possible induction of EMT or motility resulting in escape of cells out of the well-structured and regulated acini. To ascertain this, we investigated the levels of vimentin, a mesenchymal marker, in the Day 20 cultures (Figure 6.3c). We observed a significant number of acini showing an up-regulation of vimentin (Figure 6.3d).

These results highlight the potential role of PAF in inducing EMT in MCF10A cells.

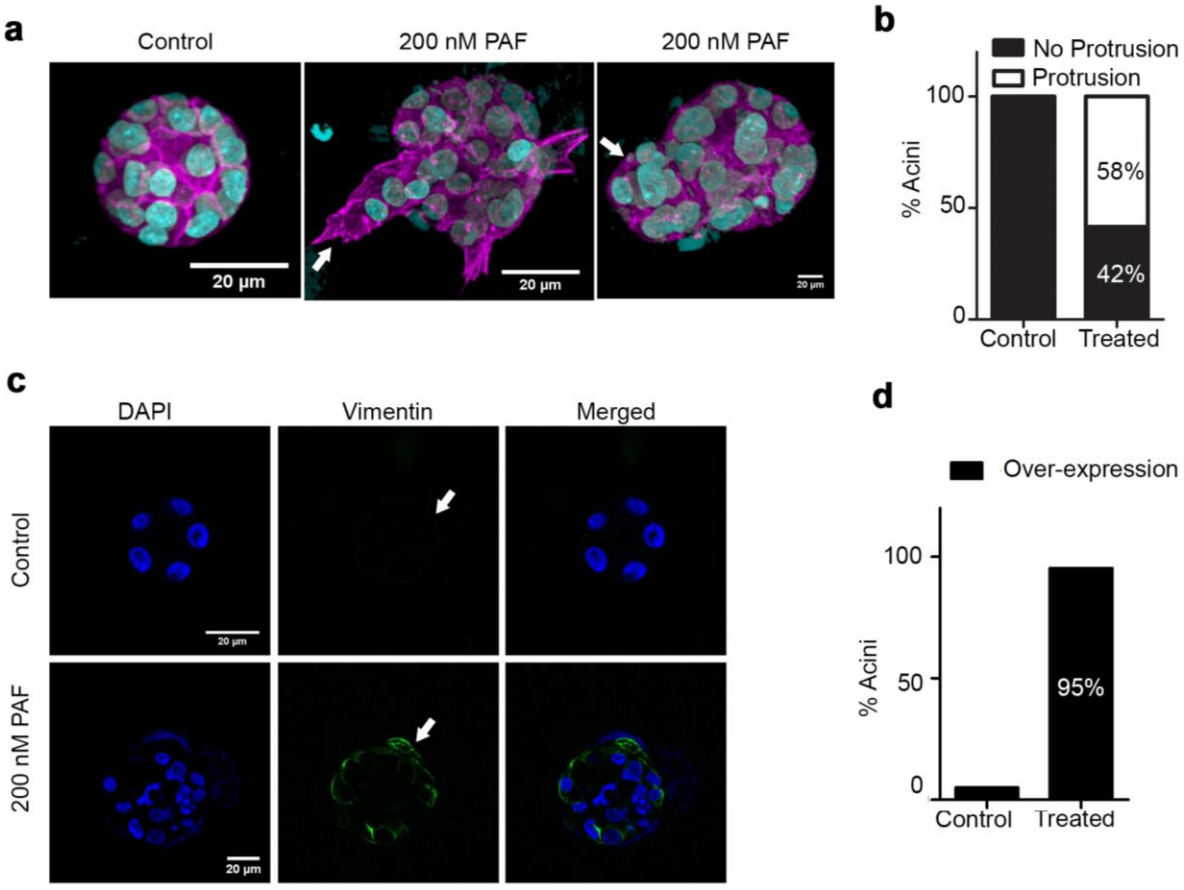

Figure 6.3: PAF exposure results in EMT in MCF10A cells grown as 3D 'on top' cultures.

MCF10A cells grown as 3D cultures were treated with 200 nM PAF every four days and maintained in culture for 20 days. (a) 3D reconstructed image of day 20 acini immunostained with Phalloidin (magenta) and nuclei counterstained with Hoechst 33342 (cyan) depicting protrusion-like or bulb-like structures. (b) Graph representing the percentage of acini showing protrusion-like phenotype. (c) Representative immunofluorescence images of day 20 acini labelled with vimentin, a mesenchymal marker (green) and nuclei counterstained with Hoechst 33342 (blue). (d) Graph representing the percentage of acini showing up-regulation of vimentin. Data is representative of >2 independent experiments. Scale bar: 20 µm

6.2.4 PAF exposure disupts basolateral and apical polarity.

Induction of EMT is usually coupled with loss of basolateral and apical polarity. To study the effect of PAF on the establishment of polarity, the day 20 cultures were immunostained with α6-integrin (basal region marker) and GM130 (marker of apical polarity). We observed loss of α6-integrin from the basal regions in a significant number of acini (Figure 6.4a and Figure 6.4b), implying the ability of cells to break the basement membrane to invade nearby tissues besides loss of basal polarity. Mis-localization of GM130 to the basal and lateral regions confirmed the loss of apical polarity (Figure 6.4a and Figure 6.4b). Further, the loss of E-cadherin (Figure 6.5a and Figure 6.5b) and diffused localization of β-catenin from the cell-cell junctions demonstrated the loss of integrity of adherens junctions (Figure 6.5c and Figure 6.5d), further supporting the claim of ability of PAF to induce EMT.

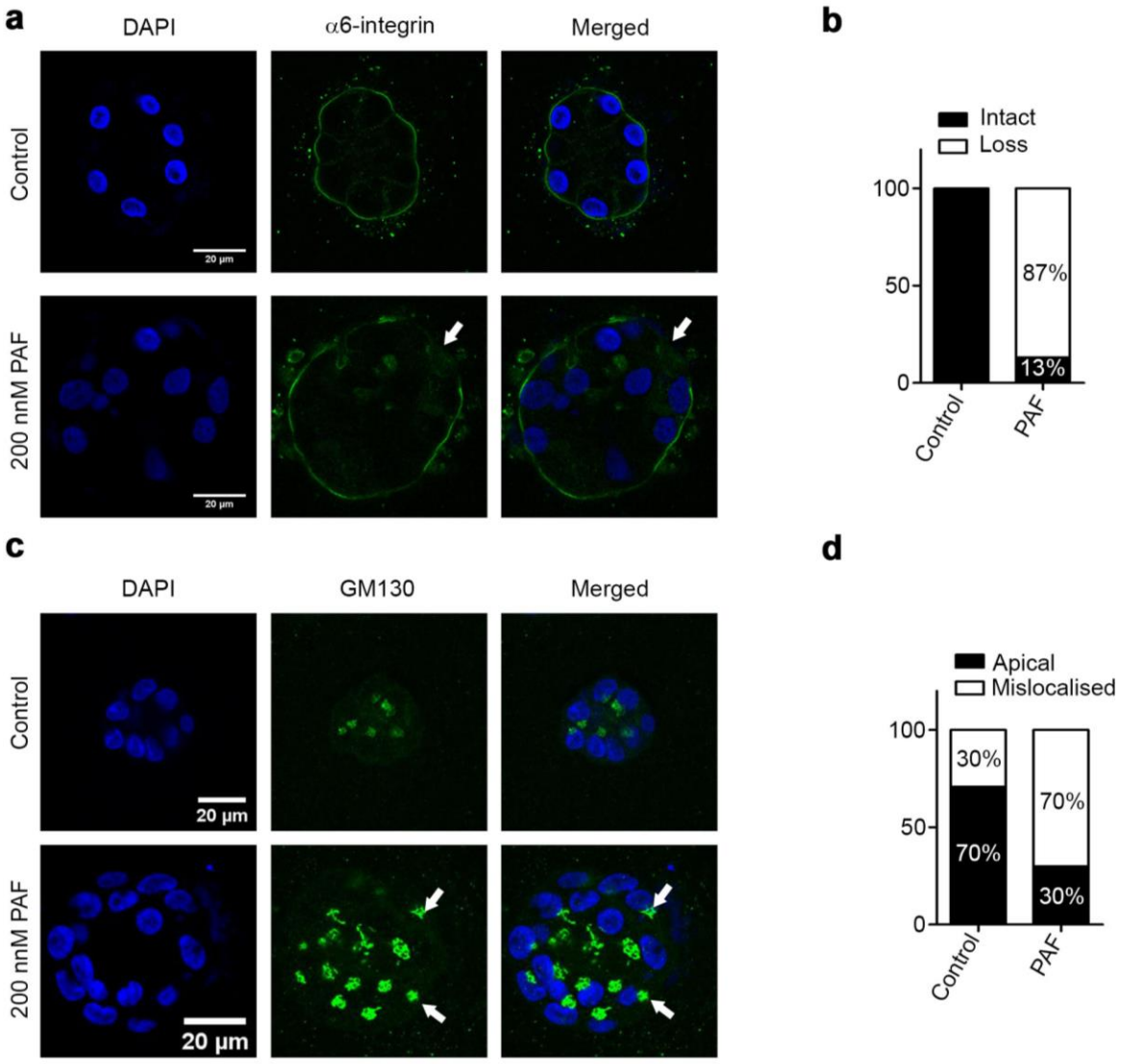

Figure 6.4: Prolonged exposure to PAF resulted in disruption of apico-basal polarity.

Day 20 spheroid cultures were immunostained for basal polarity markers. (a) Representative images of centermost z section of spheroids immunostained with α6-integrin (green). (b) Graph depicting the percentage of acini showing discontinuous α6-integrin staining in basal region. (c) Representative immunofluorescence images of day 20 acini labelled with GM130, a Golgi marker (green). (d) Graph depicting the percentage of acini showing mis-localization of Golgi. White arrows indicate the regions of mis-localization of α6-integrin and

GM130. Data is representative of >2 independent experiments. Scale bar: 20 μm.

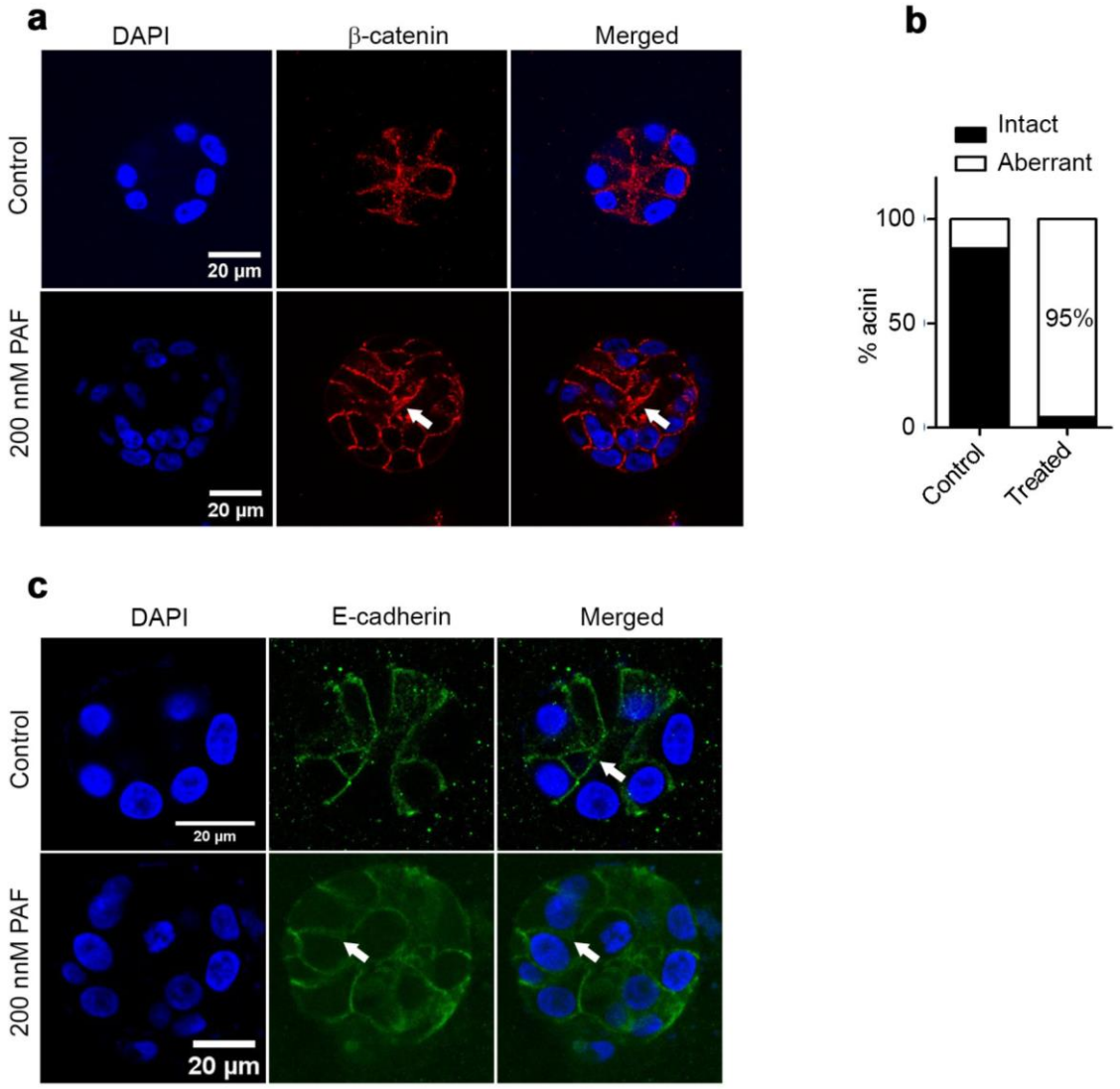

Figure 6.5: Prolonged exposure of MCF10A cells to PAF disrupts adherens junctions.

Day 16 cultures of MCF10A cells were immunostained for markers of adherens junctions and analyzed for their integrity. (a) Representative immunofluorescence images of acini labelled with β-catenin (red). (b) Graph representing the % of acini showing diffused phenotype. (c) Representative immunofluorescence images of acini labelled with E-cadherin (green). (d) Graph representing the

percentage of acini showing loss phenotype. Data is representative of >2 independent experiments. Scale bar: 20 μm

6.3 Discussion

Tumor microenvironment has been considered one of the potential factors involved in tumor progression and ‘ tumor promoting inflammation’ has been enlisted as the “enabling characteristics” by Hannan and Weinberg (Hanahan and Weinberg, 2011). This mainly refers to the tumor promoting effects of the components of the inflammatory reaction cascade. Various bioactive molecules are known to be present in the tumor milieu. Platelet activating factor, a phospholipid mediator, is one such bioactive molecule known to be present at sites of inflammation. Apart from inflammation, PAF is known to be involved in a wide range of physiological and pathological processes. Thus, it is secreted in response to various stimuli either in response to a physiological cue or in response to oxidative, non-physiological as well as non-specific stimuli. Among the various phospholipid mediators, PAF is the least studied in relation to breast cancer. This study aims at studying role of PAF in breast tumorigenesis. Under physiological conditions the amount of PAF in a particular tissue is controlled by a specific class of enzymes such as PAF-AH (Platelet activating factor acetyl hydrolase) which inactivate PAF. These enzymes are present ubiquitously in all tissues and hence there is tight regulation of the signalling elicited by PAF and PAF-like lipids. Chronic inflammatory states are known to result in accumulation of various inflammatory mediators including PAF. Such inflammatory states are also known as predisposing factors to various cancers including breast cancer. PAF and PAF-like lipids are known to be secreted by variety of cells including macrophages, neutrophils, endothelial cells as well as breast cancer cells per se. Camussi’s group also demonstrated the presence of PAF in human breast cancer tissues in amounts significantly higher than the normal tissues as well as associated with increase neo-vascularisation (Montrucchio *et al*., 1998). Further, Bougnoux group also reported presence of PAF in breast cancer tissue and it correlated with axillary lymph node metastasis

(Pitton *et al*., 1989). Cigarette smoke is considered as one of the factors which result in the accumulation of PAF by inhibiting PAF-AH (Kispert *et al*., 2015; Sharma *et al*., 2011). Although role of PAF in various cancers is well established, its role in breast cancer is least studied. Bussolati *et al* have reported the ability of PAF to induce enhanced motility of breast cancer cell lines and have demonstrated the potential of PAF to induce neo-angiogenesis. Further, accumulated PAF (due to cigarette smoke exposure) was illustrated by Mc Howat's group to enhance adherence of metastatic breast cancer cells to lung endothelium (Kispert *et al*., 2014). However none of the reports have studied the effects of PAF in early transformation. Given the presence of PAF in breast tissues we investigated the effects of PAF on non-transformed breast epithelial cells.

Prolonged exposure of PAF induced formation of larger spheroids with significantly more number of cells as compared to untreated cells. Such a phenotype being an indicator of enhanced proliferation, we confirmed it using a proliferation marker, Ki67. These results are in concordance with report by Bussolati *et al*., where they demonstrate the potential of PAF to induce proliferation of breast cancer cells (Bussolati *et al*., 2000). Lumen formation, which depends on equilibrated balance between proliferation and apoptosis was also found to be disrupted (Debnath *et al*., 2002). Partially filled lumen specially characterized by presence of multiple layers of cells surrounding the central lumen were observed in acini formed by PAF treated cells. This continuous proliferation of cells observed in day 20 acini indicates loss of homeostasis since by this time point the non-transformed cells are growth arrested. Given that, epithelial cells exhibit distinguishing characteristics such as apico–basal polarity, presence of adherens junctions as well as contacts with basement membrane which are tightly regulated and contribute to the maintenance of tissue architecture as well as homeostasis (Debnath *et al*., 2003), we investigated the effects of PAF on polarity. We observed loss of apico-basal polarity as well as presence of aberrant cell-cell contacts following PAF exposure. The loss of α6-

integrin from the basal region indicated the loss of contact with the basement membrane and possible induction of invasiveness. Up-regulation of vimentin in PAF treated acini implied possible induction of EMT, initial step in induction of invasion and metastasis. Cells grown on 3D substrata that have undergone epithelial-mesenchymal transition (EMT) give rise to protrusion-like structures. When a few cells migrate into such protrusions, these structures may appear as “bulb-like” structures (Godinho *et al*., 2014; Oyanagi *et al*., 2012). In our study we observed that the overall morphology of acini was disrupted. While untreated cells formed a spheroid on Matrigel^{TM}, PAF treated cells formed acini with protrusion-like structures. Thus, these results confirmed the induction of EMT-like phenotype as well as migratory behavior. These results corroborate with the reports in literature wherein PAF has been demonstrated to promote invasion and metastasis in different cancers including ovarian cancer (Yu et al., 2014; Zhang et al., 2010), prostate cancer (Ji et al., 2016; Xu et al., 2013) as well as melanoma cells stimulated by cytokines (Melnikova and Bar-Eli, 2007; Melnikova et al., 2008). PAF has also been shown to induce invasion in HUVECs. In prostate cancer, PAF has been reported to reduce E-cadherin levels (Ji et al., 2016; Xu et al., 2013) while in Kaposis sarcoma it has been shown to reduce endogenous expression of cell-cell adherens junctions (Bussolino et al., 1995). Thus, suggesting a possible role in EMT. In concordance with the published reports, loss of E-cadherin from the cell-cell junctions in breast epithelial cells was observed in our study. Further, Bennett *et al*, have demonstrated the potential of PAF to induce phenotypic transformation of rat embryonic cells which further supports our claim of ability of PAF to transform breast epithelial cells (Bennett et al., 1993).

Taken together, we report that prolonged exposure of non-transformed breast epithelial cells to PAF results in phenotypic transformation (Summarized in Figure 6.6). However, further studies are essential to investigate whether the transformation observed is malignant. Given that PAF acts through PAF-R and PAF exposure results in such drastic changes in acinar morphology, there may

be a possibility of increased expression of PAF-R and this might probably induce transformation. On the other hand, continuous exposure to PAF can result in continuous stimulation of PAF-R, resulting in enhanced signalling and hence transformation. The former hypothesis can be validated by investigating the level of PAF-R in the PAF transformed cells and later knocking down PAF-R in MDA-MB231 cells (invasive breast cancer cell lines) to observe a partial reversal of transformed phenotype.

Nevertheless, these preliminary results imply that presence of PAF in the microenvironment is capable of inducing transformation of breast epithelial cells. These facts indicate strongly the requirement of investigating the role of PAF in transformation in breast epithelial cells of MCF10A and also essentially the pathway followed to undergo transformation. Identification of key players in the pathway(s) may serve as potential targets and aid in better therapeutic interventions.

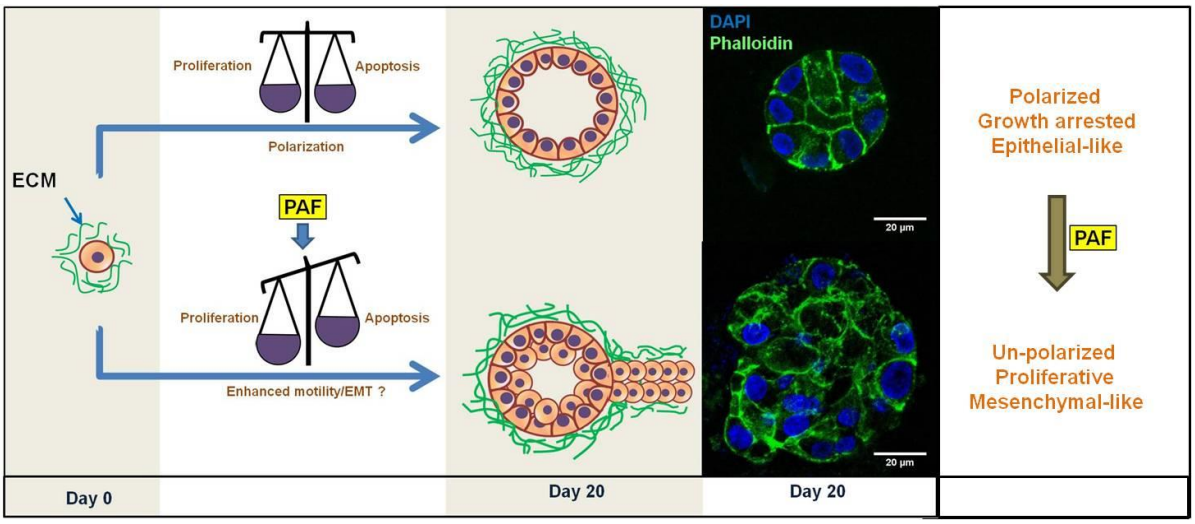

Figure 6.6: Schematic summarizing the phenotypic transformation phenotypes induced by continuous exposure to PAF.

Partially filled lumen specially characterized by presence of multiple layers of cells surrounding the central lumen was observed in acini formed by PAF treated cells. This suggests disruption of the equilibrated balance between proliferation and apoptosis which regulates lumen formation. The protrusion-like phenotype

induced upon PAF induction mimics EMT-like and invasive phenotype. The study further confirmed induction of Phenotypic transformation by investigating markers of polarity and EMT. *(Adapted from Libi Anandi., 2016)*.

Chapter 7: Conclusion and Future perspectives

This thesis explored the two “enabling characteristics” namely genomic instability and tumor promoting inflammation; enumerated by Hanahan & Weinberg in “Hallmarks of Cancer, Cell 2010", using 3-dimensional cultures of non-transformed breast epithelial cells as the model system.

To our knowledge, this is the first study to have demonstrated the ability of alkylating agents to induce tumorigenesis. Though MNU has been widely used to induce mammary tumors in rat, the exact mechanism of tumorigenesis has not been elucidated till date. This lacuna prompted us to decipher the mechanism. We identified DNA-PK, a apical kinase involved in the non-homologous end joining pathway of the DNA damage response, to be a central player in the process. This novel role of DNA-PK can be further validated by investigating clinical samples. Total level as well as the level of phosphorylated DNA-PKcs needs to be determined. The target population for this study would be the patients who have had relapse after chemotherapy or radiation therapy. Further, patients without a family history of breast cancer (sporadic cases) can also be tested for the above. These studies can thus help in establishing DNA-PKcs total and/or phosphorylated form as a biomarker and help modulate the existing therapies.

Although DNA-PK has been identified as the key player in the process of DNA damage induced transformation, involvement of alternate pathway(s) cannot be ignored. Based on literature, supported by the preliminary data we have predicted plausible pathway(s) (Figure 7.1). Published reports suggest the possible role of JNK in DNA damage induced transformation. DNA breaks are known to activate NF-κB which results in secretion of TNF-α leading to the activation of JNK pathway(Picco and Pages, 2013). Consistent with these reports, our western data suggests activation of cJun, immediate downstream target of JNK, in acini formed by MNU treated cells. cJun is also known to up-regulate Snail (Lemieux et al., 2009). We observed activation of cJun and up-regulation of Snail in our study, suggesting the activation of JNK pathway to play a role in transformation. Apart from this, we also observed an up-regulation of Api5 (Apoptosis inhibitor 5). Api5 is an oncogene, implicated in various cancers. It is known to induce invasion

through up-regulation of FGF2 (Cho et al., 2014), thus suggesting that MNU possibly can induce invasion in MCF10A cells. In addition to this, FGF2 and Snail are known to induce invasion via MMP9 (Cho et al., 2014; Jorda et al., 2005), corroborating with our results of presence of active MMP9 in the conditioned media. Akt is known to be phosphorylated by DNA-PKcs at serine 473 position following DNA damage. Enhanced phosphorylation of Akt observed at day 16, coupled with the constitutive activation of DNA-PKcs, suggests the possible activation of Akt by DNA-PKcs in our study. Activated Akt can stabilize Snail through activation of NF-κB or through phosphorylation of GSK3β (Julien et al., 2007; Wang et al., 2013). ALC1 interacts with Api5 as well as DNA-PKcs; Api5 has been shown to interact with proteins involved in the DNA damage pathway, up-regulation of Api5 observed in our study implies the possible role of this protein in transformation following DNA damage. However, our study reveals that up-regulation of Api5 *per se* can induce transformation. Nevertheless, the mechanism of transformation remains to be elucidated.

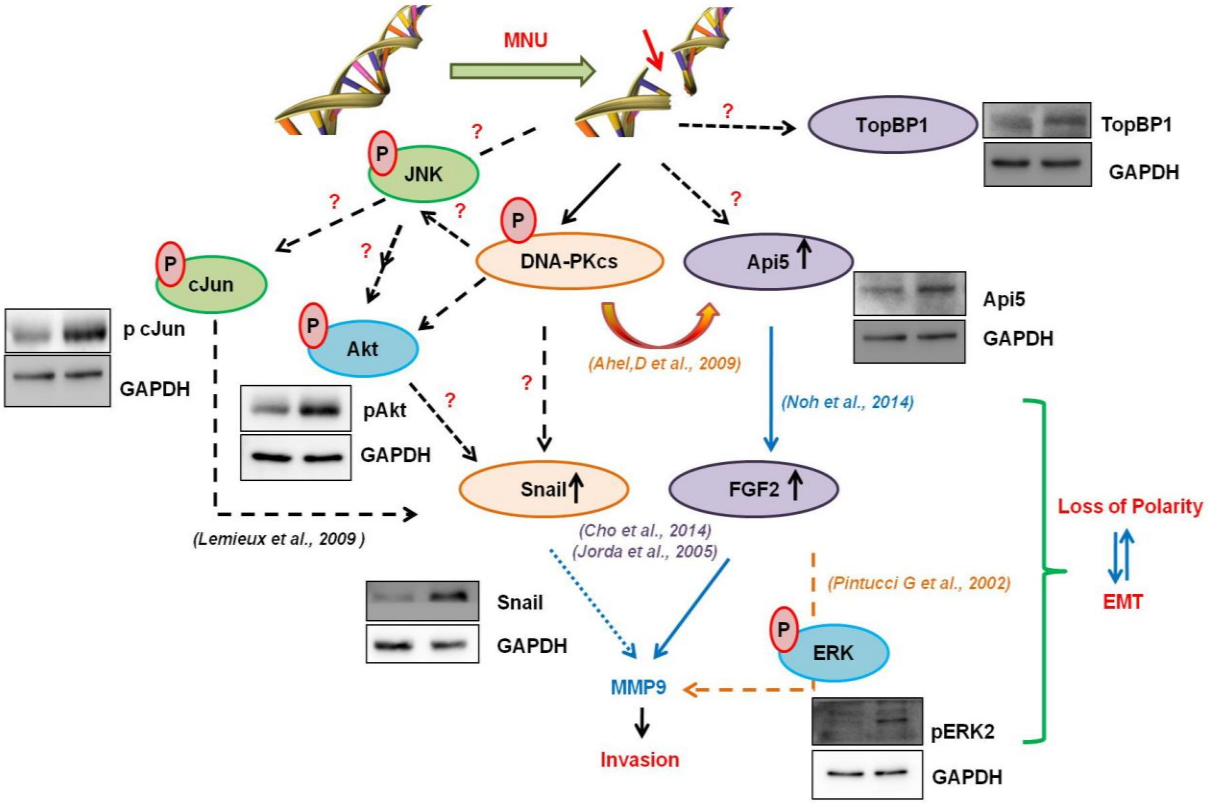

Figure 7.1: Plausible signaling pathways for MNU-induced DNA damage leading to transformation.

Interestingly, our study reveals that up-regulation of Api5 *per se* can induce transformation. Nevertheless, the mechanism of transformation remains to be elucidated. Api5 over-expression in MCF10 cells resulted in the formation of acini with phenotypes implying transformation. Considering the various phenotypes observed and based on available literature, plausible pathway has been predicted (Figure 7.2). Api5 is known to enhance transcriptional activation of G1/S cell cycle genes mediated by E2F1; thus, hyper-proliferation, a key phenotype observed in our study may be attributed to effect on E2F1 following Api5 over-expression (Garcia-Jove Navarro et al., 2013). FGF2 is known to be up-regulated following Api5 up-regulation (Noh et al., 2014); FGF2 through activation of FGFR signaling activates ERK; activated ERK (Api5 mediated) results in transcriptional activation of AP-1 which eventually results in secretion of MMP9 (Song et al., 2014). Thus, the induction of EMT and the possible induction of invasive phenotype observed in our study coupled with the reports suggesting role of API5 in cancer cell invasion (Kim et al., 2000) and EMT in urothelial carcinoma cell lines (Tomlinson et al., 2012) can be attributed to the activation of ERK by Api5 through FGF2. FGF2 is known to down-regulate E-cadherin in ovarian cancer cells (Lau et al., 2013) which corroborates with our observation of 60% acini formed by Api5 over-expressed cells showing loss of E-cadherin. However, further experiments have to be designed to validate the predicted pathways.

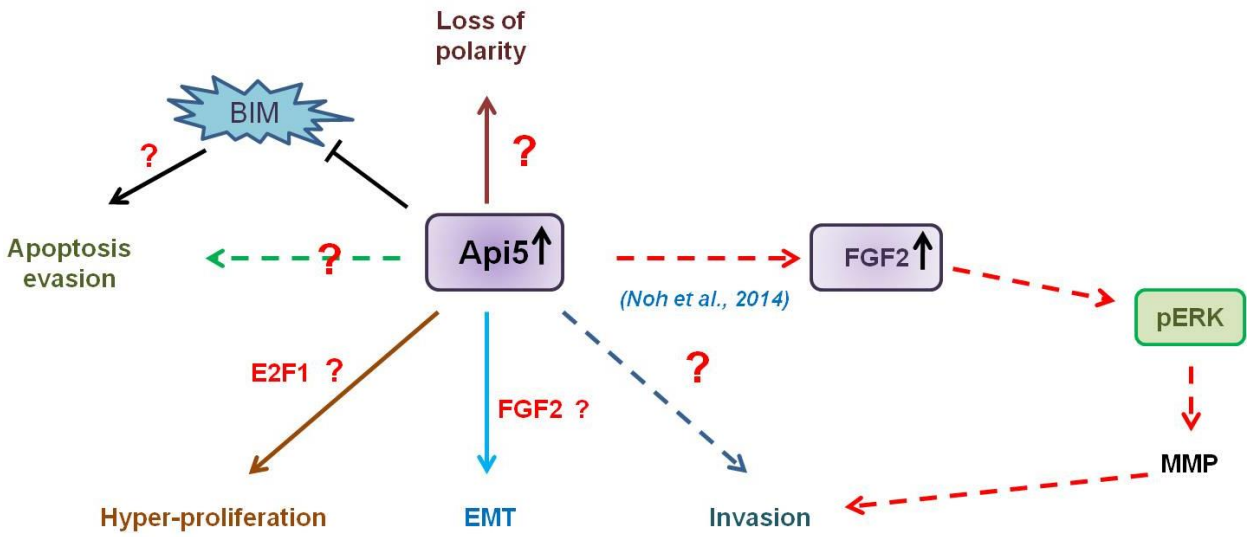

Figure 7.2: Schematic depicting the various phenotypes observed in 3-D "on top" cultures following API5 over-expression.

It’s a well known fact that DNA damage, if left unrepaired can lead to nuclear effects which might result in genomic instability. This paradigm of effect of DNA damage has been well characterized. However, very little is known till date about the effects of DNA damage on other cellular organelles. Our study has precisely provided this missing link. We observed dispersal of Golgi as well as impaired trafficking. Dispersal of Golgi was found to be mediated by DNA-PK. Apart from this; we observed that DNA damage induced reorganization of the cytoskeletal network. This reorganization was found to be mediated by DNA-PK via activation of JNK, Akt. Microtubule reorganization was found to be actin dependent. We have predicted the pathway based on preliminary data (Figure 7.3). The precise mechanism has not been deciphered and validation of the predicted pathway needs to be done. Further studies in deciphering mechanism would shed light into reorganization phenomenon and provide insights into the implication of such an organization.

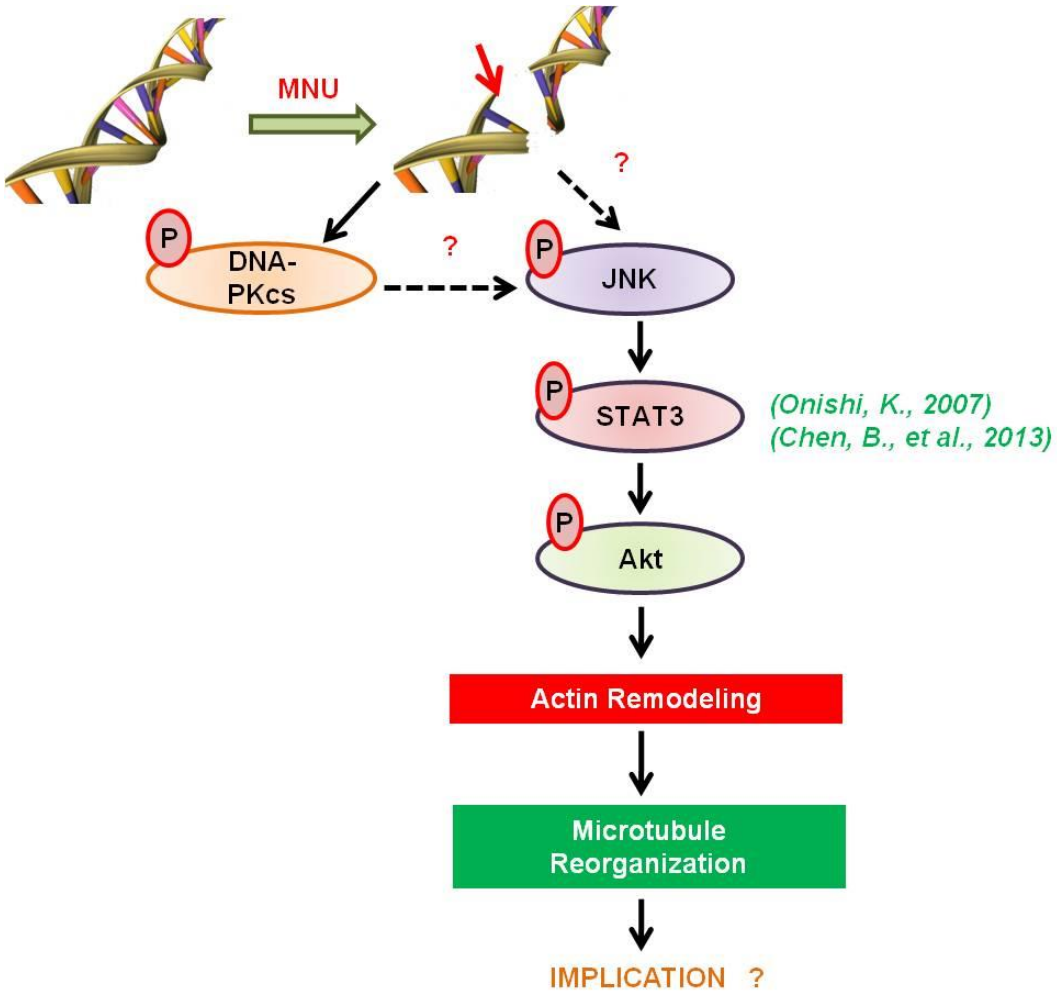

Figure 7.3: Schematic depicting the plausible pathway involved in re-organization of cytoskeleton following DNA damage.

Prolonged exposure to PAF resulted in the formation of abnormal acinar structures. Loss of polarity and induction of EMT-like phenotype was also observed. In conclusion, PAF exposure resulted in phenotypic transformation of breast epithelial cells. Based on literature we have tried predicting the plausible pathway of PAF induced transformation (Figure 7.4: Plausible pathways of PAF induced transformation based on published literature.). PAF is known to activate various signal transduction pathways in different cell types. Preliminary data from lab indicate the possible role of PI3K and/or JNK pathway in PAF induced enhanced migration of MDA-MB 231 breast cancer cells (Anandi et al., 2016). On similar lines, in esophageal squamous cell carcinoma cells Kravenchenko *et al* have reported activated PAF-R to activate Akt (PI3K pathway) which further activates NF-κβ to upregulate oncogenes (Kravchenko et al., 1995). In another study, Congjan Xu's group has demonstrated PAF to act through PAF receptor and activate EGFR finally activating ERK pathway (Yu et al., 2014). In HUVECs, PAF has been demonstrated to activate the JAK-STAT pathway resulting in nuclear localization of STAT-3 and induction of proliferation, invasion and metastasis (Deo et al., 2002). In addition to this, they have also demonstrated activation of PAF-R by PAF activated Src which in turn resulted in PAF production from lyso PAF through activation of Ras, Erk, PLA_2 in a sequential manner (Aponte et al., 2008).

Investigation of status of PAF-R in Indian patients will be investigated. Further, the findings from the lab will be compared to the clinical samples to establish the correlation and hence validate the pathway deciphered

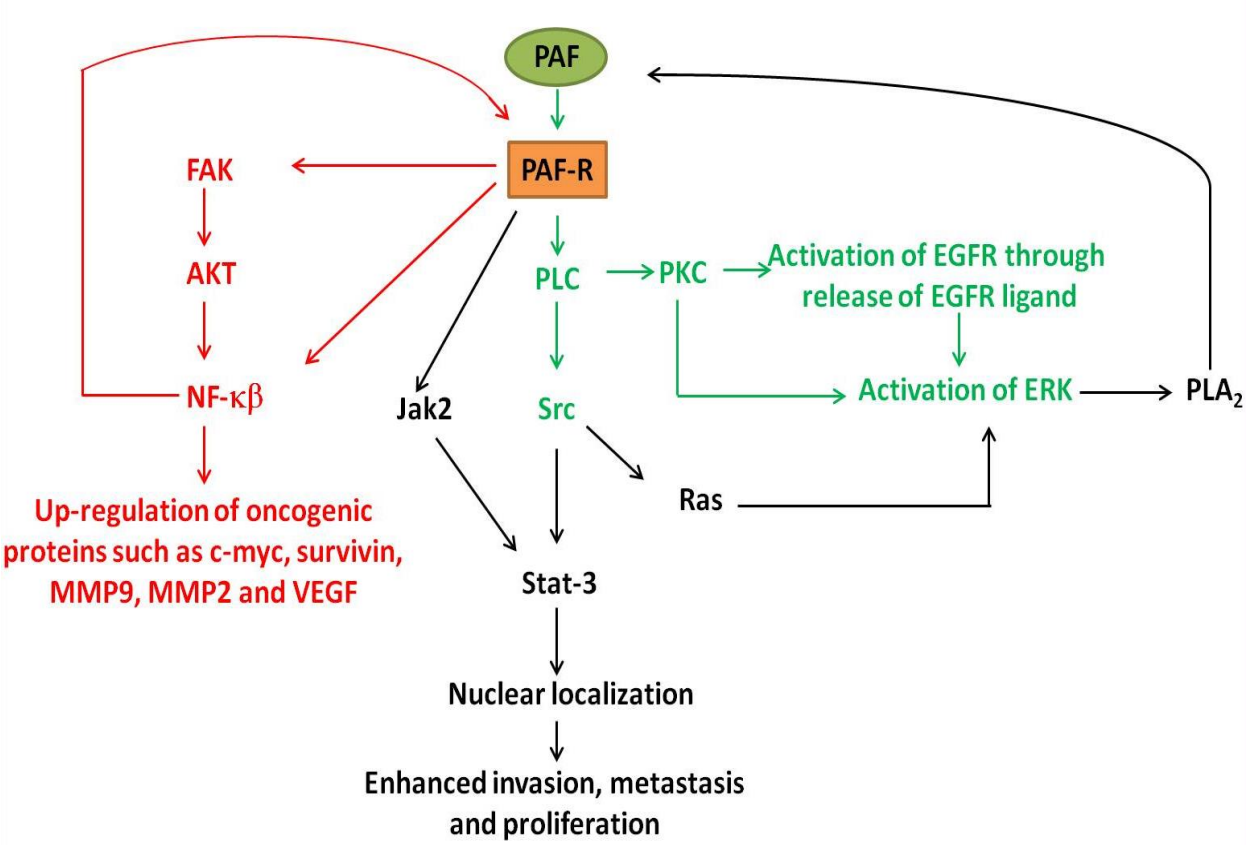

Figure 7.4: Plausible pathways of PAF induced transformation based on published literature.

.

BIBLIOGRAPHY

Acevedo-Arozena, A., Wells, S., Potter, P., Kelly, M., Cox, R.D., and Brown, S.D. (2008). ENU mutagenesis, a way forward to understand gene function. Annual review of genomics and human genetics *9*, 49-69.

Agarwal, G., and Ramakant, P. (2008). Breast Cancer Care in India: The Current Scenario and the Challenges for the Future. Breast Care (Basel) *3*, 21-27.

Aich, R., Mondal, N., Chhatui, B., Sepai, H., Aich, R., Acharyya, A., Manir, K., and Bhattacharaya, J. (2016). Relevance of risk factors of breast cancer in women: An Eastern Indian scenario. Journal of Cancer Research and Therapeutics *12*, 302-308.

Allred, D.C., Mohsin, S.K., and Fuqua, S.A. (2001). Histological and biological evolution of human premalignant breast disease. Endocr Relat Cancer *8*, 47-61.

Allred, D.C., Wu, Y., Mao, S., Nagtegaal, I.D., Lee, S., Perou, C.M., Mohsin, S.K., O'Connell, P., Tsimelzon, A., and Medina, D. (2008). Ductal carcinoma in situ and the emergence of diversity during breast cancer evolution. Clin Cancer Res *14*, 370-378.

Anandi, V.L., Ashiq, K.A., Nitheesh, K., and Lahiri, M. (2016). Platelet-activating factor promotes motility in breast cancer cells and disrupts non-transformed breast acinar structures. Oncology reports *35*, 179-188.

Anderson, C.W., and Lees-Miller, S.P. (1992). The nuclear serine/threonine protein kinase DNA-PK. Critical reviews in eukaryotic gene expression *2*, 283-314.

Andrin, C., McDonald, D., Attwood, K.M., Rodrigue, A., Ghosh, S., Mirzayans, R., Masson, J.Y., Dellaire, G., and Hendzel, M.J. (2012). A requirement for polymerized actin in DNA double-strand break repair. Nucleus *3*, 384-395.

Anitei, M., and Hoflack, B. (2011). Bridging membrane and cytoskeleton dynamics in the secretory and endocytic pathways. Nature cell biology *14*, 11-19.

Aponte, M., Jiang, W., Lakkis, M., Li, M.-J., Edwards, D., Albitar, L., Vitonis, A., Mok, S.C., Cramer, D.W., and Ye, B. (2008). Activation of Platelet-Activating Factor Receptor and Pleiotropic Effects on Tyrosine Phospho-EGFR/Src/FAK/Paxillin in Ovarian Cancer. Cancer research *68*, 5839-5848.

Aranda, V., Haire, T., Nolan, M.E., Calarco, J.P., Rosenberg, A.Z., Fawcett, J.P., Pawson, T., and Muthuswamy, S.K. (2006). Par6-aPKC uncouples ErbB2 induced disruption of polarized epithelial organization from proliferation control. Nature cell biology *8*, 1235-1245.

Arpino, G., Laucirica, R., and Elledge, R.M. (2005). Premalignant and in situ breast disease: biology and clinical implications. Ann Intern Med *143*, 446-457.

Atkinson, H.G. (2003). Alcohol's "darker side." A drink a day may raise a woman's risk of breast cancer. Health News *9*, 4.

Ayollo, D.V., Zhitnyak, I.Y., Vasiliev, J.M., and Gloushankova, N.A. (2009). Rearrangements of the actin cytoskeleton and E-cadherin-based adherens junctions caused by neoplasic transformation change cell-cell interactions. PloS one *4*, e8027.

Barrows, L.R., and Magee, P.N. (1982). Nonenzymatic methylation of DNA by S-adenosylmethionine in vitro. Carcinogenesis *3*, 349-351.

Bartek, J., Mistrik, M., and Bartkova, J. (2012). Thresholds of replication stress signaling in cancer development and treatment. Nature structural & molecular biology *19*, 5-7.

Bartkova, J., Rezaei, N., Liontos, M., Karakaidos, P., Kletsas, D., Issaeva, N., Vassiliou, L.V., Kolettas, E., Niforou, K., Zoumpourlis, V.C.*, et al.* (2006). Oncogene-induced senescence is part of the tumorigenesis barrier imposed by DNA damage checkpoints. Nature *444*, 633-637.

Baumgart, P.M., Kliem, H.C., Gottfried-Anacker, J., Wiessler, M., and Schmeiser, H.H. (1993). Site-specific mutagenesis induced by single O6-alkylguanines (O6-n-propyl, O6-n-butyl, O6-n-octyl) in vivo. Nucleic acids research *21*, 3755-3760.

Belin, B.J., Lee, T., and Mullins, R.D. (2015). DNA damage induces nuclear actin filament assembly by Formin -2 and Spire-(1/2) that promotes efficient DNA repair. [corrected]. eLife *4*, e07735.

Bennett, S.A., Leite, L.C., and Birnboim, H.C. (1993). Platelet activating factor, an endogenous mediator of inflammation, induces phenotypic transformation of rat embryo cells. Carcinogenesis *14*, 1289-1296.

Bernstein, L., Henderson, B.E., Hanisch, R., Sullivan-Halley, J., and Ross, R.K. (1994). Physical exercise and reduced risk of breast cancer in young women. J Natl Cancer Inst *86*, 1403-1408.

Bissell, M.J., and Radisky, D. (2001). Putting tumours in context. Nat Rev Cancer *1*, 46-54.

Bissell, M.J., Weaver, V.M., Lelievre, S.A., Wang, F., Petersen, O.W., and Schmeichel, K.L. (1999). Tissue structure, nuclear organization, and gene expression in normal and malignant breast. Cancer research *59*, 1757-1763s; discussion 1763s-1764s.

Bodakuntla, S., V, L.A., Sural, S., Trivedi, P., and Lahiri, M. (2014). N-nitroso-N-ethylurea activates DNA damage surveillance pathways and induces transformation in mammalian cells. BMC Cancer *14*, 1-14.

Bodian, C.A., Perzin, K.H., Lattes, R., and Hoffmann, P. (1993). Reproducibility and validity of pathologic classifications of benign breast disease and implications for clinical applications. Cancer *71*, 3908-3913.

Boncompain, G., Divoux, S., Gareil, N., de Forges, H., Lescure, A., Latreche, L., Mercanti, V., Jollivet, F., Raposo, G., and Perez, F. (2012). Synchronization of secretory protein traffic in populations of cells. Nature methods *9*, 493-498.

Bonner, M.R., Han, D., Nie, J., Rogerson, P., Vena, J.E., Muti, P., Trevisan, M., Edge, S.B., and Freudenheim, J.L. (2005). Breast cancer risk and exposure in early life to polycyclic aromatic hydrocarbons using total suspended particulates as a proxy measure. Cancer epidemiology, biomarkers & prevention : a

publication of the American Association for Cancer Research, cosponsored by the American Society of Preventive Oncology *14*, 53-60.

Bouffler, S.D., Hofland, N., Cox, R., and Fodde, R. (2000). Evidence for Msh2 haploinsufficiency in mice revealed by MNU-induced sister-chromatid exchange analysis. British journal of cancer *83*, 1291-1294.

Brown, P., and Allen, A.R. (2002). Obesity linked to some forms of cancer. The West Virginia medical journal *98*, 271-272.

Burkhardt, J.K. (1998). The role of microtubule-based motor proteins in maintaining the structure and function of the Golgi complex. Biochimica et biophysica acta *1404*, 113-126.

Bussolati, B., Biancone, L., Cassoni, P., Russo, S., Rola-Pleszczynski, M., Montrucchio, G., and Camussi, G. (2000). PAF produced by human breast cancer cells promotes migration and proliferation of tumor cells and neo-angiogenesis. The American journal of pathology *157*, 1713-1725.

Bussolino, F., Arese, M., Montrucchio, G., Barra, L., Primo, L., Benelli, R., Sanavio, F., Aglietta, M., Ghigo, D., Rola-Pleszczynski, M.R.*, et al.* (1995). Platelet activating factor produced in vitro by Kaposi's sarcoma cells induces and sustains in vivo angiogenesis. The Journal of clinical investigation *96*, 940-952.

Byrne, A.-M., Bekiaris, S., Duggan, G., Prichard, D., Kirca, M., Finn, S., Reynolds, J.V., Kelleher, D., and Long, A. (2015). Golgi phosphoprotein 2 (GOLPH2) is a novel bile acid-responsive modulator of oesophageal cell migration and invasion. British journal of cancer *113*, 1332-1342.

Cancer, C.G.o.H.F.i.B. (2001). Familial breast cancer: collaborative reanalysis of individual data from 52 epidemiological studies including 58,209 women with breast cancer and 101,986 women without the disease. Lancet *358*, 1389-1399.

Carter, C.L., Corle, D.K., Micozzi, M.S., Schatzkin, A., and Taylor, P.R. (1988). A prospective study of the development of breast cancer in 16,692 women with benign breast disease. Am J Epidemiol *128*, 467-477.

Cellai, C., Laurenzana, A., Vannucchi, A.M., Caporale, R., Paglierani, M., Di Lollo, S., Pancrazzi, A., and Paoletti, F. (2006). Growth inhibition and differentiation of human breast cancer cells by the PAFR antagonist WEB-2086. British journal of cancer *94*, 1637-1642.

Cerutti, P.A. (1994). Oxy-radicals and cancer. Lancet *344*, 862-863.

Chabin-Brion, K., Marceiller, J., Perez, F., Settegrana, C., Drechou, A., Durand, G., and Pous, C. (2001). The Golgi complex is a microtubule-organizing organelle. Molecular biology of the cell *12*, 2047-2060.

Chaney, S.G., and Sancar, A. (1996). DNA repair: enzymatic mechanisms and relevance to drug response. J Natl Cancer Inst *88*, 1346-1360.

Chao, W., and Olson, M.S. (1993). Platelet-activating factor: receptors and signal transduction. The Biochemical journal *292 (Pt 3)*, 617-629.

Chen, A., Beetham, H., Black, M.A., Priya, R., Telford, B.J., Guest, J., Wiggins, G.A., Godwin, T.D., Yap, A.S., and Guilford, P.J. (2014). E-cadherin loss alters cytoskeletal organization and adhesion in non-malignant breast cells but is insufficient to induce an epithelial-mesenchymal transition. BMC Cancer *14*, 552.

Chen, J., Miller, E.M., and Gallo, K.A. (2010). MLK3 is critical for breast cancer cell migration and promotes a malignant phenotype in mammary epithelial cells. Oncogene *29*, 4399-4411.

Chen, W.Y., Colditz, G.A., Rosner, B., Hankinson, S.E., Hunter, D.J., Manson, J.E., Stampfer, M.J., Willett, W.C., and Speizer, F.E. (2002). Use of postmenopausal hormones, alcohol, and risk for invasive breast cancer. Annals of internal medicine *137*, 798-804.

Cheung-Ong, K., Giaever, G., and Nislow, C. (2013). DNA-Damaging Agents in Cancer Chemotherapy: Serendipity and Chemical Biology. Chemistry & Biology *20*, 648-659.

Cho, H., Chung, J.Y., Song, K.H., Noh, K.H., Kim, B.W., Chung, E.J., Ylaya, K., Kim, J.H., Kim, T.W., and Hewitt, S.M. (2014). Apoptosis inhibitor-5

overexpression is associated with tumor progression and poor prognosis in patients with cervical cancer. BMC Cancer *14*, 545.

Chopra, B., Kaur, V., Singh, K., Verma, M., Singh, S., and Singh, A. (2014). Age shift: Breast cancer is occurring in younger age groups - Is it true? Clinical Cancer Investigation Journal *3*, 526-529.

Christiansen, J.J., and Rajasekaran, A.K. (2006). Reassessing epithelial to mesenchymal transition as a prerequisite for carcinoma invasion and metastasis. Cancer research *66*, 8319-8326.

Ciani, L., and Salinas, P.C. (2007). c-Jun N-terminal kinase (JNK) cooperates with Gsk3β to regulate Dishevelled-mediated microtubule stability. BMC Cell Biology *8*, 27.

Cimino, D., Fuso, L., Sfiligoi, C., Biglia, N., Ponzone, R., Maggiorotto, F., Russo, G., Cicatiello, L., Weisz, A., Taverna, D.*, et al.* (2008). Identification of new genes associated with breast cancer progression by gene expression analysis of predefined sets of neoplastic tissues. International journal of cancer *123*, 1327-1338.

Cornell, L., Munck, J.M., Alsinet, C., Villanueva, A., Ogle, L., Willoughby, C.E., Televantou, D., Thomas, H.D., Jackson, J., Burt, A.D.*, et al.* (2015). DNA-PK—A Candidate Driver of Hepatocarcinogenesis and Tissue Biomarker That Predicts Response to Treatment and Survival. Clinical Cancer Research *21*, 925-933.

Crick, F.H., Barnett, L., Brenner, S., and Watts-Tobin, R.J. (1961). General nature of the genetic code for proteins. Nature *192*, 1227-1232.

Darbre, P.D., Aljarrah, A., Miller, W.R., Coldham, N.G., Sauer, M.J., and Pope, G.S. (2004). Concentrations of parabens in human breast tumours. Journal of applied toxicology : JAT *24*, 5-13.

Davis, J.D., and Lin, S.Y. (2011). DNA damage and breast cancer. World journal of clinical oncology *2*, 329-338.

De Matteis, M.A., and Luini, A. (2008). Exiting the Golgi complex. Nat Rev Mol Cell Biol *9*, 273-284.

Debnath, J., and Brugge, J.S. (2005). Modelling glandular epithelial cancers in three-dimensional cultures. Nat Rev Cancer *5*, 675-688.

Debnath, J., Mills, K.R., Collins, N.L., Reginato, M.J., Muthuswamy, S.K., and Brugge, J.S. (2002). The role of apoptosis in creating and maintaining luminal space within normal and oncogene-expressing mammary acini. Cell *111*, 29-40.

Debnath, J., Muthuswamy, S.K., and Brugge, J.S. (2003). Morphogenesis and oncogenesis of MCF-10A mammary epithelial acini grown in three-dimensional basement membrane cultures. Methods *30*, 256-268.

Deo, D.D., Axelrad, T.W., Robert, E.G., Marcheselli, V., Bazan, N.G., and Hunt, J.D. (2002). Phosphorylation of STAT-3 in response to basic fibroblast growth factor occurs through a mechanism involving platelet-activating factor, JAK-2, and Src in human umbilical vein endothelial cells. Evidence for a dual kinase mechanism. The Journal of biological chemistry *277*, 21237-21245.

Dey, D., Saxena, M., Paranjape, A.N., Krishnan, V., Giraddi, R., Kumar, M.V., Mukherjee, G., and Rangarajan, A. (2009). Phenotypic and functional characterization of human mammary stem/progenitor cells in long term culture. PloS one *4*, e5329.

Dhimolea, E., Maffini, M.V., Soto, A.M., and Sonnenschein, C. (2010). The role of collagen reorganization on mammary epithelial morphogenesis in a 3D culture model. Biomaterials *31*, 3622-3630.

Di Micco, R., Fumagalli, M., Cicalese, A., Piccinin, S., Gasparini, P., Luise, C., Schurra, C., Garre, M., Nuciforo, P.G., Bensimon, A.*, et al.* (2006). Oncogene-induced senescence is a DNA damage response triggered by DNA hyper-replication. Nature *444*, 638-642.

Dow, L.E., and Humbert, P.O. (2007). Polarity regulators and the control of epithelial architecture, cell migration, and tumorigenesis. International review of cytology *262*, 253-302.

Du, J., Sun, C., Hu, Z., Yang, Y., Zhu, Y., Zheng, D., Gu, L., and Lu, X. (2010). Lysophosphatidic acid induces MDA-MB-231 breast cancer cells migration through activation of PI3K/PAK1/ERK signaling. PloS one *5*, e15940.

Dupont, W.D., Parl, F.F., Hartmann, W.H., Brinton, L.A., Winfield, A.C., Worrell, J.A., Schuyler, P.A., and Plummer, W.D. (1993). Breast cancer risk associated with proliferative breast disease and atypical hyperplasia. Cancer *71*, 1258-1265.

Etienne-Manneville, S. (2004). Actin and microtubules in cell motility: which one is in control? Traffic *5*, 470-477.

Farber-Katz, S.E., Dippold, H.C., Buschman, M.D., Peterman, M.C., Xing, M., Noakes, C.J., Tat, J., Ng, M.M., Rahajeng, J., Cowan, D.M.*, et al.* (2014). DNA damage triggers Golgi dispersal via DNA-PK and GOLPH3. Cell *156*, 413-427.

Feng, W., Di Rienzi, S.C., Raghuraman, M.K., and Brewer, B.J. (2011). Replication stress-induced chromosome breakage is correlated with replication fork progression and is preceded by single-stranded DNA formation. G3 (Bethesda) *1*, 327-335.

Ford, D., and Easton, D.F. (1995). The genetics of breast and ovarian cancer. British journal of cancer *72*, 805-812.

Fournier, M.V., Martin, K.J., Kenny, P.A., Xhaja, K., Bosch, I., Yaswen, P., and Bissell, M.J. (2006). Gene expression signature in organized and growth-arrested mammary acini predicts good outcome in breast cancer. Cancer research *66*, 7095-7102.

Friedenreich, C.M., Bryant, H.E., and Courneya, K.S. (2001). Case-control study of lifetime physical activity and breast cancer risk. American journal of epidemiology *154*, 336-347.

Garcia-Jove Navarro, M., Basset, C., Arcondeguy, T., Touriol, C., Perez, G., Prats, H., and Lacazette, E. (2013). Api5 contributes to E2F1 control of the G1/S cell cycle phase transition. PLoS One *8*, e71443.

Giannelli, G., and Antonaci, S. (2000). Biological and clinical relevance of Laminin-5 in cancer. Clinical & experimental metastasis *18*, 439-443.

Givelber, H.M., and DiPaolo, J.A. (1969). Teratogenic effects of N-ethyl-N-nitrosourea in the Syrian hamster. Cancer Res *29*, 1151-1155.

Godinho, S.A., Picone, R., Burute, M., Dagher, R., Su, Y., Leung, C.T., Polyak, K., Brugge, J.S., Thery, M., and Pellman, D. (2014). Oncogene-like induction of cellular invasion from centrosome amplification. Nature *510*, 167-171.

Goodwin, J.F., and Knudsen, K.E. (2014). Beyond DNA repair: DNA-PK function in cancer. Cancer discovery *4*, 1126-1139.

Goodwin, J.F., Kothari, V., Drake, J.M., Zhao, S., Dylgjeri, E., Dean, J.L., Schiewer, M.J., McNair, C., Jones, J.K., Aytes, A.*, et al.* (2015). DNA-PKcs-Mediated Transcriptional Regulation Drives Prostate Cancer Progression and Metastasis. Cancer Cell *28*, 97-113.

Gorgoulis, V.G., Vassiliou, L.V., Karakaidos, P., Zacharatos, P., Kotsinas, A., Liloglou, T., Venere, M., Ditullio, R.A., Jr., Kastrinakis, N.G., Levy, B.*, et al.* (2005). Activation of the DNA damage checkpoint and genomic instability in human precancerous lesions. Nature *434*, 907-913.

Gullino, P.M., Pettigrew, H.M., and Grantham, F.H. (1975). N-Nitrosomethylurea as Mammary Gland Carcinogen in Rats. J Natl Cancer Inst *54*, 401-414.

Guo, H.B., Johnson, H., Randolph, M., Nagy, T., Blalock, R., and Pierce, M. (2010). Specific posttranslational modification regulates early events in mammary carcinoma formation. Proc Natl Acad Sci U S A *107*, 21116-21121.

Guzman, R.C., Osborn, R.C., Bartley, J.C., and Nandi, S. (1988). Metabolism of 7,12-dimethylbenz[a]anthracene by mouse mammary epithelial cells cultured serum-free inside collagen gels. Cancer letters *40*, 123-132.

Hanahan, D., and Weinberg, R.A. (2011). Hallmarks of cancer: the next generation. Cell *144*, 646-674.

Helmrich, S.P., Shapiro, S., Rosenberg, L., Kaufman, D.W., Slone, D., Bain, C., Miettinen, O.S., Stolley, P.D., Rosenshein, N.B., Knapp, R.C*., et al.* (1983). Risk factors for breast cancer. American journal of epidemiology *117*, 35-45.

Henderson, B.E., Ross, R., and Bernstein, L. (1988). Estrogens as a cause of human cancer: the Richard and Hinda Rosenthal Foundation award lecture. Cancer research *48*, 246-253.

Henry, L.A., Johnson, D.A., Sarrio, D., Lee, S., Quinlan, P.R., Crook, T., Thompson, A.M., Reis-Filho, J.S., and Isacke, C.M. (2011). Endoglin expression in breast tumor cells suppresses invasion and metastasis and correlates with improved clinical outcome. Oncogene *30*, 1046-1058.

Herr, R., Wohrle, F.U., Danke, C., Berens, C., and Brummer, T. (2011). A novel MCF-10A line allowing conditional oncogene expression in 3D culture. Cell Commun Signal *9*, 17.

Hirose, K., Tajima, K., Hamajima, N., Takezaki, T., Inoue, M., Kuroishi, T., Miura, S., and Tokudome, S. (2001). Association of family history and other risk factors with breast cancer risk among Japanese premenopausal and postmenopausal women. Cancer causes & control : CCC *12*, 349-358.

Hirschberg, K., Miller, C.M., Ellenberg, J., Presley, J.F., Siggia, E.D., Phair, R.D., and Lippincott-Schwartz, J. (1998). Kinetic analysis of secretory protein traffic and characterization of golgi to plasma membrane transport intermediates in living cells. The Journal of cell biology *143*, 1485-1503.

Hsia, T.C., Tu, C.Y., Chen, H.J., Chen, S.C., Liang, J.A., Chen, C.Y., Wang, Y.C., and Chien, C.R. (2014). A population-based study of primary chemoradiotherapy in clinical stage III non-small cell lung cancer: intensity-modulated radiotherapy versus 3D conformal radiotherapy. Anticancer research *34*, 5175-5180.

Imbalzano, K.M., Tatarkova, I., Imbalzano, A.N., and Nickerson, J.A. (2009). Increasingly transformed MCF-10A cells have a progressively tumor-like phenotype in three-dimensional basement membrane culture. Cancer Cell Int *9*, 7.

Innes, C., Hesse, J., Palii, S., Helmink, B., Holub, A., Sleckman, B., and Paules, R. (2013). DNA damage activates a complex transcriptional response in murine lymphocytes that includes both physiological and cancer-predisposition programs. BMC Genomics *14*, 1-10.

Insall, R.H., and Machesky, L.M. (2009). Actin dynamics at the leading edge: from simple machinery to complex networks. Developmental cell *17*, 310-322.

Ji, W., Chen, J., Mi, Y., Wang, G., Xu, X., and Wang, W. (2016). Platelet-activating factor receptor activation promotes prostate cancer cell growth, invasion and metastasis via ERK1/2 pathway. International journal of oncology *49*, 181-188.

Jorda, M., Olmeda, D., Vinyals, A., Valero, E., Cubillo, E., Llorens, A., Cano, A., and Fabra, A. (2005). Upregulation of MMP-9 in MDCK epithelial cell line in response to expression of the Snail transcription factor. Journal of cell science *118*, 3371-3385.

Julien, S., Puig, I., Caretti, E., Bonaventure, J., Nelles, L., van Roy, F., Dargemont, C., de Herreros, A.G., Bellacosa, A., and Larue, L. (2007). Activation of NF-[kappa]B by Akt upregulates Snail expression and induces epithelium mesenchyme transition. Oncogene *26*, 7445-7456.

Kajita, M., McClinic, K.N., and Wade, P.A. (2004). Aberrant expression of the transcription factors snail and slug alters the response to genotoxic stress. Molecular and cellular biology *24*, 7559-7566.

Kenny, P.A., and Bissell, M.J. (2007). Targeting TACE-dependent EGFR ligand shedding in breast cancer. The Journal of clinical investigation *117*, 337-345.

Kim, J.W., Cho, H.S., Kim, J.H., Hur, S.Y., Kim, T.E., Lee, J.M., Kim, I.K., and Namkoong, S.E. (2000). AAC-11 overexpression induces invasion and protects cervical cancer cells from apoptosis. Lab Invest *80*, 587-594.

Kispert, S., Marentette, J., and McHowat, J. (2015). Cigarette smoke induces cell motility via platelet-activating factor accumulation in breast cancer cells: a potential mechanism for metastatic disease. Physiological reports *3*.

Kispert, S.E., Marentette, J.O., and McHowat, J. (2014). Enhanced breast cancer cell adherence to the lung endothelium via PAF acetylhydrolase inhibition: a potential mechanism for enhanced metastasis in smokers. American journal of physiology Cell physiology *307*, C951-956.

Knox, S.S. (2010). From 'omics' to complex disease: a systems biology approach to gene-environment interactions in cancer. Cancer cell international *10*, 11.

Koci, L., Chlebova, K., Hyzdalova, M., Hofmanova, J., Jira, M., Kysela, P., Kozubik, A., Kala, Z., and Krejci, P. (2012). Apoptosis inhibitor 5 (API-5; AAC-11; FIF) is upregulated in human carcinomas in vivo. Oncol Lett *3*, 913-916.

Kondo, N., Takahashi, A., Ono, K., and Ohnishi, T. (2010). DNA damage induced by alkylating agents and repair pathways. Journal of nucleic acids *2010*, 543531.

Kotula, E., Berthault, N., Agrario, C., Lienafa, M.C., Simon, A., Dingli, F., Loew, D., Sibut, V., Saule, S., and Dutreix, M. (2015). DNA-PKcs plays role in cancer metastasis through regulation of secreted proteins involved in migration and invasion. Cell Cycle *14*, 1961-1972.

Kravchenko, V.V., Pan, Z., Han, J., Herbert, J.M., Ulevitch, R.J., and Ye, R.D. (1995). Platelet-activating factor induces NF-kappa B activation through a G protein-coupled pathway. The Journal of biological chemistry *270*, 14928-14934.

Krejci, P., Pejchalova, K., Rosenbloom, B.E., Rosenfelt, F.P., Tran, E.L., Laurell, H., and Wilcox, W.R. (2007). The antiapoptotic protein Api5 and its partner, high molecular weight FGF2, are up-regulated in B cell chronic lymphoid leukemia. J Leukoc Biol *82*, 1363-1364.

Kulshammer, E., and Uhlirova, M. (2013). The actin cross-linker Filamin/Cheerio mediates tumor malignancy downstream of JNK signaling. Journal of cell science *126*, 927-938.

Lau, M.T., So, W.K., and Leung, P.C. (2013). Fibroblast growth factor 2 induces E-cadherin down-regulation via PI3K/Akt/mTOR and MAPK/ERK signaling in ovarian cancer cells. PLoS One *8*, e59083.

Lee, H.S., Cho, S.B., Lee, H.E., Kim, M.A., Kim, J.H., Park, D.J., Yang, H.K., Lee, B.L., and Kim, W.H. (2007). Protein expression profiling and molecular classification of gastric cancer by the tissue array method. Clinical cancer research : an official journal of the American Association for Cancer Research *13*, 4154-4163.

Lee, K.J., Lin, Y.F., Chou, H.Y., Yajima, H., Fattah, K.R., Lee, S.C., and Chen, B.P. (2011). Involvement of DNA-dependent protein kinase in normal cell cycle progression through mitosis. The Journal of biological chemistry *286*, 12796-12802.

Lees-Miller, S.P. (1996). The DNA-dependent protein kinase, DNA-PK: 10 years and no ends in sight. Biochemistry and cell biology = Biochimie et biologie cellulaire *74*, 503-512.

Lemieux, E., Bergeron, S., Durand, V., Asselin, C., Saucier, C., and Rivard, N. (2009). Constitutively active MEK1 is sufficient to induce epithelial-to-mesenchymal transition in intestinal epithelial cells and to promote tumor invasion and metastasis. International journal of cancer *125*, 1575-1586.

Lin, H.H., Yang, T.P., Jiang, S.T., Yang, H.Y., and Tang, M.J. (1999). Bcl-2 overexpression prevents apoptosis-induced Madin-Darby canine kidney simple epithelial cyst formation. Kidney international *55*, 168-178.

Liu, Z., Zhu, G., Getzenberg, R.H., and Veltri, R.W. (2015). The Upregulation of PI3K/Akt and MAP Kinase Pathways is Associated with Resistance of

Microtubule-Targeting Drugs in Prostate Cancer. Journal of cellular biochemistry *116*, 1341-1349.

Lopez-Carrillo, L., Hernandez-Ramirez, R.U., Calafat, A.M., Torres-Sanchez, L., Galvan-Portillo, M., Needham, L.L., Ruiz-Ramos, R., and Cebrian, M.E. (2010). Exposure to phthalates and breast cancer risk in northern Mexico. Environmental health perspectives *118*, 539-544.

Marchbanks, P.A., McDonald, J.A., Wilson, H.G., Folger, S.G., Mandel, M.G., Daling, J.R., Bernstein, L., Malone, K.E., Ursin, G., Strom, B.L.*, et al.* (2002). Oral contraceptives and the risk of breast cancer. The New England journal of medicine *346*, 2025-2032.

Martin, A.-M., and Weber, B.L. (2000). Genetic and Hormonal Risk Factors in Breast Cancer. Journal of the National Cancer Institute *92*, 1126-1135.

Matter, K., and Mellman, I. (1994). Mechanisms of cell polarity: sorting and transport in epithelial cells. Current opinion in cell biology *6*, 545-554.

McCready, J., Arendt, L.M., Rudnick, J.A., and Kuperwasser, C. (2010). The contribution of dynamic stromal remodeling during mammary development to breast carcinogenesis. Breast cancer research : BCR *12*, 205.

Melnikova, V., and Bar-Eli, M. (2007). Inflammation and melanoma growth and metastasis: the role of platelet-activating factor (PAF) and its receptor. Cancer metastasis reviews *26*, 359-371.

Melnikova, V.O., Villares, G.J., and Bar-Eli, M. (2008). Emerging roles of PAR-1 and PAFR in melanoma metastasis. Cancer microenvironment : official journal of the International Cancer Microenvironment Society *1*, 103-111.

Menke, M., Meister, A., and Schubert, I. (2000). N-Methyl-N-nitrosourea-induced DNA damage detected by the comet assay in Vicia faba nuclei during all interphase stages is not restricted to chromatid aberration hot spots. Mutagenesis *15*, 503-506.

Montrucchio, G., Sapino, A., Bussolati, B., Ghisolfi, G., Rizea-Savu, S., Silvestro, L., Lupia, E., and Camussi, G. (1998). Potential angiogenic role of platelet-activating factor in human breast cancer. The American journal of pathology *153*, 1589-1596.

Morozov, V.E., Falzon, M., Anderson, C.W., and Kuff, E.L. (1994). DNA-dependent protein kinase is activated by nicks and larger single-stranded gaps. The Journal of biological chemistry *269*, 16684-16688.

Musch, A. (2004). Microtubule organization and function in epithelial cells. Traffic *5*, 1-9.

Mustafa, R.A., Abdelbadie, A., Osman, I., and Omer, H. (2013). CORRELATION BETWEEN BREAST CANCER AND RISK FACTORS. IJCRR *5*, 57-60.

Muthuswamy, S.K., Li, D., Lelievre, S., Bissell, M.J., and Brugge, J.S. (2001). ErbB2, but not ErbB1, reinitiates proliferation and induces luminal repopulation in epithelial acini. Nature cell biology *3*, 785-792.

Natali, P.G., Nicotra, M.R., Botti, C., Mottolese, M., Bigotti, A., and Segatto, O. (1992). Changes in expression of alpha 6/beta 4 integrin heterodimer in primary and metastatic breast cancer. British journal of cancer *66*, 318-322.

Neft, R.E., and Conner, M.K. (1989). Induction of sister chromatid exchange in multiple murine tissues in vivo by various methylating agents. Teratogenesis, carcinogenesis, and mutagenesis *9*, 219-237.

Neft, R.E., Schol, H.M., and Casciano, D.A. (1989). Comparison of sister chromatid exchanges in spleen and thymus lymphocytes from AKR, C57BL/6N x DBA/2J F1, and CBA mice following in vivo exposure to N-methyl-N-nitrosourea. Cancer research *49*, 4504-4508.

Noh, K.H., Kim, S.H., Kim, J.H., Song, K.H., Lee, Y.H., Kang, T.H., Han, H.D., Sood, A.K., Ng, J., Kim, K.*, et al.* (2014). API5 confers tumoral immune escape through FGF2-dependent cell survival pathway. Cancer Res *74*, 3556-3566.

Olive, P.L., and Banath, J.P. (2006). The comet assay: a method to measure DNA damage in individual cells. Nature protocols *1*, 23-29.

Onishi, K., Higuchi, M., Asakura, T., Masuyama, N., and Gotoh, Y. (2007). The PI3K-Akt pathway promotes microtubule stabilization in migrating fibroblasts. Genes to cells : devoted to molecular & cellular mechanisms *12*, 535-546.

Oyanagi, J., Ogawa, T., Sato, H., Higashi, S., and Miyazaki, K. (2012). Epithelial-mesenchymal transition stimulates human cancer cells to extend microtubule-based invasive protrusions and suppresses cell growth in collagen gel. PloS one *7*, e53209.

Page, D.L., and Dupont, W.D. (1993). Anatomic indicators (histologic and cytologic) of increased breast cancer risk. Breast Cancer Res Treat *28*, 157-166.

Page, D.L., Dupont, W.D., Rogers, L.W., and Rados, M.S. (1985). Atypical hyperplastic lesions of the female breast. A long-term follow-up study. Cancer *55*, 2698-2708.

Palmer, J.R., and Rosenberg, L. (1993). Cigarette smoking and the risk of breast cancer. Epidemiologic reviews *15*, 145-156.

Paszek, M.J., Zahir, N., Johnson, K.R., Lakins, J.N., Rozenberg, G.I., Gefen, A., Reinhart-King, C.A., Margulies, S.S., Dembo, M., Boettiger, D*., et al.* (2005). Tensional homeostasis and the malignant phenotype. Cancer cell *8*, 241-254.

Petrosyan, A., Holzapfel, M.S., Muirhead, D.E., and Cheng, P.-W. (2014). Restoration of Compact Golgi Morphology in Advanced Prostate Cancer Enhances Susceptibility to Galectin-1–Induced Apoptosis by Modifying Mucin O-Glycan Synthesis. Molecular Cancer Research *12*, 1704.

Picco, V., and Pages, G. (2013). Linking JNK Activity to the DNA Damage Response. Genes & cancer *4*, 360-368.

Pitton, C., Lanson, M., Besson, P., Fetissoff, F., Lansac, J., Benveniste, J., and Bougnoux, P. (1989). Presence of PAF-Acether in Human Breast Carcinoma:

Relation to Axillary Lymph Node Metastasis. Journal of the National Cancer Institute *81*, 1298-1302.

Polyak, K. (2008). Is breast tumor progression really linear? Clin Cancer Res *14*, 339-341.

Porch, J.V., Lee, I.M., Cook, N.R., Rexrode, K.M., and Burin, J.E. (2002). Estrogen-progestin replacement therapy and breast cancer risk: the Women's Health Study (United States). Cancer causes & control : CCC *13*, 847-854.

Prescott, S.M., Zimmerman, G.A., Stafforini, D.M., and McIntyre, T.M. (2000). Platelet-activating factor and related lipid mediators. Annual review of biochemistry *69*, 419-445.

Presley, J.F., Cole, N.B., Schroer, T.A., Hirschberg, K., Zaal, K.J., and Lippincott-Schwartz, J. (1997). ER-to-Golgi transport visualized in living cells. Nature *389*, 81-85.

Preston, D.L., Mattsson, A., Holmberg, E., Shore, R., Hildreth, N.G., and Boice, J.D., Jr. (2002). Radiation effects on breast cancer risk: a pooled analysis of eight cohorts. Radiation research *158*, 220-235.

Pyun, B.J., Seo, H.R., Lee, H.J., Jin, Y.B., Kim, E.J., Kim, N.H., Kim, H.S., Nam, H.W., Yook, J.I., and Lee, Y.S. (2013). Mutual regulation between DNA-PKcs and Snail1 leads to increased genomic instability and aggressive tumor characteristics. Cell death & disease *4*, e517.

Qian, Y., Corum, L., Meng, Q., Blenis, J., Zheng, J.Z., Shi, X., Flynn, D.C., and Jiang, B.H. (2004). PI3K induced actin filament remodeling through Akt and p70S6K1: implication of essential role in cell migration. American journal of physiology Cell physiology *286*, C153-163.

Ramdas, P., Rajihuzzaman, M., Veerasenan, S.D., Selvaduray, K.R., Nesaretnam, K., and Radhakrishnan, A.K. (2011). Tocotrienol-treated MCF-7 human breast cancer cells show down-regulation of API5 and up-regulation of MIG6 genes. Cancer Genomics Proteomics *8*, 19-31.

Reginato, M.J., Mills, K.R., Becker, E.B., Lynch, D.K., Bonni, A., Muthuswamy, S.K., and Brugge, J.S. (2005). Bim regulation of lumen formation in cultured mammary epithelial acini is targeted by oncogenes. Molecular and cellular biology *25*, 4591-4601.

Rigou, P., Piddubnyak, V., Faye, A., Rain, J.C., Michel, L., Calvo, F., and Poyet, J.L. (2009). The antiapoptotic protein AAC-11 interacts with and regulates Acinus-mediated DNA fragmentation. EMBO J *28*, 1576-1588.

Robert, E.G., and Hunt, J.D. (2001). Lipid messengers as targets for antiangiogenic therapy. Current pharmaceutical design *7*, 1615-1626.

Rodriguez-Boulan, E., Kreitzer, G., and Musch, A. (2005). Organization of vesicular trafficking in epithelia. Nat Rev Mol Cell Biol *6*, 233-247.

Royer, C., and Lu, X. (2011). Epithelial cell polarity: a major gatekeeper against cancer? Cell death and differentiation *18*, 1470-1477.

Rudrapatna, V.A., Bangi, E., and Cagan, R.L. (2014). A Jnk-Rho-Actin remodeling positive feedback network directs Src-driven invasion. Oncogene *33*, 2801-2806.

Ryan, S.D., Harris, C.S., Mo, F., Lee, H., Hou, S.T., Bazan, N.G., Haddad, P.S., Arnason, J.T., and Bennett, S.A. (2007). Platelet activating factor-induced neuronal apoptosis is initiated independently of its G-protein coupled PAF receptor and is inhibited by the benzoate orsellinic acid. Journal of neurochemistry *103*, 88-97.

Sarafian, T.A., and Bredesen, D.E. (1994). Is apoptosis mediated by reactive oxygen species? Free radical research *21*, 1-8.

Sasaki, H., Moriyama, S., Yukiue, H., Kobayashi, Y., Nakashima, Y., Kaji, M., Fukai, I., Kiriyama, M., Yamakawa, Y., and Fujii, Y. (2001). Expression of the antiapoptosis gene, AAC-11, as a prognosis marker in non-small cell lung cancer. Lung Cancer *34*, 53-57.

Schreck, R., Albermann, K., and Baeuerle, P.A. (1992). Nuclear factor kappa B: an oxidative stress-responsive transcription factor of eukaryotic cells (a review). Free radical research communications *17*, 221-237.

Shao, S.L., Cai, Y., Wang, Q.H., Yan, L.J., Zhao, X.Y., and Wang, L.X. (2007). Expression of GLUT-1, p63 and DNA-Pkcs in serous ovarian tumors and their significance. Zhonghua zhong liu za zhi [Chinese journal of oncology] *29*, 697-700.

Sharma, J., Turk, J., Mancuso, D.J., Sims, H.F., Gross, R.W., and McHowat, J. (2011). Activation of group VI phospholipase A2 isoforms in cardiac endothelial cells. American journal of physiology Cell physiology *300*, C872-879.

Silber, J.R., Blank, A., Bobola, M.S., Mueller, B.A., Kolstoe, D.D., Ojemann, G.A., and Berger, M.S. (1996). Lack of the DNA repair protein O6-methylguanine-DNA methyltransferase in histologically normal brain adjacent to primary human brain tumors. Proceedings of the National Academy of Sciences of the United States of America *93*, 6941-6946.

Song, K.H., Kim, S.H., Noh, K.H., Bae, H.C., Kim, J.H., Lee, H.J., Song, J., Kang, T.H., Kim, D.W., Oh, S.J.*, et al.* (2014). Apoptosis Inhibitor 5 Increases Metastasis via Erk-mediated MMP expression. BMB Rep.

Sonnenberg, A., Calafat, J., Janssen, H., Daams, H., van der Raaij-Helmer, L.M., Falcioni, R., Kennel, S.J., Aplin, J.D., Baker, J., Loizidou, M.*, et al.* (1991). Integrin alpha 6/beta 4 complex is located in hemidesmosomes, suggesting a major role in epidermal cell-basement membrane adhesion. The Journal of cell biology *113*, 907-917.

Sotiriou, C., Wirapati, P., Loi, S., Harris, A., Fox, S., Smeds, J., Nordgren, H., Farmer, P., Praz, V., Haibe-Kains, B.*, et al.* (2006). Gene expression profiling in breast cancer: understanding the molecular basis of histologic grade to improve prognosis. J Natl Cancer Inst *98*, 262-272.

Stafforini, D.M., McIntyre, T.M., Zimmerman, G.A., and Prescott, S.M. (2003). Platelet-activating factor, a pleiotrophic mediator of physiological and pathological processes. Critical reviews in clinical laboratory sciences *40*, 643-672.

Stoica, G., Jacobs, R., Koestner, A., O'Leary, M., and Welsch, C. (1991). ENU-induced in vitro neoplastic transformation of rat mammary epithelial cells. Anticancer research *11*, 1783-1792.

Stoica, G., Koestner, A., and Capen, C.C. (1983). Characterization of N-ethyl-N-nitrosourea--induced mammary tumors in the rat. The American journal of pathology *110*, 161-169.

Stoica, G., Koestner, A., and Capen, C.C. (1984). Neoplasms induced with high single doses of N-ethyl-N-nitrosourea in 30-day-old Sprague-Dawley rats, with special emphasis on mammary neoplasia. Anticancer research *4*, 5-12.

Sugino, Y. (1966). Mutants of Escherichia coli sensitive to methylene blue and acridines. Genet Res *7*, 1-11.

Tait, L., Soule, H.D., and Russo, J. (1990). Ultrastructural and immunocytochemical characterization of an immortalized human breast epithelial cell line, MCF-10. Cancer research *50*, 6087-6094.

Tang, H.L., Tang, H.M., Mak, K.H., Hu, S., Wang, S.S., Wong, K.M., Wong, C.S.T., Wu, H.Y., Law, H.T., Liu, K.*, et al.* (2012). Cell survival, DNA damage, and oncogenic transformation after a transient and reversible apoptotic response. Molecular Biology of the Cell *23*, 2240-2252.

Tang, P., Hajdu, S.I., and Lyman, G.H. (2007). Ductal carcinoma in situ: a review of recent advances. Curr Opin Obstet Gynecol *19*, 63-67.

Tewari, M., Yu, M., Ross, B., Dean, C., Giordano, A., and Rubin, R. (1997). AAC-11, a novel cDNA that inhibits apoptosis after growth factor withdrawal. Cancer Res *57*, 4063-4069.

Thiery, J.P. (2003). Epithelial-mesenchymal transitions in development and pathologies. Current opinion in cell biology *15*, 740-746.

Tomlinson, D.C., Baxter, E.W., Loadman, P.M., Hull, M.A., and Knowles, M.A. (2012). FGFR1-induced epithelial to mesenchymal transition through MAPK/PLCgamma/COX-2-mediated mechanisms. PLoS One *7*, e38972.

Vaca, C.E., Wilhelm, J., and Harms-Ringdahl, M. (1988). Interaction of lipid peroxidation products with DNA. A review. Mutation research *195*, 137-149.

Valderrama, F., Duran, J.M., Babia, T., Barth, H., Renau-Piqueras, J., and Egea, G. (2001). Actin microfilaments facilitate the retrograde transport from the Golgi complex to the endoplasmic reticulum in mammalian cells. Traffic *2*, 717-726.

van de Vijver, M.J., He, Y.D., van't Veer, L.J., Dai, H., Hart, A.A., Voskuil, D.W., Schreiber, G.J., Peterse, J.L., Roberts, C., Marton, M.J.*, et al.* (2002). A gene-expression signature as a predictor of survival in breast cancer. The New England journal of medicine *347*, 1999-2009.

Vargo-Gogola, T., and Rosen, J.M. (2007). Modelling breast cancer: one size does not fit all. Nat Rev Cancer *7*, 659-672.

Vaughan, K.T. (2005). Microtubule plus ends, motors, and traffic of Golgi membranes. Biochimica et biophysica acta *1744*, 316-324.

Vidi, P.-A., Chandramouly, G., Gray, M., Wang, L., Liu, E., Kim, J.J., Roukos, V., Bissell, M.J., Moghe, P.V., and Lelièvre, S.A. (2012). Interconnected contribution of tissue morphogenesis and the nuclear protein NuMA to the DNA damage response. Journal of Cell Science *125*, 350-361.

Vidi, P.A., Bissell, M.J., and Lelievre, S.A. (2013). Three-dimensional culture of human breast epithelial cells: the how and the why. Methods Mol Biol *945*, 193-219.

Walker, S., Foster, F., Wood, A., Owens, T., Brennan, K., Streuli, C.H., and Gilmore, A.P. (2016). Oncogenic activation of FAK drives apoptosis suppression in a 3D-culture model of breast cancer initiation. Oncotarget *7*, 70336-70352.

Wang, F., Hansen, R.K., Radisky, D., Yoneda, T., Barcellos-Hoff, M.H., Petersen, O.W., Turley, E.A., and Bissell, M.J. (2002). Phenotypic reversion or death of cancer cells by altering signaling pathways in three-dimensional contexts. Journal of the National Cancer Institute *94*, 1494-1503.

Wang, H., Fang, R., Wang, X.F., Zhang, F., Chen, D.Y., Zhou, B., Wang, H.S., Cai, S.H., and Du, J. (2013). Stabilization of Snail through AKT/GSK-3beta signaling pathway is required for TNF-alpha-induced epithelial-mesenchymal transition in prostate cancer PC3 cells. European journal of pharmacology *714*, 48-55.

Wang, Z., Liu, H., Liu, B., Ma, W., Xue, X., Chen, J., and Zhou, Q. (2010). Gene expression levels of CSNK1A1 and AAC-11, but not NME1, in tumor tissues as prognostic factors in NSCLC patients. Med Sci Monit *16*, CR357-364.

Wehland, J., Henkart, M., Klausner, R., and Sandoval, I.V. (1983). Role of microtubules in the distribution of the Golgi apparatus: effect of taxol and microinjected anti-alpha-tubulin antibodies. Proceedings of the National Academy of Sciences of the United States of America *80*, 4286-4290.

Wellings, S.R., and Jensen, H.M. (1973). On the origin and progression of ductal carcinoma in the human breast. J Natl Cancer Inst *50*, 1111-1118.

Wu, X., and Gallo, K.A. (2013). The 18-kDa translocator protein (TSPO) disrupts mammary epithelial morphogenesis and promotes breast cancer cell migration. PloS one *8*, e71258.

Xiang, B., and Muthuswamy, S.K. (2006). Using three-dimensional acinar structures for molecular and cell biological assays. Methods in enzymology *406*, 692-701.

Xu, B., Gao, L., Wang, L., Tang, G., He, M., Yu, Y., Ni, X., and Sun, Y. (2013). Effects of platelet-activating factor and its differential regulation by androgens and steroid hormones in prostate cancers. British journal of cancer *109*, 1279-1286.

Yoo, S., and Dynan, W.S. (1999). Geometry of a complex formed by double strand break repair proteins at a single DNA end: Recruitment of DNA-PKcs induces inward translocation of Ku protein. Nucleic acids research *27*, 4679-4686.

Yu, Y., Zhang, M., Zhang, X., Cai, Q., Zhu, Z., Jiang, W., and Xu, C. (2014). Transactivation of epidermal growth factor receptor through platelet-activating factor/receptor in ovarian cancer cells. Journal of experimental & clinical cancer research : CR *33*, 85.

Zhang, L., Wang, D., Jiang, W., Edwards, D., Qiu, W., Barroilhet, L.M., Rho, J.H., Jin, L., Seethappan, V., Vitonis, A.*, et al.* (2010). Activated networking of platelet activating factor receptor and FAK/STAT1 induces malignant potential in BRCA1-mutant at-risk ovarian epithelium. Reproductive biology and endocrinology : RB&E *8*, 74.

Zhong, S., Ye, W., Lin, S.H., Liu, J.Y., Leong, J., Ma, C., and Lin, Y.C. (2011). Zeranol induces cell proliferation and protein disulfide isomerase expression in mammary gland of ACI rat. Anticancer research *31*, 1659-1665.

Zhu, T., Gobeil, F., Vazquez-Tello, A., Leduc, M., Rihakova, L., Bossolasco, M., Bkaily, G., Peri, K., Varma, D.R., Orvoine, R.*, et al.* (2006). Intracrine signaling through lipid mediators and their cognate nuclear G-protein-coupled receptors: a paradigm based on PGE2, PAF, and LPA1 receptors. Canadian journal of physiology and pharmacology *84*, 377-391.

Zink, D., Fischer, A.H., and Nickerson, J.A. (2004). Nuclear structure in cancer cells. Nat Rev Cancer *4*, 677-687.

Zoller, J., Brandle, K., and Bereiter-Hahn, J. (1997). Cellular motility in vitro as revealed by scanning acoustic microscopy depends on cell-cell contacts. Cell and tissue research *290*, 43-50.

APPENDIX

Appendix I: Media composition

MCF10A media composition:

Components	Stock concentration	Growth Medium	Resuspension Medium	Assay Medium
Horse Serum (Invitrogen)		5%	20%	2%
Insulin (Sigma-Aldrich)	10 mg/ml	10 µg/ml	-	10 µg/ml
Hydrocortisone (Sigma-Aldrich)	1 mg/ml	0.5 µg/ml	-	0.5 µg/ml
Choleratoxin (Sigma-Aldrich)	1 mg/ml	100ng/ml	-	100ng/ml
Epidermal growth factor (EGF-Sigma-Aldrich)	100 µg/ml	20 ng/ml	-	5 ng/ml
Matrigel® (BD Biosciences)	NA	-	-	2%
Pencillin-Streptamycin (Invitrogen)	100X	2X	2X	2X

Appendix II: Buffers for Immunofluorescence:

1. Phosphate buffered Saline (PBS)

Component	Concentration
Na_2HPO_4	10 mM
KH_2PO_4	1.8 mM
NaCl	137 mM
KCl	2.7 mM

2. Phosphate buffer Saline-EDTA (PBS-EDTA)

Component	Concentration
EDTA	5 mM
Sodium orthovanadate	1 mM
Sodium Fluoride	1.5 mM
Protease Inhibitor Cocktail	1X
PBS	1X

3. Immunofluorescence Buffer (IF Buffer)

Component	Concentration
PBS	I X
Sodium Azide	0.05% [w/v]
BSA	0.1% [w/v]
Triton-X-100	0.2% [v/v]
Tween 20	0.05%
PBS	I X

4. VSVG wash buffer

Component	Concentration
House Serum	2%
Sodium Azide	0.1%
PBS	1X

Appendix III: Buffers for Immunoblotting

1. 6X sample buffer (10 ml)

Component	Concentration
Tris (pH 6.8)	3.5 ml
Glycerol	3.6 ml
DTT	0.093 gm
Bromo phenol blue	0.6 ml
SDS	1.1 gm

2. 10 X SDS running Buffer (1 L)

Component	Concentration
Trizma base	30.3
Glycine	144 gm
SDS	10 gm

3. 10X Transfer Buffer (1 L)

Component	Concentration
Trizma base	29 gm
Glycine	146.5

4. TBS-Tween

Component	Concentration
Tris (pH 7.6)	25 mM
NaCl	150 mM
KCl	2 mM
Tween 20	0.1%

Appendix IV: Buffers and staining solution for Gelatin Zymograph

1. Non-reducing sample buffer

Component	Concentration
Tris-HCl (pH 7.5)	25mM
NaCl	100mM
NP-40	1%

2. Renaturing buffer

Component	Concentration
Triton X-100	2.5%
Water	100ml

3. Developing buffer

Component	Concentration
Tris-HCL (pH-7.8)	0.5 M
NaCl	2M
CaCl2	0.05M
Brij35	0.2%

4. Staining solution

Component	Concentration
Coomassie blue	0.1% w/v
Methanol	50% v/v
Acetic acid	10% v/v

5. Destaining solution

Component	Concentration
Methanol	40% v/v
Acetic acid	10% v/v

Appendix V: Cloning of Api5 into CSII-EF-MCS

1. Plasmid map

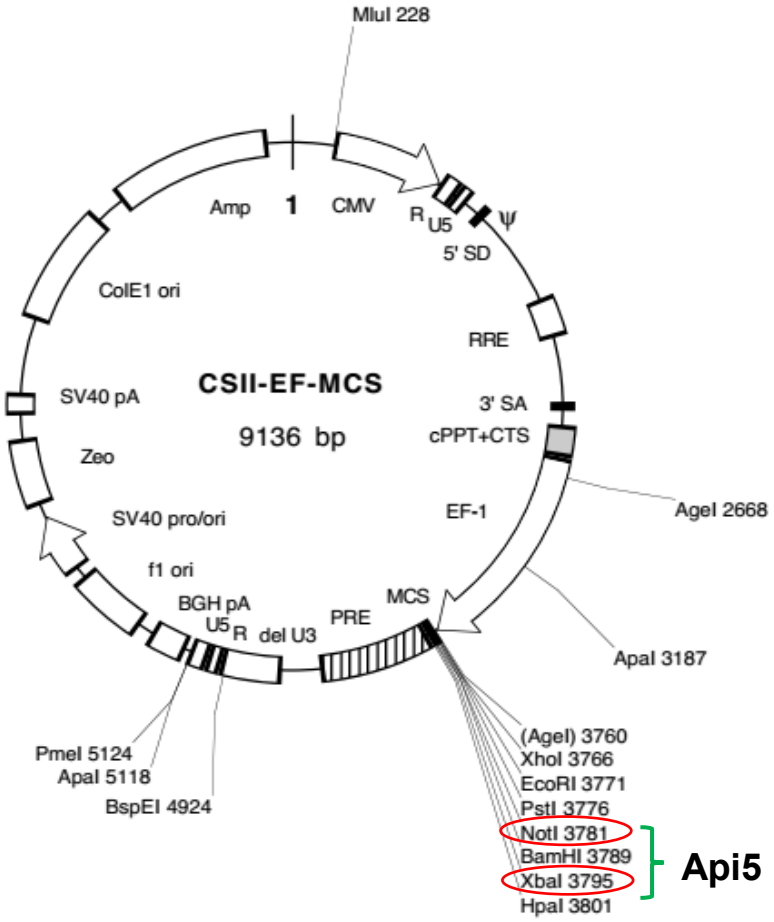

Plasmid name: CSII-EF-MCS

Source: RIKEN BRC DNA bank

Restriction sites: Not1 and Xba1

Primer sequences used for amplification of Api5:

Forward: AAGGAAAAAAGCGGCCGCAT`ATGCCGACAGTAGAGGAGCT`

Reverse: GCTCTAGATCAGTAGAGTCTTCCCCGAC

2. PCR amplification of Api5 from Api5-mVenus C1

DNA Template	3 μl
Forward Primer	3 μl
Reverse Primer	3 μl
10 mM dNTPs	12.5 μl
10X Pfu buffer	10 μl
DMSO	5 μl
dH_2O	6.5 μl
Pfu polymerase	2 μl

3. PCR cycle for Amplification

95°C - 2 min

95°C - 1 min
60°C - 1 min } X 30 Cycles

72°C - 3 min

72°C - 6 min

4°C – hold

4. Digestion of PCR product and CSII-EF-MCS-mCherry

DNA Template	5 μg
10 X Cut smart buffer	5 μl
Not 1 HF	5 μl
Xba 1	5 μl
dH_2O	To make up the reaction to 50 μl

5. Ligation reaction

Insert	74.25 ng
Vector	153.45 ng
10X T4 Ligase buffer	1 μl
T4 DNA Ligase	1 μl
dH_2O	To make up the reaction to 10 μl

PUBLICATIONS

List of Publications:

Research articles

1. **Libi Anandi, V.,** Chakravarty, V., Ashiq, K.A., Bodakuntla, S., and Lahiri, M. A central role for DNA-PK activation in transformation of breast epithelial cells following MNU-induced DNA damage. ***(Manuscript submitted)***
2. **Anandi V Libi**, Ashiq, Nitheesh, Lahiri. Platelet-activating factor promotes motility in breast cancer cells and disrupts non-transformed breast acinar structures. ***Oncology Reports.*** 2016;35(1):179-88.
3. Bodakuntla, S., **Anandi V, Libi**., Sural, S., Trivedi, P and Lahiri, M. (2014) N-nitroso-N-ethylurea activates DNA damage surveillance pathways and induces transformation in mammalian cells. **BMC Cancer** 14 (1): 287. doi:10.1186/1471-2407-14-287.

Review articles

1. **Anandi, L.,** Chakravarty, V. and Lahiri, M. (2016) Investigating two Hallmarks of Cancer - Genome Instability and Tumor Promoting Inflammation. **Indian Society of Cell Biology Newsletter** 35 (2):ISSN: 2349:8307
2. **Libi Anandi, V** and Lahiri,M. Platelet activating factor leads to initiation and promotion of breast cancer. ***Cancer cell and microenvironment.*** 3 (3): e1370 (Invited Research highlights)

Collaborative research articles

1. Paul D, **Libi Anandi,** Lahiri M, Santra MK. Protein phosphatase 1 regulatory subunit p90 suppresses tumor growth through inactivation of MAPK pathway. *(Manuscript under preparation)*
2. Jain DR, **Anandi VL**, Lahiri M, Ganesh KN. (2014) Influence of pendant chiral C(gamma)-(alkylideneamino/guanidino) cationic side-chains of PNA backbone on hybridization with complementary DNA/RNA and cell permeability. ***The Journal of organic chemistry*.**;79(20):9567-77. Epub 2014/09/16.

RESEARCH ARTICLES

BMC Cancer

RESEARCH ARTICLE Open Access

N-nitroso-N-ethylurea activates DNA damage surveillance pathways and induces transformation in mammalian cells

Satish Bodakuntla[1], Libi Anandi V[1], Surojit Sural[1,2], Prasad Trivedi[1,3] and Mayurika Lahiri[1*]

Abstract

Background: The DNA damage checkpoint signalling cascade sense damaged DNA and coordinates cell cycle arrest, DNA repair, and/or apoptosis. However, it is still not well understood how the signalling system differentiates between different kinds of DNA damage. N-nitroso-N-ethylurea (NEU), a DNA ethylating agent induces both transversions and transition mutations.

Methods: Immunoblot and comet assays were performed to detect DNA breaks and activation of the canonical checkpoint signalling kinases following NEU damage upto 2 hours. To investigate whether mismatch repair played a role in checkpoint activation, knock-down studies were performed while flow cytometry analysis was done to understand whether the activation of the checkpoint kinases was cell cycle phase specific. Finally, breast epithelial cells were grown as 3-dimensional spheroid cultures to study whether NEU can induce upregulation of vimentin as well as disrupt cell polarity of the breast acini, thus causing transformation of epithelial cells in culture.

Results: We report a novel finding that NEU causes activation of major checkpoint signalling kinases, Chk1 and Chk2. This activation is temporally controlled with Chk2 activation preceding Chk1 phosphorylation, and absence of cross talk between the two parallel signalling pathways, ATM and ATR. Damage caused by NEU leads to the temporal formation of both double strand and single strand breaks. Activation of checkpoints following NEU damage is cell cycle phase dependent wherein Chk2 is primarily activated during G2-M phase whilst in S phase, there is immediate Chk1 phosphorylation and delayed Chk2 response. Surprisingly, the mismatch repair system does not play a role in checkpoint activation, at doses and duration of NEU used in the experiments. Interestingly, NEU caused disruption of the well-formed polarised spheroid architecture and upregulation of vimentin in three-dimensional breast acini cultures of non-malignant breast epithelial cells upon NEU treatment indicating NEU to have the potential to cause early transformation in the cells.

Conclusion: NEU causes damage in mammalian cells in the form of double strand and single strand breaks that temporally activate the major checkpoint signalling kinases without the occurrence of cross-talk between the pathways. NEU also appear to cause transformation in three-dimensional spheroid cultures.

Keywords: N-nitroso-N-ethylurea, DNA lesions, Epithelial - mesenchymal transition, Mismatch repair, O^6-ethylguanine, DNA damage response, Checkpoints, Cell cycle, Comet assay, 3-dimesional cultures, Transformation

* Correspondence: mayurika.lahiri@iiserpune.ac.in
[1]Indian Institute of Science Education and Research, Pune, Maharashtra 411008, India
Full list of author information is available at the end of the article

Background

Alkylating agents are a structurally diverse group of DNA damaging compounds which form adducts at ring nitrogen (N) and extracyclic oxygen (O) atoms of DNA bases [1]. N-nitroso-N-ethylurea (NEU), a simple monofunctional S_N1 type-DNA ethylating agent, forms the modified base O^6-ethylguanine (O^6EtG) which mispairs with thymine during DNA replication and thus primarily induces A:T to T:A transversions or A:T to G:C transition mutations [2,3]. NEU has been traditionally characterised as a severely potent transplacental teratogen and carcinogen in rodents [4,5]. In vertebrates, the mismatch repair proteins, namely Msh2-Msh6 and Mlh1-Pms2 heterodimers, play a pivotal role in mediating the mutagenic and cytotoxic effects of O^6EtG lesions [6,7]; however the mechanisms are still controversial. According to one model, futile cycles of mismatch repair-induced excision and repair of erroneously paired thymine nucleotides opposite O^6EtG lesions cause formation of recurring single strand breaks (SSBs). These gaps in the genome and double strand breaks (DSBs) that form at these sites during the next replication cycle have been proposed to be mediating the cytotoxic effects of different alkylating agents [8]. However according to an alternate model, recognition of O^6EtG:T mispairs by the mismatch repair proteins can directly recruit DNA damage response kinases at the site of DNA damage which possibly elicits cell cycle checkpoint activation and apoptosis [9]. Interestingly, at high doses, cytotoxicity of S_N1 type-alkylating agents has been shown to be largely mismatch repair independent [10]. Hence the cellular pathways that collectively modulate sensitivity to DNA alkylation damage involve direct crosstalk, overlap in substrates and recruitment of alternative pathways for processing of intermediates.

The pathways that sense damaged DNA and coordinate DNA repair, cell cycle arrest and/or apoptosis comprise the DNA damage checkpoint signalling cascade. The sensor or apical kinases that detect the damaged DNA belong to the phosphoinositide 3-kinase related kinase (PIKK) family. These kinases, namely ATM (ataxia-telangiectasia mutated) and ATR (ATM and Rad3-related), initiate a cascade of phosphorylation events which mediate cell cycle arrest, DNA repair and apoptosis [11]. The increased local concentration of ATM at the DSB sites is important to boost phosphorylation of ATM targets, including signal mediators such as the Chk2 kinase [12]. ATR responds primarily to stalled replication forks, base adducts and DNA cross-links, and relays the signal by phosphorylating Chk1 kinase and a large subset of ATM substrates [13]. However this paradigm of ATM and ATR signalling through two independent and alternate pathways was recently challenged and redefined by several reports showing that ATR can be activated directly in response to DSBs specifically in S and G2 phases of the cell cycle [14,15]. Recruitment of ATR to ionising radiation (IR)-induced DSBs occurs in an ATM and Mre11-Rad50-Nbs1 (MRN) complex-dependent manner at time points following ATM activation [16]. Though DNA alkylating agents do not directly induce strand breaks, low doses of S_N1 type-methylating agents have been shown to induce activation of the apical kinases, ATM and ATR, and their downstream substrates [10,17]. Most studies suggest that checkpoint activation can occur only in the second G2 phase after DNA alkylation damage, however few findings have reported ATM activation within 3 hrs of treatment with a prototypical S_N1 type-methylating agent [18]. Furthermore, SSBs have been shown to accumulate as primary lesions in cells after 2 hrs of NEU damage [19]. These findings, being contrary to the standard model of DNA alkylation damage, have led to the possibility that S_N1 type-alkylating agents can induce strand breaks in a replication-independent manner.

Loss of cellular architechture and polarity of breast tissue is one of the early markers for onset of breast cancer. This loss in cellular morphology can be phenocopied using three-dimensional (3D) cultures of human mammary epithelial cells, MCF10A. MCF10A are immortalised, non-transformed human mammary epithelial cells when grown in 3D matrices, exhibit a number of features of normal breast epithelium [20]. MCF10A cells form multicellular acini-like spheroids which represent the layer of basal epithelial cells surrounding a hollow lumen in the lobule of human mammary gland [21]. The morphology of these acini are disrupted in malignancy, such as an increase in size and elongation of acini [22]. As transformation progresses, the acini lose their polarisation and some may even form multi-acinar structures [21]. Another characteristic of transformed cells is their ability to invade and metastasise to the other tissues. During the process of transformation the epithelial cells are said to undergo 'epithelial - mesenchymal' (EMT) transition [23-25].

In this study, we have investigated the activation of DNA damage response kinases in human cancer cell lines following 2 hours treatment with different doses of NEU. Mismatch repair-proficient and mismatch repair-deficient cells were used to address the dependence on an active mismatch repair system for signalling to apical kinases of the DNA damage response signalling cascade after ethylation damage. We also explored the possibility of crosstalk and/or interdependence between the two canonical DNA damage response pathways, namely ATM through Chk2 and ATR through Chk1, post-NEU treatment for 2 hours. The data indicate presence of a mismatch repair-independent and cell cycle phase-dependent mechanism of checkpoint activation in mammalian cells immediately after treatment with a prototypical S_N1 type-ethylating agent. Using the 3D platform to investigate

whether NEU has the potential to cause transformation of breast epithelial cells grown as spheroids, it was observed that upon NEU treatment to MCF10A acinar cultures, the well organised polarised structures were completely distrupted upon transformation. Vimentin, an EMT marker was also observed in the NEU-treated breast acini, thereby indicating NEU to cause an EMT-like phenotype in the transformed breast epithelial cells grown in 3D.

Methods

Cell lines and culture conditions

MCF7 cell line was purchased from European Collection of Cell Cultures (ECACC). HeLa and HCT 116 cell lines were generous gifts from Dr. Sorab Dalal (ACTREC, Mumbai, India). DLD1 cell line was a kind gift from Dr. Thomas Ried (NCI, NIH, USA). MCF10A cell line was a generous gift from Prof. Raymond C. Stevens (The Scripps Research Institute, California, USA). All cell lines were grown in High Glucose Dulbecco's Modified Eagle Medium (DMEM; Invitrogen or Lonza) containing 10% fetal bovine serum (FBS; Invitrogen), 2 mM L-glutamine (Invitrogen) and 100 units/mL penicillin-streptomycin (Invitrogen). MCF10A cells were grown in High Glucose DMEM without sodium pyruvate (Invitrogen) containing 5% horse serum (Invitrogen), 20 ng/mL EGF (Sigma), 0.5 μg/mL hydrocortisone (Sigma), 100 ng/mL cholera toxin (Sigma), 10 μg/mL insulin (Sigma) and 100 units/mL penicillin-streptomycin (Invitrogen) and were resuspended during sub-culturing in High Glucose DMEM without sodium pyruvate containing 20% horse serum and 100 units/mL penicillin-streptomycin (Invitrogen). Cells were maintained in 100 mm tissue-culture treated dishes (Corning) at 37°C in humidified 5% CO_2 incubator (Thermo Scientific).

Chemicals and antibodies

Dimethyl sulfoxide (DMSO), N-nitroso-N-ethylurea (NEU), neocarzinostatin (NCS), thiazolyl blue tetrazolium bromide (MTT), thymidine, nocodazole, RNase A and propidium iodide (PI) were purchased from Sigma-Aldrich. Selective ATM inhibitor KU 55933 and DNA-PK inhibitor DMNB were obtained from Tocris Bioscience. VE 821, a potent and selective ATR kinase inhibitor was purchased from Axon Medichem. Monoclonal antibodies for Chk1 and Msh2 were bought from Santa Cruz Biotechnology. Polyclonal antibodies for phospho-Chk1 (Ser345), phospho-Chk2 (Thr68) and monoclonal antibodies for Chk2 and RPA32 were purchased from Cell Signaling Technology. Polyclonal antibody for phospho-RPA (Thr21) and monoclonal antibodies for phospho-ATM (Ser1981) and ATM were obtained from Abcam. Monoclonal antibodies for γH2AX (Ser139) and α6 integrin were bought from Millipore while α-tubulin was from Sigma. Monoclonal antibodies for vimentin, E-cadherin and β-catenin were purchased from Abcam. Peroxidase-conjugated AffiniPure goat anti-mouse, anti-rabbit and anti-rat IgG (H + L) as well as AffiniPure $F(ab')_2$ fragment goat anti-mouse IgG, $F(ab')_2$ fragment specific were obtained from Jackson Immuno Research. 4′, 6-Diamidino-2-phenylindole dihydrochloride (DAPI), Alexa Fluor 488 donkey anti-rabbit IgG (H + L) and Alexa Fluor 568 goat anti-mouse IgG (H + L) were bought from Invitrogen.

MTT-based cytotoxicity assay

Cells were seeded at a density of 10^4 cells per well in 96-well flat bottom tissue culture treated plates (Corning) and maintained at 37°C for 16 hours. Cells were then treated with NEU for 2 hours. Medium containing drug was aspirated and fresh growth medium containing 0.5 mg/mL MTT was added to cells. Plates were maintained in dark at 37°C for 4 hours. Medium-MTT mixture was aspirated and MTT-formazan crystals were dissolved in DMSO. Plates were kept on a nutating shaker at room temperature (RT) for 5 minutes and absorbance was recorded at 570 nm using a Varioskan Flash Multimode Plate Reader (Thermo Scientific).

Drug treatment and time course assays

Cells were seeded at a density of 10^6 cells per well in 6-well tissue culture treated plates (Corning) and maintained at 37°C for 16 hours. Cells were then treated with NEU by direct addition of drug to the culture medium for 2 hours (unless otherwise indicated). Control cells were treated with equivalent volume of DMSO (drug solvent). For ATM and DNA-PK inhibition, cells were treated with 10 μM KU 55933 and 25 μM DMNB, respectively, immediately prior to addition of drug while for ATR inhibition 10 μM VE 821 was added one hour prior to addition of NEU to the cells. For time course studies, cells were treated with NEU for different time periods ranging from 0 to 120 minutes. After drug treatment, medium containing NEU was aspirated and cells were washed once with 1X phosphate buffered saline (PBS; PAN-Biotech GmbH). Cells were lysed in sample buffer containing 0.06 mM Tris (pH 6.8), 6% glycerol, 2% sodium dodecyl sulphate (SDS), 0.1 M dithiothreitol (DTT) and 0.006% bromophenol blue and lysates were stored at - 40°C.

Single cell gel electrophoresis (Comet assay)

DNA strand breaks were detected using single cell gel electrophoresis/comet assay, using standard protocols [26]. Comet slides were then stained with ethidium bromide at a concentration of 2 μg/ml for 5 minutes and then were scored for comets immediately. Images were acquired using epiflourescence microscope at 20X magnification. Randomly selected 50 cells were analysed per sample. Amount of DNA SSBs and DSBs were measured and represented as length of tail and relative DNA content in tail.

siRNA knockdown

siRNA duplexes targeting Msh2, Msh6 and LacZ were purchased from Dharmacon (Thermo Scientific). Sense sequences of the siRNA are: Msh2, 5′-ACAGAAUA GAGGAGAGAUUUU-3′; Msh6, 5′-GAAUACGAGUU GAAAUCUAdTdT-3′; LacZ, 5′-CGUACGCGGAAUA CUUCGAdTdT-3′. HeLa cells were seeded at a density of 0.3 X 10^5 cells per well in 12-well tissue culture treated plates (Corning) and maintained at 37°C for 24 hours. Transfections were performed with a final siRNA concentration of 100 nM using X-tremeGENE siRNA transfection reagent (Roche) diluted in Opti-MEM I Reduced Serum Medium (Invitrogen). DMEM supplemented with 30% FBS was added 4 hours post-transfection to achieve a final FBS concentration of 10% in the wells. After 24 hours, siRNA transfection was repeated for each set. Cells were maintained at 37°C for an additional 48 hours and NEU damage was induced before lysis using same procedure as described earlier.

Immunoblot analysis

Cell lysates were resolved using sodium dodecyl sulphate polyacrylamide gel electrophoresis (SDS-PAGE) and transferred to Immobilon-P polyvinylidene difluoride (PVDF) membrane (Millipore). Blocking was performed in 5% (w/v) skimmed milk (SACO Foods, USA) for non-phospho antibodies or 4% (w/v) Block Ace (AbD Serotec) for phospho-specific antibodies prepared in 1X tris buffered saline containing 0.1% Tween 20 (1X TBS-T) for 1 hour at RT. Blots were incubated for 3 hours at RT (or for 16 hours at 4°C) in primary antibody solution. Following washes, blots were incubated with peroxidase-conjugated secondary antibody solution prepared in 5% (w/v) skimmed milk in 1X TBS-T for 1 hour at RT following which blots were developed using Immobilon Western Detection Reagent kit (Millipore) and visualised using ImageQuant LAS 4000 (GE Healthcare). All western data were quantified using minimum three independent experiments and have been denoted as fold-difference over respective controls for each blot.

Cell cycle synchronisation

Cell cycle synchronisation for S (double thymidine block) and G2 (thymidine-nocodazole block) phases were performed following the protocol mentioned by Whitfield et al. [27]. For the S phase synchronisation, HeLa cells were seeded at a density of 10^5 cells per well in 6-well tissue-culture treated plates while for synchronisation in G2 phase, cells were seeded at 2.5 X 10^5 cells per well in 6-well tissue-culture treated plates. The cells were released into DMEM containing 10 mM NEU and harvested at different time points.

Cell cycle analysis

HeLa cells were synchronised as mentioned above and harvested by trypsinisation. Cells were washed twice with 1X PBS and fixed with 70% ethanol at least overnight at 4°C. Cells were then washed twice with 1X PBS, resuspended in a solution containing 20 mg/ml RNase A and 1 mg/ml PI and incubated at 37°C for 1 hr. Cell cycle analysis was performed using FACS-Calibur flow cytometer (BD Biosciences) and data was analysed using ModFit (Verity Software House, Topsham, ME, USA).

Immunofluorescence analysis

Cells were seeded at a density of 2 X 10^5 cells per well on top of glass cover slips (Micro-Aid, India). Following drug treatment, cells were fixed using 4% formalin (Macron Chemicals) and were permeabilised using 0.5% Triton-X-100 for 5 minutes at RT. Cells were blocked with 10% (v/v) goat serum (Abcam), stained with primary antibody and then incubated with secondary antibody. For FITC-conjugated γH2AX (Ser139), the secondary antibody step was skipped. Cells were then counterstained with 0.5 μg/ml DAPI and mounted on glass slides (Micro-Aid, India). Slides were visualised under an Axio Imager.Z1 ApoTome microscope or a LSM 710 laser scanning confocal microscope (Carl Zeiss, GmbH). All microscopy images, unless otherwise specified, were captured using 63X oil-immersion objective.

3D "on-top" culture

The 3D on top cultures were set up in 8-well chamber coverglass (Nunc Lab tek, Thermo Scientific) using protocol described previously [21,28]. Cells were seeded at a density of 0.5 X 10^4 cells per well. Cultures were maintained for 20 days and medium was supplemented every 4 days [21]. For drug treatments, NEU was directly added to the culture medium on day 0 and 2. (Day 0 being the day of seeding).

In-well 3D culture extraction and immunofluorescence

The acini were fixed on the 20^{th} day using 4% paraformaldehyde (PFA) (freshly prepared in PBS, pH 7.4), permeabilised using PBS containing 0.5% Triton-X-100 for 10 minutes at 4°C, and immunostaining was done using standard protocols [21,28]. 3D structures were visualised under a Zeiss LSM 710 laser scanning confocal microscope (Zeiss, GmbH). All immunofluorescence images, unless otherwise specified, were captured using 63X oil-immersion objective.

Statistical analysis

Data represented in comet assay graphs are mean +/− standard error of parameters recorded from three independent experiments. Student's t-test was used to analyse

the statistical significance of fold-difference between treated and control samples in the western blots. Student's t-test was also used to analyse the statistical significance of difference in tail length. The results for % DNA in tail were analysed using nonparametric test one-tailed Mann Whitney U test. One way ANOVA was used to analyse the statistical significance of difference in the relative DNA content in tail for time course experiments. The results for % DNA in tail were also confirmed using nonparametric tests (Kruskal-Wallis test). The data was analysed using GraphPad Prism software (GraphPad Software, La Jolla, CA, USA), and $p < 0.05$ has been considered as significantly different.

Results

NEU damage activates DNA damage response kinases

To evaluate the cytotoxicity induced by NEU in MCF7 (breast adenocarcinoma origin) and HeLa (cervical adenocarcinoma origin) cell lines, MTT-based cell viability assay was used (see Additional file 1: Figure S1, A and B respectively). In the dose range at which cell viability was between 50% and 100%, NEU induced phosphorylation of the DNA damage response kinases ATM, Chk2 and Chk1 was observed in MCF7 and HeLa cells in a dose dependent manner (Figure 1A and Additional file 1: Figure S1C). To investigate whether DNA damage cascades are activated on exposure to NEU doses at which cell viability is higher than 70%, we treated MCF7 and HeLa cells with drug concentrations lower than 2 mM. Interestingly, phosphorylation of ATM, Chk2 and Chk1 were also detected in the low dose range of NEU (Figure 1B and Additional file 1: Figure S1D). Since both DSB and SSB response pathways were activated after exposure to NEU, we sought to visualise the presence of these breaks immediately after NEU damage. γH2AX foci formation was observed in HeLa and MCF7 cells after 1 hour of NEU damage and these nuclear foci intensified with increase in concentration of the drug (Figure 1C and Additional file 1: Figure S1E). NEU damage also led to phosphorylation of RPA at threonine 21 residue and induced localisation of phospho-RPA proteins to nuclear foci in HeLa cells within 2 hour of addition of the drug (Figure 1D and E). Neutral and alkaline comet assays were performed to further confirm the formation of DSBs and SSBs respectively. A significant increase in comet formation was observed in MCF7 cells post NEU damage for 2 hours (Figure 1F and G; Additional file 2: Figure S2A and B) compared to control cells. Together these data suggests that NEU induces formation of both SSBs and DSBs within two hours, which leads to the activation of the DNA damage response signalling cascades, namely Chk1 and Chk2 with formation of damage-induced foci.

NEU-induced DNA damage response activation is independent of the mismatch repair system

Earlier reports have shown mismatch repair proteins to mediate checkpoint activation and downstream cytotoxic effects induced upon exposure to DNA alkylating agents [10,17,29,30]. To investigate whether activation of DNA damage response after NEU damage was dependent on mismatch repair, we performed individual knockdowns of the mammalian MutS homologs, Msh2 and Msh6, in HeLa cells. Knocking down of Msh2 or Msh6 using siRNAs against the endogenous proteins did not affect the checkpoint response following 2 hours of NEU treatment (Figure 2A). Phosphorylation of Chk1 at serine 345 and of Chk2 at threonine 68 was observed in Msh2 or Msh6 knocked down cells following NEU damage. The levels of phospho-Chk1 (Ser 345) in NEU-treated Msh2 or Msh6 RNAi-depleted cells were simlar to that of LacZ RNAi knocked down cells in the presence of NEU (1.3 fold for Msh2 and Msh6 siRNA lanes compared to LacZ control in the presence of damage). Similarly the levels of Chk2 phosphorylation in Msh2 or Msh6 RNAi-depleted cells following NEU damage were 1 and 0.7 fold difference in comparison to NEU damaged LacZ lane and hence the activation of both Chk1 and Chk2 remain unperturbed in NEU-treated Msh2 or Msh6 RNAi-depleted cells. To further explore DNA damage response activation after NEU damage mismatch repair-deficient cell lines, HCT 116, a MLH1 deficient cell line of colon cancer origin and DLD1, a MSH6 deficient (frame-shift mutation in Msh6) cell line derived from colorectal adenocarcinoma were used in the experiments. In HCT 116, activation of the DNA damage response kinases ATM, Chk2 and Chk1 were observed after exposure to NEU concentrations from 2 mM to 10 mM for 2 hours (Figure 2B). Similar results were obtained for DLD1 cells (Figure 2C). Though it has been previously reported that the DLD1 cell line is Chk2 deficient [31], we could detect low amounts of phosphorylation of Chk2 at threonine 68 position in DLD1 cells which was reduced in presence of an ATM autophosphorylation inhibitor, KU 55933 (Figure 2D). To confirm that DNA damage response activation in mismatch repair-deficient cells occurs due to formation of breaks in the genome after NEU damage, we investigated the formation of γH2AX foci in DLD1 cells after exposure to NEU (Figure 2E). We observed that similar to mismatch repair-proficient cells, γH2AX foci were prevalent in DLD1 cells after 1 hour of NEU damage. These results collectively suggest that activation of DNA damage cascades after exposure to the S_N1 type-ethylating agent NEU for 2 hours is largely mismatch repair-independent.

Activation of ATM-Chk2 checkpoint pathway precedes but is not required for activation of ATR-Chk1 response pathway

Since we observed phosphorylation of ATM and Chk2 as well as that of Chk1 kinase after treatment of MCF7

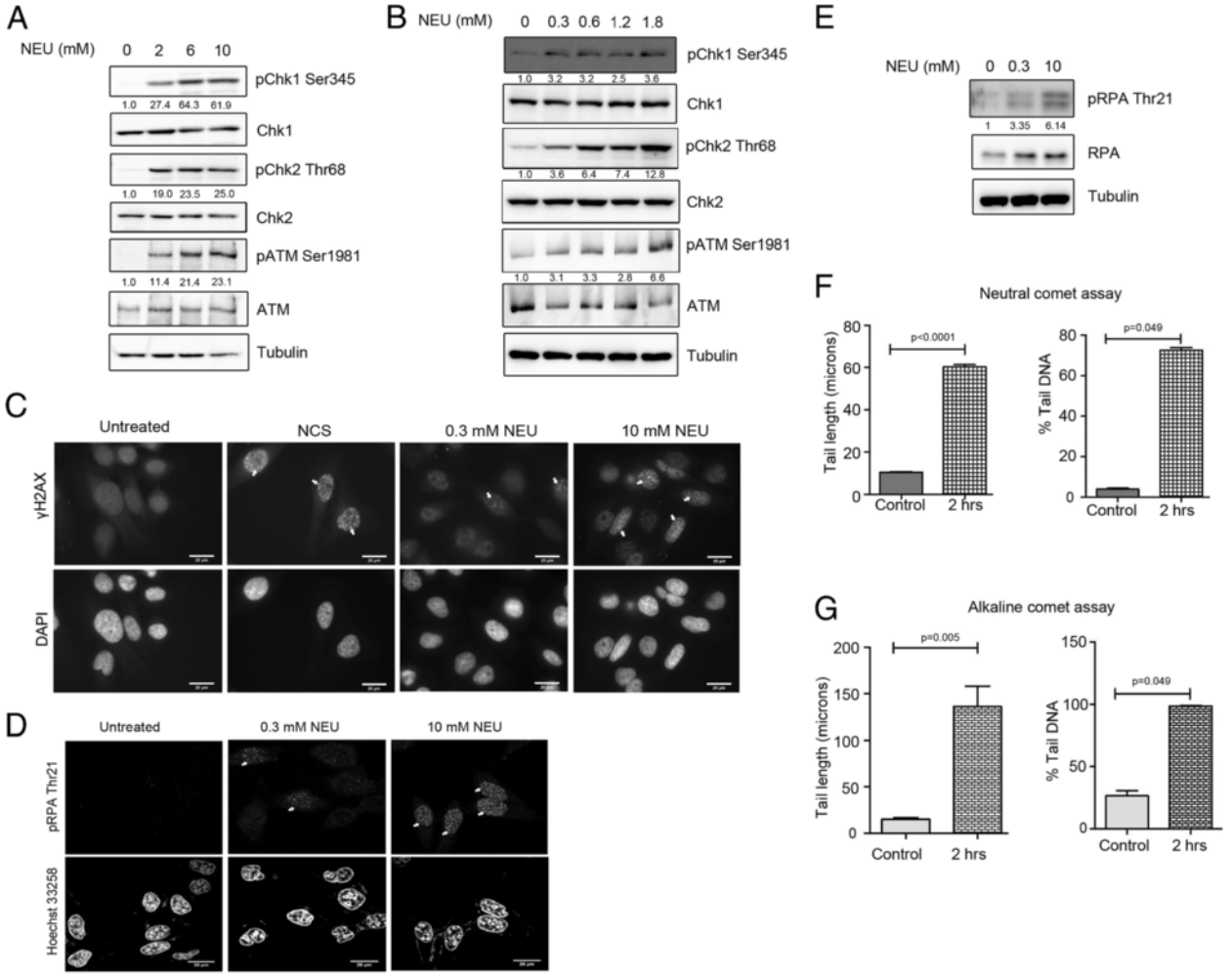

Figure 1 NEU causes activation of checkpoint signalling pathways in a dose dependent manner. (A) MCF7 cells were treated with 0, 2, 6 and 10 mM NEU for 2 hours and lysates were analysed for activation of checkpoint proteins by immunoblotting. **(B)** MCF7 cells were treated with 0, 0.3, 0.6, 1.2 and 1.8 mM NEU for 2 hours and lysates were analysed for activation of checkpoint proteins by immunoblotting. **(C)** HeLa cells were treated with 0.3 and 10 mM NEU for 1 hour, fixed and analysed for γH2AX foci formation by immunostaining. DMSO was used as negative control and neocarzinostatin (NCS), an IR-mimetic drug, was used as positive control at a concentration of 200 ng/ml. Scale bar: 20 μM. **(D)** HeLa cells were treated with 0.3 and 10 mM NEU for 2 hours, fixed and analysed for pRPA foci formation by immunostaining. DMSO was used as negative control. Scale bar: 20 μM. **(E)** HeLa cells were treated with 0, 0.3 and 10 mM NEU for 2 hours and lysates were analysed for phosphorylation of RPA. **(F and G)** MCF7 cells treated with 0 and 10 mM NEU for 2 hours were collected, embedded in agarose and layered on slides. Cells were subjected to lysis followed by electrophoresis in neutral and alkaline conditions respectively. N = 150 cells (50 cells/experiment). Data shown are mean +/− standard error. The results for % DNA in tail and tail length are significantly different at $p < 0.05$ in Mann Whitney U test and student's t test respectively.

and HeLa cells for 2 hours with NEU, we investigated the temporal sequence of activation of these two canonical DNA damage response pathways. On performing a time course assay in MCF7 and HeLa cells, we could detect phosphorylation of ATM and Chk2 10 minutes after initial exposure to NEU while Chk1 phosphorylation was detected 20 minutes after drug damage (Figures 3A and 4A). This pattern of checkpoint activation was similar to a previously reported ATM-to-ATR switch that has been shown to be involved in resection of DSBs [32]. To confirm our results regarding temporal activation of DNA damage response pathways, MCF7 cells treated with 10mM NEU for similar time points were subjected to neutral and alkaline comet assay (Figure 3B and Figure 3C). In the neutral comet assay (Figure 3B and Additional file 2: Figure S2C), tails were visible at 10 minutes post NEU damage. The comet tails in the NEU-damaged cells were significantly longer with higher percentage of DNA compared to the control cells. In the alkaline comet assay, comet tails were observed 20

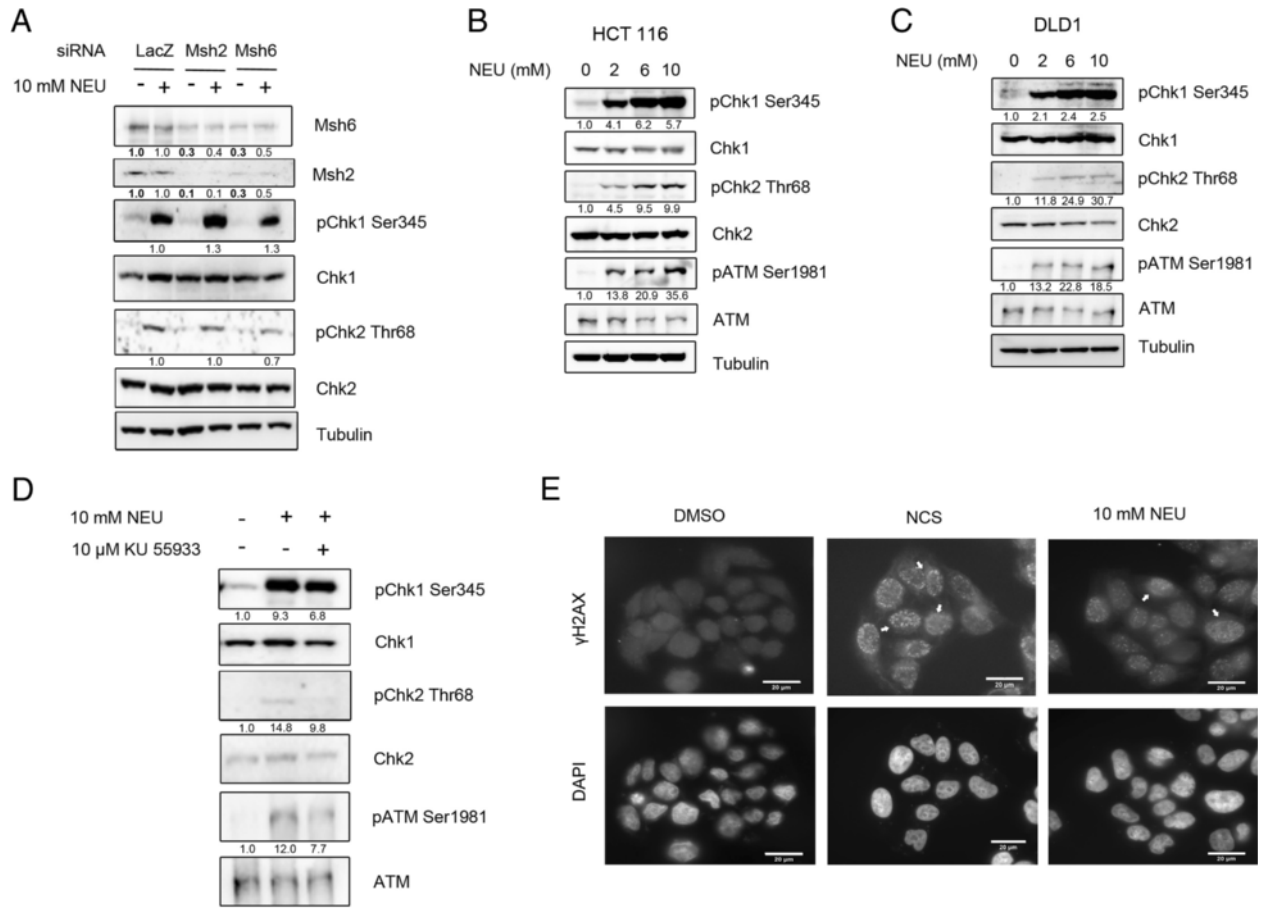

Figure 2 Checkpoint activation in response to NEU-induced damage is independent of mismatch repair. (A) siLacZ, siMsh2 and siMsh6 transfected HeLa cells were treated with 10 mM NEU for 2 hours and lysates were analysed for activation of checkpoint proteins by immunoblotting. **(B)** HCT116, a MLH1-deficient cell line, was treated with 0, 2, 6 and 10 mM NEU for 2 hours and lysates were analysed for activation of checkpoint proteins by immunoblotting. **(C)** DLD1, a MSH6 deficient cell line, was treated with 0, 2, 6 and 10 mM NEU for 2 hours and lysates were analysed for activation of checkpoint proteins by immunoblotting. **(D)** DLD1 cells were treated with 10 mM NEU in presence of 10 μM KU 55933 (ATM inhibitor) for 2 hours and lysates were analysed for activation of checkpoint proteins by immunoblotting. **(E)** DLD1 cells were treated with 10 mM NEU for 1 hour, fixed and analysed for formation of γH2AX foci by immunostaining. DMSO was used as negative control and 200 ng/ml NCS, an IR-mimetic drug, was used as positive control. Scale bar: 20 μM.

minutes after NEU treatment (Figure 3C and Additional file 2: Figure S2D). There was not much tail formation in the 10 minute NEU-treated cells while the 20 minute NEU-damaged cells showed a significant increase in tail length and percentage tail DNA when compared to the untreated cells. KU 55933, an inhibitor of ATM autophosphorylation was used to investigate whether activation of upstream kinases in the DSB response pathway is essential for activation of the SSB response kinase Chk1 after DNA damage. Interestingly, though ATM and Chk2 phosphorylation were almost completely diminished after pre-treatment of MCF7 cells with KU 55933 prior to NEU treatment, unlike the findings in the previous study [32], Chk1 phosphorylation remained unhampered and was observed in 10 mM NEU damaged MCF7 cells treated with the ATM inhibitor (Figure 3D). DMNB, a DNA-PK inhibitor, was used either separately or along with KU 55933 in this experiment since members of the PIKK family of kinases show functional redundancy in ATM-deficient cells [33]. However DNA-PK inhibition did not have any significant effect on the phosphorylation profile of checkpoint proteins after NEU damage (Figure 3D). To investigate whether inhibition of DSB response pathway alters the temporal profile of Chk1 activation after treatment with NEU, a time course assay was performed in MCF7 cells pre-incubated with KU 55933. ATM and Chk2 phosphorylation was totally abolished at all time points in cells pre-treated with the ATM inhibitor before addition of NEU. Interestingly, Chk1 phosphorylation appeared at the same time point (20 minutes) after NEU damage (2.9 fold difference over control) as was observed in the absence of ATM inhibition

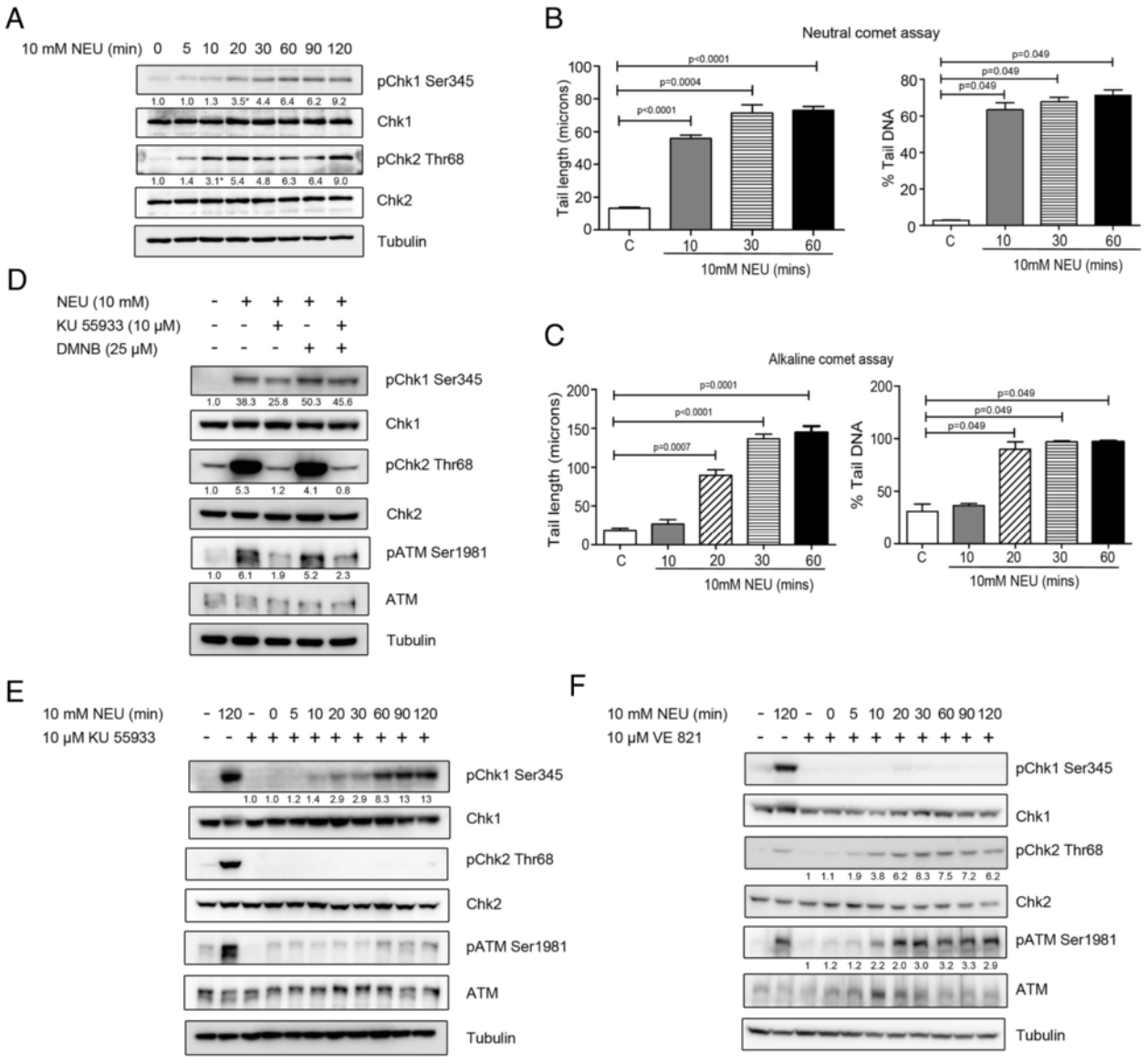

Figure 3 ATM and Chk2 activation precedes but is not required for Chk1 activation. (A) MCF7 cells were treated with 10 mM NEU for different time intervals and lysates were analysed for activation of checkpoint proteins by immunoblotting. **(B and C)** MCF 7 cells treated with 10 mM NEU at different time points were used for analysing DNA DSBs (neutral comet assay) and SSBs (alkaline comet assay) respectively. N = 150 cells (50 cells/experiment). Data shown are mean +/− standard error. The results for % DNA in tail and tail length are significantly different at $p < 0.05$ in Mann Whitney U test and student's t test respectively. **(D)** MCF7 cells were treated with 10 mM NEU in presence of 10 μM KU 55933 (ATM inhibitor) or 25 μM DMNB (DNA-PK inhibitor) or a combination of both for 2 hours and lysates were analysed for activation of checkpoint proteins by immunoblotting. **(E)** MCF7 cells were treated with 10 mM NEU in presence of 10 μM KU 55933 for different time intervals and lysates were analysed for activation of checkpoint proteins by immunoblotting. **(F)** MCF7 cells were treated with 10 mM NEU in presence of 10 μM VE 821 for different time intervals and lysates were analysed for activation of checkpoint proteins by immunoblotting.

(Figure 3E). To completely rule out cross-talk between the two canonical signalling pathways, VE 821, a potent ATP-competitive inhibitor of ATR [34] was added to cells prior to NEU treatment and a time-course assay was performed (Figure 3F). VE 821 compleletly abrogated Chk1 phosphorylation in cells damaged with NEU at all time points. However, both Chk2 and ATM phosphorylation was observed at 10 mins post NEU treatment (3.8 and 2.2 fold difference over control for pChk2 and pATM respectively). In summary, these results point towards a temporal delay in activation of the Chk1 kinase in comparison to that of ATM-Chk2 kinases after DNA damage induced by NEU, however activation of both pathways are independent of each other.

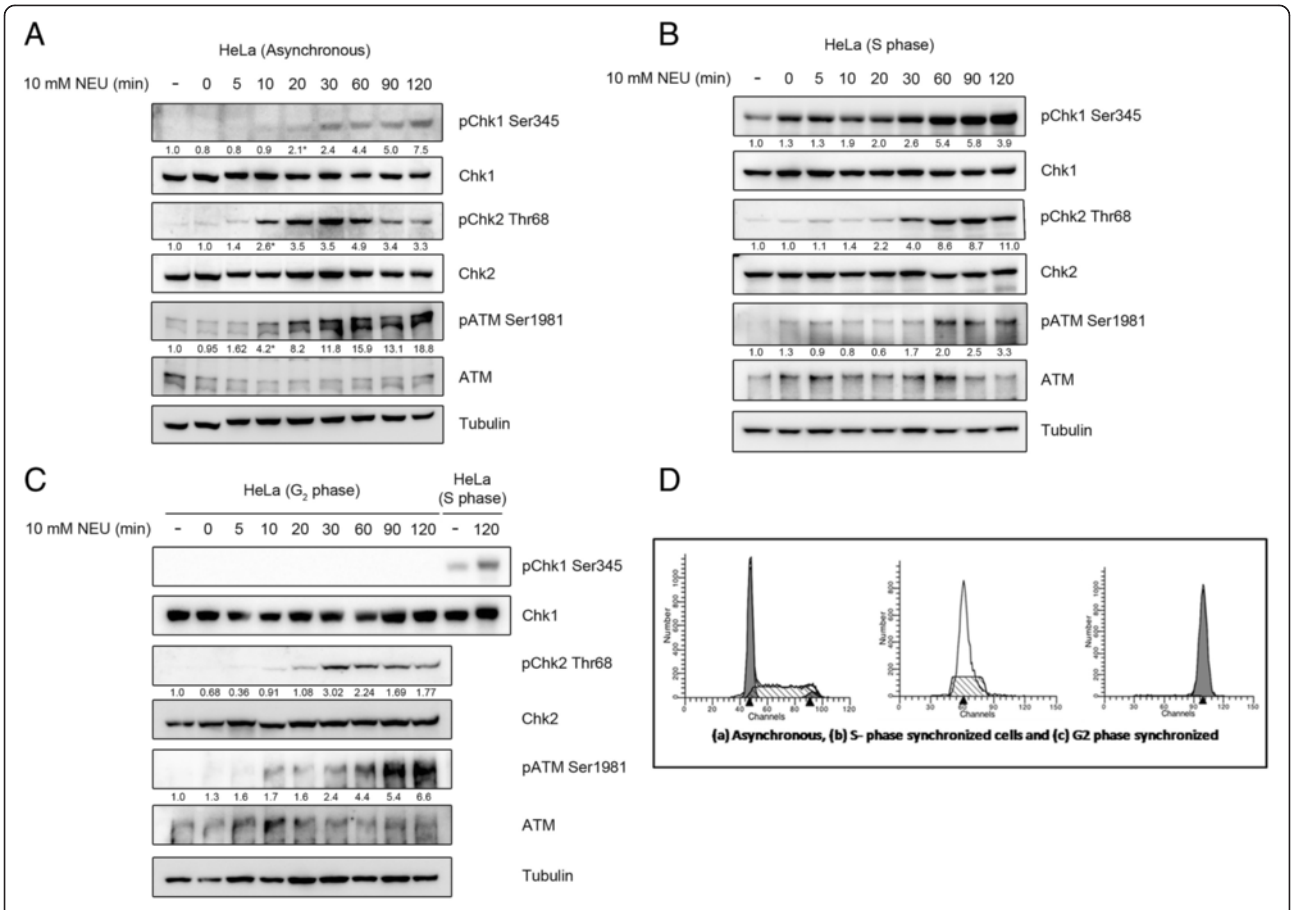

Figure 4 NEU-induced activation of DNA damage response pathway is cell cycle phase dependent. (A) HeLa cells were treated with 10 mM NEU for different time intervals and lysates were analysed for activation of checkpoint proteins by immunoblotting. **(B)** HeLa cells synchronised in S phase using double thymidine block were treated with 10 mM NEU for different time intervals and lysates were analysed for activation of checkpoint proteins by immunoblotting. **(C)** HeLa cells synchronised in G2 phase using thymidine-nocodazole block were treated with 10 mM NEU for different time intervals and lysates were analysed for activation of checkpoint proteins by immunoblotting. **(D)** Cell cycle profile of propidium iodide (PI) stained asynchronous, S phase synchronised and G2-M phase synchronised HeLa cells using Flow Cytometer.

NEU-induced activation of SSB response pathway is cell cycle phase dependent

Since the nature of DNA damage induced by alkylating agents has been proposed to be dependent on replication of DNA at the damaged site [35,36], we compared the temporal profile of checkpoint activation after NEU damage in asynchronous and phase-synchronised HeLa cell populations (Figure 4). In asynchronous HeLa cells, ATM and Chk2 were phosphorylated after 10 minutes of NEU damage while Chk1 phosphorylation was detected after 20 minutes of initial exposure to the drug (Figure 4A). Interestingly, Chk1 phosphorylation was detected as early as 0 minutes after NEU damage in S phase synchronised HeLa cells (Figure 4B). Also, these cells showed a delayed activation of ATM and Chk2 following exposure to NEU (Figure 4B). In cells synchronised in the G2-M phase, the temporal profile of ATM and Chk2 activation after NEU treatment was slightly delayed to that in asynchronous cells (30 minutes instead of 20 minutes as shown in Figure 4C. However NEU did not induce activation of Chk1 even after 2 hours of treatment to G2-M phase synchronised HeLa cells (Figure 4C). Collectively, we conclude that the profile of NEU-induced activation of ATM and Chk2 kinases was conserved across cell cycle phases while the susceptibility to activation of Chk1 kinase after DNA damage induced by NEU was highest in the S phase and least in the G2-M phase. A temporal delay in activation of ATM-Chk2 in S phase may be due to a delay in formation of DSBs during that phase.

NEU disrupts cell polarity and induces upregulation of vimentin in MCF10A acini grown in 3D matrices

NEU was shown to disrupt polarisation in MCF10A breast epithelial cells grown as 3D 'on top' cultures. MCF10A epithelial cells when grown on Matrigel® differentiate to form polarised acinar structures with hollow

lumen attached to the basement membrane, as shown in Figure 5A. On treatment with two doses of NEU (day 0 and 2), the polarisation appears to get disrupted, as seen by the presence of α-6 integrin on the baso-lateral and apical regions, rather than its strong basal and weak lateral localisation. Also, a few acini showed loss of integrin in certain regions (as shown by white arrows in Figure 5A). Similar loss has been observed in cells that metastasise to the parenchyma and pleural cavity [37-39]. β-catenin was found to be disrupted and its presence was seen in the cytoplasm rather than at the cell-cell junctions (membraneous localisation). In addition to the disruption of cell polarity, an upregulation of vimentin was observed following NEU-treatment (Figure 5B). E-cadherin also showed a marginal decrease (Figure 5C) indicating a reduction of this epithelial cell marker.

Discussion

Here, we report a novel finding that damage induced on DNA by a prototypical S_N1 type-ethylating agent, NEU caused rapid activation of major kinases (ATM, Chk2 and Chk1) involved in the checkpoint signalling pathway as well as has the potential to cause transformation in breast acini grown as 3D cultures. The activation of the kinases is cell cycle phase dependent and is temporally controlled without any cross talk between the two parallel signalling pathways, ATM and ATR. Interestingly, mismatch repair system does not seem to play a role at the doses of NEU used in the experiments and the time of exposure of the cells to the chemical agent.

Activation of both Chk1 and Chk2, which are the two major signal relay proteins in the checkpoint signalling cascade and ATM, an apical sensor kinase, were observed in the presence of increasing dose of NEU. Activation of the above-mentioned kinases following NEU damage is indicative of lesions, both DSBs and SSBs being formed on DNA. This is interesting since within a short time interval of NEU damage, there is an immediate checkpoint response which is in contrast to earlier studies where alkylation damage forms detectable lesions

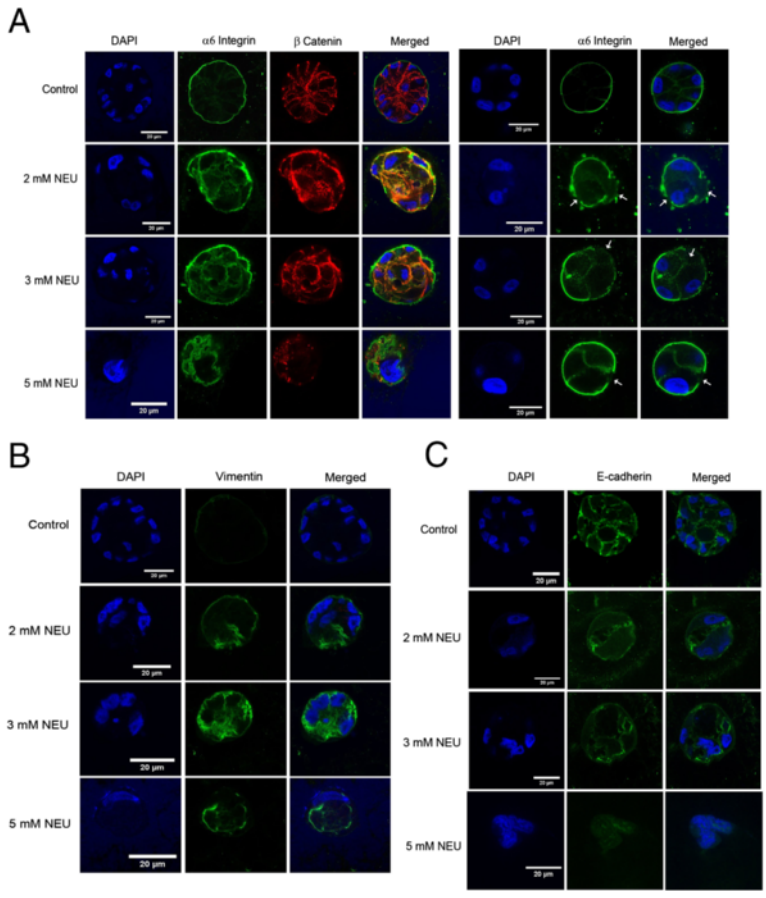

Figure 5 NEU induces upregulation of vimentin and disrupts polarity in MCF10A breast acini. MCF10A cells were grown as 3D 'on top' cultures in Matrigel™. 2, 3 and 5 mM NEU was administered on Day 0 and Day 2. The acini were cultured for 20 days and then immunostained for **(A)** α6-integrin (green), β-catenin (red) and DAPI (blue) to stain nuclei **(B)** Vimentin (green) a marker for EMT and **(C)** E-cadherin (green). The data is representative of 40 – 50 acini from three biologically independent experiments.

following one to two cell division cycles (10). Neutral and alkaline comet assays [19,40-42] as well as phosphorylation of γH2AX on serine 139 and phosphorylation of RPA on threonine 21 confirmed the presence of breaks, both double and single stranded following 2 hours of NEU damage to cells.

Activation of the DNA damage checkpoint pathway is thought to involve the independent recruitment and localisation of the ATM-Chk2 and ATR-Chk1 pathways [11-13]. Challenging this notion, recent reports have shown the existence of considerable cross talk between the two pathways [14,43]. Our data showed the activation of both ATM-Chk2 and ATR-Chk1 pathways in a temporal manner with activation of ATM-Chk2 and Chk1 kinases at 10 minutes and 20 minutes respectively after addition of NEU for 2 hours to the cells (as depicted in Figure 6). This pattern of NEU-induced checkpoint activation is similar to a previous study where IR-induced damage resulted in an ATM–to–ATR switch via single-stranded intermediates [32]. The absence of cross talk between the two signalling modules was ruled out by using ATM and ATR kinase inhibitors, KU 55933 and VE 821 respectively.

It has been previously reported that damage caused by DNA alkylating agents is recognized and repaired by the mismatch repair pathway, which includes the MutSα complex comprising of Msh2 and Msh6 proteins [10,17,29,30]. A number of downstream targets including Chk1, Chk2, p53 and CDC25A have shown to be activated in an mismatch repair-dependent manner [17,44], thereby positioning mismatch repair proteins at a level above ATR kinase. We observed activation of Chk1 and Chk2 kinases, after individual knockdown of Msh6 or Msh2 in HeLa cells post 10 mM NEU damage. Interestingly, knock down of Msh2 also led to a decrease in Msh6 expression in the cells and *vice versa*. This is corroborative with a previous study where the expression of both proteins was required to maintain a steady-state regulation of the mismatch repair system [45]. Our observation was further confirmed when we observed phosphorylation of Chk1 and Chk2 following 2 hours of NEU induced damage in mismatch repair-deficient cell lines, namely HCT116 and DLD1. Overall, the checkpoint activation profile in mismatch repair deficient cell lines post NEU damage was found to be similar to that of mismatch repair proficient cells.

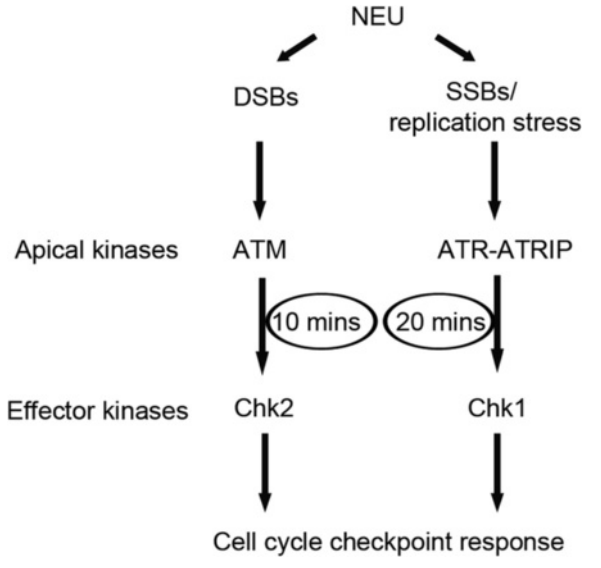

Figure 6 Model depicting temporal activation of checkpoint signalling cascade following NEU damage on cells. According to the model, ATM-Chk2 pathway gets activated at 10 minutes post NEU damage followed by activation of Chk1 signalling cascade at 20 minutes.

In order to test the hypothesis that cells in different phases of the cell cycle could respond differently to the DNA damaging agent, cells were synchronised at S and G2/M phases. S-phase synchronised cells showed activation of Chk1 as soon as they were released from the block, while phosphorylation of Chk2 was observed from 20 minutes. The immediate activation of Chk1 may be speculated to be due to sensitivity of the cells to NEU damage during the replication cycle. There is a higher propensity of single-stranded regions being exposed during this cell cycle phase and therefore immediate activation of Chk1. ATM as well as Chk2 activation was delayed since activation of this pathway requires DSBs or changes in chromatin structure [46]. Interestingly, the checkpoint activation profile was observed to be different during G2/M synchrony where a complete abrogation of Chk1 was observed while ATM and Chk2 activation was observed at 30 minutes post release from G2/M block in NEU drug. This may be speculated to be due to a higher incidence of sister chromatid exchange (SCE) in cells treated with NEU as has been previously observed by Kaina and his colleagues [47] and therefore propensity for increased DSBs to occur during that time. Another reasoning could be the presence of abasic sites formed following the removal of the NEU adduct formed on DNA, giving rise to gaps which may be recognised as DSBs which then leads to the activation of ATM-Chk2 kinases as has been observed in our data.

This study has shed light on some of the players of the DNA damage surveillance pathway that are activated when a prototypical S_N1 type-ethylating agent, NEU, causes insult to DNA. There is a good number of studies on methylating agents and their possible mechanism of action in cells as well as their effect on some of the cellular pathways such as DNA repair. Most research articles have addressed O^6meG and repair by mismatch repair, but literature addressing O^6EtG lesions and its repair is lacking.

Further investigations are necessary to understand the DNA repair pathways that may be involved in repairing the lesions induced by incorporation of an ethyl group to DNA as well as any other sensor protein complex that may first detect the mis-incorporation and then signal to the apical checkpoint kinases. Although it has been reported that DNA alkylating agents do not directly form DSBs, but are formed after processing of lesions induced by the alkylating agent, our study provides evidence that on addition of NEU, the ATM and Chk2 pathway is activated, as early as 10 minutes. This is in contrast to earlier published work where γH2AX foci formation was detected after 24 hours [46]. Therefore, it will be interesting to investigate how NEU alkylation damage is able to convert to a DSB lesion that is capable of activating the DSB response pathway within a short interval of time.

NEU is known to cause point mutations which ultimately lead to the formation of mammary tumours in rat models. NEU has been shown to induce neoplastic transformation *in vitro* of rat mammary epithelial cell [48]. *In vitro* studies have also shown NEU to act as an active rat mammary gland genotoxic carcinogen [4,49]. During the process of neoplastic transformation, one of the earliest stages of invasion is epithelial to mesenchymal transition (EMT) wherein the epithelial cells acquire mesenchymal characteristic so as to invade the surrounding extracellular matrix and migrate towards distant organs [50,51]. EMT is characterised by loss of polarity of the epithelial cells, appearance of mesenchymal markers (upregulation of vimentin, fibronectin, N-cadherin) and down regulation of the epithelial markers (E-cadherin, occludins, cytokeratin 19, claudins) [52,53]. During EMT, β-catenin which is membranous has been found to relocalise in the cytoplasm and/or nucleus [54]. Immortalised breast epithelial cells (MCF10A) when treated with NEU showed upregulation of vimentin. There was marginal loss of E-cadherin following treatment, and complete loss at 5 mM NEU treatment. NEU treatment at all doses also led to disruption of polarity of cells in the acini, overall giving rise to an EMT-like phenotype. Thus, it may be speculated that NEU may play a role in causing transformation in breast acini grown as 3D cultures.

Conclusions

In conclusion, our study reports two novel findings. First, NEU causes DNA lesions within 2 hours of administration that causes the activation of checkpoint signalling kinases, Chk1 and Chk2 in a temporal manner. This activation does not depend upon the mismatch repair complex and is cell cycle phase-dependent. The second finding is that NEU can cause disruption of polarity in cells forming the breast acini grown in 3D as well as upregulate vimentin, thereby leading to transformation *in vitro*. Therefore, NEU can potentially be used as an agent to induce such a phenotype. This strategy will not only permit the study of novel genes that are required for normal mammary development but also shed light on genes that get disrupted in breast cancer.

Additional files

Additional file 1: Figure S1. Checkpoint activation in MCF7 and HeLa cells post NEU damage. **(A)** and **(B)** MCF7 and HeLa cells respectively were treated with increasing NEU concentrations ranging from 0.2 mM to 18 mM for 2 hours. Percent viability was determined for each NEU dose by normalising corresponding absorbance at 570 nm with respect to that of untreated cells. **(C)** HeLa cells were treated with 0, 2, 6 and 10 mM NEU for 2 hours and lysates were analysed for activation of checkpoint proteins by immunoblotting. **(D)** HeLa cells were treated with 0, 0.3, 0.6, 1.2 and 1.8 mM NEU for 2 hours and lysates were analysed for activation of checkpoint proteins by immunoblotting. **(E)** MCF7 cells were treated with 10 mM NEU for 1 hour, fixed and analysed for γH2AX foci formation by immunostaining. DMSO was used as negative control and 200 ng/ml neocarzinostatin (NCS), an IR mimetic drug, was used as positive control. Scale bar: 20 μM.

Additional file 2: Figure S2. NEU induced formation of DSBs and SSBs in MCF7 cells. DNA damage in NEU treated MCF7 cells were measured using comet assay. Cells treated with 10 mM NEU for two hours were subjected to **(A)** neutral comet assay and **(B)** alkaline comet assay. **(A and B)** Representative images of ethidium bromide stained control cells, showing intact super coiled DNA (left) and treated cells showing damaged DNA migrating out of the cell (right). **(C and D)** Cells treated with 10 mM NEU at different time points were subjected to neutral comet assay and alkaline comet assay. Representative images of ethidium bromide stained control cells showing intact super coiled DNA and treated cells at **(C)** 10, 30 and 60 minutes for neutral comet and **(D)** 10, 20, 30 and 60 minutes for alkaline comet showing damaged DNA migrating out of the cell.Scale bar: 50 μM.

Abbreviations

NEU: N-nitroso-N-ethylurea; SSBs: Single strand breaks; DSBs: Double strand breaks; EMT: Epithelial to Mesenchymal transition; MMR: Mismatch repair; O^6EtG: O^6-ethylguanine; DDR: DNA damage response; ATM: Ataxia-telangiectasia mutated; ATR: ATM and Rad3-related; PIKK: Phosphoinositide 3-kinase related kinase; RT: Room temperature.

Competing interests

The authors declare that they have no competing interests.

Authors' contributions

All the authors contributed to the design of the project. Monolayer culture experiments were performed by SB, SS and PT, while three dimensional culture experiments were performed by LAV. ML, SB, SS and LAV wrote the manuscript. All authors read and approved the final manuscript.

Acknowledgements

We thank Dr. Lee Zou, Prof LS Shashidhara and Dr. Girish Deshpande for critical reading of the manuscript and providing useful suggestions. We also thank Lahiri lab members for helpful comments and discussions. The authors greatly acknowledge help from Vijay Vittal at the IISER, Pune Microscopy facility, Dr. S Chiplunker at the flow cytometry facility at ACTREC, Navi Mumbai and Dr. Deepak Barua for help with statistical analysis. This work was supported by Indian Institute of Science Education and Research, Pune Core funding. BS is funded through IISER, Pune Core funds. LAV is funded through DST-INSPIRE fellowship and SS was funded by KVPY fellowship.

Author details

[1]Indian Institute of Science Education and Research, Pune, Maharashtra 411008, India. [2]Current address: Department of Molecular and Integrative Physiology, University of Michigan, Anne Arbor, MI 48109, USA. [3]Current address: Department of Biochemistry & Molecular Genetics, University of Virginia Medical Center, Charlottesville, VA 22908, USA.

Received: 13 November 2013 Accepted: 16 April 2014
Published: 24 April 2014

References

1. Shrivastav N, Li D, Essigmann JM: **Chemical biology of mutagenesis and DNA repair: cellular responses to DNA alkylation.** *Carcinogenesis* 2010, **31:**59–70.
2. Engelbergs J, Thomale J, Rajewsky MF: **Role of DNA repair in carcinogen-induced ras mutation.** *Mutat Res* 2000, **450:**139–153.
3. Barbaric IWS, Russ A, Dear TN: **Spectrum of ENU-induced mutations in phenotype-driven and gene-driven screens in the mouse.** *Environ Mol Mutagen* 2007, **48:**124–142.
4. Stoica G, Koestner A, Capen CC: **Characterization of N-ethyl-N-nitrosourea-induced mammary tumors in the rat.** *Am J Pathol* 1983, **110:**161–169.
5. Givelber HM, DiPaolo JA: **Teratogenic effects of N-ethyl-N-nitrosourea in the Syrian hamster.** *Cancer Res* 1969, **29:**1151–1155.
6. van Boxtel R, Toonen PW, van Roekel HS, Verheul M, Smits BMG, Korving J, de Bruin A, Cuppen E: **Lack of DNA mismatch repair protein MSH6 in the rat results in hereditary non-polyposis colorectal cancer-like tumorigenesis.** *Carcinogenesis* 2008, **29:**1290–1297.
7. Feitsma H, Akay A, Cuppen E: **Alkylation damage causes MMR-dependent chromosomal instability in vertebrate embryos.** *Nucleic Acids Res* 2008, **36:**4047–4056.
8. Fu D, Calvo JA, Samson LD: **Balancing repair and tolerance of DNA damage caused by alkylating agents.** *Nat Rev Cancer* 2012, **12:**104–120.
9. Liu Y, Fang Y, Shao H, Lindsey-Boltz L, Sancar A, Modrich P: **Interactions of human mismatch repair proteins MutSalpha and MutLalpha with proteins of the ATR-Chk1 pathway.** *J Biol Chem* 2010, **285:**5974–5982.
10. Stojic L, Cejka P, Jiricny J: **High doses of SN1 type methylating agents activate DNA damage signaling cascades that are largely independent of mismatch repair.** *Cell Cycle* 2005, **4:**473–477.
11. Ciccia A, Elledge SJ: **The DNA damage response: making it safe to play with knives.** *Mol Cell* 2010, **40:**179–204.
12. Shiloh Y: **The ATM-mediated DNA-damage response: taking shape.** *Trends Biochem Sci* 2006, **31:**402–410.
13. Cimprich KA, Cortez D: **ATR: an essential regulator of genome integrity.** *Nat Rev Mol Cell Biol* 2008, **9:**616–627.
14. Jazayeri A, Falck J, Lukas C, Bartek J, Smith GCM, Lukas J, Jackson SP: **ATM- and cell cycle-dependent regulation of ATR in response to DNA double-strand breaks.** *Nat Cell Biol* 2006, **8:**37–45.
15. Helt CE, Cliby WA, Keng PC, Bambara RA, O'Reilly MA: **Ataxia telangiectasia mutated (ATM) and ATM and Rad3-related protein exhibit selective target specificities in response to different forms of DNA damage.** *J Biol Chem* 2005, **280:**1186–1192.
16. Adams KE, Medhurst AL, Dart DA, Lakin ND: **Recruitment of ATR to sites of ionising radiation-induced DNA damage requires ATM and components of the MRN protein complex.** *Oncogene* 2006, **25:**3894–3904.
17. Stojic L, Mojas N, Cejka P, Di Pietro M, Ferrari S, Marra G, Jiricny J: **Mismatch repair-dependent G2 checkpoint induced by low doses of SN1 type methylating agents requires the ATR kinase.** *Genes Dev* 2004, **18:**1331–1344.
18. Adamson AW, Kim WJ, Shangary S, Baskaran R, Brown KD: **ATM is activated in response to N-methyl-N′-nitro-N-nitrosoguanidine-induced DNA alkylation.** *J Biol Chem* 2002, **277:**38222–38229.
19. Kawaguchi S, Nakamura T, Honda G, Yokohama N, Sasaki YF: **Detection of DNA single strand breaks induced by chemical mutagens using the acellular comet assay.** *Genes Environ* 2008, **30:**77–85.
20. Soule HD, Maloney TM, Wolman SR, Peterson WD Jr, Brenz R, McGrath CM, Russo J, Pauley RJ, Jones RF, Brooks SC: **Isolation and characterization of a spontaneously immortalized human breast epithelial cell line, MCF-10.** *Cancer Res* 1990, **50:**6075–6086.
21. Debnath J, Muthuswamy SK, Brugge JS: **Morphogenesis and oncogenesis of MCF-10A mammary epithelial acini grown in three-dimensional basement membrane cultures.** *Methods* 2003, **30:**256–268.
22. Dey D, Saxena M, Paranjape AN, Krishnan V, Giraddi R, Kumar MV, Mukherjee G, Rangarajan A: **Phenotypic and functional characterization of human mammary stem/progenitor cells in long term culture.** *PLoS One* 2009, **4:**e5329.
23. Kallergi G, Papadaki MA, Politaki E, Mavroudis D, Georgoulias V, Agelaki S: **Epithelial to mesenchymal transition markers expressed in circulating tumour cells of early and metastatic breast cancer patients.** *Breast Cancer Res* 2011, **13:**R59.
24. Huang Y, Fernandez SV, Goodwin S, Russo PA, Russo IH, Sutter TR, Russo J: **Epithelial to mesenchymal transition in human breast epithelial cells transformed by 17beta-estradiol.** *Cancer Res* 2007, **67:**11147–11157.
25. Tiezzi DG, Fernandez SV, Russo J: **Epithelial mesenchymal transition during the neoplastic transformation of human breast epithelial cells by estrogen.** *Int J Oncol* 2007, **31:**823–827.
26. Olive PL, Banath JP: **The comet assay: a method to measure DNA damage in individual cells.** *Nat Protoc* 2006, **1:**23–29.
27. Whitfield ML, Sherlock G, Saldanha AJ, Murray JI, Ball CA, Alexander KE, Matese JC, Perou CM, Hurt MM, Brown PO, Botstein D: **Identification of genes periodically expressed in the human cell cycle and their expression in tumors.** *Mol Biol Cell* 2002, **13:**1977–2000.
28. Lee GY, Kenny PA, Lee EH, Bissell MJ: **Three-dimensional culture models of normal and malignant breast epithelial cells.** *Nat Methods* 2007, **4:**359–365.
29. Christmann M, Kaina B: **Nuclear translocation of mismatch repair proteins MSH2 and MSH6 as a response of cells to alkylating agents.** *J Biol Chem* 2000, **275:**36256–36262.
30. Aquilina G, Crescenzi M, Bignami M: **Mismatch repair, G(2)/M cell cycle arrest and lethality after DNA damage.** *Carcinogenesis* 1999, **20:**2317–2326.
31. Jallepalli PV, Lengauer C, Vogelstein B, Bunz F: **The Chk2 tumor suppressor is not required for p53 responses in human cancer cells.** *World J Biol Chem* 2003, **278:**20475–20479.
32. Shiotani B, Zou L: **Single-stranded DNA orchestrates an ATM-to-ATR switch at DNA breaks.** *Mol Cell* 2009, **33:**547–558.
33. Tomimatsu N, Mukherjee B, Burma S: **Distinct roles of ATR and DNA-PKcs in triggering DNA damage responses in ATM-deficient cells.** *EMBO Rep* 2009, **10:**629–635.
34. Reaper PM, Griffiths MR, Long JM, Charrier JD, Maccormick S, Charlton PA, Golec JM, Pollard JR: **Selective killing of ATM- or p53-deficient cancer cells through inhibition of ATR.** *Nat Chem Biol* 2011, **7:**428–430.
35. Kaina B: **Critical steps in alkylation-induced aberration formation.** *Mutat Res* 1998, **404:**119–124.
36. Kondo N, Takahashi A, Ono K, Ohnishi T: **DNA damage induced by alkylating agents and repair pathways.** *J Nucleic Acids* 2010, **2010:**543531.
37. Pignatelli M, Cardillo MR, Hanby A, Stamp GW: **Integrins and their accessory adhesion molecules in mammary carcinomas: loss of polarization in poorly differentiated tumors.** *Hum Pathol* 1992, **23:**1159–1166.
38. Natali PG, Nicotra MR, Botti C, Mottolese M, Bigotti A, Segatto O: **Changes in expression of alpha 6/beta 4 integrin heterodimer in primary and metastatic breast cancer.** *Br J Cancer* 1992, **66:**318–322.
39. Davis TL, Cress AE, Dalkin BL, Nagle RB: **Unique expression pattern of the alpha6beta4 integrin and laminin-5 in human prostate carcinoma.** *Prostate* 2001, **46:**240–248.
40. Collins AR, Dobson VL, Dusinska M, Kennedy G, Stetina R: **The comet assay: what can it really tell us?** *Mutat Res* 1997, **375:**183–193.
41. Collins AR: **The comet assay for DNA damage and repair: principles, applications, and limitations.** *Mol Biotechnol* 2004, **26:**249–261.
42. Fortini P, Raspaglio G, Falchi M, Dogliotti E: **Analysis of DNA alkylation damage and repair in mammalian cells by the comet assay.** *Mutagenesis* 1996, **11:**169–175.
43. Cuadrado M, Martinez-Pastor B, Fernandez-Capetillo O: **ATR activation in response to ionizing radiation: still ATM territory.** *Cell Div* 2006, **1:**7.
44. Wang Y, Qin J: **MSH2 and ATR form a signaling module and regulate two branches of the damage response to DNA methylation.** *Proc Natl Acad Sci U S A* 2003, **100:**15387–15392.
45. Chang DK, Ricciardiello L, Goel A, Chang CL, Boland CR: **Steady-state regulation of the human DNA mismatch repair system.** *J Biol Chem* 2000, **275:**18424–18431.
46. Bakkenist CJ, Kastan MB: **DNA damage activates ATM through intermolecular autophosphorylation and dimer dissociation.** *Nature* 2003, **421:**499–506.
47. Kaina B, Aurich O: **Dependency of the yield of sister-chromatid exchanges induced by alkylating agents on fixation time. Possible involvement of secondary lesions in sister-chromatid exchange induction.** *Mutat Res* 1985, **149:**451–461.
48. Stoica G, Jacobs R, Koestner A, O'Leary M, Welsch C: **ENU-induced in vitro neoplastic transformation of rat mammary epithelial cells.** *Anticancer Res* 1991, **11:**1783–1792.
49. Stoica G, Koestner A, Capen CC: **Neoplasms induced with high single doses of N-ethyl-N-nitrosourea in 30-day-old Sprague–Dawley rats, with special emphasis on mammary neoplasia.** *Anticancer Res* 1984, **4:**5–12.

50. Trimboli AJ, Fukino K, de Bruin A, Wei G, Shen L, Tanner SM, Creasap N, Rosol TJ, Robinson ML, Eng C, Ostrowski MC, Leone G: **Direct evidence for epithelial-mesenchymal transitions in breast cancer.** *Cancer Res* 2008, **68:**937–945.
51. Tse JC, Kalluri R: **Mechanisms of metastasis: epithelial-to-mesenchymal transition and contribution of tumor microenvironment.** *J Cell Biochem* 2007, **101:**816–829.
52. Thiery JP, Sleeman JP: **Complex networks orchestrate epithelial-mesenchymal transitions.** *Nat Rev Mol Cell Biol* 2006, **7:**131–142.
53. Ksiazkiewicz M, Markiewicz A, Zaczek AJ: **Epithelial-mesenchymal transition: a hallmark in metastasis formation linking circulating tumor cells and cancer stem cells.** *Pathobiology* 2012, **79:**195–208.
54. Kim K, Daniels KJ, Hay ED: **Tissue-specific expression of beta-catenin in normal mesenchyme and uveal melanomas and its effect on invasiveness.** *Exp Cell Res* 1998, **245:**79–90.

doi:10.1186/1471-2407-14-287
Cite this article as: Bodakuntla *et al.*: N-nitroso-N-ethylurea activates DNA damage surveillance pathways and induces transformation in mammalian cells. *BMC Cancer* 2014 **14**:287.

Electronic supplementary material

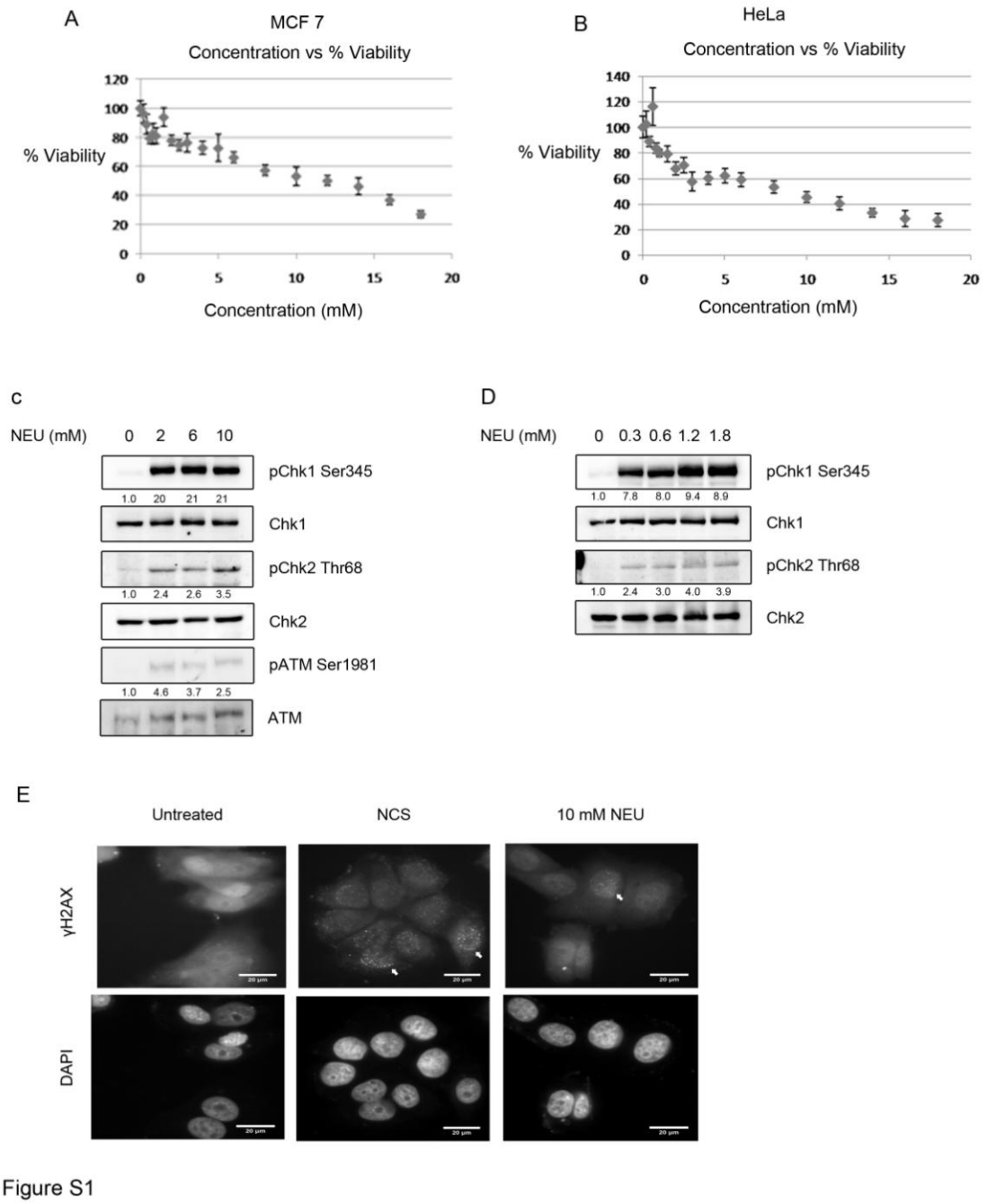

Figure S1

Additional file 1: Figure S1: Checkpoint activation in MCF7 and HeLa cells post NEU damage. **(A)** and **(B)** MCF7 and HeLa cells respectively were treated with increasing NEU concentrations ranging from 0.2 mM to 18 mM for 2 hours. Percent viability was determined for each NEU dose by normalising corresponding absorbance at 570 nm with respect to that of untreated cells. **(C)** HeLa cells were treated with 0, 2, 6 and 10 mM NEU for 2 hours and lysates were analysed for activation of checkpoint proteins by immunoblotting. **(D)** HeLa cells were treated with 0, 0.3, 0.6,

1.2 and 1.8 mM NEU for 2 hours and lysates were analysed for activation of checkpoint proteins by immunoblotting. **(E)** MCF7 cells were treated with 10 mM NEU for 1 hour, fixed and analysed for γH2AX foci formation by immunostaining. DMSO was used as negative control and 200 ng/ml neocarzinostatin (NCS), an IR mimetic drug, was used as positive control. Scale bar: 20 μM.

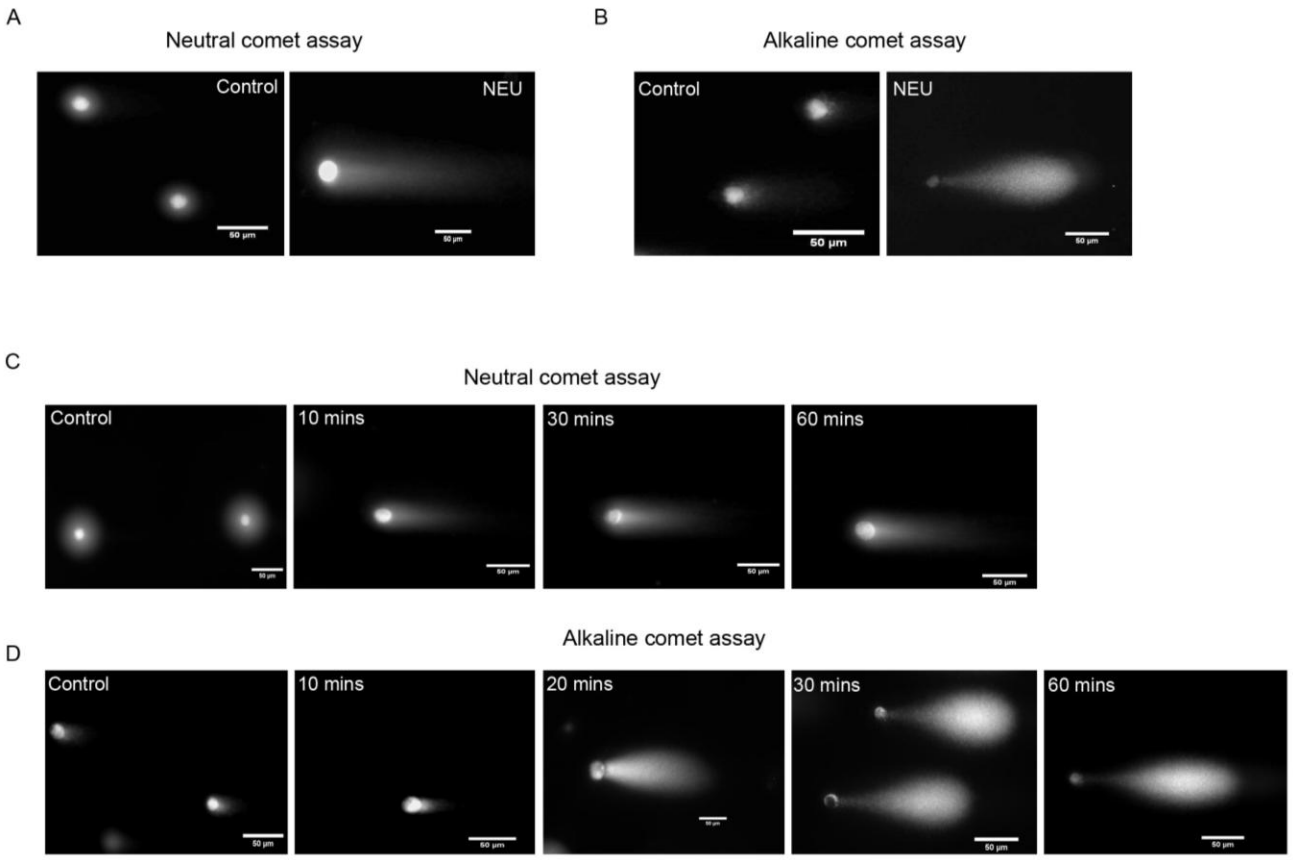

Figure S2

Additional file 2: Figure S2: NEU induced formation of DSBs and SSBs in MCF7 cells. DNA damage in NEU treated MCF7 cells were measured using comet assay. Cells treated with 10 mM NEU for two hours were subjected to **(A)** neutral comet assay and **(B)** alkaline comet assay. **(A and B)** Representative images of ethidium bromide stained control cells, showing intact super coiled DNA (left) and treated cells showing damaged DNA migrating out of the cell (right). **(C and D)** Cells treated with 10 mM NEU at different time points were subjected to neutral comet assay and alkaline comet assay. Representative images of ethidium bromide stained control cells showing intact super coiled DNA and treated cells at **(C)** 10, 30 and 60 minutes for neutral comet and **(D)** 10, 20, 30 and 60 minutes for alkaline comet showing damaged DNA migrating out of the cell.Scale bar: 50 μM.

Platelet-activating factor promotes motility in breast cancer cells and disrupts non-transformed breast acinar structures

V. LIBI ANANDI, K.A. ASHIQ*, K. NITHEESH* and M. LAHIRI

Indian Institute of Science Education and Research, Pashan, Pune, Maharashtra 411008, India

Received July 20, 2015; Accepted September 4, 2015

DOI: 10.3892/or.2015.4387

Abstract. A plethora of studies have demonstrated that chronic inflammatory microenvironment influences the genesis and progression of tumors. Such microenvironments are enriched with various lipid mediators. Platelet activating factor (PAF, 1-alkyl-2-acetyl-sn-glycero-3-phosphocholine) is one such lipid mediator that is secreted by different immune cell types during inflammation and by breast cancer cells upon stimulation with growth factors. Overexpression of PAF-receptor has also been observed in many other cancers. Here we report the possible roles of PAF in tumor initiation and progression. MCF10A, a non-transformed and non-malignant mammary epithelial cell line, when grown as 3D 'on-top' cultures form spheroids that have a distinct hollow lumen surrounded by a monolayer of epithelial cells. Exposure of these spheroids to PAF resulted in the formation of large deformed acinar structures with disrupted lumen, implying transformation. We then examined the response of transformed cells such as MDA-MB 231 to stimulation with PAF. We observed collective cell migration as well as motility at the single cell level on PAF induction, suggesting its role during metastasis. This increase in collective cell migration is mediated via PI3-kinase and/or JNK pathway and is independent of the MAP-kinase pathway. Taken together this study signifies a novel role of PAF in inducing transformation of non-tumorigenic cells and the vital role in promotion of breast cancer cell migration.

Correspondence to: Dr Mayurika Lahiri, Indian Institute of Science Education and Research, Dr Homi Bhabha Road, Pashan, Pune, Maharashtra 411008, India
E-mail: mayurika.lahiri@iiserpune.ac.in

*Contributed equally

Abbreviations: PAF, platelet-activating factor; PAF-R, platelet-activating factor receptor; 3D, three-dimensional; JNK, c-Jun N-terminal kinase; MAP, mitogen-activated kinase; PI3K, phosphoinositide 3-kinase; EGF, epidermal growth factor; EHS, Engelbreth-Holm-Swarm

Key words: platelet-activating factor, collective cell migration, single-cell motility, breast cancer, transformation, spheroids

Introduction

Microenvironment and tumor infiltrate have been shown to have a profound effect on different stages of cancer development ranging from cancer cell initiation, promotion and progression (1,2). Chronic inflammatory microenvironments have been demonstrated to be a major predisposing factor for different cancers including breast and ovarian cancers (3-5). Phospholipid mediators such as prostaglandins (PG), lysophosphatidic acid (LPA) and platelet-activating factor (PAF) have been shown to play a role in a number of biological pathways including inflammatory diseases, cardiovascular homeostasis as well as in cancer (6-8). The role of PAF in various immunological responses like platelet aggregation, stimulation of neutrophils and macrophages, inflammation and allergic responses has also been demonstrated (9). PAF has been shown to induce apoptotic cell death in primary neurons of mice independent of the PAF receptors (10). PAF is one of the most potent mediators, which has been shown to play a vital role in neo-angiogenesis (3,5,11). Interference with the PAF pathway in breast cancer, prostate cancer and Kaposi's sarcoma has been demonstrated to inhibit growth of tumors primarily due to inhibition of angiogenesis (12). Signaling through PAF has been suggested to play a role in murine melanoma lung metastasis (13,14). Association of PAF to early events of transformation has been shown in BRCA-1 mutant ovarian cells (15).

PAF mediated activity occurs via its cell surface and intracellular G protein-coupled receptors known as PAF receptors (PAF-R) (16,17). Overexpression of PAF-R was shown to induce melanocytic tumorigenesis in transgenic mice (18). Also, upregulation of PAF receptors has been observed in invasive breast cancer cells (16,17). Furthermore, use of PAF-R antagonist inhibited growth and differentiation of human breast cancer cells (19). In case of nude mice, treatment with PAF-R antagonist caused inhibition of xenografts of human prostatic carcinoma (20). Thus, highlighting the role of PAF-PAF-R pathway in the genesis and maintenance of the tumor.

Bussolati *et al* (16) reported that breast cancer cells MDA-MB 231, a metastatic cell line and MCF7, adenocarcinoma, secreted PAF under the influence of different growth factors, and that PAF increased the motility of MDA-MB 231 cells. However the role of PAF in breast cancer has not been studied extensively, particularly with respect to

early events in breast cancer initiation. This study elucidated the role of PAF in breast cancer initiation, progression and promotion. To investigate the potential of PAF to induce early transformation, 3-dimensional cultures of non-tumorigenic mammary epithelial cells were grown on laminin-rich basement membrane and allowed to differentiate and organize to form polarized structures called spheroids. These spheroids have an outer layer of epithelial cells encircling a hollow lumen (21,22). This well-architectured structure is vital for the form and function of the epithelial cells (23). The disruption of the well-formed polarized architecture is seen during early stages of breast cancer (21). Exposure of MCF10A, a non-tumorigenic mammalian breast epithelial cell to PAF resulted in the formation of abnormal acinar structures. These abnormal acini showed different phenotypes such as spheroids with multiple layers of cells surrounding the lumen or absence of a distinct lumen as well some acini had protrusion-like structures. The PAF-treated spheroids also showed an increase in size with a significant increase in the number of cells in each acini compared to the untreated acini. Collectively these phenotypes signify transformation. Thus, this study reports for the first time the potential of PAF to induce early transformation in breast epithelial cells.

Furthermore, to investigate the role of PAF in cancer promotion, MDA-MB 231 invasive breast cancer cells were treated with PAF to test for its ability to enhance migration. 'Collective cell migration' has been reported to play a vital role in invasion and metastasis (24). We studied this dynamic process using wound-healing assay as reported previously (25). Our study demonstrated the ability of PAF to induce enhanced collective cell migration and henceforth indicating its possible role in breast cancer promotion. At the single cell level, PAF induction showed increased motility of MDA-MB 231 cells when compared to un-induced cells, which was measured by taking into account motility parameters such as distance and displacement of an individual cell. Significant increase in velocity (rate of migration) of the cells was observed similarly to that demonstrated previously (16), however, there was no change in directionality between untreated and PAF-treated cells.

Materials and methods

Cells and culture conditions. MDA-MB 231 and MCF10A cell lines were generous gifts from Dr Kundan Sengupta (IISER, Pune) and Professor Raymond C. Stevens (The Scripps Research Institute, CA, USA), respectively. MDA-MB 231 cells were cultured in Dulbecco's modified Eagle's medium (DMEM), supplemented with 10% fetal bovine serum (FBS; Invitrogen), 2 mM L-glutamine and 100 U/ml penicillin-streptomycin (Invitrogen). Cells were grown in 100-mm tissue culture treated dishes (Corning) at 37˚C in a humidified 5% CO_2 incubator. MCF10A cells were cultured in growth medium containing high glucose DMEM without sodium pyruvate and 5% horse serum (both from Invitrogen), 20 ng/ml EGF, 0.5 μg/ml hydrocortisone, 100 ng/ml cholera toxin and 10 μg/ml insulin (all from Sigma) and 100 U/ml penicillin-streptomycin (Invitrogen). High glucose DMEM without sodium pyruvate containing 20% horse serum and 100 U/ml penicillin-streptomycin (Invitrogen) was used for resuspension during sub-culturing.

RNA extraction and cDNA synthesis for PAF receptor expression analysis. Cells were harvested from the culture dish using TRIzol (Ambion) by scraping cells using cell scraper (Corning), followed by DNAse I treatment using TURBO DNA-free™ kit as per the manufactures protocol. Extracted RNA was quantified and cDNA was prepared using standard protocols with 5 μg of RNA, 1 μl oligodT (50 mM; Invitrogen) in nuclease free water (NFW), dNTP (2.5 mM) and MLMV-reverse transcriptase (Promega). Reverse transcriptase was heat inactivated at 67˚C for 10 min. The cDNA was further used to analyze the expression of PAF receptor in the cell lines. Amplification of the target was performed in thermal mastercyclers (Eppendorf) using forward, (5'-TACTGCTCTGTGGCCTTCCT-3') and reverse, (5'-CTGCCCTTCTCGTAATGCTC-3') primers. GAPDH was used as the house-keeping gene and was amplified with forward, (5'-ACCACAGTCCATGCCATCAC-3') and reverse (5'-TCCACACCCTGTTGCTGTA-3') primers. The following PCR cycle was used for the amplification 95˚C for 60 sec, 55˚C for 45 sec, 72˚C for 60 sec and final extension for 3 min. The experiments were repeated three times to confirm the receptor status. The quantification (densitometry) was done using the gel analysis function of ImageJ software and normalized to the housekeeping gene (GAPDH) and further adjusted with respect to MCF10A expression (considering MCF10A PAF-R expression to be 1).

Wound-healing assay. Cells were seeded at a density of $5x10^5$ cells/ml of complete culture medium in culture plates with wound healing inserts (Ibidi GmbH, Munich, Germany), as per manufacturers protocol for 16-18 h. The monolayer was then treated with 10 μg/ml mitomycin C (Sigma) in serum free media for 2 h so as to inhibit cell proliferation (26). Cells were pre-treated with various inhibitors as per the experiment. WEB 2086 (200 μM) (PAF receptor antagonist) (27,28) was added 10 min prior to start of the experiment. UO126 (10 μM), a MEK inhibitor (29), was added 30 min before PAF induction while wortmannin (200 nM) (30), PI3-K inhibitor and SP 600125 (75 μM), JNK inhibitor (31) were added 60 min prior to PAF induction. Following treatment with inhibitors and before addition of PAF (200 nM), the inserts were removed carefully and cells were washed gently using 1X phosphate-buffered saline (PBS; PAN-Biotech GmbH) to remove floating cells and cells were replenished with complete media containing inhibitors. Images of the wounds were acquired using phase contrast microscope (Nikon) at x10 magnification at different time-points (namely 0, 18 and 24 h) after PAF induction. The results presented are average from three independent biological replicates. Wound areas were quantified using ImageJ and graphs were plotted using GraphPad Prism 6. The percentage of wound closure was calculated as:

$$\% \text{ Wound closure} = \frac{(\text{Initial wound area} - \text{final wound area})}{\text{Initial wound area}} \times 100$$

Single cell migration assay. Cells were seeded at a density of 5,000 cells/well in an 8-well chamber cover glass (LabTek) precoated with 10 μg/ml fibronectin (2-3 h treatment at 37˚C). Cells were maintained at 37˚C in complete medium for 18-20 h. For live cell imaging, cells were supplemented with L-15 medium

containing 10% FBS and 100 U/ml penicillin-streptomycin (both from Invitrogen) containing WEB 2086 and PAF as per the experiment. Time-lapse microscopy for 4 h was carried out in a stage incubator using Zeiss LSM 710 laser scanning confocal microscope at x10 magnification. Cells were tracked in ImageJ analysis software using manual tracking plugin. Randomly selected cells from three to five independent experiments were tracked and distance travelled, displacement and velocity of a cell were calculated using Chemotaxis and Migration tool (Ibidi GmbH).

3D 'on top' cultures and immunofluorescence analysis. MCF10A cells were grown as 3D-'on top' cultures according to standard protocols (21,32,33). PAF was added on day 4, 8, 12 and 16 into the culture medium (day of seeding was considered as day 0) and the acini were harvested on day 20 and immunostained as outlined earlier (21,32,33) with phalloidin (Invitrogen) instead of Alexa Fluor-conjugated secondary antibody to label the actin cytoskeleton. Images were acquired using Zeiss LSM 710 laser scanning confocal microscope at x63 magnification. The results depicted are representative images from three independent biological experiments. A total of ~90 acini were imaged and optical sections were analyzed and classified based on the observed phenotype. Graphs were plotted and statistical analysis was done using GraphPad Prism software (GraphPad Software, La Jolla, CA, USA). Measurement of the volume of acini and counting of number of nuclei were done using Image-Pro Plus software (Media Cybernetics, USA). Around 30 acini were analyzed each in control and treated.

Ethics. This study did not involve utilization of human subject and has been carried out using cell lines.

Statistical analysis. Wound healing data are presented as mean ± SEM. One-way ANOVA was used to test the significance of difference of the percentage of wound closure across treatments. Mann-Whitney U test was used to analyze the significance of difference between parameters used in single cell migration assay (accumulated distance, euclidean distance, velocity and directionality and 3D morphometric analysis). $P<0.05$ was considered statistically significant. ***, ** and * indicate $P<0.0001$, $P<0.01$, and $P<0.05$, respectively.

Results

PAF induces formation of abnormal acinar structures in immortalized non-tumorigenic breast epithelial cell line MCF10A grown as 3D 'on-top' cultures. MCF10A cells are spontaneously immortalized, non-tumorigenic cells of normal breast epithelial origin. These cells when grown on laminin rich extracellular matrix form multicellular acini-like structures resembling epithelial cells lining the acinus, the smallest functional unit of a human mammary gland (34). MCF10A cells give rise to acinar structures wherein the hollow lumen is surrounded by a single layer of epithelial cells as shown in Fig. 1A (top panel). Upon exposure to PAF, these well-organized structures were observed to be disrupted. Sixty-five percent of the spheroids showed multiple layers of cells surrounding a lumen or absence of a distinct lumen (Fig. 1A; middle panel and B) while ~58% showed formation of protrusion-like structures as seen in Fig. 1A (bottom panel) and C. Further morphometric analysis revealed that the PAF-treated acini were larger in size as indicated by a significant increase in volume compared to untreated acini (Fig. 1E). Also there was a significant increase in the number of cells per acini (Fig. 1F), which implied that PAF induces proliferation of MCF10A cells in the acini. Taken together, PAF was found to disrupt overall morphology of the spheroids as well as induce proliferation, an indicator of transformation.

PAF increases collective cell migration in MDA-MB 231. Since PAF treatment induced formation of disrupted acinar structures, we checked for the PAF-R status in MCF10A as well as in two other breast cancer cells, MDA-MB 231 and MCF7s, using RT-PCR. PAF-R expression levels in these cell lines were correlated with their tumorigenic potential. MDA-MB 231 and MCF7 cells showed overexpression of PAF-receptors while MCF10A showed weak expression (Fig. 2A and B). However there was no appreciable change in the expression levels of the receptor with increase in dose of PAF (data not shown). The effect of PAF on collective cell migration was investigated using wound healing assay. MDA-MB 231 cells were treated with different doses of PAF ranging from 10 to 200 nM. PAF (200 nM) showed an appreciable increase in motility by 18 h (data not shown). Thus, further experiments were performed using 200 nM PAF. On exposure of MDA-MB 231 cells to 200 nM PAF, the cells showed a significant increase in migration with almost 80% wound closure at 18 h (Fig. 2C and D). This increase in motility was inhibited upon pre-treatment of cells with WEB 2086, a PAF receptor antagonist (27,28). Thus, confirming role of PAF in inducing increased migration of highly invasive MDA-MB 231 cells.

PAF-induced migration is mediated via PI3-kinase pathway and/or JNK pathway, but not via MAP-kinase pathway. To predict the possible pathway(s) involved in PAF-induced cell migration scratch assays along with inhibitors for generally known motility pathways were performed. It was observed that the MAP-kinase pathway did not mediate PAF-induced migration since inhibition of the pathway with a MEK inhibitor, UO126 (29), did not have an effect on wound closure (Fig. 3A).

PAF stimulated cells, upon pre-treatment with wortmannin, a PI3-K inhibitor (30), showed wound closure which was similar to unstimulated and untreated cells and was significantly less than PAF-treated cells (Fig. 3B). Thus, indicating a possible role of PI3-K pathway in PAF induced motility. However, the wound closure of unstimulated wortmannin-treated cells was significantly less than control cells indicating the role of PI3-kinase pathway in normal MDA-MB 231 cell motility (Fig. 3B).

Use of the JNK inhibitor SP600125 (31), also abrogated both PAF-induced as well as inherent motility of MDA-MB 231 cells (Fig. 3C). However, the extent of inhibition of migration of PAF stimulated cells as well as untreated cells by the inhibitor suggests the possible role of JNK pathway in PAF induced motility.

PAF induces chemokinesis at the single cell level in MDA-MB 231 cells. To determine the effect of PAF on

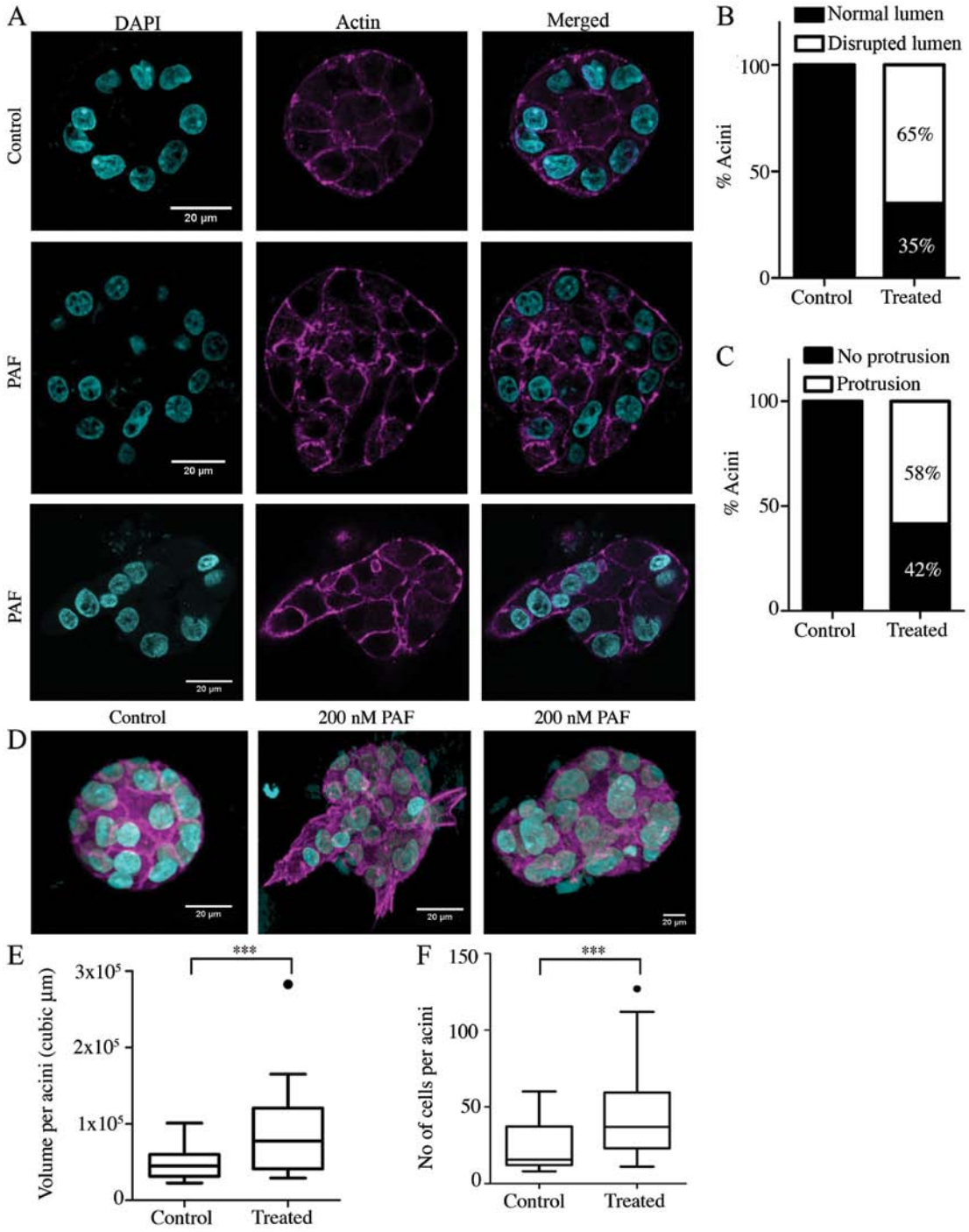

Figure 1. PAF induces formation of abnormal acinar structures in immortalized non-tumorigenic breast epithelial cell line MCF10A grown as 3D on-top cultures. (A) Representative images of day 20 MCF10A acini (centre optical section, 0.35 μm thickness). Top panel: untreated acini showing presence of distinct hollow lumen. Middle panel: acini treated with 200 nM PAF on day 4, 8, 12 and 16; showing multiple layers of cells encircling a not so distinct lumen. Bottom panel: spheroids with protrusion-like structures extending out of acini. Graphs represent data quantified based on visual observation of 3D structures for (B) normal or disrupted lumen and (C) presence of protrusion like or 'bulb'-like structures. Data represent the pooled results from more than 3 independent experiments; n=94 acini. (D) 3D re-construction of the Z-optical sections to aid in visualization of the protrusions in acini following PAF treatment. (E and F) Box plots representing number of cell/acini and volume per acini respectively, quantified using Image-Pro Plus software (Media Cybernetics, USA). Mann-Whitney test was used to test the statistical significance, ***P<0.0001. Number of acini analyzed; n>30.

motility of MDA-MB 231 cells at the single cell level time-lapse microscopy of sparsely seeded MDA-MB 231 cells on fibronectin coated chamber cover glass was performed for 4 h. Tracking of cells was done and trajectory plots were obtained for the following cell treatments: untreated, PAF stimulated, WEB 2086 pre-treated followed by PAF stimulation and only WEB 2086 treated as shown in Fig. 4B. Further analysis of the cells revealed an increase in motility of cells upon PAF induction. There was a significant increase in the distance covered by the PAF-treated cells when compared to untreated cells as well as to cells that were pre-treated with WEB 2086 followed by PAF-stimulation in the time and conditions used in the study (Fig. 5A). Other parameters such as displacement (Fig. 5B) and velocity (Fig. 5C) were

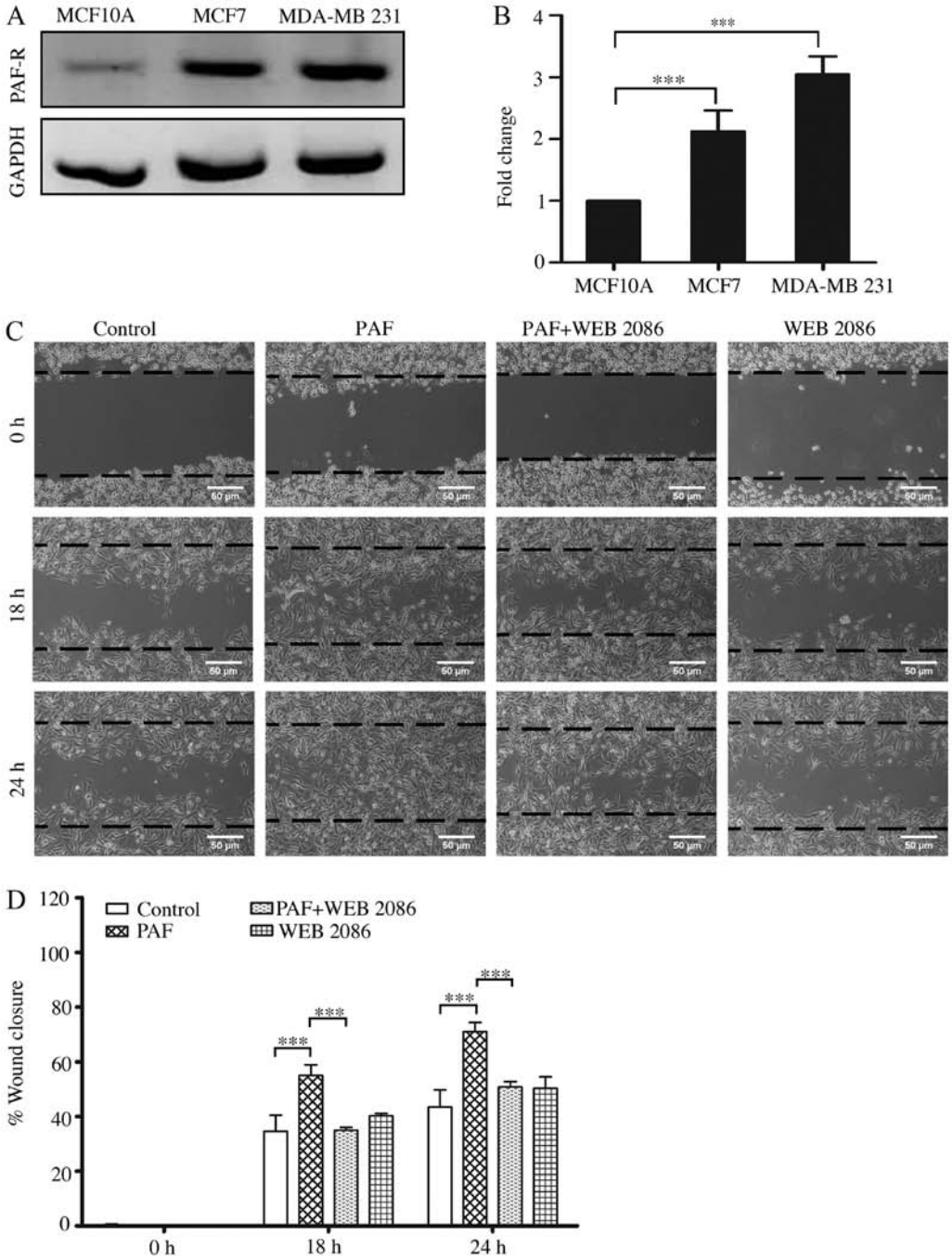

Figure 2. PAF increases collective cell migration in MDA-MB 231 cells. (A) RT-PCR analysis of PAF-receptor expression in non-transformed breast epithelial cell line MCF10A and breast cancer cell lines MCF-7 and MDA-MB 231. (B) Graphs represent mean ± SEM fold change of expression level normalized to MCF10A PAF-R expression. Two-fold difference was considered to be significant. (C) Wound-healing assay demonstrating collective migration of MDA-MB 231 cells with or without treatment of 200 nM PAF and/or 200 μM WEB 2086 (PAF receptor antagonist). Scale bar: 50 μm. (D) Quantitative results for the data shown in (C). Percentage wound closures were calculated. Data represent mean ± SEM (n=3 independent experiments). Student's t-test was used to test the statistical significance of data, ***P<0.001.

observed to increase significantly following PAF treatment in comparison to untreated or PAF-stimulated and WEB 2086 pre-treated cells. All these effects induced by PAF were reversed upon pretreatment of cells with WEB 2086. The directionality, which is the ratio of euclidean distance to accumulated distance, did not show a significant change (Fig. 5D). Thus, the above results signify that PAF is capable of inducing motility and promoting random non-directional movement of MDA-MB 231 cells.

Discussion

Progression of cancer occurs due to a complex combination of uncontrolled growth of transformed cells, evasion of apoptosis and invasion of cancer cells into nearby tissues, finally resulting in metastasis and secondary tumor formation (24). Uncontrolled cell division coupled with evasion of apoptosis and migration (as single cells or clusters) can thus be considered as some of the key features of cancer cells.

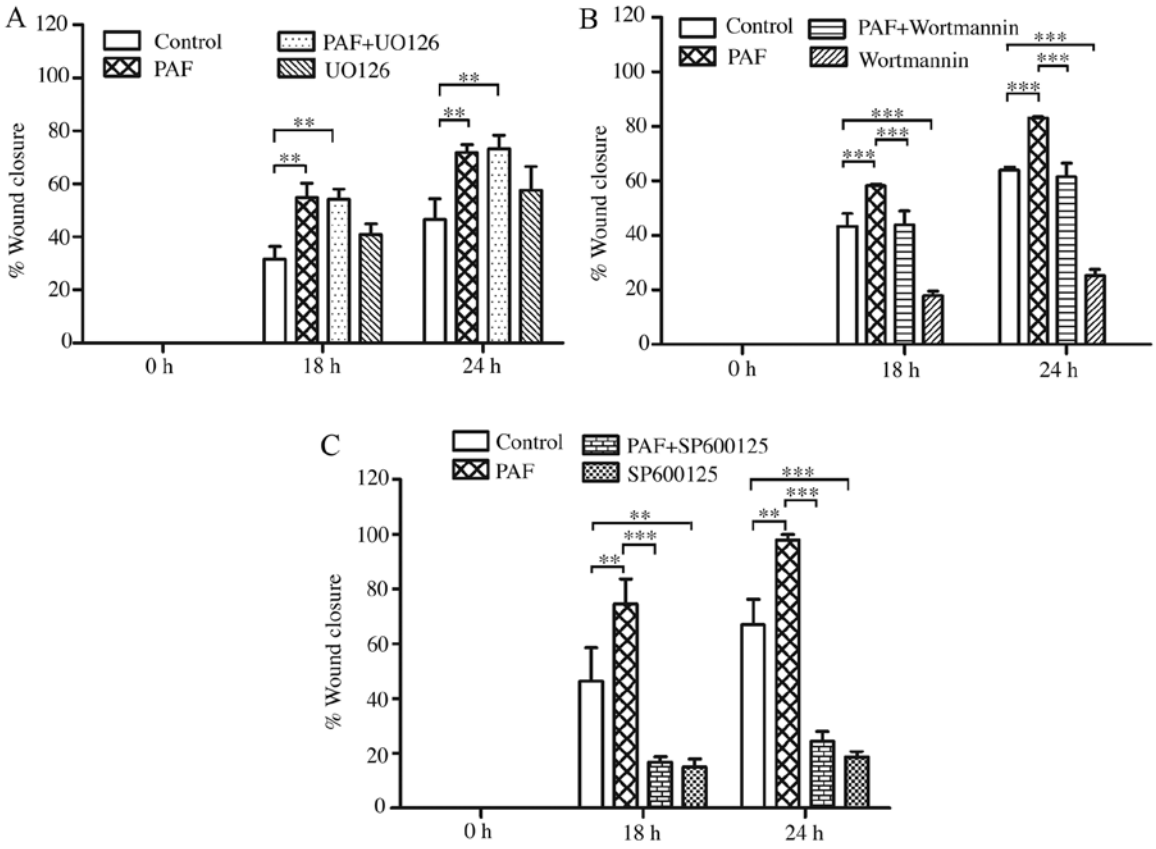

Figure 3. PAF induced migration is mediated via PI3-kinase pathway and/or JNK pathway but not via MAP-kinase pathway. Wound-healing assay of MDA-MB 231 cells with or without treatment of (A) PAF (200 nM) and/or 10 μM UO126 (MEK inhibitor). (B) PAF (200 nM) and/or 200 nM wortmannin (PI3-K inhibitor). (C) PAF (200 nM) and/or 75 μM SP600125 (JNK inhibitor). Wound closure was measured at 0, 18 and 24 h for all treatments. Data represent mean ± SEM (n=3 independent experiments). Wound area was measured using ImageJ software. Statistical significance was analyzed using Student's t-test, $P<0.05$ is considered to be significant; $^{**}P<0.01$, $^{***}P<0.001$.

Migration of cancer cells can be considered at two levels, namely, single cell migration and collective migration. Some of the carcinomas are known to progress through epithelial to mesenchymal transition, wherein the cells lose their cell-cell adhesion and disseminate independently as single cells and finally lodge into a distant organ (35,36). Besides single cell migration, recently, collective cell migration has also been implicated as the predominant mode of cancer cell invasion and metastasis (37). This process has been exhibited by most of the epithelial cancers including breast cancer, colorectal carcinoma, rhabdomyosarcoma, melanoma and oral squamous cell carcinoma (38-40). Histopathological studies of epithelial cancers in tumor regions, suggest the presence of clusters, sheets or chains of secondary cancer cells in the stroma surrounding the primary tumor (41). In addition to this, draining lymphatics were also found to contain clusters of metastasizing tumor cells, implying that small groups of tumor cells are capable of invading vasculatures and lymphatics in individuals with cancer (42). Thus migration, either collective or single cell is a vital phenomenon in the multi-step process of invasion and metastasis.

PAF and PAF-like lipids are present across various cell types and tissues such as neutrophils, macrophages and endothelial cells (43), as well as breast cancer tissues (11). One of the major sources of these lipids is chronic inflammatory microenvironments as well as the cancer cells *per se* (3-5,16). Different types of cells have been found to respond to such chemical stimuli, present in the microenvironment, in several ways such as proliferation, apoptosis, migration, to name a few. To investigate the role of PAF in early transformation, we used 3-dimensional cultures of MCF10A cells, which are non-transformed breast epithelial cells. 3D cultures of cells have been found to recapitulate the *in vivo* scenario largely. This model involves growing of cells on various extracellular matrix, one of the widely used matrix being Matrigel® which is derived from EHS tumors (23). This model aids in the easy identification of a transformed cell from a non-tumorigenic cell (21). The normal breast epithelial cells form growth-arrested multicellular acinar-like structures with a hollow lumen which closely resemble the epithelial cells lining the duct in the mammary tissue *in vivo* (34). In case of cancer cells, this well formed structure is disrupted leading to the formation of spheroids which are devoid of or have irregular lumen, multiple lumens or clusters of cells (44). The morphological features are a clear indication of the tumorigenic status of the cell lines. In our experiment MCF10A cells were under continuous exposure to 200 nM PAF. While investigating the presence of a transformed phenotype, we observed 65% of the acini showing protrusion-like or 'bud like' phenotype. Such phenotypes have been related to collective migratory behavior of transformed cells (44,45). Of the total acini imaged, 58% showed disrupted lumen, which may imply that the cells in

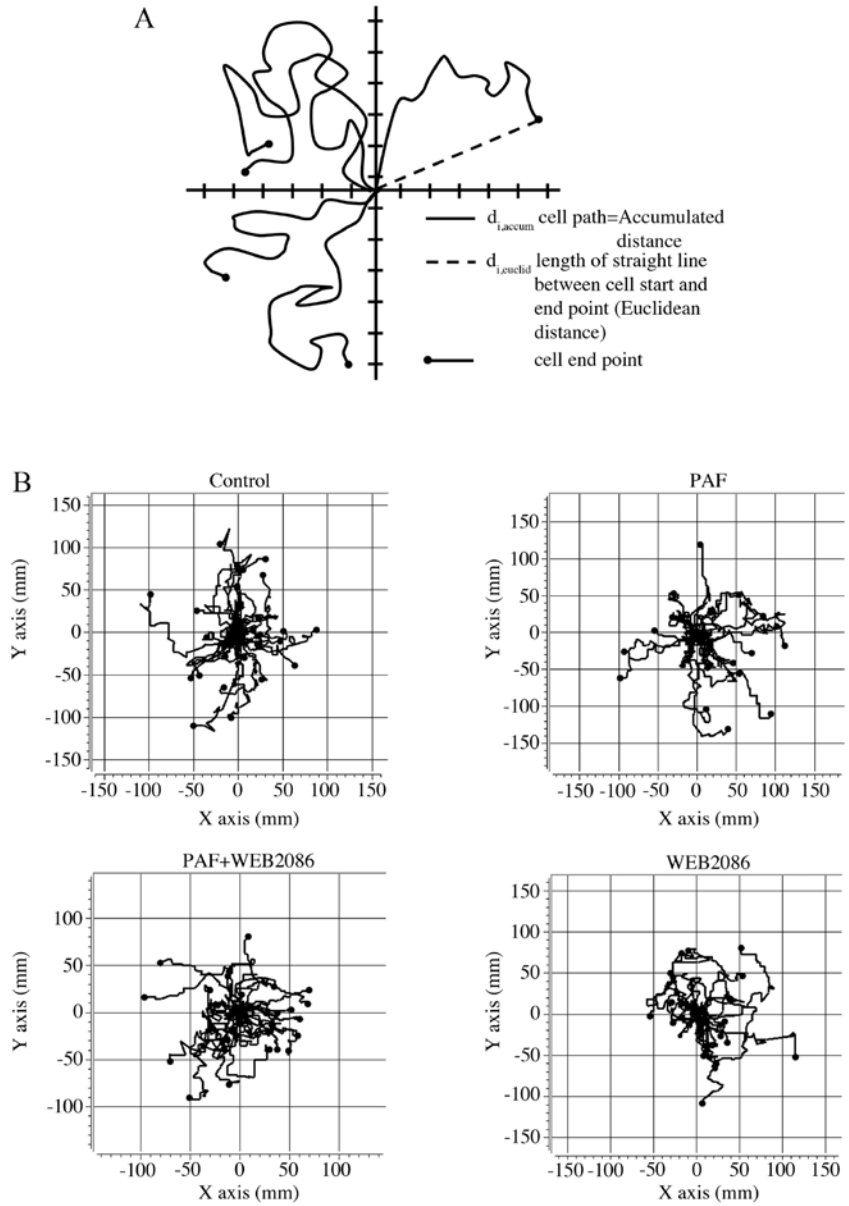

Figure 4. PAF induces chemokinesis at the single cell level in MDA-MB 231 cells. Time-lapse imaging of MDA-MB 231 cells seeded as sparse populations on fibronectin-coated dishes, with or without 200 nM PAF and/or 200 μM WEB 2086 was performed for a period of 4 h with images taken at 2-min intervals. Cells were tracked using ImageJ manual tracking plugin and analyzed using Chemotaxis and Migration tool (Ibidi GmbH, Munich, Germany) to calculate different motility parameters. (A) Diagrammatic representation of a trajectory plot depicting the calculation of the various chemokinetic parameters adapted from Ibidi chemotaxis and migration tool user manual. (B) Trajectory plots of various treatment combinations obtained using chemotaxis and migration tool.

the lumen may restrain apoptosis, which is another hallmark of epithelial cancers (21,44,46). Apart from this, there was a significant increase in the number of cells per transformed acini, which may indicate the induction of proliferation or 'escape from the proliferative arrest', one of the hallmarks of cancer (44,47). This is supported by published reports wherein PAF has been shown to induce proliferation in mouse vascular smooth muscle cells (48) as well as breast adenocarcinoma cells in tissue culture dishes (16). There have been contradictory reports to the same suggesting that the effect of PAF varies according to the type of cells and type of cancer (49). However, our results demonstrate the potential of PAF to induce proliferation in MCF10A cells under continuous exposure to PAF. These results appeal for further intervention with respect to the changes at the molecular level, which have subsequently given rise to such a drastic change in the morphogenesis of the non-tumorigenic cells.

PAF has been demonstrated to induce migration in many cell types such as eosinophils (50), human endothelial cells (43), peripheral blood lymphocytes (51), using *in vivo* as well as *in vitro* models and assays. However, to our knowledge, only one report pertained to the role of PAF in motility of breast cancer cells wherein PAF was demonstrated to induce chemotaxis as well as chemokinesis in the cells (16). Our results are in agreement with the published report by Bussolati *et al* (16), where we show PAF-induced chemokinesis at the single cell level in breast cancer cells. As per the dose and conditions used in our assay, we observed that PAF stimulated cells moved at a significantly increased velocity as well as traversed a larger distance as compared to untreated cells. Displacement was

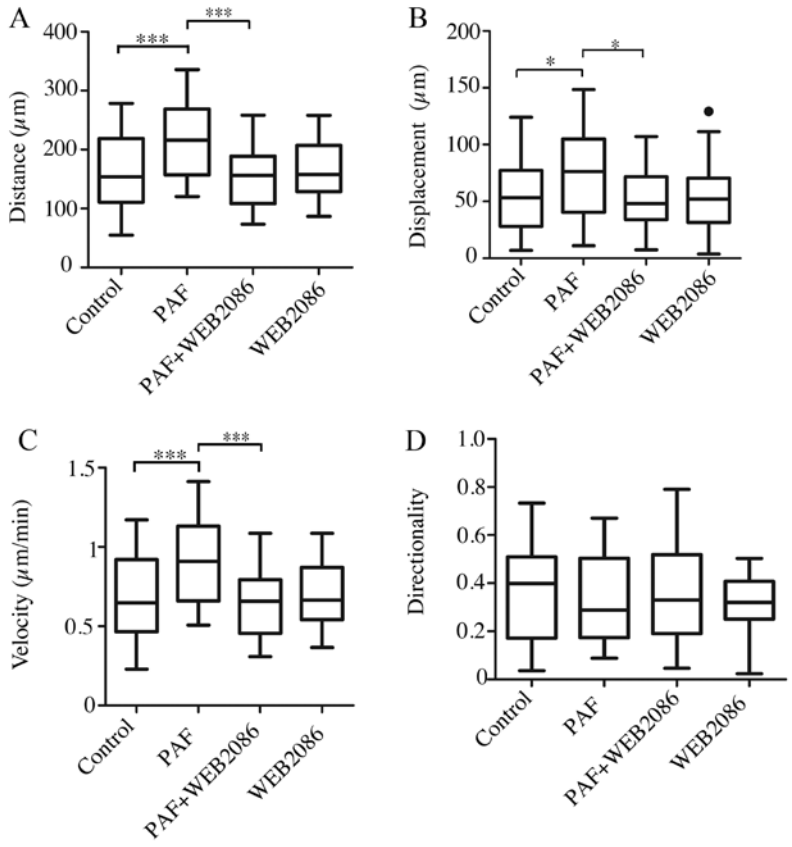

Figure 5. PAF induces chemokinesis without change in directionality at the single cell level in MDA-MB 231 cells. (A) Accumulated distance, (B) displacement, (C) velocity, (D) directionality. Box plots represent distribution of values calculated about the median. (n=3 independent experiments). Mann-Whitney test was used to test the statistical significance of data. $^{*}P<0.05$, $^{**}P<0.01$, $^{***}P<0.001$.

also significantly increased. However, there was no significant difference in the directionality indicating that PAF stimulation enhanced the random movement of the cells without inducing directionality. In order to investigate the role of PAF in collective cell migration, wound-healing assay, a traditional method to study the dynamic process of collective cell migration was performed (25). Wound-healing assay results implicated that PAF is capable of inducing collective cell migration in invasive MDA-MB 231 breast cancer cells. Pretreatment of cells with WEB 2086, a PAF receptor antagonist resulted in a significant decrease in PAF-stimulated motility of cells. Thus further substantiating the crucial role played by PAF in collective cell migration. Collectively these results imply that PAF can enhance cell migration and hence possibly promote metastasis *in vivo*.

To dissect out the motility pathway(s) that are involved in signaling in the highly metastatic MDA-MB 231 cells upon PAF induction, wound-healing assays were performed. PAF is known to act through PAF receptor and stimulate a number of signal transduction pathways and effectors such as PKCs, MAPKs, phospholipase C, paxillin, FAK, EGFR, and Src (4,11,52). However, the downstream effectors of PAF and PAF-R, especially with respect to breast cancer progression and more precisely related to PAF-induced migration are not well elucidated. Metastasis is one of the areas of current interest in the field of cancer and search for better therapies related to it, still continues. Clarification on the downstream effectors of PAF-PAFR pathway involved in motility may, to some extent contribute to the designing of new strategies to treat this heterogeneous condition. To address this, MDA-MB 231 cells were subjected to treatment with inhibitors of well-known motility related pathways (53-55). PAF was found to induce collective cell migration in cells that were independent of the MAPK pathway but dependent on PI3-K as well as JNK pathways. However, inhibition of c-Jun reduced PAF motility almost completely while PI3-K inhibition resulted in partial inhibition of motility. Thus, these results indicate a possible role of PI3-K and/or JNK pathway in PAF-induced motility. However, this demands further investigation to elucidate the exact signal transduction pathway of PAF-induced motility.

In conclusion, role of PAF in cancer progression has been studied in the past (56). However, many questions pertaining to its role in breast cancer are yet to be answered. In this study, we have demonstrated the possible role of PAF in inducing transformation of non-tumorigenic breast epithelial cells grown as spheroids as well as promoting migration of metastatic breast cancer cells. Nonetheless, this study calls for further detailed investigation to unravel some of the interesting questions raised with respect to the involvement of signaling pathways in PAF-induced motility.

Acknowledgements

We thank Professor L.S. Shashidhara for critical reading of the manuscript and providing useful suggestions, Lahiri lab members for helpful comments and discussions, Drs Aurnab

Ghose and Nagaraj Balasubramanian for their suggestions with the single cell migration assay, Vijay Vittal at the IISER, Pune Microscopy facility for his help with microscopy and Dr Kundan Sengupta for sharing with us the Image-Pro Plus software (Media Cybernetics, USA). This study is supported by Indian Institute of Science Education and Research, Pune Core funding (BT/PR8699/MED/30/1018/2013). L.A.V. is funded through DST-INSPIRE fellowship while A.K.A. and N.K. are funded through DST-INSPIRE scholarship.

References

1. Ramos-Nino ME: The role of chronic inflammation in obesity-associated cancers. ISRN Oncol 2013: 697521, 2013.
2. Sounni NE and Noel A: Targeting the tumor microenvironment for cancer therapy. Clin Chem 59: 85-93, 2013.
3. Bussolino F, Arese M, Montrucchio G, Barra L, Primo L, Benelli R, Sanavio F, Aglietta M, Ghigo D and Rola-Pleszczynski MR: Platelet activating factor produced in vitro by Kaposi's sarcoma cells induces and sustains in vivo angiogenesis. J Clin Invest 96: 940-952, 1995.
4. Caiazza F, Harvey BJ and Thomas W: Cytosolic phospholipase A2 activation correlates with HER2 overexpression and mediates estrogen-dependent breast cancer cell growth. Mol Endocrinol 24: 953-968, 2010.
5. Camussi G, Montrucchio G, Lupia E, Arese M and Bussolino F: Platelet-activating factor and angiogenesis. In: Platelet-Activating Factor and Related Lipid Mediators 2. Nigam S, Kunkel G and Prescott S (eds). Vol. 416, Springer US, pp231-234, 1996.
6. Zhu T, Gobeil F, Vazquez-Tello A, Leduc M, Rihakova L, Bossolasco M, Bkaily G, Peri K, Varma DR, Orvoine R, *et al*: Intracrine signaling through lipid mediators and their cognate nuclear G-protein-coupled receptors: A paradigm based on PGE2, PAF, and LPA1 receptors. Can J Physiol Pharmacol 84: 377-391, 2006.
7. Stafforini DM, McIntyre TM, Zimmerman GA and Prescott SM: Platelet-activating factor, a pleiotrophic mediator of physiological and pathological processes. Crit Rev Clin Lab Sci 40: 643-672, 2003.
8. Prescott SM, Zimmerman GA, Stafforini DM and McIntyre TM: Platelet-activating factor and related lipid mediators. Annu Rev Biochem 69: 419-445, 2000.
9. Chao W and Olson MS: Platelet-activating factor: Receptors and signal transduction. Biochem J 292: 617-629, 1993.
10. Ryan SD, Harris CS, Mo F, Lee H, Hou ST, Bazan NG, Haddad PS, ArnasonJT and Bennett SA: Platelet activating factor-induced neuronal apoptosis is initiated independently of its G-protein coupled PAF receptor and is inhibited by the benzoate orsellinic acid. J Neurochem 103: 88-97, 2007.
11. McHowat J, Gullickson G, Hoover RG, Sharma J, Turk J and Kornbluth J: Platelet-activating factor and metastasis: Calcium-independent phospholipase A2β deficiency protects against breast cancer metastasis to the lung. Am J Physiol Cell Physiol 300: C825-C832, 2011.
12. Melnikova V and Bar-Eli M: Inflammation and melanoma growth and metastasis: The role of platelet-activating factor (PAF) and its receptor. Cancer Metastasis Rev 26: 359-371, 2007.
13. Im SY, Ko HM, Kim JW, Lee HK, Ha TY, Lee HB, Oh SJ, Bai S, Chung KC, Lee YB, *et al*: Augmentation of tumor metastasis by platelet-activating factor. Cancer Res 56: 2662-2665, 1996.
14. Melnikova VO, Villares GJ and Bar-Eli M: Emerging roles of PAR-1 and PAFR in melanoma metastasis. Cancer Microenviron 1: 103-111, 2008.
15. Zhang L, Wang D, Jiang W, Edwards D, Qiu W, Barroilhet LM, Rho JH, Jin L, Seethappan V, Vitonis A, *et al*: Activated networking of platelet activating factor receptor and FAK/STAT1 induces malignant potential in BRCA1-mutant at-risk ovarian epithelium. Reprod Biol Endocrinol 8: 74, 2010.
16. Bussolati B, Biancone L, Cassoni P, Russo S, Rola-Pleszczynski M, Montrucchio G and Camussi G: PAF produced by human breast cancer cells promotes migration and proliferation of tumor cells and neo-angiogenesis. Am J Pathol 157: 1713-1725, 2000.
17. Kravchenko VV, Pan Z, Han J, Herbert JM, Ulevitch RJ and Ye RD: Platelet-activating factor induces NF-kappa B activation through a G protein-coupled pathway. J Biol Chem 270: 14928-14934, 1995.
18. Ishii S, Nagase T, Tashiro F, Ikuta K, Sato S, Waga I, Kume K, Miyazaki J and Shimizu T: Bronchial hyperreactivity, increased endotoxin lethality and melanocytic tumorigenesis in transgenic mice overexpressing platelet-activating factor receptor. EMBO J 16: 133-142, 1997.
19. Cellai C, Laurenzana A, Vannucchi AM, Caporale R, Paglierani M, Di Lollo S, Pancrazzi A and Paoletti F: Growth inhibition and differentiation of human breast cancer cells by the PAFR antagonist WEB-2086. Br J Cancer 94: 1637-1642, 2006.
20. Robert EG and Hunt JD: Lipid messengers as targets for antiangiogenic therapy. Curr Pharm Des 7: 1615-1626, 2001.
21. Debnath J, Muthuswamy SK and Brugge JS: Morphogenesis and oncogenesis of MCF-10A mammary epithelial acini grown in three-dimensional basement membrane cultures. Methods 30: 256-268, 2003.
22. Petersen OW, Rønnov-Jessen L, Howlett AR and Bissell MJ: Interaction with basement membrane serves to rapidly distinguish growth and differentiation pattern of normal and malignant human breast epithelial cells. Proc Natl Acad Sci USA 89: 9064-9068, 1992.
23. Bissell MJ and Radisky D: Putting tumours in context. Nat Rev Cancer 1: 46-54, 2001.
24. Deisboeck TS and Couzin ID: Collective behavior in cancer cell populations. Bioessays 31: 190-197, 2009.
25. Riahi R, Yang Y, Zhang DD and Wong PK: Advances in wound-healing assays for probing collective cell migration. J Lab Autom 17: 59-65, 2012.
26. Kuroda Y and Furuyama J: Physiological and biochemical studies of effects of mitomycin C on strain HeLa cells in cell culture. Cancer Res 23: 682-687, 1963.
27. Casals-Stenzel J, Muacevic G and Weber KH: Pharmacological actions of WEB 2086, a new specific antagonist of platelet activating factor. J Pharmacol Exp Ther 241: 974-981, 1987.
28. Cellai C, Laurenzana A, Vannucchi AM, Della Malva N, Bianchi L and Paoletti F: Specific PAF antagonist WEB-2086 induces terminal differentiation of murine and human leukemia cells. FASEB J 16: 733-735, 2002.
29. Du J, Sun C, Hu Z, Yang Y, Zhu Y, Zheng D, Gu L and Lu X: Lysophosphatidic acid induces MDA-MB-231 breast cancer cells migration through activation of PI3K/PAK1/ERK signaling. PLoS One 5: e15940, 2010.
30. Powis G, Bonjouklian R, Berggren MM, Gallegos A, Abraham R, Ashendel C, Zalkow L, Matter WF, Dodge J, Grindey G, *et al*: Wortmannin, a potent and selective inhibitor of phosphatidylinositol-3-kinase. Cancer Res 54: 2419-2423, 1994.
31. Bennett BL, Sasaki DT, Murray BW, O'Leary EC, Sakata ST, Xu W, Leisten JC, Motiwala A, Pierce S, Satoh Y, *et al*: SP600125, an anthrapyrazolone inhibitor of Jun N-terminal kinase. Proc Natl Acad Sci USA 98: 13681-13686, 2001.
32. Bodakuntla S, Libi AV, Sural S, Trivedi P and Lahiri M: N-nitroso-N-ethylurea activates DNA damage surveillance pathways and induces transformation in mammalian cells. BMC Cancer 14: 287, 2014.
33. Lee GY, Kenny PA, Lee EH and Bissell MJ: Three-dimensional culture models of normal and malignant breast epithelial cells. Nat Methods 4: 359-365, 2007.
34. Vidi PA, Bissell MJ and Lelièvre SA: Three-dimensional culture of human breast epithelial cells: The how and the why. Methods Mol Biol 945: 193-219, 2013.
35. Sleeman JP and Thiery JP: SnapShot: The epithelial-mesenchymal transition. Cell 145: 162.e1, 2011.
36. Thiery JP, Acloque H, Huang RY and Nieto MA: Epithelial-mesenchymal transitions in development and disease. Cell 139: 871-890, 2009.
37. Bidard FC, Pierga JY, Vincent-Salomon A and Poupon MF: A 'class action' against the microenvironment: Do cancer cells cooperate in metastasis? Cancer Metastasis Rev 27: 5-10, 2008.
38. Friedl P, Noble PB, Walton PA, Laird DW, Chauvin PJ, Tabah RJ, Black M and Zänker KS: Migration of coordinated cell clusters in mesenchymal and epithelial cancer explants in vitro. Cancer Res 55: 4557-4560, 1995.
39. Hegerfeldt Y, Tusch M, Bröcker EB and Friedl P: Collective cell movement in primary melanoma explants: Plasticity of cell-cell interaction, beta1-integrin function, and migration strategies. Cancer Res 62: 2125-2130, 2002.
40. Nabeshima K, Inoue T, Shimao Y, Kataoka H and Koono M: Cohort migration of carcinoma cells: Differentiated colorectal carcinoma cells move as coherent cell clusters or sheets. Histol Histopathol 14: 1183-1197, 1999.

41. Friedl P and Gilmour D: Collective cell migration in morphogenesis, regeneration and cancer. Nat Rev Mol Cell Biol 10: 445-457, 2009.
42. Rørth P: Collective cell migration. Annu Rev Cell Dev Biol 25: 407-429, 2009.
43. Montrucchio G, Lupia E, Battaglia E, Del Sorbo L, Boccellino M, Biancone L, Emanuelli G and Camussi G: Platelet-activating factor enhances vascular endothelial growth factor-induced endothelial cell motility and neoangiogenesis in a murine matrigel model. Arterioscler Thromb Vasc Biol 20: 80-88, 2000.
44. Debnath J and Brugge JS: Modelling glandular epithelial cancers in three-dimensional cultures. Nat Rev Cancer 5: 675-688, 2005.
45. Friedl P, Hegerfeldt Y and Tusch M: Collective cell migration in morphogenesis and cancer. Int J Dev Biol 48: 441-449, 2004.
46. Debnath J, Mills KR, Collins NL, Reginato MJ, Muthuswamy SK and Brugge JS: The role of apoptosis in creating and maintaining luminal space within normal and oncogene-expressing mammary acini. Cell 111: 29-40, 2002.
47. Hanahan D and Weinberg RA: Hallmarks of cancer: The next generation. Cell 144: 646-674, 2011.
48. Gaumond F, Fortin D, Stankova J and Rola-Pleszczynski M: Differential signaling pathways in platelet-activating factor-induced proliferation and interleukin-6 production by rat vascular smooth muscle cells. J Cardiovasc Pharmacol 30: 169-175, 1997.
49. Wang H and Chakrabarty S: Platelet-activating factor activates mitogen-activated protein kinases, inhibits proliferation, induces differentiation and suppresses the malignant phenotype of human colon carcinoma cells. Oncogene 22: 2186-2191, 2003.
50. Schweizer RC, van Kessel-Welmers BA, Warringa RA, Maikoe T, Raaijmakers JA, Lammers JW and Koenderman L: Mechanisms involved in eosinophil migration. Platelet-activating factor-induced chemotaxis and interleukin-5-induced chemokinesis are mediated by different signals. J Leukoc Biol 59: 347-356, 1996.
51. McFadden RG, Bishop MA, Caveney AN and Fraher LJ: Effect of platelet activating factor (PAF) on the migration of human lymphocytes. Thorax 50: 265-269, 1995.
52. Aponte M, Jiang W, Lakkis M, Li MJ, Edwards D, Albitar L, Vitonis A, Mok SC, Cramer DW and Ye B: Activation of platelet-activating factor receptor and pleiotropic effects on tyrosine phospho-EGFR/Src/FAK/paxillin in ovarian cancer. Cancer Res 68: 5839-5848, 2008.
53. Huang C, Rajfur Z, Borchers C, Schaller MD and Jacobson K: JNK phosphorylates paxillin and regulates cell migration. Nature 424: 219-223, 2003.
54. Lopez-Ilasaca M: Signaling from G-protein-coupled receptors to mitogen-activated protein (MAP)-kinase cascades. Biochem Pharmacol 56: 269-277, 1998.
55. Wymann MP and Pirola L: Structure and function of phosphoinositide 3-kinases. Biochim Biophys Acta 1436: 127-150, 1998.
56. Tsoupras AB, Iatrou C, Frangia C and Demopoulos CA: The implication of platelet activating factor in cancer growth and metastasis: Potent beneficial role of PAF-inhibitors and antioxidants. Infect Disord Drug Targets 9: 390-399, 2009.

REVIEW ARTICLES

Cancer Cell & Microenvironment 2016; 3: e1370. doi: 10.14800/ccm.1370; © 2016 by Libi Anandi, *et al*.
http://www.smartscitech.com/index.php/ccm

RESEARCH HIGHLIGHT

Platelet activating factor leads to initiation and promotion of breast cancer

Libi Anandi, Mayurika Lahiri

Biology Division, Indian Institute of Science Education and Research, Pune, 411008, India

Correspondence: Mayurika Lahiri
E-mail: mayurika.lahiri@iiserpune.ac.in
Received: June 13, 2016
Published online: July 21, 2016

Bioactive molecules present in the tumor milieu are known to contribute substantially to tumor progression. Phospholipid mediators are a group of molecules that have roles in normal physiology as well as in pathological conditions. Platelet activating factor (PAF), a phospholipd mediator, secreted by cells present in tumor microenvironment has been implicated to have a possible role in cancer progression. Here, we highlight our study of the potential role of PAF in inducing transformation of breast epithelial cells grown as three dimensional cultures. We have also attempted to dissect the motility related molecular pathway activated upon PAF stimulation in MDA-MB 231 cells. This study further calls for detailed analysis of pathways downstream of PAF signalling which would aid in identification of targets and designing of treatment strategies.

Keywords: platelet activating factor; collective cell migration; single cell motility; breast cancer; transformation

To cite this article: Libi Anandi, *et al*. Platelet activating factor leads to initiation and promotion of breast cancer. Can Cell Microenviron 2016; 3: e1370. doi: 10.14800/ccm.1370.

Breast cancer is one of the most common cancers and a leading cause of death in women worldwide. It is a multi-factorial disease caused by a complex combination of genetic and environmental factors. Apart from these, tumor microenvironment has recently been identified as a key factor playing a pivotal role in cancer progression [1]. The microenvironment is believed to evolve into an 'activated state' thus resulting in a 'dynamic signaling circuitry' capable of initiating cancer [2]. Immune cells have been found to be one of the major components of this microenvironment. Nevertheless, inflammatory response associated with the tumor has been demonstrated to have tumor promoting capabilities. The inflammatory cells can release various bio-molecules, which may have tumor inducing as well as promoting capabilities. One such group of molecules is the phospholipid mediators, namely LPA (lysophosphatidic acid) PGs (Prostaglandins) and PAF (Platelet activating factor) including PAF - like lipids [3-5]. These molecules are known to be secreted by these cells and have been implicated in various physiological and pathological conditions. PAF has been hypothesized to act as an intracellular mediator or messenger and is known to act through the PAF receptor (PAF-R), which is a G - protein coupled receptor [6]. Furthermore, given that PAF is a phospholipid mediator, most of the associated pathological effects occur due to excessive accumulation of PAF which maybe a result of either impaired degradation and/or enhanced synthesis [4]. Biologically active PAF is synthesized by the cells by hydrolysis of membrane phospholipids catalyzed by phospholipase A2 (PLA2) followed by trans-acetylation by

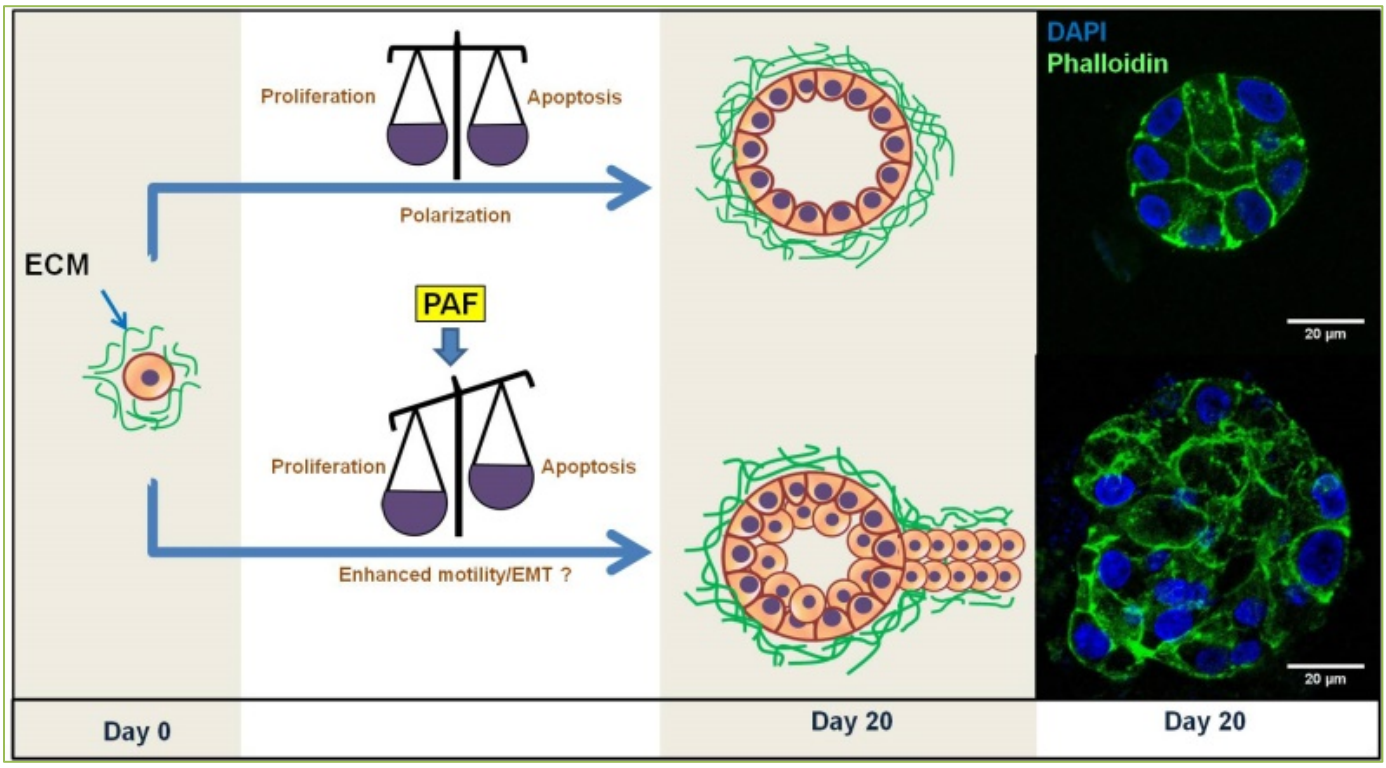

Figure 1. Schematic depicting the abnormal acinar structure formed by breast epithelial cells grown under continuous stimulation with PAF.

lysoPAF-acetyltransferase [7] while degradation is carried out by PAF-acetyl hydrolase (PAF-AH), enzyme which hydrolyses and thus inactivates PAF [8, 9]. The synthesis generally, may occur in response to physiological cues or due to unregulated oxidative reactions stimulated by various cellular or environmental factors [5]. For instance, UV-B irradiations have been demonstrated to induce PAF production by epidermal keratinocytes [10]. Apart from this, macrophages, neutrophils and endothelial cells are known to secrete PAF. Bussolati *et al* have also demonstrated the ability of breast cancer cells to secrete PAF upon growth factor stimulation [11]. This correlates with the observation by Camussi's group that significant amount of PAF is present in breast cancer tissues [12]. Impaired degradation is another reason for PAF accumulation, which may result from the inhibition or absence of PAF-AH. Cigarette smoke is considered as one of the factors which result in the accumulation of PAF by inhibiting PAF-AH [13, 14]. This accumulated PAF enhances adherence of metastatic breast cancer cells to lung endothelium [15].

Apart from the well-established role of PAF in various immunological processes, PAF has been demonstrated to play a role in neo-angiogenesis [16] and the inhibition of this process has been shown to inhibit growth of tumor in Kaposi's sarcoma [17], prostate cancer and breast cancer [18]. Hepatocyte growth factor (HGF), TNF-α (Tumor Necrosis Factor- α) and thrombopoietin-induced angiogenesis is mediated through PAF[19]. In addition to this, PAF has been shown to induce transformation in rat embryonic cells [20] as well as BRCA-1 mutant ovarian cancer cells [21]. Axelrad *et al* reported that PAF induced migration and invasion of HUVECs; these effects could be reversed using a PAF - R antagonist [22]. PAF is capable of inducing invasive phenotypes in melanoma cells stimulated by cytokines [23]. Apart from this in liver metastasis of colorectal cancer PAF has been shown to promote bFGF (basic fibroblast growth factor) and VEGF (Vascular endothelial growth factor) -induced neoangiogenesis [24]. PAF secretion by keratinocytes following UV-B radiation exposure has been reported to be an important mediator of UV-B induced immunosuppression [10]. In addition to this, presence of PAF has been shown to reduce the ability of cells to repair DNA damage induced by UV radiations [25]. The two phenomena have been hypothesized to be responsible for skin cancer induction [26].

PAF receptor shows differential expression across various cell types. Investigation of the PAF-R status revealed that MDA MB-231 and MCF7 cells showed higher expression as compared to MCF10A cells, which showed a very low expression. A recent study from our lab demonstrated that PAF may play a role in cancer initiation as well as promote cancer progression [27]. Three dimensional (3D) cultures of

normal breast epithelial cells as well as cancerous cells have been exploited to study the process of morphogenesis and tumorigenesis [28-30]. We used 3D 'on top' cultures of breast epithelial cells to investigate the cancer initiation potential of PAF. In this culture system, breast epithelial cells when grown on laminin-rich extracellular matrix form growth-arrested polarized spheroids that structurally and functionally closely resemble the 'acini' of the mammary gland [28-30]. Maintenance of such an architecture mainly depends on the balance between proliferation and apoptosis which translate in 3D cultures into either increase in the number of cells per acini or a luminal filling phenotype [28, 29], as depicted in Figure 1. We observed that when MCF10A cells, considered as 'near normal' breast epithelial cells were grown in presence of PAF, resulted in the formation of acinar structures which had a larger volume. Consistent with this finding, we also observed significant increase in the number of cells per acini. Luminal phenotype was also disrupted with a significant number of acini having multiple layers of cells enclosing the luminal space. All these phenotypes demonstrate the ability of PAF to induce proliferation of breast epithelial cells, implying possible attainment of hyperproliferative state, referred to as "escape from proliferative state", one of the "hallmarks of cancer" [31]. PAF has been shown to induce proliferation of differentiated keratinocytes [32], rat vascular smooth muscle cells [33], epidermal cells [34] as well as breast adenocarcinoma cells. In contrast, PAF is known to induce apoptosis in neurons [35] as well as inhibit proliferation of colon carcinoma cells [36]. Another striking feature of the acini grown in presence of PAF was the formation of "protrusion-like" or "bulb-like" structures. Such structures are known to be characteristic features of invasiveness or migratory cells. Cells grown on 3D substrata that have undergone epithelial-mesenchymal transition (EMT) give rise to protrusion-like structures. When a few cells migrate into such protrusions, these structures may appear as "bulb-like" structures [37, 38]. With the known role of PAF in inducing motility of different kinds of cells including breast cancer cells, these abnormal structures imply possible induction of EMT or motility resulting in escape of cells out of the well structured and regulated acini. Taken together these preliminary results imply that presence of PAF in the microenvironment is capable of inducing transformation. However, studies are being performed to further investigate this process and delineate the mechanism thereof.

To study the role of PAF in breast cancer progression, effect of PAF on migration was studied [27]. Metastasis of cancer cells is one of the many aspects which remain unexplored in cancer pathogenesis and effectively curtailing this phenomenon is the need of the hour [39]. Acquiring migratory potential is one of the early processes in metastasis. Cancer cells are known to invade the surrounding tissue and disseminate to the secondary sites. Research has revealed presence of cluster of cells, which move as sheets during metastasis. This is also supported by the observation of clusters of cells infiltrating the secondary tumor sites. On the other hand, cells with invasive and metastatic characteristic can travel as single entities and lodge themselves into the secondary site. Stimulation of cells with PAF induces motility in a variety of cells including peripheral blood lymphocytes [40] human endothelial cells [41] as well as eosinophils [42] and breast cancer cells. However the mechanism(s) for PAF-induced motility of breast cancer cells remains unknown. Thus, an attempt was made to identify the key pathway(s) involved in PAF-induced increased migration of breast cancer cells. Firstly, we investigated the effect of PAF, under the conditions of our study, on both collective cell migration as well as single cell migration of MDA-MB 231 cells. Previous reports have shown growth factor stimulation to induce PAF secretion and PAF stimulation induced chemotaxis as well as chemokinesis in breast cancer cells such as MDA-MB231 [11]. In addition, a recent report showed the ability of cigarette smoke to enhance motility of MDA-MB 231 cells by inducing PAF accumulation via inhibiting PAF-AH. In agreement with these reports we also observed increased collective cell migration of MDA-MB 231 cells upon PAF treatment in the wound healing assay. At the single cell level, PAF enhanced the velocity as well as distance traversed by the cells without change in directionality [27]. Further, to unravel the mechanistic aspect of PAF induced motility we used small molecule inhibitors of probable pathways predicted from available literature. PAF through PAF-R is known to activate various signal transduction pathways in different cell types. In ovarian cancer cells, Bin Ye's group have reported PAF induced MMP9 and MMP2 secretion through activation of EGFR/Src/FAK/paxilin and this activation was mediated through PAF-R [43]. Further, PAF-R activates c-Jun N-terminal kinase in hippocampal cells, regulates cell growth, survival and proliferation of macrophage cell line through GBγ- activatable PI3K kinaseγ and while in various cells activates p38 MAP kinases [44]. Apart from this, G-proteins like Ral, Rap as well as other signaling molecules like PLCγ□□PLD are regulated by PAF-R [45, 46]. In ovarian cancer cells PAF promotes cancer progression through EGFR/ERK transactivation pathway as well as activates PKC pathway, which couples with activated ERK [47]. FAK and Paxillin are activated following PAF induction in human endothelial cells [48] while in non-cancerous cell lines such as neutrophils [49] and eosinophils [50], it activates various protein kinases such as G-protein kinase, PKC as well as tyrosine protein kinase [48]. Since MAPK pathway and PI3K pathway were the most common downstream targets of PAF in various cell types as well as these pathways are well

known motility pathways, we investigated whether PAF induced motility in invasive breast cancer cells through the MAPK pathway. Our data indicated that the ERK pathway did not play a role in PAF induced motility. Inhibition of the PI3K pathway as well as JNK pathway resulted in the inhibition of motility as compared to PAF stimulated cells. However, PI3K pathway inhibition appeared to partially reduce the motility of PAF stimulated cells. This coupled with the observation that significant reduction of motility was seen in control untreated cells treated with wortmannin (a PI3K inhibitor) alludes to the possible role of PI3K in either PAF induced motility or the inherent motility of MDA-MB 231 cells. On the other hand, JNK pathway inhibition resulted in inhibition of PAF stimulated enhanced motility as well as motility of unstimulated cells, confirming its role in PAF increased motility as well as inherent motility. Taken together, these results raise the possibility that PAF induced increased motility may be occurring through PI3K as well as JNK pathways [27]. Ongoing studies are being performed to dissect out the exact mechanistic pathway involved in PAF stimulated motility in cells.

Role of PAF in various cancers have been studied to some extent. The exact role of PAF and the mechanism(s) thereof have not been reported till date. The results discussed above and supported by few reports available in literature suggests the possible role of PAF in breast cancer initiation as well as promotion of breast cancer by enhancing migratory ability of cells. However, this work warrants further investigation to delineate the pathway(s) involved, which would further help in designing novel therapeutic strategies to combat this heterogeneous condition.

Conflicting interests

The authors have declared that no conflict of interest exists.

Author contributions

L.A.V. performed 3D experiments and prepared the figure. L.A.V. and M.L. wrote the manuscript.

Acknowledgements

This study is supported by Indian Institute of Science Education and Research, Pune Core funding and grant from Department of Biotechnology, Government of India (BT/PR8699/MED/30/1018/2013). L.A.V. is funded through DST-INSPIRE fellowship.

Abbreviations

PAF: Platelet activating factor; LPA: lysophosphatidic acid; PGs: Prostaglandins; PAF-R: PAF receptor; PLA2: phospholipase A2; PAF-AH: PAF-acetyl hydrolase; HGF: Hepatocyte growth factor; TNF-α Tumor Necrosis Factor- α; Bfgf: basic fibroblast growth factor; VEGF, Vascular endothelial growth factor; 3D: Three dimensional; EMT, epithelial-mesenchymal transition; MAPK: Mitogen-activated protein kinase; EGFR: Epidermal growth factor receptor; ERK, extracellular signal–regulated kinases; PI3K: phosphatidylinositide 3-kinases; JNK: c-Jun N-terminal kinases; HUVEC: Human Umbilical Vein Endothelial Cells; FAK: Focal adhesion kinase; PLCγ: Phospholipase C; PLD: Phospholipase D; PKC: Protein kinase C.

References

1. Lorusso G, Ruegg C. The tumor microenvironment and its contribution to tumor evolution toward metastasis. Histochem Cell Biol 2008; 130:1091-1103.
2. Pietras K, Ostman A. Hallmarks of cancer: interactions with the tumor stroma. Exp Cell Res 2010; 316:1324-1331.
3. Zhu T, Gobeil F, Vazquez-Tello A, Leduc M, Rihakova L, Bossolasco M, Bkaily G, Peri K, Varma DR, Orvoine R *et al*. Intracrine signaling through lipid mediators and their cognate nuclear G-protein-coupled receptors: a paradigm based on PGE2, PAF, and LPA1 receptors. Can J Physiol Pharmacol 2006; 84:377-391.
4. Prescott SM, Zimmerman GA, Stafforini DM, McIntyre TM. Platelet-activating factor and related lipid mediators. Annu Rev Biochem 2000; 69:419-445.
5. Stafforini DM, McIntyre TM, Zimmerman GA, Prescott SM. Platelet-activating factor, a pleiotrophic mediator of physiological and pathological processes. Crit Rev Clin Lab Sci 2003; 40:643-672.
6. Kravchenko VV, Pan Z, Han J, Herbert JM, Ulevitch RJ, Ye RD. Platelet-activating factor induces NF-kappa B activation through a G protein-coupled pathway. J Biol Chem 1995; 270:14928-14934.
7. McHowat J, Kell PJ, O'Neill HB, Creer MH. Endothelial cell PAF synthesis following thrombin stimulation utilizes Ca(2+)-independent phospholipase A(2). Biochemistry 2001; 40:14921-14931.
8. Wardlow ML, Cox CP, Meng KE, Greene DE, Farr RS. Substrate specificity and partial characterization of the PAF-acylhydrolase in human serum that rapidly inactivates platelet-activating factor. J Immunol 1986; 136(9):3441-3446.
9. Stafforini DM, Prescott SM, Zimmerman GA, McIntyre TM. Platelet-activating factor acetylhydrolase activity in human tissues and blood cells. Lipids 1991; 26:979-985.
10. Walterscheid JP, Ullrich SE, Nghiem DX. Platelet-activating factor, a molecular sensor for cellular damage, activates systemic immune suppression. J Exp Med 2002; 195:171-179.
11. Bussolati B, Biancone L, Cassoni P, Russo S, Rola-Pleszczynski M, Montrucchio G, Camussi G. PAF produced by human breast cancer cells promotes migration and proliferation of tumor cells and neo-angiogenesis. Am J Pathol 2000; 157:1713-1725.

12. Montrucchio G, Sapino A, Bussolati B, Ghisolfi G, Rizea-Savu S, Silvestro L, Lupia E, Camussi G. Potential angiogenic role of platelet-activating factor in human breast cancer. Am J Pathol 1998; 153:1589-1596.
13. Sharma J, Turk J, Mancuso DJ, Sims HF, Gross RW, McHowat J. Activation of group VI phospholipase A2 isoforms in cardiac endothelial cells. Am J Physiol Cell Physiol 2011; 300:C872-879.
14. Kispert S, Marentette J, McHowat J. Cigarette smoke induces cell motility via platelet-activating factor accumulation in breast cancer cells: a potential mechanism for metastatic disease. Physiol Rep 2015; 3.
15. Kispert SE, Marentette JO, McHowat J. Enhanced breast cancer cell adherence to the lung endothelium via PAF acetylhydrolase inhibition: a potential mechanism for enhanced metastasis in smokers. Am J Physiol Cell Physiol 2014; 307:C951-956.
16. Camussi G, Montrucchio G, Lupia E, Arese M, Bussolino F: Platelet-Activating Factor and Angiogenesis. In: Platelet-Activating Factor and Related Lipid Mediators 2. Volume 416, edn. Edited by Nigam S, Kunkel G, Prescott S: Springer US; 1996; 231-234.
17. Bussolino F, Arese M, Montrucchio G, Barra L, Primo L, Benelli R, Sanavio F, Aglietta M, Ghigo D, Rola-Pleszczynski MR *et al*. Platelet activating factor produced in vitro by Kaposi's sarcoma cells induces and sustains in vivo angiogenesis. J Clin Invest 1995; 96:940-952.
18. Melnikova V, Bar-Eli M. Inflammation and melanoma growth and metastasis: the role of platelet-activating factor (PAF) and its receptor. Cancer Metastasis Rev 2007; 26:359-371.
19. Melnikova VO, Villares GJ, Bar-Eli M. Emerging roles of PAR-1 and PAFR in melanoma metastasis. Cancer Microenviron 2008; 1:103-111.
20. Bennett SA, Leite LC, Birnboim HC. Platelet activating factor, an endogenous mediator of inflammation, induces phenotypic transformation of rat embryo cells. Carcinogenesis 1993; 14:1289-1296.
21. Zhang L, Wang D, Jiang W, Edwards D, Qiu W, Barroilhet LM, Rho JH, Jin L, Seethappan V, Vitonis A *et al*. Activated networking of platelet activating factor receptor and FAK/STAT1 induces malignant potential in BRCA1-mutant at-risk ovarian epithelium. Reprod Biol Endocrinol 2010; 8:74.
22. Axelrad TW, Deo DD, Ottino P, Van Kirk J, Bazan NG, Bazan HE, Hunt JD. Platelet-activating factor (PAF) induces activation of matrix metalloproteinase 2 activity and vascular endothelial cell invasion and migration. FASEB J 2004; 18:568-570.
23. Fallani A, Calorini L, Mannini A, Gabellieri S, Mugnai G, Ruggieri S. Platelet-activating factor (PAF) is the effector of IFN gamma-stimulated invasiveness and motility in a B16 melanoma line. Prostaglandins Other Lipid Mediat 2006; 81:171-177.
24. Denizot Y, Descottes B, Truffinet V, Valleix D, Labrousse F, Mathonnet M. Platelet-activating factor and liver metastasis of colorectal cancer. Int J Cancer 2005; 113:503-505.
25. Sreevidya CS, Fukunaga A, Khaskhely NM, Masaki T, Ono R, Nishigori C, Ullrich SE. Agents that reverse UV-Induced immune suppression and photocarcinogenesis affect DNA repair. J Invest Dermatol 2010; 130:1428-1437.
26. Damiani E, Puebla-Osorio N, Gorbea E, Ullrich SE. Platelet-Activating Factor Induces Epigenetic Modifications in Human Mast Cells. J Invest Dermatol 2015; 135:3034-3040.
27. Anandi, Ashiq, Nitheesh, Lahiri. Platelet-activating factor promotes motility in breast cancer cells and disrupts non-transformed breast acinar structures. Oncology Reports 2016; 35:179-188.
28. Debnath J, Brugge JS. Modelling glandular epithelial cancers in three-dimensional cultures. Nat Rev Cancer 2005; 5:675-688.
29. Debnath J, Muthuswamy SK, Brugge JS. Morphogenesis and oncogenesis of MCF-10A mammary epithelial acini grown in three-dimensional basement membrane cultures. Methods 2003; 30:256-268.
30. Vidi PA, Bissell MJ, Lelievre SA. Three-dimensional culture of human breast epithelial cells: the how and the why. Methods Mol Biol 2013; 945:193-219.
31. Hanahan D, Weinberg RA. Hallmarks of cancer: the next generation. Cell 2011; 144:646-674.
32. Feuerherm AJ, Jorgensen KM, Sommerfelt RM, Eidem LE, Laegreid A, Johansen B. Platelet-activating factor induces proliferation in differentiated keratinocytes. Mol Cell Biochem 2013; 384:83-94.
33. Gaumond F, Fortin D, Stankova J, Rola-Pleszczynski M. Differential signaling pathways in platelet-activating factor-induced proliferation and interleukin-6 production by rat vascular smooth muscle cells. J Cardiovasc Pharmacol 1997; 30:169-175.
34. Marques SA, Dy LC, Southall MD, Yi Q, Smietana E, Kapur R, Marques M, Travers JB, Spandau DF. The platelet-activating factor receptor activates the extracellular signal-regulated kinase mitogen-activated protein kinase and induces proliferation of epidermal cells through an epidermal growth factor-receptor-dependent pathway. J Pharmacol Exp Ther 2002; 300:1026-1035.
35. Ryan SD, Harris CS, Mo F, Lee H, Hou ST, Bazan NG, Haddad PS, Arnason JT, Bennett SA. Platelet activating factor-induced neuronal apoptosis is initiated independently of its G-protein coupled PAF receptor and is inhibited by the benzoate orsellinic acid. J Neurochem 2007; 103:88-97.
36. Wang H, Chakrabarty S. Platelet-activating factor activates mitogen-activated protein kinases, inhibits proliferation, induces differentiation and suppresses the malignant phenotype of human colon carcinoma cells. Oncogene 2003; 22:2186-2191.
37. Oyanagi J, Ogawa T, Sato H, Higashi S, Miyazaki K. Epithelial-mesenchymal transition stimulates human cancer cells to extend microtubule-based invasive protrusions and suppresses cell growth in collagen gel. PLoS One 2012; 7:e53209.
38. Godinho SA, Picone R, Burute M, Dagher R, Su Y, Leung CT, Polyak K, Brugge JS, Thery M, Pellman D. Oncogene-like induction of cellular invasion from centrosome amplification. Nature 2014; 510:167-171.
39. Chambers AF, Groom AC, MacDonald IC. Dissemination and growth of cancer cells in metastatic sites. Nat Rev Cancer 2002; 2:563-572.
40. McFadden RG, Bishop MA, Caveney AN, Fraher LJ. Effect of platelet activating factor (PAF) on the migration of human lymphocytes. Thorax 1995; 50:265-269.
41. Montrucchio G, Lupia E, Battaglia E, Del Sorbo L, Boccellino M, Biancone L, Emanuelli G, Camussi G. Platelet-activating factor

enhances vascular endothelial growth factor-induced endothelial cell motility and neoangiogenesis in a murine matrigel model. Arterioscler Thromb Vasc Biol 2000; 20:80-88.

42. Schweizer RC, van Kessel-Welmers BA, Warringa RA, Maikoe T, Raaijmakers JA, Lammers JW, Koenderman L. Mechanisms involved in eosinophil migration. Platelet-activating factor-induced chemotaxis and interleukin-5-induced chemokinesis are mediated by different signals. J Leukoc Biol 1996; 59:347-356.
43. Aponte M, Jiang W, Lakkis M, Li MJ, Edwards D, Albitar L, Vitonis A, Mok SC, Cramer DW, Ye B. Activation of platelet-activating factor receptor and pleiotropic effects on tyrosine phospho-EGFR/Src/FAK/paxillin in ovarian cancer. Cancer Res 2008; 68:5839-5848.
44. Honda Z-i, Ishii S, Shimizu T. Platelet-Activating Factor Receptor. Journal of Biochemistry 2002; 131:773-779.
45. Liu B, Nakashima S, Takano T, Shimizu T, Nozawa Y. Implication of protein kinase C alpha in PAF-stimulated phospholipase D activation in Chinese hamster ovary (CHO) cells expressing PAF receptor. Biochem Biophys Res Commun 1995; 214:418-423.
46. M'Rabet L, Coffer P, Zwartkruis F, Franke B, Segal AW, Koenderman L, Bos JL. Activation of the small GTPase rap1 in human neutrophils. Blood 1998; 92:2133-2140.
47. Yu Y, Zhang M, Zhang X, Cai Q, Zhu Z, Jiang W, Xu C. Transactivation of epidermal growth factor receptor through platelet-activating factor/receptor in ovarian cancer cells. J Exp Clin Cancer Res 2014; 33:85.
48. Soldi R, Sanavio F, Aglietta M, Primo L, Defilippi P, Marchisio PC, Bussolino F. Platelet-activating factor (PAF) induces the early tyrosine phosphorylation of focal adhesion kinase (p125FAK) in human endothelial cells. Oncogene 1996; 13:515-525.
49. Mollapour E, Linch DC, Roberts PJ. Activation and priming of neutrophil nicotinamide adenine dinucleotide phosphate oxidase and phospholipase A(2) are dissociated by inhibitors of the kinases p42(ERK2) and p38(SAPK) and by methyl arachidonyl fluorophosphonate, the dual inhibitor of cytosolic and calcium-independent phospholipase A(2). Blood 2001; 97:2469-2477.
50. Sotsios Y, Ward SG. Phosphoinositide 3-kinase: a key biochemical signal for cell migration in response to chemokines. Immunol Rev 2000; 177:217-235.

Investigating two Hallmarks of Cancer – Genome Instability and Tumor Promoting Inflammation

Libi Anandi, Vaishali Chakravarty and Mayurika Lahiri*

Indian Institute of Science Education and Research, Dr Homi Bhabha Road, Pashan, Pune 411008

*email: mayurika.lahiri@iiserpune.ac.in

According to the GLOBACON report of 2012, India has the highest incidence as well as highest mortality in breast cancer among women [1, 2]. A closer look at the statistics reveals that one in every two women diagnosed with breast cancer die of the disease. Furthermore, it also reveals that there has been a shift in the age of occurrence of breast cancer among Indian women with the average age at diagnosis being between 45-50 years, in contrast to above 60 years in the western countries. In addition to this, these cancers, especially in the young population are more aggressive as compared to the Caucasian population [3, 4]. Interestingly, it has been observed that only 15% cases of breast cancer are due to inherited mutations whereas the remaining 85% cases are sporadic in nature [4]. This fact draws our attention to the large proportion of sporadic cases and the various factors which can play a vital role in initiation of breast cancer as well its progression.

Hanahan and Weinberg in 2011 proposed certain capabilities acquired by the cell during tumor development termed as “Hallmarks of Cancer” as depicted in figure 1. According to them, ‘genomic instability’ and ‘tumor promoting inflammation’ are two characteristics, which aid in acquiring the hallmark capabilities. Various environmental factors such as radiations, environmental pollutants, cigarette smoke as well as chemotherapy itself, are potential agents which can induce genomic instability and hence act as “enabling factors” to acquire cancerous phenotype. On the other hand inflammation is capable of accumulating cells of the immune system in the microenvironment thereby resulting in secretion of certain biomolecules like reactive oxygen species (ROS), cytokines and phospholipid mediators. These are potential signaling molecules and thus convert the microenvironment into an “active state” and probably contribute to initiation or progression of the multistep process of tumorigenesis. (summarized in figure 1).

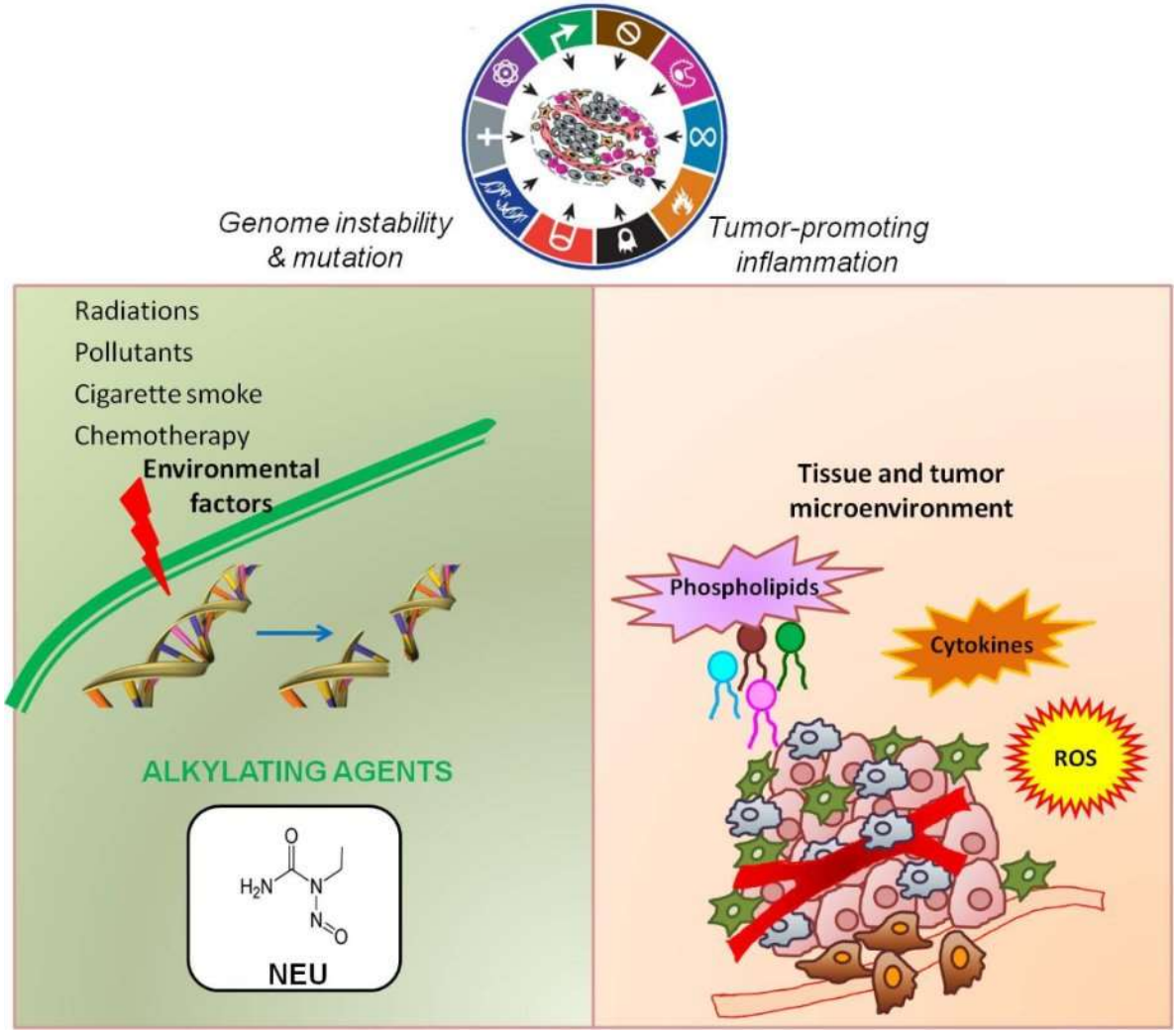

Figure 1: Schematic depicting the "enabling characteristics" that cell acquires to become cancerous.

Alkylating agents, one of the major components of cigarette smoke and cancer chemotherapy, are well known DNA damaging agents as well as known or suspected carcinogens. It is well known that, exposure to such genotoxic agents results in DNA breaks which in turn activates ATM and ATR kinases, key proteins in the DNA Damage Response (DDR) pathway which further phosphorylates their downstream targets, Chk2 and Chk1, respectively [5]. In our recent study, using N-nitroso-N-ethylurea (NEU), a simple monofunctional S_N1 type-DNA ethylating agent, we investigated the activation of DDR kinases following DNA damage induced by NEU in human cancer cell lines [6]. In our study, NEU damage led to phosphorylation of Chk1 and Chk2 in a dose-dependent as well as temporal manner. In contrast to earlier reports where

alkylation damage was detectable only after 1-2 cell divisions [7], our study revealed the activation of Chk2 and Chk1 in 10 and 20 minutes, respectively. Contrary to other reports where □H2AX activation was observed after 24hrs of DNA damage [8], in our study, □H2AX foci were detectable within 2 hrs of NEU damage, which further supported the activation of Chk2 kinase within 10 minutes. Given that alkylating agents cannot directly induce double strand breaks, our results called for further investigations to understand how NEU-induced alkylation damage was being processed to form DSBs within 10 minutes.

Reports suggested that post ionizing radiation (IR) treatment, phosphorylation of Chk2 precedes Chk1 activation and as phosphorylation of Chk2 decreases, Chk1 activation gradually increases indicating the presence of crosstalk between ATM and ATR pathways [9]. Since both the checkpoint kinase activations were observed in our study, it was intriguing to check the presence of a crosstalk between the two canonical pathways. We observed absence of any possible crosstalk between the two pathways following damage by NEU. Furthermore, alkylating agents have been shown to alkylate "N" and "O" positions of DNA leading to the formation of 12 different DNA adducts which in turn may result in A:T to T:A transversions or G:C to A:T transition mutations [10, 11]. The DNA adducts formed by these agents are generally recognised by the mismatch repair (MMR) proteins, namely Msh2-Msh6 and Mlh1-Pms2 heterodimers during the first round of replication. Further, it has been observed that p53, Chk1, Chk2 as well as Cdc25A are activated in a MMR dependent manner [7, 12], thus implying that MMR proteins played an important role in the DDR pathway. To investigate the role of MMR proteins in NEU induced DNA damage, a MMR deficient cell line was exposed to NEU damage. Surprisingly, activation of Chk1 as well as Chk2 was observed, thus clearly indicating at the dose and time of damage, mismatch repair proteins did not play any significant role in NEU induced DNA damage.

Apart from the DNA damaging effects, alkylating agents have been demonstrated to cause mammary tumors in rodent models [13, 14]. Rat mammary epithelial cells, following 30 days post NEU exposure (at different doses) underwent point mutations which as an accumulative effect provided the cells the ability to form multilayered colonies. They also acquired the ability to form colonies on soft agar and could produce noticeable sized tumors when grafted into

female athymic nude mice [15]. These results pointed towards neoplastic transformation due to alkylation damage. Following exposure to NEU, we investigated the ability of NEU to induce transformation using three-dimensional (3D) cultures of non-transformed MCF0A epithelial cells. 3D cultures aid in distinguishing transformed cells from the non-transformed cells by changes in morphology of the acinar structures formed when these cells are grown on extracellular matrix. Such acini resemble the *in vivo* breast acini structurally and functionally. In our study we have shown the characteristic features of epithelial-mesenchymal (EMT) where loss of polarity, establishment of mesenchymal characteristics and down-regulation of epithelial like characters were observed in MCF10A cells treated with NEU at the single cell stage. □-6 integrin, which marks the basal region, showed mislocalization. E-cadherin and □-catenin, both cell-cell junction markers [16], showed aberrant staining patterns, with E-cadherin showing a loss phenotype while □-catenin showed cytoplasmic localization. Vimentin, which is a characteristic mesenchymal marker showed strong expression in the NEU-treated acini. These phenotypes were distinct at all doses of NEU, that is, at 2, 3 and 5 mM NEU and also confirmed that a EMT-like phenotype was acquired by breast epithelial cells upon NEU treatment. These results gave strong implications of transformation occurring in breast epithelial cells on exposure of an alkylating agent, NEU.

Apart from the various environmental factors which influence the induction and progression of cancers, bioactive molecules present in the tissue microenvironment as well as tumor milieu can contribute to the occurrence and progression of the disease. Phospholipid mediators such as lysophosphatadic acid, prostaglandins, platelet activating factor and platelet activating factor-like molecules are secreted by cells of the immune system and are present in the microenvironment. Under chronic inflammatory conditions the proportion of these molecules increases in the adjoining tissues. Given the contribution of chronic inflammation in various cancers, the possibility of these molecules behaving as potential factors for cancer initiation and progression has increased multifold. Level of LPA has been shown to be high in various cell lines as well as in ovarian cancer patients and has been demonstrated to play a vital role in tumor angiogenesis, migration, proliferation, invasion and metastasis [17-19]. Similarly, platelet activating factor (PAF), acting through PAF-R (Platelet activating factor receptor, a G protein-coupled receptor) has been demonstrated to play important roles in various cancers. Apart from the well-known

roles of PAF in inflammation, platelet aggregation various groups have demonstrated the contributing role of PAF in cancer progression. PAF has been shown to play a role in neo-angiogenesis mediated by bFGF (basic fibroblast growth factor) and VEGF (vascular endothelial growth factor) as well as angiogenesis mediated by thrombopoietin, TNF-α (Tumor Necrosis Factor- α), CD-40 and hepatocyte growth factor (HGF). In addition to this, PAF induces motility of HUVECs, endothelial cells [20], peripheral blood lymphocytes[21] eosinophils, [22] as well as breast cancer cells. Our recent study, demonstrated the ability of PAF to enhance migration in MDA-MB 231 cells (invasive breast cancer cells) corroborates with these published reports. Crucial role played by MAPK pathway (JNK, ERK and p38) in regulating cell movement is well known. ERK is known to phosphorylate myosin light chain kinase, FAK or calpain to regulate cell migration [23]. Apart from this, ERK has been shown to be involved in the migration of breast cancer cells exhibiting lung metastasis [24]. In contrast to published reports, we observed that PAF-induced enhanced motility was independent of ERK activation. However inhibition of JNK pathway reduced motility of PAF-stimulated and un-stimulated cells suggesting that JNK pathway was involved in both PAF-induced as well as in the inherent motility of breast cancer cells. PI3K pathway, another pathway well known to play a vital role in cell motility, was investigated to understand its role in motility of PAF-stimulated cells. Surprisingly, we observed that inhibition of this pathway though reduced inherent motility of cells, it could only partially rescue increased motility, thus implying the role of PI3K pathway in inherent motility of cells and a possible role in PAF-induced motility. Further studies are being performed to decipher the pathway through which PAF elicits motility in breast cancer cells. Literature suggests various pathways activated upon exposure to PAF suggesting that in different cell types, PAF may stimulate different signal transduction pathways to elicit various responses. In HUVECs, PAF exposure was found to induce transformation while in neurons, it induced apoptosis [25, 26]. Role of PAF in various cancers has been well studied; however the precise role in breast cancer initiation remains to be elucidated. PAF has been found to be present in breast tissue of patients suffering from breast cancer and has also been shown to correlate with lymph node metastasis [27, 28]. Accumulation of PAF could occur either due to enhanced production and secretion or due to abnormal degradation. In support to this, Kispert *et al* reported the inhibitory effect of cigarette smoke on platelet PAF-acetyl hydrolase (PAF-AH, enzyme inactivating PAF), thus resulting in accumulation of PAF, which enhanced motility of breast cancer cells as well as

increased adherence to lung endothelium [29]. However, the possibility of PAF inducing transformation in breast epithelial cells has not yet been explored. We observed that in non-transformed breast epithelial cells, PAF induced formation of abnormal acinar structures when cells were grown as 3D cultures under constant stimulation of PAF. Apart from the increase in the number of cells in the acini, indicative of proliferation or evasion of apoptosis, the acinar structures also showed presence of protrusion-like structures indicative of EMT-like phenotype. Taken together, we demonstrated the ability of PAF to induce transformation of non-transformed breast epithelial cells. These results appeal for further investigations to delineate the pathway and identify novel targets to design novel therapeutics.

References

1. Ferlay J SI, Ervik M, Dikshit R, Eser S, Mathers C, Rebelo M, Parkin DM, Forman D, Bray, F.: GLOBOCAN 2012 v1.0, Cancer Incidence and Mortality Worldwide: IARC CancerBase No. 11. In.; 2012.
2. International Agency for Research on Cancer [http://globocan.iarc.fr]
3. Three year report of the population based cancer registries 2009-2011: Report of 25 PBCRs. In: *National Cancer Registry Programme.* India: Indian Council Medical Research.
4. Leong SP, Shen ZZ, Liu TJ, Agarwal G, Tajima T, Paik NS, Sandelin K, Derossis A, Cody H, Foulkes WD: Is breast cancer the same disease in Asian and Western countries? *World journal of surgery* 2010, 34(10):2308-2324.
5. Abraham RT: PI 3-kinase related kinases: 'big' players in stress-induced signaling pathways. *DNA repair* 2004, 3(8-9):883-887.
6. Bodakuntla S, Libi AV, Sural S, Trivedi P, Lahiri M: N-nitroso-N-ethylurea activates DNA damage surveillance pathways and induces transformation in mammalian cells. *BMC cancer* 2014, 14:287.
7. Stojic L, Cejka P, Jiricny J: High doses of SN1 type methylating agents activate DNA damage signaling cascades that are largely independent of mismatch repair. *Cell Cycle* 2005, 4(3):473-477.
8. Bakkenist CJ, Kastan MB: DNA damage activates ATM through intermolecular autophosphorylation and dimer dissociation. *Nature* 2003, 421(6922):499-506.
9. Shiotani B, Zou L: Single-stranded DNA orchestrates an ATM-to-ATR switch at DNA breaks. *Molecular cell* 2009, 33(5):547-558.
10. Engelbergs J, Thomale J, Rajewsky MF: Role of DNA repair in carcinogen-induced ras mutation. *Mutation Research* 2000, 450(1-2):139-153.
11. Barbaric I WS, Russ A, Dear TN: Spectrum of ENU-induced mutations in phenotype-driven and gene-driven screens in the mouse. *Environ Mol Mutagen* 2007, 48(2):124-142.
12. Wang Y, Qin J: MSH2 and ATR form a signaling module and regulate two branches of the damage response to DNA methylation. *Proceedings of the National Academy of Sciences of the United States of America* 2003, 100(26):15387-15392.
13. Stoica G, Koestner A, Capen CC: Characterization of N-ethyl-N-nitrosourea-induced mammary tumors in the rat. *Am J Pathol* 1983, 110(0002-9440 (Print)):161-169.

14. Givelber HM, DiPaolo JA: Teratogenic effects of N-ethyl-N-nitrosourea in the Syrian hamster. *Cancer Research* 1969, 29(0008-5472 (Print)):1151-1155.
15. Stoica G, Jacobs R, Koestner A, O'Leary M, Welsch C: ENU-induced in vitro neoplastic transformation of rat mammary epithelial cells. *Anticancer research* 1991, 11(5):1783-1792.
16. Kim K, Daniels KJ, Hay ED: Tissue-specific expression of beta-catenin in normal mesenchyme and uveal melanomas and its effect on invasiveness. *Experimental cell research* 1998, 245(1):79-90.
17. Shida D, Kitayama J, Yamaguchi H, Okaji Y, Tsuno NH, Watanabe T, Takuwa Y, Nagawa H: Lysophosphatidic acid (LPA) enhances the metastatic potential of human colon carcinoma DLD1 cells through LPA1. *Cancer research* 2003, 63(7):1706-1711.
18. Yu X, Zhang Y, Chen H: [Lysophosphatidic acid (LPA) stimulates invasion and metastatic colonization of ovarian cancer cells through Rac activation]. *Zhonghua zhong liu za zhi [Chinese journal of oncology]* 2015, 37(2):95-100.
19. Goldsmith ZG, Ha JH, Jayaraman M, Dhanasekaran DN: Lysophosphatidic Acid Stimulates the Proliferation of Ovarian Cancer Cells via the gep Proto-Oncogene Galpha(12). *Genes & cancer* 2011, 2(5):563-575.
20. Montrucchio G, Lupia E, Battaglia E, Del Sorbo L, Boccellino M, Biancone L, Emanuelli G, Camussi G: Platelet-activating factor enhances vascular endothelial growth factor-induced endothelial cell motility and neoangiogenesis in a murine matrigel model. *Arteriosclerosis, thrombosis, and vascular biology* 2000, 20(1):80-88.
21. McFadden RG, Bishop MA, Caveney AN, Fraher LJ: Effect of platelet activating factor (PAF) on the migration of human lymphocytes. *Thorax* 1995, 50(3):265-269.
22. Schweizer RC, van Kessel-Welmers BA, Warringa RA, Maikoe T, Raaijmakers JA, Lammers JW, Koenderman L: Mechanisms involved in eosinophil migration. Platelet-activating factor-induced chemotaxis and interleukin-5-induced chemokinesis are mediated by different signals. *J Leukoc Biol* 1996, 59(3):347-356.
23. Huang C, Jacobson K, Schaller MD: MAP kinases and cell migration. *Journal of cell science* 2004, 117(Pt 20):4619-4628.
24. Choi C, Helfman DM: The Ras-ERK pathway modulates cytoskeleton organization, cell motility and lung metastasis signature genes in MDA-MB-231 LM2. *Oncogene* 2014, 33(28):3668-3676.
25. Ryan SD, Harris CS, Mo F, Lee H, Hou ST, Bazan NG, Haddad PS, Arnason JT, Bennett SA: Platelet activating factor-induced neuronal apoptosis is initiated independently of its G-protein coupled PAF receptor and is inhibited by the benzoate orsellinic acid. *Journal of neurochemistry* 2007, 103(1):88-97.
26. Axelrad TW, Deo DD, Ottino P, Van Kirk J, Bazan NG, Bazan HE, Hunt JD: Platelet-activating factor (PAF) induces activation of matrix metalloproteinase 2 activity and vascular endothelial cell invasion and migration. *FASEB journal : official publication of the Federation of American Societies for Experimental Biology* 2004, 18(3):568-570.
27. Pitton C, Lanson M, Besson P, Fetissoff F, Lansac J, Benveniste J, Bougnoux P: Presence of PAF-acether in human breast carcinoma: relation to axillary lymph node metastasis. *Journal of the National Cancer Institute* 1989, 81(17):1298-1302.
28. Montrucchio G, Sapino A, Bussolati B, Ghisolfi G, Rizea-Savu S, Silvestro L, Lupia E, Camussi G: Potential angiogenic role of platelet-activating factor in human breast cancer. *The American journal of pathology* 1998, 153(5):1589-1596.

29. Kispert S, Marentette J, McHowat J: Cigarette smoke induces cell motility via platelet-activating factor accumulation in breast cancer cells: a potential mechanism for metastatic disease. *Physiological reports* 2015, 3(3).